U.PORTO

DOUTORAMENTO

BIOLOGIA MOLECULAR E CELULAR

Unveiling biosynthetic pathways for the production of extracellular polymeric substances (EPS) in cyanobacteria and possible applications of the polymers

Marina Patrícia Fonseca Santos

D

2021

U.PORTO

Marina Patrícia Fonseca Santos. Unveiling biosynthetic pathways for the production of extracellular polymeric substances (EPS) in cyanobacteria and possible applications of the polymers

D.ICBAS 2021

Unveiling biosynthetic pathways for the production of extracellular polymeric substances (EPS) in cyanobacteria and possible applications of the polymers

Marina Patrícia Fonseca Santos

SEDE ADMINISTRATIVA

INSTITUTO DE CIÊNCIAS BIOMÉDICAS ABEL SALAZAR

FACULDADE DE CIÊNCIAS

MARINA PATRÍCIA FONSECA SANTOS

Unveiling biosynthetic pathways for the production of extracellular polymeric substances (EPS) in cyanobacteria and possible applications of the polymers

Tese de Candidatura ao grau de Doutor em Biologia Molecular e Celular;
Programa Doutoral da Universidade do Porto
(Instituto de Ciências Biomédicas de Abel Salazar
e Faculdade de Ciências)

Orientador:
Paula Tamagnini
Professora Associada
Faculdade de Ciências,
i3S - Instituto de Investigação e Inovação em Saúde
IBMC - Instituto de Biologia Molecular e Celular
Universidade do Porto, Portugal.

Co-orientador:
Elton Paul Hudson
Associate Professor
Department of Protein Science
School of Engineering Sciences in Chemistry,
Biotechnology and Health
KTH Royal Institute of Technology
Science for Life Laboratory (SciLifeLab)
Stockholm, Sweden.

Co-orientador:
Luís Gales
Professor Associado
Instituto de Ciências Biomédicas Abel Salazar
i3S - Instituto de Investigação e Inovação em Saúde
IBMC - Instituto de Biologia Molecular e Celular
Universidade do Porto, Portugal.

Acknowledgements / Agradecimentos

In the first place, I would like to thank everyone that contributed, directly or indirectly, to the work presented here.

To my supervisor, Prof. Dr. Paula Tamagnini, whom I have to thank for the opportunity to work in the Bioengineering and Synthetic Microbiology (BSM) group, and for all the time, patience, support, important advice as well as the guidance of the work in the framework of my PhD.

I would like to express my most sincere thank you to both of my co-supervisors, Prof. Dr. Elton Paul Hudson and Prof. Dr. Luís Gales. Paul, for the wonderful time I had in Stockholm learning how to use CRISPRi. Prof. Luís for always being in a good mood, and available when I needed him.

To Prof. Dr. Cláudio Sunkel, the scientific committee and the "comissão de acompanhamento" (Professors Vítor Costa and Anabela Cordeiro da Silva) of the Doctoral Program in Molecular and Cellular Biology from ICBAS, I thank you for all the logistical support and advice throughout these last years.

To all the people in i3S, Faculty of Sciences, Faculty of Pharmacy, ICBAS, University of Sheffield and University of Florence, both collaborators and technical staff, that helped me throughout my PhD project such as: Paula Magalhães and Tânia Meireles (CCGen), Frederico Silva and Fátima Fonseca (B2Tech), Rui Fernandes and Ana Rita Malheiro (HEMS), Hugo Osório (Proteomics Platform), Narciso Couto and Esther Karunakaran (University of Sheffield), Federico Rossi and Prof. Dr. Roberto de Philippis (University of Florence), Sara Cravo and Professor Emília Sousa (University of Porto), Catarina Carona and Helena Martins. Thank you all for the help and the kindness!

To Prof. Arlete Santos (who was an important presence in my academic life) and Prof. Roberto Salema, who were mentors for all things related to electron microscopy.

To other members/former members from the Structural Biochemistry and Yeast Signalling Networks groups (i3S), and the HudsonLab (KTH Royal Institute of Technology, SciLifeLab) that were also very important throughout my PhD journey. Namely, Prof. Dr. João Morais Cabral, Prof. Dr. Pedro Moradas Ferreira, Clara Pereira, Telma Martins, Lun

Yao, Michael Jahn, Ivana Cengic, Kiyan Shabestary (lunch time!), Markus Janash and Johannes Asplund-Samuelsson (all the Stockholm museums and exhibits!) and Dóra Vitay.

To all current and former members of the BSM group for making the lab a fun and relaxed place, for always being available to lend a helping hand, for providing helpful insights, valuable discussions, and even tell a joke or two: namely D. Helena, Marta Mendes, Pedro Albuquerque, Filipe Pinto, Rute Oliveira (all the advice and support), Filipe Marques, João Rodrigues (Uppsala mini tour!), Cátia Gonçalves, Delfim Cardoso (the memes), Catarina Príncipe and Zsófia Büttel.

An enormous thank you to Paulo Oliveira and Catarina Pacheco, that were pivotal in helping me navigate my PhD, and were always available to plan, talk and discuss the work, to provide a helping hand, to challenge me, to suggest new possibilities or sometimes just to give me advice. Thank you for your mentorship and companionship.

To current and former “Team EPS” members namely, Sara Pereira, Rita Mota, and Carlos Flores. I thank Sara for being there to mentor, guide and support me, to discuss results and hypothesis with me, to help when necessary, and for being my friend. I thank Rita for all the support, the perspective, the good mood, and all the fun (and not so fun) moments spent trying to optimize this or that. And lastly, I thank Carlos who was my “EPS PhD buddy”, someone who is a friend, who was present through a lot of this journey and helped make it easier.

To Ângela Brito, Zé Pedro, Eunice Ferreira and Steeve Lima who were truly wonderful lab colleagues and friends. Thank you for all the wonderful and fun times, the friendly teasing, the music and movie recommendations (Zé), the book recommendations and incredibly nerdy jokes (Steeve). But mostly, thank you for all the words of strength and motivation, and for the companionship throughout this journey.

To my friends who let me ramble about everything, and think I’m speaking in tongues when I’m talking about work, but still let me do it (yeah…)! You are a much needed break from the toughest parts of life and I thank you for always having been there and continuing to do so, even if sometimes it is long distance ;P .

Finalmente, o meu maior obrigada para a minha família, que me apoiou em todos os momentos! Para os meus tios (Nelo, Armando, Sérgio, Zé e Lipe) e tias (Bela e Vanessa), primos (Tiago e Diogo) e primas (Bruna, Susana e Joana), o meu muito obrigada por todos os momentos em família (aqui e na aldeia!), são memórias que vou guardar para sempre. Bruna, eu sou filha única, mas sinto que tenho uma irmã. Susana, uma década é pouca coisa! Para o meu avô Aníbal e especialmente para a minha avó Lurdes, que sempre

será a pessoa mais extraordinária que alguma vez conheci, e o maior exemplo de bondade, força e resiliência que alguma vez terei. Vou guardar todas as memórias, todos os momentos, todo o carinho e dedicação. Obrigada avó, sempre foste e sempre serás um exemplo para mim.

E por último, para as pessoas que me conhecem melhor do que ninguém: os meus pais, Fernando e Maria do Céu Santos. Não existem palavras suficientes para vos agradecer todo o amor, todo o carinho, toda a força, motivação e apoio, todos os momentos, todas as alegrias e até, todas as vezes que me relembram da canção do Heathcliff. Obrigada por tudo o me ensinaram e todos os valores que me transmitiram. Obrigada por serem parte integral da pessoa que sou hoje, por sempre me terem dado a liberdade de escolher o meu caminho, mas estarem sempre presentes quando mais preciso. Mãe e Pai (e Polly!), obrigada por absolutamente tudo, incluindo todo o apoio que me deram para enfrentar e terminar esta etapa da minha vida. Amo-vos.

Financial Support

This work was financed by FEDER-Fundo Europeu de Desenvolvimento Regional funds through the COMPETE 2020-Operacional Programme for Competitiveness and Internationalisation (POCI), Portugal 2020, and by Portuguese funds through the Fundação para a Ciência e a Tecnologia (FCT)/Ministério da Ciência, Tecnologia e Ensino Superior, in the framework of the PhD Grant SFRH/BD/119920/2016, and the projects POCI-01-0145-FEDER-028779 (PTDC/BIA-MIC/28779/2017), and the projects Norte-01-0145-FEDER-000012, supported by Norte Portugal Regional Operational Programme (NORTE 2020), and also supported by national funds through the FCT, I.P., under the projects UIDB/04293/2020 and UIDP/04293/2020.

"The most exciting phrase to hear in science, the one that heralds new discoveries, is not 'Eureka!', but 'That's funny ...' "

– Isaac Asimov

Table of Contents

List of Publications

This thesis is based on the following publications and some unpublished results:

Pereira, S. B.*, **SANTOS, M.***, Leite, J. P., Flores, C., Eisfeld, C., Buttel, Z., Mota,R., Rossi, F., De Philippis, R., Cabral, J. M. & Tamagnini, P. (2019) The role of the tyrosine kinase Wzc (Sll0923) and the phosphatase Wzb (Slr0328) in the production of extracellular polymeric substances (EPS) by *Synechocystis* PCC 6803. *MicrobiologyOpen*, *8*:e00753. https://doi.org/10.1002/mbo3.753 *These authors contributed equally to this work

SANTOS, M., Pereira, S. B., Flores, C., Príncipe, C., Couto, N., Karunakaran, E., Cravo, S. M., Oliveira, P. & Tamagnini, P. (2021) Absence of KpsM (Slr0977) impairs the secretion of extracellular polymeric substances (EPS) and impacts carbon fluxes in *Synechocystis* sp. PCC 6803. *mSphere*, *6*:e00003-21. https://doi.org/10.1128/mSphere.00003-21

SANTOS, M., Pacheco, C. C., Yao, L., Hudson, E. P. & Tamagnini, P. CRISPRi as a tool to repress multiple copies of extracellular polymeric substances (EPS)-related genes in the cyanobacterium *Synechocystis* sp. PCC 6803. *Life*, 11:1198. https://doi.org/10.3390/life11111198

Other Publications:

Pereira, S. B., Sousa, A., **SANTOS, M.**, Araújo, M., Serôdio, F., Granja, P. L. & Tamagnini, P. (2019) Strategies to obtain designer polymers based on cyanobacterial extracellular polymeric substances (EPS). *International Journal of Molecular Sciences, 20*:5693. https://doi.org/10.3390/ijms20225693

Flores, C., **SANTOS, M.**, Pereira, S.B., Mota, R., Rossi, F., De Philippis, R., Couto, N., Karunakaran, E., Wright, P.C., Oliveira, P. & Tamagnini, P. (2019) The alternative sigma factor SigF is a key player in the control of secretion mechanisms in *Synechocystis* sp. PCC 6803. *Environmental Microbiology*, *21*, 343-359. https://doi.org/10.1111/1462-2920.14465

List of Abbreviations

2-OG	2-oxoglutarate
3D	Three dimensional
ABC	Ammonium bicarbonate
Acetyl-CoA	Acetyl-Coenzyme A
AGC	Automatic gain control
Amp	Ampicillin
ANOVA	Analysis of variance
ATP	Adenosine triphosphate
ATPase	ATP synthase
AU	Arbitrary units
BCA	Bicinchoninic acid assay
BLAST	Basic local alignment search tool
bp	Base pairs
BY-kinases	Bacterial tyrosine kinases
Car	Carotenoids
cDNA	Complementary DNA
CHCA	alpha-Cyano-4-hydroxycinnamic acid
Chl a	Chlorophyll a
Cm	Chloramphenicol
CPS	Capsular polysaccharides
CRISPR	Clustered regularly interspaced short palindromic repeats
CRISPRi	Clustered regularly interspaced short palindromic repeats interference
DAD	Diode array detection
dCas9	Nuclease-deficient Cas9
DDM	Dodecyl-β-D-maltoside
DIG	Digoxigenin
DNA	Deoxyribonucleic acid
DTT	Dithiothreitol
EDTA	Ethylenediaminetetraacetic acid
EMVs	Everted membrane vesicles
Eno	Enolase
EPS	Extracellular polymeric substances
FDR	False Discovery Rate
GEO	Great Oxigenation Event
GEO	Gene Expression Omnibus

HCD	High-energy collision dissociation
HEP	Heterocyst outermost exopolysaccharide
His	Histidine
HPLC	High-performance liquid chromatography
HRP	Horse radish peroxidase
IT	Injection time
iTRAQ	Isobaric tags for relative and absolute quantitation
JTT	Jones-Taylor-Thornton
kDA	Kilodalton
KEGG	Kyoto Encyclopedia of Genes and Genomes
Km	Kanamycin
LC-MS	Liquid chromatography-mass spectrometry
LFQ	Label-free quantification
LMW-PTP	Low molecular weight protein tyrosine phosphatase
LPS	Lipopolysaccharides
MALDI	Matrix-assisted laser desorption/ionization
Mbp	Megabase pair
mRNA	Messenger RNA
MS	Mass spectrometry
MW	Molecular weight
MWCO	Molecular weight cut-off
NADH	Nicotinamide adenine dinucleotide (reduced form)
NCBI	National center for biotechnology information, US
np	Not present
ns	No significant differences
OAg	O-antigen
OCP	Orange carotenoid binding protein
OD	Optical density
OPX	Outer membrane export
ORF	Open reading frame
OxPPP	Oxidative pentose phosphate pathway
PAGE	Polyacrylamide gel electrophoresis
PCC	Pasteur Culture Collection
PCP	Polysaccharide co-polymerase
PCR	Polymerase chain reaction
PDB	Protein data bank

Pgm	Phosphoglycerate mutase
PHA	Poly-hydroxyalkanoate
PhaP	Phasin
PHB	Poly-hydroxybutyrate
PilA	Pilin protein
PMF	Peptide mass fingerprinting
PMSF	Phenylmethylsulfonyl fluoride
pNP	p-nitrophenol
pNPP	p-nitrophenyl phosphate
PPI	Protein-protein interaction
ppm	Parts per million
RNA	Ribonucleic acid
RNAseq	RNA sequencing
ROS	Reactive oxygen species
RPKM	Reads Per Kilobase
rpm	Revolutions per minute
RPS	Released polysaccharides
RT-PCR	Reverse transcription polymerase chain reaction
RT-qPCR	Reverse transcription quantitative polymerase chain reaction
RuBisCo	Ribulose-1,5-bisphosphate carboxylase/oxygenase
SD	Standard deviation
SDS	Sodium dodecyl sulfate
SEC	Size exclusion chromatography
sgRNA	Small-guide RNA
SigF/SigJ/SigE	Alternative sigma factor F, J, E
Sm/Sp	Streptomycin/spectinomycin
sp.	Species
TEAB	Triethylammonium bicarbonate
TEM	Transmission electron microscopy
TES	N-tris(hydroxymethyl)methyl-2-aminoethanesulfonic acid
TFA	Trifluoroacetic acid
TktA	Transketolase
TPR	Tetratricopeptide
Tr	Traces
TSS	Transcriptional start unit
TU	Transcriptional unit

UV	Ultraviolet
wt	Wild-type
Y	Tyrosine

Abstract

Cyanobacteria are photosynthetic prokaryotes that can directly convert CO_2 into organic compounds, thus having a major ecological role as primary producers. Their high genomic and metabolic plasticity, has granted them the capacity to survive in the most varied/inhospitable environments. Furthermore, these microorganisms produce so many natural compounds, that they have gained notoriety as possible “green cell-factories”. Most cyanobacteria produce extracellular polymeric substances (EPS), which are mainly composed of heteropolysaccharides that can either remain attached to cell surface or be released into the extracellular media, being referred to as released polysaccharides (RPS). Cyanobacterial EPS have distinct features compared to their bacterial counterparts, which makes them relevant for use in biotechnological and biomedical applications. However, the knowledge on the cyanobacterial EPS biosynthesis, assembly and export pathways is limited, hindering not only the optimization of polymer yields and tailoring of polymer properties, but also the possibility to efficiently redirect the carbon flux toward the production of other compounds, thus restricting the implementation of industrial systems based on cyanobacterial “cell factories”.

Throughout this work, an in depth characterization of some knockout and CRIPSRi mutants was performed to validate and elucidate the role/effect of some genes/proteins in EPS production, and general cell homeostasis, using the model cyanobacterium *Synechocystis* sp. PCC 6803. To start, we showed that absence of Wzb (Slr0328) and Wzc (Sll0923) affects both the amount and composition of the polymers produced. Moreover, we clarified the roles of both proteins through biochemical and structural analysis, providing the first insights into the molecular mechanisms of EPS production in *Synechocystis*, and highlighting, for the first time, tyrosine-phosphorylation as possible regulatory mechanism of EPS production in cyanobacteria. Furthermore, a double mutant lacking both Wzb and Wzc showed an increase of RPS which lead us to look towards the involvement of other players/a crosstalk between components associated with different pathways. Thus, we generated a mutant lacking KpsM (Slr0977), a homologue to a component of the bacterial ABC-transporter dependent pathway. The *kpsM* mutant has a significant reduction of RPS and a smaller decrease of capsular polysaccharides (CPS), but it accumulates more poly-hydroxybutyrate (PHB) than the wild-type. In addition, the *kpsM* mutant exhibits a light/cell density-dependent clumping phenotype, and the absence of KpsM affects the amount of carotenoids present in the extracellular media, protein secretion, and pilin glycosylation. In addition, proteomic and transcriptomic analyses revealed significant changes in the mechanisms of energy production and conversion, namely, photosynthesis, oxidative phosphorylation, and carbon metabolism. This work showed that cells with impaired EPS

secretion undergo broad transcriptomic and proteomic adjustments, highlighting the importance of EPS as a major carbon sink in cyanobacteria. In addition, by characterizing a CRISPRi mutant, where the three putative *kpsM* homologues (*slr0977*, *slr2107* and *sll0574*) were repressed, and comparing its phenotype to those of the three conventional single *kpsM* mutants (*slr0977*, *slr2107* and *sll0574*), it seems likely that Slr0977 is the key KpsM homologue in *Synechocystis*.

Overall, this work contributed to a better and more in depth understanding of the molecular mechanisms underlying the last steps of EPS production in *Synechocystis*, to unveil the role of some key proteins involved in these pathways, and to provide a better understanding of the importance of cyanobacterial EPS as a carbon-sink. It also acts as a starting point in the study of the genetic functional redundancy, which is common in cyanobacteria and hinders the study of these complex biosynthetic pathways.

Keywords: cyanobacteria, *Synechocystis*, extracellular polymeric substances (EPS), secretion, poly-hydroxybutyrate (PHB), carbon fluxes, functional redundancy, CRISPRi

Resumo

As cianobactérias são procariontes fotossintéticos que, por converterem diretamente CO_2 em compostos orgânicos, têm uma elevada importância ecológica como produtores primários. A sua alta plasticidade genómica e metabólica confere-lhes a capacidade de sobreviver nos mais variados/inóspitos ambientes. Além disso, estes microrganismos produzem uma vasta gama de compostos naturais tendo por isso alcançado notoriedade como possíveis "fábricas verdes". A maior parte das cianobactérias produz substâncias poliméricas extracelulares (EPS), compostas principalmente de heteropolissacarídeos, que podem permanecer associados à superfície celular ou serem libertados para o ambiente extracelular sendo, neste último caso denominados *released polysaccharides* (RPS). Os polímeros das cianobactérias têm características distintas dos produzidos por outras bactérias, o que os torna relevantes para aplicações biotecnológicas e biomédicas. O conhecimento sobre as suas vias biossintéticas e secretoras é, contudo, limitado, dificultando não só a otimização da produção e manipulação das propriedades do polímero, mas também a possibilidade de redirecionar de forma eficiente o fluxo de carbono para a produção de outros compostos, limitando deste modo a implementação de sistemas industriais baseados em "fábricas cianobacterianas".

Ao longo deste trabalho, foi feita uma caracterização detalhada de alguns mutantes de deleção e de repressão para elucidar o papel de alguns genes/proteínas na produção de EPS, usando como modelo a cianobactéria *Synechocystis* sp. PCC 6803. Inicialmente, demonstramos que a ausência das proteínas Wzb (Slr0328) e Wzc (Sll0923) afeta a quantidade e a composição do polímero produzido. Além disso, clarificamos os papéis destas proteínas, usando análises bioquímicas e estruturais, o que permitiu começar a conhecer os mecanismos moleculares de produção de EPS em *Synechocystis* e a levantar, pela primeira vez, a hipótese de a fosforilação de tirosinas ser um possível mecanismo regulador da produção de EPS em cianobactérias. Por outro lado, verificamos que um mutante duplo em que estão ausentes as proteínas Wzb e Wzc, produz mais RPS que a estirpe selvagem, o que nos levou a considerar o envolvimento de outros componentes ou a existência de uma possível interação entre componentes associados a diferentes vias. Assim, geramos um mutante de deleção num homólogo de um componente da via bacteriana dependente de um transportador ABC - KpsM (Slr0977). O mutante *kpsM* exibe uma redução significativa de RPS e uma diminuição menor de polissacarídeos capsulares (CPS), mas acumula mais polihidroxibutirato (PHB) do que a estirpe selvagem. O mutante *kpsM* apresenta também, um fenótipo de aglutinação dependente da luz/densidade celular, e a ausência da KpsM afeta a quantidade de carotenóides presentes no meio extracelular, a secreção de proteínas e a glicosilação de um componente das pili. As análises de

proteómica e transcriptómica revelaram ainda alterações significativas nos mecanismos de produção e conversão de energia, nomeadamente fotossíntese, fosforilação oxidativa e metabolismo do carbono. No geral, este trabalho mostrou que células em que a secreção de EPS está afetada sofrem vários ajustes a nível do seu transcriptoma e proteoma, destacando a importância das EPS como uma reserva de carbono nas cianobactérias. Por último, a caracterização de um mutante gerado por CRISPRi, onde os três homólogos *kpsM* (*slr0977*, *slr2107* e *sll0574*) foram reprimidos, em comparação com o fenótipo dos três mutantes de deleção *kpsM* convencionais (*slr0977*, *slr2107* e *sll0574*), parece sugerir que Slr0977 é o KpsM mais importante em *Synechocystis*.

Globalmente, este trabalho contribui para uma melhor e mais profunda compreensão dos mecanismos moleculares subjacentes à produção de EPS em *Synechocystis*, para elucidar o papel de algumas proteínas-chave e para melhor compreender a importância das EPS cianobacterianas como uma reserva de carbono. Este trabalho constitui também um ponto de partida para o estudo da redundância funcional genética, que é comum nas cianobactérias e dificulta o estudo destas vias biossintéticas tão complexas.

Palavras-chave: cianobactérias, *Synechocystis*, substâncias poliméricas extracelulares (EPS), secreção, polihidroxibutirato (PHB), fluxos de carbono, redundância funcional, CRISPRi

CHAPTER I

General Introduction

General Introduction

1. Cyanobacteria

1.1. The "architects of our planet"

Cyanobacteria are photosynthetic organisms that produce oxygen as a byproduct of photosynthesis. These microorganisms survive in aerobic and anaerobic environments and this characteristic is believed to be the reason that they not only survived the methane-rich primitive atmosphere, but to have transformed the geochemistry of our planet with the *en masse* oxigenation of the oceans (Soo et al., 2017). So, they were the first group of photoautotrophs able to produce molecular oxygen through water oxidation, and thus triggering the transition from the primitive anaerobic state of the Earth's atmosphere to its aerobic counterpart (Farquhar et al., 2000; Kasting & Siefert, 2002; Saito, 2009; Schopf, 2002). In addition, the study of ancient cyanobacterial strains supported that aerobic respiration evolved after oxygenic photosynthesis through independent acquisition of aerobic respiratory complexes by these organisms (Soo et al., 2017). The key-role of cyanobacteria in the development of life on Earth, through their involvement in the Great Oxigenation Event (GEO) (Blaustein, 2016; Knoll, 2008) is indisputable. However, their contribution goes beyond that, as it is widely accepted that a symbiosis event that took place among a free-living cyanobacterium and a phagotrophic organism, led to the formation of the first photosynthetic eukaryote. The cyanobacterium engulfed by the heterotrophic host cell was believed to have been involved in the origin of the first plastids of algae and higher plants, around 1.5 billion years ago (Dyall et al., 2004; Ochoa de Alda et al., 2014). These plastids further evolved into semiautonomous organelles known as chloroplasts, representing a critical step in the evolution and diversification of algae and higher plants (Dyall et al., 2004; Maréchal, 2018). The resemblance between plant cell plastids and cyanobacteria was first noted by the ecologist Schimper in 1883 in what was the starting point for a concept which is now designated the Endosymbiotic Theory on the origin of eukaryotic organelles. This theory was further advanced and supported with microbiological and fossil record evidences by others (Margulis, 1970; Sagan, 1967). Later on, the use of electron microscopy and molecular techniques produced more data that supported this theory (Deusch et al., 2008; McFadden, 2014; Woese, 1987). Nowadays, with a global biomass estimated to exceed 10^{15} g (Garcia-Pichel, 2009), they are regarded as important primary producers because of their crucial roles in the nitrogen and carbon cycles (Canfield et al., 2010; Galloway et al., 2004; Raven et al., 2012; Savage et al., 2010). Overall, it is understandable that some authors refer to these microorganisms as the "architects of our planet", given their role in shaping the characteristics of the planet we now inhabit.

1.2. Environmental adaptation, phenotypic diversity & general classification

Nowadays, cyanobacteria are described as a group of ancient, morphologically diverse, and ecologically important photosynthetic prokaryotes with a ubiquitous geographical distribution that is due to their innate ability to adapt to virtually any environmental conditions, including extreme ones. Their ability to live autotrophycally and/or diazotrophycally contributes to their capacity to adapt and proliferate in a variety of habitats, from fresh and brackish to salt water, soil and even extreme environments, such as hot springs, polar regions, hot and cold deserts and hypersaline areas (Bahl et al., 2011; Garcia-Pichel, 2009; Whitton, 2012). Cyanobacteria are a morphologically diverse group of microorganisms that can exist in forms such as unicellular, colonial, and filamentous. Furthermore, their capacity to respond to biotic and abiotic stresses allowed cyanobacteria to evolve and develop a series of features, ultimately giving rise to several different taxa.

Although a relatively recent classification system proposed their division into 8 orders (Komárek, 2016) the taxonomy of these group of organisms is still a controversial subject. One of the commonly used classifications, based on the type of reproduction, cell differentiation, and molecular/biochemical attributes, divides cyanobacteria into five Subsections (Rippka et al., 1979; Castenholz, 2001), that broadly coincide with five orders (Dvořák et al., 2015): Subsection I (Chroococcales), Subsection II (Pleurocapsales), Subsection III (Oscillatoriales), Subsection IV (Nostocales) and Subsection V (Stigonematales). Subsections I and II comprise unicellular cyanobacteria, single cells or forming colonial aggregates held together by additional outer cell wall layers. For cyanobacteria of Subsection I reproduction occurs mainly by binary fission, while for Subsection II it occurs by multiple fission giving rise to small and easily dispersible daughter cells (baeocytes), or by both multiple and binary fission (Rippka et al., 1979). Subsections III to V include filamentous cyanobacteria with varying levels of multicellular complexity. Genera belonging to Subsection III are comprised of filaments composed by vegetative cells only, in which division occurs only on one plane (Rippka et al., 1979). For cyanobacteria classified as belonging to Subsections IV and V, in the absence of combined nitrogen, the filaments differentiate heterocysts (cells specialized in nitrogen fixation), while some also produce akinetes (resting cells for survival under stress conditions) (Rippka et al., 1979). The characteristic that distinguishes Subsections IV and V is the plane in which division occurs, with it occurring in a single plane (at right angles to the long axis of the trichome) for Subsection IV and in multiple planes (development of lateral branches that are not at right angles to the long axis of the trichome) for Subsection V (Rippka et al., 1979).

As stated above, some cyanobacteria have the capacity to fix atmospheric nitrogen (N_2), this ability is quite remarkable because the nitrogenase, the N_2-reducing enzymatic

complex, is oxygen (O_2)-sensitive (Kasting & Siefert, 2002), forcing the cyanobacteria to adopt a number of different strategies to protect their enzymes. Two common strategies adopted by cyanobacteria are the differentiation of heterocysts (for filamentous cyanobacteria), spatially separating N_2 fixation from photosynthesis, or temporally separating the nitrogenase activity from the photosynthetic activity, using night time to fix nitrogen while the photosynthetic reactions occur during the day (light/dark cycles). Furthermore, despite being classified as Gram-negative bacteria, cyanobacteria possess a cell envelope that combines characteristics from both Gram-negative and Gram-positive bacteria, like the presence of lipopolysaccharides (LPS) in the outer membrane (Gram-negative) and the thickness and cross-linking degree of the peptidoglycan layer (Gram-positive) (Hahn & Schleiff, 2014), reinforcing their uniqueness as a group.

2. Extracellular polymeric substances (EPS)

2.1. A brief historical perspective

Extracellular polymeric substances (EPS) are one of the oldest studied substances and are produced by species from all the three life domains. The EPS naturally produced by cyanobacteria are the main focus of this thesis. To start at the beginning, Ernst Haeckel hypothesized in the 1868 publication titled “The History of Creation” that life originated from a sticky substance that he baptized as “primordial slime”. Years later, the biologist Thomas Henry Huxley discovered an albuminaceous slime in the Atlantic seafloor that he believed to be the substance Haeckel described and thus, named it *Bathybius haeckelii* in his honor. Although this substance was mistakenly associated with the origin of life by both Haeckel and Huxley, it is remarkable to see the importance that these slime-like substances, later defined as polysaccharide-based molecules, currently have. Quite a few decades went by, until in 1978 a seminal publication in Scientific American, appropriately titled “*How bacteria stick*”, described that the matrix which embeds bacteria consisted mainly of “polysaccharide fibers, fabricated and oriented by the cell itself”. The term EPS as “extracellular polymeric substances” was used for the first time shortly after in 1982 (Flemming, 2016). Subsequently, in 1988 these molecules were defined as “organic polymers of microbial origin which in biofilm systems are frequently responsible for binding cells and other particulate materials together (cohesion) and to the substratum (adhesion)”. Nowadays, the term EPS is used for polymers which include not only polysaccharides, but also proteins, lipids and nucleic acids (Flemming, 2016). Production of these molecules is a common feature among bacteria. Fundamentally, this represents an important process for the maintenance of bacterial cell homeostasis, either as a sink of carbon/energy and other molecules, or as an adaptative response to environmental stimuli.

2.2. Physiological roles of cyanobacterial EPS and environmental conditions that affect production

Most cyanobacteria produce EPS, mainly composed of heteropolysaccharides. These polymers can remain attached to the cell surface and depending on their thickness, consistency and degree of association with the cell surface can be classified as capsules or capsular polysaccharides (CPS) (thick and slimy layer intimately associated with the cell surface), sheaths (thin and dense layer loosely surrounding cells) or slime (mucilaginous material dispersed around the cells), or be released to the extracellular media, being referred to as released polysaccharides (RPS) (Rossi & De Philippis, 2016). The production and composition of EPS can be dependent on environmental conditions, such as pH, light, temperature and nutrient availability (Bahat-Samet et al., 2004; Fisher et al., 2013; Otero & Vincenzini, 2003; Rossi & De Philippis, 2016), which will be expanded upon below.

EPS produced by cyanobacteria are reported to be involved in a multiplicity of functions: protective barrier for cells, to minimise cell desiccation; protection against UV (Chen et al., 2009) and salt and metal stresses (Jittawuttipoka et al., 2013); promoting aggregation (Xu et al., 2014); adherence to surfaces (Fisher et al., 2013); formation and maintenance of biofilms (Sutherland, 2001); motility (Khayatan et al., 2015; Wilde & Mullineaux, 2015); cell-cell recognition; biosorption of exogenous compounds and establishment of symbiotic interactions (Kehr & Dittmann, 2015). Thus, although EPS production is a costly metabolic process for the cell, it provides physiological/adaptative advantages to the producing strain, justifying the maintenance of this high energy-consuming metabolic process. Although targeted genetic manipulation is the prime strategy to optimize and customize EPS production, there is also the possibility to increase or decrease the production of these biopolymers by manipulating the culture conditions.

Environmental factors can be one of the main influences in cyanobacterial EPS production, affecting not only the amount of EPS produced, but also, their composition, structure and consequently their chemical and functional properties. The influence of these factors is strongly strain-dependent (Pereira et al., 2009). Light, both intensity and quality, is one of the main factors influencing EPS production by cyanobacteria. For some strains, exposure to continuous or high-light intensities can enhance EPS production (Khattar et al., 2010; Otero & Vincenzini, 2003). In particular cases, specific light wavelengths promoted EPS production, such as UVB radiation for *Nostoc commune* and *Nostoc flagelliforme* (Ehling-Schulz et al., 1997; Han et al., 2018); or blue, red, purple and green light wavelenghts for *Nostoc flagelliforme*, which not only increased the amount of EPS produced, but also significantly changed the monosaccharide composition of their EPS (Han et al., 2014a, 2015, 2018). Although not commonly addressed, a second factor that

can affect EPS production is temperature, as EPS production tends to be higher under slightly higher temperatures than the ones used for optimal cell growth (Moreno et al., 1998; Su et al., 2007; Trabelsi et al., 2009; Yu et al., 2010), though others have reported opposite results (Gris et al., 2017; Nicolaus et al., 1999; Otero & Vincenzini, 2004), which suggests a strain-specific response to temperature fluctuations. Nutrient availability (for e.g. phosphate, sulphate and magnesium) and its ratio inside the cell (for e.g. Carbon:Nitrogen – C:N) are also determinant for cyanobacterial EPS production. For instance, phosphate-starvation induced production of both poly-hydroxybutyrate (PHB) and EPS in the nitrogen-fixing *Anabaena variabilis* and the non-nitrogen fixing *Microcystis aeruginosa* (Deb et al., 2019). In general, higher availability of carbon and/or nitrogen leads to higher production (De Philippis et al., 1996; Lama et al., 1996; Otero & Vincenzini, 2003). However, nitrogen starvation may also lead to higher EPS production, probably because this contributes to the increase in the C:N ratio, thus promoting the incorporation of carbon into polymers (De Philippis et al., 1998; De Philippis et al., 1993; Otero & Vincenzini, 2004). The metabolite 2-oxoglutarate (2-OG) was proposed to be the key to sense C:N balance in cyanobacteria (Forchhammer & Selim, 2020) and alterations in its concentration are sensed by the PII-protein, which was recently suggested as standing at the center of the C:N balance in cyanobacteria (Forchhammer & Selim, 2020; Hagemann et al., 2021; Orthwein et al., 2021). This mechanism is intrinsically linked to central metabolism, suggesting that all and any environmental factor(s) that affect central metabolism can disrupt or improve EPS production. Another factor that is frequently described as enhancing EPS production by cyanobacteria is salt stress. While this stress is a common stimulator of carbohydrate synthesis for the production of compatible solutes, it can also increase EPS production, enhancing salt stress tolerance (Bemal & Anil, 2018; Ozturk & Aslim, 2010; Shah et al., 1999; Yoshimura et al., 2012), and even altering the monosaccharidic composition of EPS produced by some cyanobacterial strains (Li et al., 2001; Yoshimura et al., 2012). Aeration, a type of shear stress, usually promotes an increase of the growth rate possibly by improving both nutrient and light availability for the cultures (Moreno et al., 1998; Su et al., 2007; Su et al., 2008). Although this parameter is not commonly evaluated, it can strongly impact EPS production in cyanobacteria by altering the culture conditions. Although a variety of environmental factors affecting cyanobacterial EPS production have been revealed, the specific way in which they trigger alterations in the production and on the characteristics of the polymers, and the molecular mechanisms they employ are still mostly unknown.

2.3. Characteristics of cyanobacterial EPS

The EPS produced by cyanobacteria are highly complex polymers with distinct features compared to their bacterial counterparts, such as: i) higher structural/compositional complexity derived from the presence of up to 13 possible different constituent monosaccharides, which can include up to two different uronic acids, ii) unusual sugars such as acetyl-, methyl- and amino-sugars, iii) peptide moieties, and iv) the presence of sulphate groups, a rare feature among bacterial EPS. Among the possible 13 different constituent monosaccharides, the most abundant is usually glucose, but also commonly identified are other hexoses (galactose, mannose and fructose), deoxyhexoses (fucose and rhamnose), pentoses (ribose, xylose and arabinose), and frequently 2 uronic acids (glucuronic and galacturonic acids). Moreover, approximately 75% of the cyanobacterial polymers characterized thus far are heteropolysaccharides comprising 6 or more different sugar residues (Okajima et al., 2018). On one side, the presence of hydrophilic moieties (such as sulphated sugars and uronic acids), and on the other, hydrophobic (such as acetyl groups, deoxysugars and peptides) confers an amphiphilic character to these macromolecules and provides greater plasticity in the capacity of the organisms to respond to the surrounding environment (Rossi & De Philippis, 2016), as the hydrophilic fractions are involved in entrapment of nutrients and water, while the hydrophobic ones enhance cell adhesion. Moreover, the presence of sulphate groups and uronic acids also contributes to the anionic nature of the EPS, conferring a negative charge and a “sticky” behavior to the macromolecule (Arias et al., 2003; De Philippis & Vincenzini, 1998; Nichols et al., 2005). Although not commonly described, other constituents, such as pyruvate and acetate, were also found in cyanobacterial EPS, namely from some *Nostoc* (De Philippis et al., 2000) and *Cyanothece* (De Philippis et al., 1998) strains. The presence of high-molecular weight fractions (reaching values ≥ 2 MDa) is another interesting feature of some cyanobacterial EPS (Flores et al., 2019a; Mota et al., 2020), and is of crucial importance for the polymers’ rheological behavior in solution (its viscosity), directly influencing possible applications of these biopolymers (Xu & Zhang, 2016). Overall, the combination of all these characteristics culminates in highly complex polymers (Abed et al., 2009; De Philippis & Vincenzini, 1998; Pereira et al., 2009; Rossi & De Philippis, 2016), which can be valuable for environmental, biomedical and biotechnological applications (Abed et al., 2009).

2.4. Cyanobacteria as “green cell-factories” for the production of EPS

The set of characteristics described above make cyanobacterial EPS promising macromolecules to be used in a variety of applications. Moreover, cyanobacteria are

photosynthetic prokaryotes that can directly convert CO_2 into organic compounds, ultimately to EPS, and thus are a very promising alternative to other, less sustainable and more pollutant methods. Therefore, the development and biotechnological application of cyanobacterial EPS-based products is increasingly attractive. Especially because now, more than ever, there is a demand for "greener products", products with a smaller ecological footprint, as a way to achieve environmental sustainability (to balance human activities while simultaneously harmonizing them with pre-existing natural processes) (Dhillon & von Wuehlisch, 2013). Thus, the "greener" side associated with cyanobacterial EPS production is both timely and relevant. Furthermore, the industrial production of these polymers presents important advantages compared to the production of biopolymers using other natural sources. Namely, the fact that they are usually actively secreted by the cells (facilitating the extraction and recovery processes), their manufacturing is not legislated by stringent rules usually applied for the production of polymers using animals or plants (for e.g. ethics and animal protection, or deforestation preventive measures) and, cyanobacteria have similar or higher growth rates compared to algae and plants (decreasing the time spent on production). In addition, the simple nutritional requirements of cyanobacteria, coupled with their photoautotrophic lifestyle, make these organisms desirable to be used in an industrial setting, due to their relatively easy and cost-effective cultivation. Therefore, recently, greater efforts are being made to both maximize and tailor the production of cyanobacterial EPS, and also of other value-added compounds, using genetic/metabolic engineering (Behler et al., 2018; Carroll et al., 2018; Hagemann & Hess, 2018; Knoot et al., 2018; Luan & Lu, 2018; Vavitsas et al., 2021). In this framework, some cyanobacterial strains emerge as promising microbial cell-factories, since they can be easily genetically engineered and there is an increasing amount of molecular and synthetic biology tools available for their manipulation. Strains such as *Synechococcus* sp. PCC 7002, *Anabaena* sp. PCC 7120, the fast-growing *Synechococcus elongatus* UTEX 2973, and, particularly, the aptly designated by Branco dos Santos et al. (2014) as the 'green *E. coli', Synechocystis* sp. PCC 6803 (Carroll et al., 2018; Ferreira et al., 2018; Gordon et al., 2016; Hagemann & Hess, 2018; Hudson, 2021; Liu & Pakrasi, 2018; Luan & Lu, 2018; Vasudevan et al., 2019; Vavitsas et al., 2019; Wendt et al., 2016; Yao et al., 2016; Yu et al., 2015), are some of the most biotechnologically promising cyanobacterial chassis due to their unique traits (Berla et al., 2013). From a metabolic engineering standpoint, it is important to highlight that glycogen, poly-hydroxybutyrate (PHB) and, more recently, the EPS are described as the major carbon sinks in cyanobacteria (Oliver & Atsumi, 2015). By subjecting organisms to different stress conditions, or by challenging the native fluxes through targeted modifications on a specific reaction of a biological pathway, plasticity/flexibility can be triggered at others (Vijay et al., 2019; Xiong et al., 2017). Thus, it stands to reason that by disrupting the

biosynthesis of a particular carbon sink in cyanobacteria and further engineering and/or re-directing other metabolic pathways, or specific nodes of these pathways, it would be possible to more efficiently re-route the carbon flux towards production of other products of interest or, at the very least, their precursor molecules (Ciebiada et al., 2020; Katayama et al., 2018; Song et al., 2021; van der Woude et al., 2014), as was already described to occur for other metabolic processes (Savakis & Hellingwerf, 2015; Thiel et al., 2017, 2019; van der Woude et al., 2014). In fact, previous work suggested that the accumulation of PHB is a direct result of glycogen turnover, during nitrogen-deficiency conditions, in *Synechocystis* sp. PCC 6803 (Koch et al., 2019, 2020; Osanai et al., 2005). Thus, this is significant not only from the perspective of increasing EPS production, but also if the goal is to use cyanobacteria as cell-factories of other compounds, since the production of EPS is a costly metabolic process, requiring a lot of energy, and thus it can strongly hinder productivity. Overall, engineering cyanobacterial carbon-related metabolism, should provide a solid strategy to re-direct carbon flux towards the preferential metabolic pathway and boost productivity of specific compounds, including the EPS, making cyanobacteria a promising chassis to be used as “green cell-factories”.

2.5. Biological activities and applications of cyanobacterial EPS

As stated in section 2.3. the cyanobacterial EPS are generally more complex than other bacterial EPS, which also results in higher versatility and allows the possibility of their use in a broader-spectrum of application fields. In fact, some polymers showed potential to be used in distinct fields, such as the polymer produced by the marine cyanobacterium *Crocosphaera chwakensis* CCY0110 (previously known as *Cyanothece* CCY 0110) that can not only be used efficiently for heavy metal remediation (Mota et al., 2016), but also as a vehicle for controlled drug delivery (Leite et al., 2017, Estevinho et al., 2019), and as a coating with anti-adhesive properties (Costa et al., 2019). Presently, the main areas of possible application for cyanobacterial EPS are bioremediation of heavy metals, soil stabilization (as nutrient supplements and physical soil amendments for the recovery of eroded cells), pharmaceutics, cosmetics/cosmeceutical industry, food supplementation or food conservation, and biomedicine and tissue engineering (reviewed in Singh et al., 2019). Concomittantly, several patents have been filled to protect the knowledge/use related to methods of cyanobacterial EPS production in large-scale, their extraction and/or downstream processing, as well as the use of the polymers (pure or combined in formulae) in specific fields (compiled in Borowitzka, 2014). Cyanobacterial EPS have been described to have a wide range of different biological activities (for e.g. quelating, immunostimulatory, antiviral, cytotoxic, anti-inflammatory and antimicrobial). From an environmental

perspective cyanobacterial EPS can be applied as a heavy metal removal approach in contaminated water or soils, while also having the potential to be used as a soil restoration method. The use of cyanobacterial EPS for heavy metal remediation constitutes an alternative to both physico-chemical methods and other bacterial EPS. Its advantages are related to: i) the high affinity of the polymer towards metal cations due to its overall negative charge, and ii) the high number of different monosaccharides that increases the number of different conformations, which could facilitate the interaction of the metal ions with the EPS-binding sites (Mota et al., 2016; Pereira et al., 2011). Moreover, EPS-rich cyanobacteria can be used as nutrient supplements and physical soil amendments for the recovery of eroded soils, due to the EPS' physiological role in increasing the water retention capacity of the affected soil (Adessi et al., 2018; Rossi et al., 2018). Furthermore, since EPS are composed of molecules with water absorption and retention capacity, such as uronic acids, their use in the cosmetics/cosmeceutical industry is also a feasible option. In fact, the water absorption and retention capacities of the EPS produced by *Nostoc commune* were described to be higher in comparison to urea and chitosan (Morone et al., 2019), highlighting their greater potential to be used as a natural humectant in the cosmetic industry. In addition, sacran, the polymer produced by *Aphanothece sacrum,* has higher viscosity, water retention, and capacity to absorb salines than hyaluronic acid (Okajima et al., 2008), which is one of the most commonly used ingredients in cosmetics but has a high cost and limited production. Moreover, the rheological properties of cyanobacterial EPS often make them promising to be used both in the cosmetic industry, as well as in the food industry as emulsifying and thickening agents. In fact, emulcyan, a polymer produced by *Phormidium*, and one of the four cyanobacterial EPS commercially available currently, was described as having flocculating and emulsifying properties (Fattom & Shilo, 1985). Similarly, cyanoflan, a polymer produced by the marine cyanobacterium *Crocosphaera chwakensis* CCY0110 (previously *Cyanothece* CCY 0110) was also described to be highly viscous in aqueous solutions and having high emulsifying activity (Mota et al., 2020). In addition, the EPS of *Nostoc flagelliforme* were also described as having high intrinsic viscosity, good emulsification activity, and excellent flocculation capability, being a very promising candidate for use in the food industry (Han et al., 2014b).

The natural ability of polysaccharides to form hydrogels, in which three dimensional (3D) cross-linked network structures retain large amounts of water, makes them incredibly useful for the production of cell-carrier systems and scaffolds (Bellini et al., 2018; Ciocci et al., 2017; Seliktar, 2012). Additionally, cyanobacterial EPS have also been tested for use as a vehicle for the controlled delivery of proteins or drugs. This could prove advantageous due to: i) the possible reduction of toxic side-effects, because it is an organic polymer, and ii) the improvement of the bioavailability of the transported molecule and possibility to

control release due to biodegradability (Estevinho et al., 2019; Leite et al., 2017; Liu et al., 2008). Currently, perhaps the most relevant and promising uses of cyanobacterial EPS are in biomedicine, being related to some of these polymers capabilities to act as antitumor, antiviral and antibacterial agents, thus emerging as new, alternative therapeutics. Spirulan, immulan and nostoflan, which are commercially available, are produced by *Arthrospira platensis* (Spirulina) (spirulan and immulan) and *Nostoc flagelliforme* (nostoflan). Spirulan and immulan possess anti-thrombin and immunostimulatory activities, respectively (Cruz et al., 2020; Hayakawa et al., 2000; Patel & Goyal, 2013; Pugh et al., 2001), while nostoflan was described as having antiviral and antitumor bioactivities (Kanekiyo et al., 2005, 2007; Yue et al., 2012). Recently, a sulfated polymer produced by a *Synechocystis* sp. PCC 6803 Δ*sigF* mutant strain was described as strongly reducing the viability of different human tumor cell lines (Flores et al., 2019a). Previously, polymers produced by *Aphanothece halophytica* (Ou et al., 2014) and *Nostoc sphaeroide* (Li et al., 2018) were also reported as having antitumor activity, making them relevant molecules for targeted therapeutics.

As of today, and to our knowledge, only four cyanobacterial EPS are commercially available (spirulan, immulan, nostoflan and emulcyan) (Cruz et al., 2020). While the overall characteristics of these polymers make them ideal to be used in a broad range of applications, they are not reaching the market as easily as other bacterial polymers. Thus, an in depth understanding of the biosynthetic mechanism(s) responsible for EPS production is necessary to allow an increase of polymer yields in a cost-effective manner (thus justifying production costs), the formulation of tailor-made polymer variants with desirable properties/enhanced performance for specific applications, and to facilitate the implementation of cyanobacterial-based industrial systems, and the broader use of cyanobacterial EPS.

2.6. EPS Biosynthetic Pathways

The machinery involved in the production, assembly and export of EPS has been extensively studied in both Gram-positive and Gram-negative bacteria (Cuthbertson et al., 2009, 2010; Islam & Lam, 2014; Whitfield et al., 2020; Whitney & Howell, 2013). In general, bacteria may display either extracellular or, more complex, intracellular EPS biosynthetic pathways (Schmid, 2018). Regarding the extracellular synthesis of polysaccharides, this process is dependent on extracellular sucrases, which are secreted and anchored to the bacterial cell wall (Schwab et al., 2007). In general, dextrans and levans, are produced by the action of these sucrase enzymes and assembled from the percursors obtained from cleavage of sucrose molecules. Depending on which monosaccharide is tranferred to a primer molecule, fructans (levan) or glucans (dextran), are produced (Schmid, 2018; Zeidan

et al., 2017). These polymers can have distinct molecular weights and be branched at different levels, depending on the reaction conditions (Leemhuis et al., 2013; Srikanth et al., 2015). Other oligosaccharides variants can be produced depending on the use of different primer molecules, such as maltose, isomaltose or nigerose, displaying interesting potential for tailored production (Hu et al., 2017). For the intracellular biosynthetic pathways, usually, this is a four-step process spanning different cellular compartments. The initial steps of EPS production are dependent on proteins involved in primary sugar metabolism, which are organism-specific and are determinant for the composition and properties of the EPS produced. In the cytoplasm, monosaccharide units are converted to activated sugar nucleotides that are transferred, by specific glycosyltransferases, to acceptor-molecules located on the plasma membrane (Whitfield, 2006; Whitfield et al., 2020). The last steps of polymerization, assembly and export appear mostly conserved throughout bacteria, following one of three model mechanisms: the Wzy-, the ABC transporter- or the Synthase-dependent pathways (Cuthbertson et al., 2010; Islam & Lam, 2014; Kehr & Dittmann, 2015; Whitney & Howell, 2013) (Figure 1).

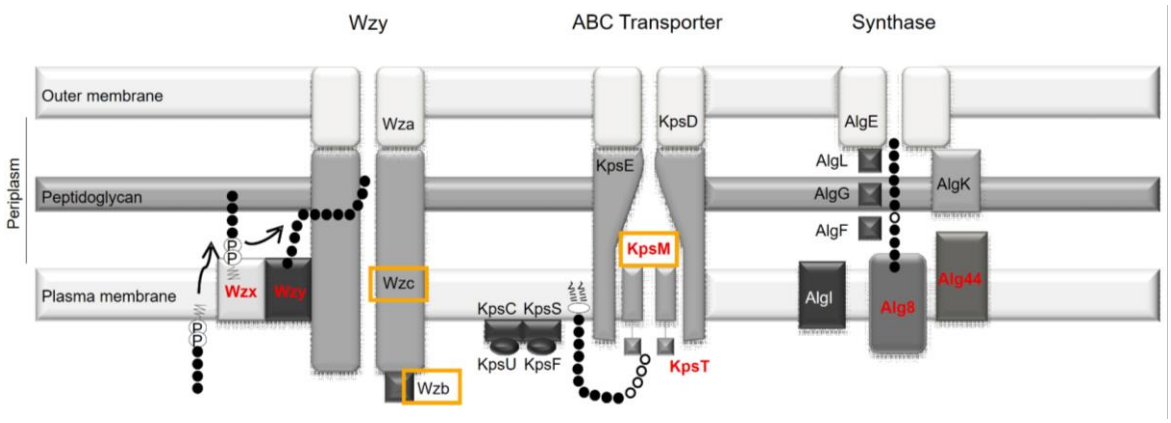

Figure 1. Representation of the three main bacterial EPS assembly and export mechanisms (*adapted from* Pereira et al., 2015). For the synthase-dependent pathway, the components involved in the synthesis of alginate are shown. Hallmark proteins from each pathway are indicated in red and bold. Cyanobacterial putative components studied in the framework of this thesis are highlighted with an orange box.

The Wzy-dependent pathway relies on the flippase Wzx to translocate oligosaccharide lipid-linked repeat units to the periplasmic space where polymerization is performed by the polymerase, Wzy. A complex spanning the citoplasmic membrane, periplasm and outer membrane, formed by the polysaccharide co-polymerase (PCP) and the outer membrane export (OPX) proteins Wzc and Wza, respectively, translocates the polymer to the extracellular side of the outer membrane (Islam & Lam, 2014). Wzc is a protein kinase, capable of auto-phosphorylation, whose phosphorylation status is regulated by the phosphatase Wzb (Obadia et al., 2007; Paiment et al., 2002). It has been hypothesized that

cycles of phosphorylation/dephosphorylation control the conformational changes of Wzc to allow the transport of the polymer to the extracellular space (Standish & Morona, 2014). In the case of the ABC transporter-dependent pathway, the fully polymerized polysaccharide is assembled in the cytoplasmic side of the plasma membrane where it is translocated to the periplasm by a two-protein complex, KpsM and KpsT, the so-called ABC-transporter. Export to the extracellular space occurs through the action of the PCP and OPX proteins KpsE and KpsD, respectively (Whitfield, 2006). Regarding the Synthase-dependent pathway, and in contrast with the ABC transporter- and Wzy-dependent pathways, this pathway initially results in the assembly of homopolysaccharides, constituted by one specific type of monosaccharide. The main examples are alginate or bacterial cellulose. It relies on a membrane embedded multi-protein complex comprised of a polysaccharide synthase and a co-polymerase that are responsible for the simultaneous polymerization and transport the polymer across the membrane complex. Final polymer secretion is dependent of a tetratricopeptide (TPR) associated to a beta-barrel porin. Modifications to the polymer are performed in the periplasm, as necessary, throughout the whole process (Low & Howell, 2018). Specifically, for the production of alginate (Figure 1), this pathway requires a synthase, Alg8, to simultaneously polymerize and export the polymer across the plasma membrane to the periplasmic site. Once in the periplasm, the polymer can be modified or degraded by a set of specific proteins such as epimerases (AlgG), lyases (AlgL) and acetylases (AlgIJFX) (Hay et al., 2013). Alginate export to the extracellular space requires the scaffold protein AlgK and the outer membrane porin AlgE (Whitfield & Trent, 2014; Whitney & Howell, 2013).

Although the last steps of EPS biosynthesis are relatively conserved throughout bacteria, the information regarding these pathways in cyanobacteria is limited and mostly inferred from homology analysis of the most conserved proteins, those involved in the last steps of assembly and export of the EPS biosynthetic pathways. In 2015, an analysis of 124 cyanobacterial genomes was performed to identify genes/proteins putatively involved in these last steps and their relative distribution among cyanobacteria (Pereira et al., 2015). For this purpose, EPS-related conserved domains were identified by screening bacterial proteins sequences which are known to be involved in well-characterized systems of EPS assembly and export. Subsequently, a homology analysis was performed to determine the presence or absence of these domains in cyanobacterial theoretical proteomes. While all the analysed strains had proteins related to the three main pathways of EPS assembly and export, not all strains possessed the full set of proteins associated with each pathway (Pereira et al., 2015). Moreover, some of the proteins were identified only in a restricted number of strains within the phylum while others are widespread. A phylum-wide distribution of proteins which are predicted to be involved in the Wzy-dependent pathway was observed:

Wza/KpsD, Wzb, Wzc/KpsE, Wzx and Wzy (Pereira et al., 2015). Furthermore, the KpsM/Wzm, associated with the ABC-transporter dependent pathway, was also widely distributed within the phylum, similarly to the protein of unknown function ExoD. The presence of genes encoding proteins related to the Synthase-dependent pathway was also found in cyanobacteria (Pereira et al., 2015). However, the domains related to most of these proteins were absent or confined to a small number of the strains with the notable exception of the synthase, Alg8, which is ubiquitously distributed (Pereira et al., 2015). Nevertheless, all cyanobacteria possess genes encoding proteins involved in the last steps of EPS assembly and export pathways. Their distribution, however, is variable and might depend on factors such as genome size, natural habitat and morphology of the cyanobacteria (Pereira et al., 2015). Commonly, EPS-related genes could be identified in more than one copy in a single cyanobacterial strain (Pereira et al., 2009; Pereira et al., 2015). For the most part, this can be correlated with the genome size, wherein the larger genomes present a higher number of copies of each gene (Pereira et al., 2015). In contrast to what is described for other bacteria, where these genes are usually organized in clusters/operons that contain the elements necessary for the synthesis of a specific polymer, in cyanobacteria, the EPS-related genes are mostly scattered throughout the genome or organized in relatively small clusters (Dimopoulou et al., 2014; Pereira et al., 2009; Pereira et al., 2015; Whitfield, 2006).

2.6.1. Genes/proteins associated with EPS production in the model cyanobacterium *Synechocystis* sp. PCC 6803

Among cyanobacteria, the freshwater unicellular cyanobacterium *Synechocystis* sp. PCC 6803 (hereafter *Synechocystis*) is commonly used as a model organism. This non–diazotrophic cyanobacterium has a ~3.6 Mbp genome encoding ~3,172 proteins and it was the first photosynthetic organism to have its genome fully sequenced (Kaneko et al., 1996), and consequently it detains the more detailed pool of information while also being easily genetically engineered.

Similarly to other cyanobacteria, the knowledge regarding EPS biosynthesis in *Synechocystis* is scarce. In 2015, Pereira et al. identified putative EPS-related genes, by a homology analysis, in *Synechocystis*, noting their presence in multiple copies (Table 1). The ExoD protein was included in this analysis even though the authors refer that its exact role and/or relationship with the main pathways remains unclear to date.

Table 1. Putative open reading frames encoding EPS-related proteins involved in the ABC-transporter, Wzy-dependent and Synthase-dependent pathways, and other proteins putatively associated with EPS production. The PCP (KpsE/Wzc) and OPX (KpsD/Wza) proteins are present in both pathways to assure the transport between the cytoplasmic face of the membrane and the outer membrane.

ABC-transporter and Wzy-dependent Pathways			
Protein		**Putative ORF**	
KpsD/Wza		*sll1581*	
KpsE/Wzc		*sll0923*	
		sll5052	
		slr0067	
ABC-transporter Dependent Pathway		**Wzy-dependent Pathway**	
Protein	**Putative ORF**	**Protein**	**Putative ORF**
KpsM	*slr0977*	Wzb	*slr0328*
	sll0574	Wzx	*slr0896*
	slr2107		*slr0488*
KpsT	*sll0575*		*slr1543*
	slr0982		*sll5049*
	slr2108		*sll0737*
KpsC/KpsS	*slr2115*	Wzy	*slr1515*
KpsU	*slr2122*		*slr1074*
KpsF	*slr2111*		*slr0728*
			sll5047
			sll5047
Synthase-dependent pathway			
Protein		**Putative ORF**	
Alg8/BcsA		*slr1566*	
		sll1377	
		sll1004	
		slr5056	
Alg44/BcsA		*sll1481*	
		sll1181	
Other Proteins associated with EPS production			
Protein		**Putative ORF**	
ExoD		*slr1875*	

Other than being present in multiple copies these genes are also scattered throughout the genome (for e.g. *wzc*, *wzx*, *wzy*, *kpsM* and *kpsT*) (Figure 2), unlike what happens for other bacteria, in which they are often in large clusters, in specific regions and as single gene copies (Rehm, 2010). Recently, however, a bacterial-like cluster was identified in the megaplasmid pSYSM of a motile *Synechocystis* sp. PCC 6803 substrain, and described as responsible for producing a sulphated polymer designated synechan (Maeda et al., 2021). Furthermore, some of the EPS-related genes represented in Fig. 2 are in relevant genomic contexts regarding EPS production, not only nearby genes encoding proteins that could be important for the initial steps of EPS production such as glycosyltransferases, but also genes encoding proteins involved in EPS modifications such as sulfo- and methyltransferases. The "*rfb* gene cluster", previously described as the "*slr0977* gene cluster" by Fisher et al., 2013, is particularly relevant since it has several components that have already been experimentally associated with EPS production (Fisher et al., 2013; Jittawuttipoka et al., 2013). For a more detailed description of this gene cluster

see Chapter III, Fig. 1. All combined, this differential distribution and redundancy results in a more complex organization than previously observed and described for other bacteria, and strongly suggests that cyanobacteria might follow divergent pathways from the well-characterized bacterial pathways.

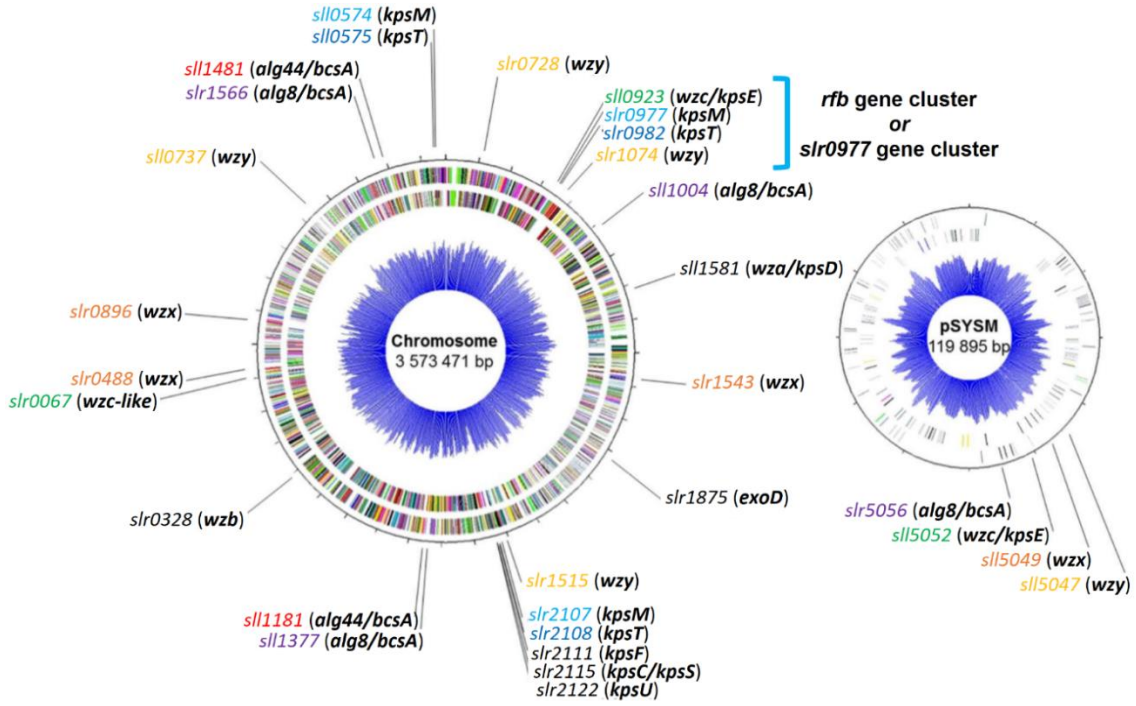

Figure 2. Genomic organization of the putative EPS-related genes associated to the bacterial ABC transporter-, Wzy- and Synthase-dependent pathways in the model cyanobacterium *Synechocystis* sp. PCC 6803. The genes are distributed between the chromosome and the megaplasmid pSYSM. Genes with more than one putative homologue are color-coded (for e.g. all *kpsM* copies are depicted in light blue) while genes present in a single copy are depicted in black.

In *Synechocystis*, some of the identified putative EPS-related genes have already been directly or indirectly implicated in EPS production, namely *sll1581* (*wza*) (Jittawuttipoka et al., 2013; Planchon et al., 2013), *sll0923* and *sll5052* (*wzc* copies) (Jittawuttipoka et al., 2013), *sll0574* and *slr0977* (*kpsM* copies) (Fisher et al., 2013), *sll0575* and *slr0982* (*kpsT* copies) (Fisher et al., 2013), and *slr1875* (*exoD*) (Jittawuttipoka et al., 2013; Planchon et al., 2013). Others have been studied as part of completely different metabolic processes such as, metal or multidrug tolerance mechanisms (*slr0946* – *wzb*; *slr0896* and *slr1543* – *wzx* copies) (Houot et al., 2007; Pengelly, 2008), photosynthesis (*slr0067* – *wzc*/*kpsE*; *slr2111* – *kpsF*) (Dai et al., 2013; He et al., 2018), and bicarbonate transport (*slr1515* – *wzy*) (Scott et al., 2006; Shibata et al., 2002). For the remaining genes, information regarding the function of their encoded proteins or their involvement in specific metabolic processes is still sparse. Studies carried out by generating and characterizing knockout mutants of EPS-related genes have already allowed the validation of some

proteins involved in the last steps of EPS assembly and export pathways in *Synechocystis*, and of the impact of the absence of these proteins on the amount and/or composition of the EPS produced. Regarding putative components of the Wzy-dependent pathway, Jittawuttipoka et al., in 2013, reported that deletion mutants of *sll0923* (*wzc*) and *sll1581* (*wza*) resulted in a decrease on the amount of CPS. Additionally, the *sll0923* (*wzc*) mutant also produced less RPS than the wild-type strain (Jittawuttipoka et al., 2013). In the same year, another *sll1581* mutant was described to produce less of both CPS and RPS (Planchon et al., 2013). It has been previously described that tyrosine phosphorylation impacts the activity of the bacterial autokinase Wzc, and has been positively correlated with alterations in the production/regulation of polysaccharide secretion and in the assembly of group 1 capsules (Obadia et al., 2007; Paiment et al., 2002; Standish & Morona, 2014). Since homologues of *wzb* and *wzc* were identified in *Synechocystis* (Jittawuttipoka et al., 2013; Planchon et al., 2013; Pereira et al., 2015), and *wzc* was already described as affecting EPS production (Jittawuttipoka et al., 2013; Planchon et al., 2013), while *wzb* was described as having phosphatase activity (Mukhopadhyay & Kennelly, 2011), the mechanism of phosphorylation/dephosphorylation could play a role in the control of EPS production/export in cyanobacteria.

Regarding the ABC transporter-dependent pathway, knockout mutants of *slr0977* (*kpsM*), *sll0574* (*kpsM*), *slr0982* (*kpsT*), and *sll0575* (*kpsT*) produce EPS with different monosaccharidic compositions from that of the wild-type polymer (Fisher et al., 2013). Moreover, both *sll0923* (*wzc*) and *slr0977* (*kpsM*) were described to be inorganic carbon (C_i) responsive genes, showing that they respond to an imbalance in the C:N ratio (Eisenhut et al., 2007). A *slr1875* (*exoD*) knockout mutant was also showed to impair CPS production, while not affecting the amount of RPS (Jittawuttipoka et al., 2013), the mechanism through which *exoD* operates, and if it cooperates with the EPS assembly and export pathways is still unknown. Recently, it was described that the SigF from *Synechocystis* is closely related to *Anabaena's* sp. PCC 7120 SigJ (Flores et al., 2019b), which is a transcription factor specifically associated with the control of EPS production, in particular with the formation of the heterocyst outermost exopolysaccharide (HEP)-layer (Yoshimura et al., 2007). *Synechocystis*' SigF is a group 3 sigma factor, encoded by *slr1564*, and was described to play a pleiotropic role in *Synechocystis* physiology, with a major impact on growth and secretion mechanisms, such as the production of extracellular polysaccharides, vesiculation and protein secretion. Not only did a mutant lacking SigF produced approximately four-fold more RPS than the wild-type, but an analysis of the putative SigF binding sites in the genome of *Synechocystis* disclosed possible genes regulated by SigF, including those encoding proteins involved in the central carbon metabolism (for e.g. glycosyltransferases), and proteins involved in CO_2 fixation and glycolysis (Flores et al.,

2019b). Considering the extensive phenotypic alterations reported for this mutant, the role of SigF in RPS production and/or export is most likely indirect. Nevertheless, in order to control all the players involved in these highly intricate biosynthetic pathways, a complex regulatory network is expected to exist and to operate harmoniously, with transcriptional regulation expected to be an important step for the control of cyanobacterial EPS production (Schmid et al., 2015). Particularly, because of the high number of identified putative EPS-related genes, and considering that some may encode proteins with redundant functions (Pereira et al., 2015).

In summary, the distinctive characteristics of cyanobacterial EPS associated with the low-cost cultivation of cyanobacteria, increased the interest in cyanobacterial EPS, and consequently their synthesis/export pathways, not only to maximize EPS production, but also to tailor polymer variants. Nevertheless, looking at things from a slightly different perspective, if the main goal is to use cyanobacteria as “cell factories” for production of other compounds of interest, the process of EPS production can strongly impair productivity. This dichotomy resulted in a refreshed interest in the cyanobacterial EPS biosynthetic pathways. Therefore, an extensive and comprehensible knowledge of these biosynthetic pathways is necessary, not only to better control the amount of polymer produced, or even modify its properties according to the desired final product, but also to efficiently redirect the carbon flux toward the production of other compounds, allowing the implementation of industrial systems based on cyanobacterial “cell factories”.

3. Main aims

The aim of this study was to contribute to the knowledge on cyanobacterial EPS-biosynthetic pathways by unveiling the last steps of assembly and export, evaluating the role of individual components on the amount and quality of the polymer(s) produced. For this purpose, the model unicellular cyanobacterium *Synechocystis* sp. PCC 6803 was used to:

1. identify and validate genes/proteins involved in the last steps of EPS production in cyanobacteria, mainly through the generation and characterization of knockout mutants (Chapters II, III and V).
2. investigate the role of some proteins involved in the cyanobacterial EPS-biosynthetic pathways (Chapter II).

3. understand the impact of the absence of EPS-related genes/proteins in general cell homeostasis (Chapter III).
4. validate the use of CRISPRi as a feasible option to address the redundancy of EPS-related genes (Chapter IV).

References

Abed, R. M. M., Dobretsov, S., & Sudesh, K. (2009). Applications of cyanobacteria in biotechnology. *Journal of Applied Microbiology*, *106*(1), 1–12. https://doi.org/10.1111/j.1365-2672.2008.03918.x

Adessi, A., Cruz de Carvalho, R., De Philippis, R., Branquinho, C., & Marques da Silva, J. (2018). Microbial extracellular polymeric substances improve water retention in dryland biological soil crusts. *Soil Biology and Biochemistry*, *116*, 67–69. https://doi.org/10.1016/j.soilbio.2017.10.002

Arias, S., del Moral, A., Ferrer, M. R., Tallon, R., Quesada, E., & Béjar, V. (2003). Mauran, an exopolysaccharide produced by the halophilic bacterium *Halomonas maura*, with a novel composition and interesting properties for biotechnology. *Extremophiles: Life under Extreme Conditions*, *7*(4), 319–326. https://doi.org/10.1007/s00792-003-0325-8

Bahat-Samet, E., Castro-Sowinski, S., & Okon, Y. (2004). Arabinose content of extracellular polysaccharide plays a role in cell aggregation of *Azospirillum brasilense*. *FEMS Microbiology Letters*, *237*(2), 195–203. https://doi.org/10.1111/j.1574-6968.2004.tb09696.x

Bahl, J., Lau, M. C. Y., Smith, G. J. D., Vijaykrishna, D., Cary, S. C., Lacap, D. C., Lee, C. K., Papke, R. T., Warren-Rhodes, K. A., Wong, F. K. Y., McKay, C. P., & Pointing, S. B. (2011). Ancient origins determine global biogeography of hot and cold desert cyanobacteria. *Nature Communications*, *2*, 163. https://doi.org/10.1038/ncomms1167

Behler, J., Vijay, D., Hess, W. R., & Akhtar, M. K. (2018). CRISPR-based technologies for metabolic engineering in cyanobacteria. *Trends in Biotechnology*, *36*(10), 996–1010. https://doi.org/10.1016/j.tibtech.2018.05.011

Bellini, E., Ciocci, M., Savio, S., Antonaroli, S., Seliktar, D., Melino, S., & Congestri, R. (2018). *Trichormus variabilis* (cyanobacteria) biomass: from the nutraceutical products to novel EPS-cell/protein carrier systems. *Marine Drugs, 16*(9). https://doi.org/10.3390/md16090298

Bemal, S., & Anil, A. C. (2018). Effects of salinity on cellular growth and exopolysaccharide production of freshwater *Synechococcus* strain CCAP1405. *Journal of Plankton Research*, *40*(1), 46–58. https://doi.org/10.1093/plankt/fbx064

Berla, B. M., Saha, R., Immethun, C. M., Maranas, C. D., Moon, T. S., & Pakrasi, H. B. (2013). Synthetic biology of cyanobacteria: Unique challenges and opportunities. *Frontiers in Microbiology*, *4*(AUG), 1–14. https://doi.org/10.3389/fmicb.2013.00246

Blaustein, R. (2016). The Great Oxidation Event: Evolving understandings of how oxygenic life on Earth began. *BioScience*, *66*(3), 189–195. https://doi.org/10.1093/biosci/biv193

Borowitzka, M.A. (2014). Patents on cyanobacteria and cyanobacterial products and uses. In Cyanobacteria (Chichester, UK: John Wiley & Sons, Ltd), pp. 329–338. https://doi.org/10.1002/9781118402238.ch21

Branco dos Santos, F., Du, W., & Hellingwerf, K. J. (2014). *Synechocystis*: not just a plug-bug for CO_2, but a green *E. coli*. *Frontiers in Bioengineering and Biotechnology, 2*, 36. https://doi.org/10.3389/fbioe.2014.00036

Canfield, D. E., Glazer, A. N., & Falkowski, P. G. (2010). The evolution and future of Earth's nitrogen cycle. *Science*, *330*(6001), 192–196. https://doi.org/10.1126/science.1186120

Carroll, A. L., Case, A. E., Zhang, A., & Atsumi, S. (2018). Metabolic engineering tools in model cyanobacteria. *Metabolic Engineering*, *50*, 47–56. https://doi.org/10.1016/j.ymben.2018.03.014

Castenholz, R. W., Wilmotte, A., Herdman, M., Rippka, R., Waterbury, J. B., Iteman, I., & Hoffmann, L. (2001). Phylum BX. Cyanobacteria. In D.R. Boone, R.W.Castenholz and G.M. Garrity. *Bergey's Manual of Systematic Bacteriology* (pp. 473-599). New York, NY: Springer. https://doi.org/10.1007/978-0-387-21609-6_27.

Chen, L. Z., Wang, G. H., Hong, S., Liu, A., Li, C., & Liu, Y. D. (2009). UV-B-induced oxidative damage and protective role of exopolysaccharides in desert cyanobacterium *Microcoleus vaginatus*. *Journal of Integrative Plant Biology*, *51*(2), 194–200. https://doi.org/10.1111/j.1744-7909.2008.00784.x

Ciebiada, M., Kubiak, K., & Daroch, M. (2020). Modifying the cyanobacterial metabolism as a key to efficient biopolymer production in photosynthetic microorganisms. *International Journal of Molecular Sciences*, *21*(19), 1–24. https://doi.org/10.3390/ijms21197204

Ciocci, M., Mochi, F., Carotenuto, F., Di Giovanni, E., Prosposito, P., Francini, R., De Matteis, F., Reshetov, I., Casalboni, M., Melino, S., & Di Nardo, P. (2017). Scaffold-in-scaffold potential to induce growth and differentiation of cardiac progenitor cells. *Stem Cells and Development*, *26*(19), 1438–1447. https://doi.org/10.1089/scd.2017.0051

Costa, B., Mota, R., Parreira, P., Tamagnini, P., L Martins, M. C., & Costa, F. (2019). Broad-spectrum anti-adhesive coating based on an extracellular polymer from a marine cyanobacterium. *Marine Drugs*, *17*(4). https://doi.org/10.3390/md17040243

Cruz, D., Vasconcelos, V., Pierre, G., Michaud, P., & Delattre, C. (2020). Exopolysaccharides from cyanobacteria: Strategies for bioprocess development. *Applied Sciences*, *10*(11). https://doi.org/10.3390/app10113763

Cuthbertson, L., Kos, V., & Whitfield, C. (2010). ABC transporters involved in export of cell surface glycoconjugates. *Microbiology and Molecular Biology Reviews*, *74*(3), 341–362. https://doi.org/10.1128/mmbr.00009-10

Cuthbertson, L., Mainprize, I. L., Naismith, J. H., & Whitfield, C. (2009). Pivotal roles of the outer membrane polysaccharide export and polysaccharide copolymerase protein families in export of extracellular polysaccharides in Gram-negative bacteria. *Microbiology and Molecular Biology Reviews*, *73*(1), 155–177. https://doi.org/10.1128/mmbr.00024-08

Dai, H., Zhang, L., Zhang, J., Mi, H., Ogawa, T., & Ma, W. (2013). Identification of a cyanobacterial CRR6 protein, Slr1097, required for efficient assembly of NDH-1 complexes in *Synechocystis* sp. PCC 6803. *Plant Journal*, *75*(5), 858–866. https://doi.org/10.1111/tpj.12251

Deb, D., Mallick, N., & Bhadoria, P. B. S. (2019). Analytical studies on carbohydrates of two cyanobacterial species for enhanced bioethanol production along with poly-β-hydroxybutyrate, C-phycocyanin, sodium copper chlorophyllin, and

exopolysaccharides as co-products. *Journal of Cleaner Production*, *221*, 695–709. https://doi.org/10.1016/j.jclepro.2019.02.254

De Philippis, R., Margheri, M. C., Materassi, R., & Vincenzini, M. (1998). Potential of unicellular cyanobacteria from saline environments as exopolysaccharide producers. *Applied and Environmental Microbiology*, *64*(3), 1130–1132. https://doi.org/10.1128/AEM.64.3.1130-1132.1998

De Philippis, R., Ena, A., Paperi, R., Sili, C., & Vincenzini, M. (2000). Assessment of the potential of *Nostoc* strains from the Pasteur Culture Collection for the production of polysaccharides of applied interest. *Journal of Applied Phycology*, *12*(3), 401–407. https://doi.org/10.1023/A:1008161815801

De Philippis, R., Margheri, M. C., Pelosi, E., & Ventura, S. (1993). Exopolysaccharide production by a unicellular cyanobacterium isolated from a hypersaline habitat. *Journal of Applied Phycology*, *5*(4), 387–394. https://doi.org/10.1007/BF02182731

De Philippis, R., Sili, C., & Vincenzini, M. (1996). Response of an exopolysaccharide-producing heterocystous cyanobacterium to changes in metabolic carbon flux. *Journal of Applied Phycology*, *8*(4), 275–281. https://doi.org/10.1007/BF02178570

De Philippis, R., & Vincenzini, M. (1998). Exocellular polysaccharides from cyanobacteria and their possible applications. *FEMS Microbiology Reviews*, *22*(3), 151–175. https://doi.org/10.1111/j.1574-6976.1998.tb00365.x

Deusch, O., Landan, G., Roettger, M., Gruenheit, N., Kowallik, K. V, Allen, J. F., Martin, W., & Dagan, T. (2008). Genes of cyanobacterial origin in plant nuclear genomes point to a heterocyst-forming plastid ancestor. *Molecular Biology and Evolution*, *25*(4), 748–761. https://doi.org/10.1093/molbev/msn022

Dhillon, R. S., & von Wuehlisch, G. (2013). Mitigation of global warming through renewable biomass. *Biomass and Bioenergy*, *48*, 75–89. https://doi.org/10.1016/j.biombioe.2012.11.005

Dimopoulou, M., Vuillemin, M., Campbell-Sills, H., Lucas, P. M., Ballestra, P., Miot-Sertier, C., Favier, M., Coulon, J., Moine, V., Doco, T., Roques, M., Williams, P., Petrel, M., Gontier, E., Moulis, C., Remaud-Simeon, M., & Dols-Lafargue, M. (2014). Exopolysaccharide (EPS) synthesis by *Oenococcus oeni*: From genes to phenotypes. *PLoS ONE*, *9*(6). https://doi.org/10.1371/journal.pone.0098898

Dyall, S. D., Brown, M. T., & Johnson, P. J. (2004). Ancient invasions: from endosymbionts to organelles. *Science*, *304*(5668), 253–257. https://doi.org/10.1126/science.1094884

Dvořák, P., Poulíčková, A., Hašler, P., Belli, M., Casamatta, D. A., & Papini, A. (2015). Species concepts and speciation factors in cyanobacteria, with connection to the problems of diversity and classification. *Biodiversity and Conservation*, *24*(4), 739–757. https://doi.org/10.1007/s10531-015-0888-6

Ehling-Schulz, M., Bilger, W., & Scherer, S. (1997). UV-B-induced synthesis of photoprotective pigments and extracellular polysaccharides in the terrestrial cyanobacterium *Nostoc commune*. *Journal of Bacteriology*, *179*(6), 1940–1945. https://doi.org/10.1128/jb.179.6.1940-1945.1997

Eisenhut, M., von Wobeser, E. A., Jonas, L., Schubert, H., Ibelings, B. W., Bauwe, H., Matthijs, H. C. P., & Hagemann, M. (2007). Long-term response toward inorganic carbon limitation in wild type and glycolate turnover mutants of the cyanobacterium

Synechocystis strain PCC 6803. *Plant Physiology*, *144*(4), 1946–1959. https://doi.org/10.1104/pp.107.103341

Estevinho, B. N., Mota, R., Leite, J. P., Tamagnini, P., Gales, L., & Rocha, F. (2019). Application of a cyanobacterial extracellular polymeric substance in the microencapsulation of vitamin B12. *Powder Technology*, *343*, 644–651. https://doi.org/10.1016/j.powtec.2018.11.079

Farquhar, J., Bao, H., & Thiemens, M. (2000). Atmospheric influence of Earth's earliest sulfur cycle. *Science*, *289*(5480), 756–758. https://doi.org/10.1126/science.289.5480.756

Fattom, A., & Shilo, M. (1985). Production of emulcyan by *Phormidium* J-1: its activity and function. *FEMS Microbiology Ecology*, *31*, 3–9. https://doi.org/10.1111/j.1574-6968.1985.tb01125.x

Ferreira, E. A., Pacheco, C. C., Pinto, F., Pereira, J., Lamosa, P., Oliveira, P., Kirov, B., Jaramillo, A., & Tamagnini, P. (2018). Expanding the toolbox for *Synechocystis* sp. PCC 6803: validation of replicative vectors and characterization of a novel set of promoters. *Synthetic Biology*, *3*(1). https://doi.org/10.1093/synbio/ysy014

Fisher, M. L., Allen, R., Luo, Y., & Curtiss, R. (2013). Export of extracellular polysaccharides modulates adherence of the cyanobacterium *Synechocystis*. *PLoS ONE*, *8*(9). https://doi.org/10.1371/journal.pone.0074514

Flemming, H.-C. (2016). EPS - Then and Now. *Microorganisms*, *4*(4), 41. https://doi.org/10.3390/microorganisms4040041

Flores, C., Lima, R. T., Adessi, A., Sousa, A., Pereira, S. B., Granja, P. L., De Philippis, R., Soares, P., & Tamagnini, P. (2019a). Characterization and antitumor activity of the extracellular carbohydrate polymer from the cyanobacterium *Synechocystis* Δ*sigF* mutant. *International Journal of Biological Macromolecules*, *136*, 1219–1227. https://doi.org/10.1016/j.ijbiomac.2019.06.152

Flores, C., Santos, M., Pereira, S. B., Mota, R., Rossi, F., De Philippis, R., Couto, N., Karunakaran, E., Wright, P. C., Oliveira, P., & Tamagnini, P. (2019b). The alternative sigma factor SigF is a key player in the control of secretion mechanisms in *Synechocystis* sp. PCC 6803. *Environmental Microbiology*, *21*(1), 343–359. https://doi.org/10.1111/1462-2920.14465

Forchhammer, K., & Selim, K. A. (2020). Carbon/nitrogen homeostasis control in cyanobacteria. *FEMS Microbiology Reviews*, *44*(1), 33–53. https://doi.org/10.1093/femsre/fuz025

Galloway, J. N., Dentener, F. J., Capone, D. G., Boyer, E. W., Howarth, R. W., Seitzinger, S. P., Asner, G. P., Cleveland, C. C., Green, P. A., Holland, E. A., Karl, D. M., Michaels, A. F., Porter, J. H., Townsend, A. R., & Vöosmarty, C. J. (2004). Nitrogen cycles: past, present, and future. *Biogeochemistry*, *70*(2), 153–226. https://doi.org/10.1007/s10533-004-0370-0

Garcia-Pichel, F. (2009). Cyanobacteria. In M. Schaechter (Ed.). *Encyclopedia of Microbiology* (3rd ed., pp. 107-124). Amsterdam: Elsevier Inc. https://doi.org/10.1016/B978-012373944-5.00250-9

Gordon, G. C., Korosh, T. C., Cameron, J. C., Markley, A. L., Begemann, M. B., & Pfleger, B. F. (2016). CRISPR interference as a titratable, trans-acting regulatory tool for

metabolic engineering in the cyanobacterium *Synechococcus* sp. strain PCC 7002. *Metabolic Engineering*, *38*, 170–179. https://doi.org/10.1016/j.ymben.2016.07.007

Gris, B., Sforza, E., Morosinotto, T., Bertucco, A., & La Rocca, N. (2017). Influence of light and temperature on growth and high-value molecules productivity from *Cyanobacterium aponinum*. *Journal of Applied Phycology*, *29*(4), 1781–1790. https://doi.org/10.1007/s10811-017-1133-3

Hagemann, M., & Hess, W. R. (2018). Systems and synthetic biology for the biotechnological application of cyanobacteria. *Current Opinion in Biotechnology*, *49*, 94–99. https://doi.org/10.1016/j.copbio.2017.07.008

Hagemann, M., Song, S. and Brouwer, E.-M. (2021). Inorganic carbon assimilation in cyanobacteria: Mechanisms, regulation, and engineering. In J. Nielsen, S. Lee, G. Stephanopoulos and P. Hudson (Eds.) *Cyanobacteria Biotechnology* (1st ed.). Hoboken, NJ: Wiley Online Library. https://doi.org/10.1002/9783527824908.ch1

Hahn, A., & Schleiff, E. (2014). The Cell Envelope. In E. Flores and A. Herrero (Eds.). *The Cell Biology of Cyanobacteria*. Rover, UK: Caister Academic Press. https://doi.org/10.21775/9781908230508

Han, P., Guo, R., Shen, S., Yan, R., Wu, Y., Yao, S., Wang, H., & Jia, S. (2018). Proteomic profiling of *Nostoc flagelliforme* reveals the common mechanism in promoting polysaccharide production by different light qualities. *Biochemical Engineering Journal*, *132*, 68–78. https://doi.org/10.1016/j.bej.2017.12.006

Han, P., Shen, S., Wang, H.-Y., Sun, Y., Dai, Y., & Jia, S. (2015). Comparative metabolomic analysis of the effects of light quality on polysaccharide production of cyanobacterium *Nostoc flagelliforme*. *Algal Research*, *9*, 143–150. https://doi.org/10.1016/j.algal.2015.02.019

Han, P., Sun, Y., Jia, S., Zhong, C., & Tan, Z. (2014a). Effects of light wavelengths on extracellular and capsular polysaccharide production by *Nostoc flagelliforme*. *Carbohydrate Polymers*, *105*, 145–151. https://doi.org/10.1016/j.carbpol.2014.01.061

Han, P., Sun, Y., Wu, Y., Yuan, J., Dai, J., & Jia, S. (2014b). Emulsifying, flocculating, and physicochemical properties of exopolysaccharide produced by cyanobacterium *Nostoc flagelliforme*. *Applied Biochemistry and Biotechnology*, *172*(1), 36–49. https://doi.org/10.1007/s12010-013-0505-7

Hay, I. D., Rehman, Z. U., Moradali, M. F., Wang, Y., & Rehm, B. H. A. (2013). Microbial alginate production, modification and its applications. *Microbial Biotechnology*, *6*(6), 637–650. https://doi.org/10.1111/1751-7915.12076

Hayakawa, Y., Hayashi, T., Lee, J. B., Ozawa, T., & Sakuragawa, N. (2000). Activation of heparin cofactor II by calcium spirulan. *Journal of Biological Chemistry*, *275*(15), 11379–11382. https://doi.org/10.1074/jbc.275.15.11379

He, Q., Tang, Q. Y., Sun, Y. F., Zhou, M., Gärtner, W., & Zhao, K. H. (2018). Chromophorylation of cyanobacteriochrome Slr1393 from *Synechocystis* sp. PCC 6803 is regulated by protein Slr2111 through allosteric interaction. *Journal of Biological Chemistry*, *293*(46), 17705–17715. https://doi.org/10.1074/jbc.RA118.003830

Houot, L., Floutier, M., Marteyn, B., Michaut, M., Picciocchi, A., Legrain, P., Aude, J. C., Cassier-Chauvat, C., & Chauvat, F. (2007). Cadmium triggers an integrated

reprogramming of the metabolism of *Synechocystis* PCC6803, under the control of the Slr1738 regulator. *BMC Genomics*, *8*, 1–16. https://doi.org/10.1186/1471-2164-8-350

Hu, Y., Winter, V., Chen, X. Y., & Gänzle, M. G. (2017). Effect of acceptor carbohydrates on oligosaccharide and polysaccharide synthesis by dextransucrase DsrM from *Weissella cibaria*. *Food Research International*, *99*(June), 603–611. https://doi.org/10.1016/j.foodres.2017.06.026

Hudson, E.P. (2021). Synthetic biology in cyanobacteria and applications for biotechnology. In J. Nielsen, S. Lee, G. Stephanopoulos and P. Hudson (Eds.). *Cyanobacteria Biotechnology* (1st ed.). Hoboken, NJ: Wiley Online Library. https://doi.org/10.1002/9783527824908.ch5

Islam, S. T., & Lam, J. S. (2014). Synthesis of bacterial polysaccharides via the Wzx/Wzy-dependent pathway. *Canadian Journal of Microbiology*, *60*(11), 697–716. https://doi.org/10.1139/cjm-2014-0595

Jittawuttipoka, T., Planchon, M., Spalla, O., Benzerara, K., Guyot, F., Cassier-Chauvat, C., & Chauvat, F. (2013). Multidisciplinary evidences that *Synechocystis* PCC6803 exopolysaccharides operate in cell sedimentation and protection against salt and metal stresses. *PLoS ONE*, *8*(2). https://doi.org/10.1371/journal.pone.0055564

Kanekiyo, K., Hayashi, K., Takenaka, H., Lee, J. B., & Hayashi, T. (2007). Anti-herpes simplex virus target of an acidic polysaccharide, nostoflan, from the edible blue-green algae *Nostoc flagelliforme*. *Biological and Pharmaceutical Bulletin*, *30*(8), 1573–1575. https://doi.org/10.1248/bpb.30.1573

Kanekiyo, K., Lee, J.-B., Hayashi, K., Takenaka, H., Hayakawa, Y., Endo, S., & Hayashi, T. (2005). Isolation of an antiviral polysaccharide, nostoflan, from a terrestrial cyanobacterium, *Nostoc flagelliforme*. *Journal of Natural Products*, *68*(7), 1037–1041. https://doi.org/10.1021/np050056c

Kaneko, T., Sato, S., Kotani, H., Tanaka, A., Asamizu, E., Nakamura, Y., Miyajima, N., Hirosawa, M., Sugiura, M., Sasamoto, S., Kimura, T., Hosouchi, T., Matsuno, A., Muraki, A., Nakazaki, N., Naruo, K., Okumura, S., Shimpo, S., Takeuchi, C., Wada, T., Watanabe, A., Yamada, M., Yasuda, M. & Tabata, S. (1996). Sequence analysis of the genome of the unicellular cyanobacterium *Synechocystis* sp. strain PCC6803. II. Sequence determination of the entire genome and assignment of potential protein-coding regions. *DNA Research*, *3*(3), 109–136. https://doi.org/10.1093/dnares/3.3.109

Kasting, J. F., & Siefert, J. L. (2002). Life and the evolution of Earth's atmosphere. *Science*, *296*(5570), 1066–1068. https://doi.org/10.1126/science.1071184

Katayama, N., Iijima, H., & Osanai, T. (2018). Production of bioplastic compounds by genetically manipulated and metabolic engineered cyanobacteria. In W. Zhang and X. Song (Eds.). *Synthetic Biology of Cyanobacteria*. Singapore: Springer. https://doi.org/10.1007/978-981-13-0854-3_7

Kehr, J. C., & Dittmann, E. (2015). Biosynthesis and function of extracellular glycans in cyanobacteria. *Life*, *5*(1), 164–180. https://doi.org/10.3390/life5010164

Khattar, J. I. S., Singh, D. P., Jindal, N., Kaur, N., Singh, Y., Rahi, P., & Gulati, A. (2010). Isolation and characterization of exopolysaccharides produced by the cyanobacterium *Limnothrix redekei* PUPCCC 116. *Applied Biochemistry and Biotechnology*, *162*(5), 1327–1338. https://doi.org/10.1007/s12010-010-8922-3

Khayatan, B., Meeks, J. C., & Risser, D. D. (2015). Evidence that a modified type IV pilus-like system powers gliding motility and polysaccharide secretion in filamentous cyanobacteria. *Molecular Microbiology*, *98*(6), 1021–1036. https://doi.org/10.1111/mmi.13205

Knoll, A. H. (2008). Cyanobacteria and Earth history. In H. Antonia and F. Enrique (Eds.). *The Cyanobacteria: Molecular Biology, Genomics and Evolution*. Rover, UK: Caister Academic Press. https://doi.org/10.21775/9781913652531

Knoot, C. J., Ungerer, J., Wangikar, P. P., & Pakrasi, H. B. (2018). Cyanobacteria: Promising biocatalysts for sustainable chemical production. *The Journal of Biological Chemistry*, *293*(14), 5044–5052. https://doi.org/10.1074/jbc.R117.815886

Koch, M., Berendzen, K. W., & Forchhammer, A. K. (2020). On the role and production of polyhydroxybutyrate (PHB) in the cyanobacterium *Synechocystis* sp. PCC 6803. *Life*, *10*(4). https://doi.org/10.3390/life10040047

Koch, M., Doello, S., Gutekunst, K., & Forchhammer, K. (2019). PHB is produced from glycogen turn-over during nitrogen starvation in *Synechocystis* sp. PCC 6803. *International Journal of Molecular Sciences*, *20*(8), 1942. https://doi.org/10.3390/ijms20081942

Komárek, J. (2016). A polyphasic approach for the taxonomy of cyanobacteria: principles and applications. *European Journal of Phycology*, *51*(3), 346–353. https://doi.org/10.1080/09670262.2016.1163738

Lama, L., Nicolaus, B., Calandrelli, V., Manca, M. C., Romano, I., & Gambacorta, A. (1996). Effect of growth conditions on endo- and exopolymer biosynthesis in *Anabaena cylindrica* 10 C. *Phytochemistry*, *42*(3), 655–659. https://doi.org/10.1016/0031-9422(95)00985-X

Leemhuis, H., Pijning, T., Dobruchowska, J. M., van Leeuwen, S. S., Kralj, S., Dijkstra, B. W., & Dijkhuizen, L. (2013). Glucansucrases: Three-dimensional structures, reactions, mechanism, α-glucan analysis and their implications in biotechnology and food applications. *Journal of Biotechnology*, *163*(2), 250–272. https://doi.org/10.1016/j.jbiotec.2012.06.037

Leite, J. P., Mota, R., Durão, J., Neves, S. C., Barrias, C. C., Tamagnini, P., & Gales, L. (2017). Cyanobacterium-derived extracellular carbohydrate polymer for the controlled delivery of functional proteins. *Macromolecular Bioscience*, *17*(2). https://doi.org/10.1002/mabi.201600206

Li, H., Su, L., Chen, S., Zhao, L., Wang, H., Ding, F., Chen, H., Shi, R., Wang, Y., & Huang, Z. (2018). Physicochemical characterization and functional analysis of the polysaccharide from the edible microalga *Nostoc sphaeroides*. *23*(2). https://doi.org/10.3390/molecules23020508

Li, P., Liu, Z., & Xu, R. (2001). Chemical characterisation of the released polysaccharide from the cyanobacterium *Aphanothece halophytica* GR02. *Journal of Applied Phycology*, *13*(1), 71–77. https://doi.org/10.1023/A:1008109501066

Liu, D., & Pakrasi, H. B. (2018). Exploring native genetic elements as plug-in tools for synthetic biology in the cyanobacterium *Synechocystis* sp. PCC 6803. *Microbial Cell Factories*, *17*(1), 48. https://doi.org/10.1186/s12934-018-0897-8

Liu, Z., Jiao, Y., Wang, Y., Zhou, C., & Zhang, Z. (2008). Polysaccharides-based nanoparticles as drug delivery systems. *Advanced Drug Delivery Reviews*, *60*(15), 1650–1662. https://doi.org/10.1016/j.addr.2008.09.001

Low, K. E., & Howell, P. L. (2018). Gram-negative synthase-dependent exopolysaccharide biosynthetic machines. *Current Opinion in Structural Biology*, *53*, 32–44. https://doi.org/10.1016/j.sbi.2018.05.001

Luan, G., & Lu, X. (2018). Tailoring cyanobacterial cell factory for improved industrial properties. *Biotechnology Advances*, *36*(2), 430–442. https://doi.org/10.1016/j.biotechadv.2018.01.005

Maeda, K., Okuda, Y., Enomoto, G., Watanabe, S., & Ikeuchi, M. (2021). Biosynthesis of a sulphated exopolysaccharide, synechan, and bloom formation in the model cyanobacterium *Synechocystis* sp. strain PCC 6803*. eLife, 10:* e66538*.* https://doi.org/10.7554/eLife.66538

Maréchal, E. (2018). Primary endosymbiosis: Emergence of the primary chloroplast and the chromatophore, two independent events. *Methods in Molecular Biology*, 1829, 3–16. https://doi.org/10.1007/978-1-4939-8654-5_1

Margulis, L. (1970). Origin of eukaryotic cells: evidence and research implications for a theory of the origin and evolution of microbial, plant, and animal cells on the Precambrian earth. New Haven: Yale University Press.

McFadden, G. I. (2014). Origin and evolution of plastids and photosynthesis in eukaryotes. *Cold Spring Harbor Perspectives in Biology*, *6*(4), a016105–a016105. https://doi.org/10.1101/cshperspect.a016105

Moreno, J., Vargas, M. A., Olivares, H., Rivas, J., & Guerrero, M. G. (1998). Exopolysaccharide production by the cyanobacterium *Anabaena* sp. ATCC 33047 in batch and continuous culture. *Journal of Biotechnology*, *60*(3), 175–182. https://doi.org/10.1016/S0168-1656(98)00003-0

Morone, J., Alfeus, A., Vasconcelos, V., & Martins, R. (2019). Revealing the potential of cyanobacteria in cosmetics and cosmeceuticals — A new bioactive approach. *Algal Research*, *41*, 101541. https://doi.org/10.1016/j.algal.2019.101541

Mota, R., Rossi, F., Andrenelli, L., Pereira, S. B., De Philippis, R., & Tamagnini, P. (2016). Released polysaccharides (RPS) from *Cyanothece* sp. CCY 0110 as biosorbent for heavy metals bioremediation: interactions between metals and RPS binding sites. *Applied Microbiology and Biotechnology*, *100*(17), 7765–7775. https://doi.org/10.1007/s00253-016-7602-9

Mota, R., Vidal, R., Pandeirada, C., Flores, C., Adessi, A., De Philippis, R., Nunes, C., Coimbra, M. A., & Tamagnini, P. (2020). Cyanoflan: A cyanobacterial sulfated carbohydrate polymer with emulsifying properties. *Carbohydrate Polymers*, *229*, 115525. https://doi.org/10.1016/j.carbpol.2019.115525

Mukhopadhyay, A., & Kennelly, P. J. (2011). A low molecular weight protein tyrosine phosphatase from *Synechocystis* sp. strain PCC 6803: enzymatic characterization and identification of its potential substrates. *The Journal of Biochemistry*, *149*(5), 551–562. https://doi.org/10.1093/jb/mvr014

Nichols, C. A. M., Guezennec, J., & Bowman, J. P. (2005). Bacterial exopolysaccharides from extreme marine environments with special consideration of the southern ocean,

sea ice, and deep-sea hydrothermal vents: A review. *Marine Biotechnology*, *7*(4), 253–271. https://doi.org/10.1007/s10126-004-5118-2

Nicolaus, B., Panico, A., Lama, L., Romano, I., Manca, M. C., De Giulio, A., & Gambacorta, A. (1999). Chemical composition and production of exopolysaccharides from representative members of heterocystous and non-heterocystous cyanobacteria. *Phytochemistry*, *52*(4), 639–647. https://doi.org/10.1016/S0031-9422(99)00202-2

Obadia, B., Lacour, S., Doublet, P., Baubichon-Cortay, H., Cozzone, A. J., & Grangeasse, C. (2007). Influence of tyrosine-kinase Wzc activity on colanic acid production in *Escherichia coli* K12 cells. *Journal of Molecular Biology*, *367*(1), 42–53. https://doi.org/10.1016/j.jmb.2006.12.048

Ochoa de Alda, J. A. G., Esteban, R., Diago, M. L., & Houmard, J. (2014). The plastid ancestor originated among one of the major cyanobacterial lineages. *Nature Communications*, *5*(1), 4937. https://doi.org/10.1038/ncomms5937

Okajima, M. K., Bamba, T., Kaneso, Y., Hirata, K., Fukusaki, E., Kajiyama, S., & Kaneko, T. (2008). Supergiant ampholytic sugar chains with imbalanced charge ratio form saline ultra-absorbent hydrogels. *Macromolecules*, *41*(12), 4061–4064. https://doi.org/10.1021/ma800307w

Okajima, M. K., Sornkamnerd, S., & Kaneko, T. (2018). Development of functional bionanocomposites using cyanobacterial polysaccharides. *Chemical Record*, *18*(7), 1167–1177. https://doi.org/10.1002/tcr.201700074

Oliver, J. W. K., & Atsumi, S. (2015). A carbon sink pathway increases carbon productivity in cyanobacteria. *Metabolic Engineering*, *29*, 106–112. https://doi.org/10.1016/j.ymben.2015.03.006

Orthwein, T., Scholl, J., Spät, P., Lucius, S., Koch, M., Macek, B., Hagemann, M., & Forchhammer, K. (2021). The novel PII-interactor PirC identifies phosphoglycerate mutase as key control point of carbon storage metabolism in cyanobacteria. *Proceedings of the National Academy of Sciences*, *118*(6), e2019988118. https://doi.org/10.1073/pnas.2019988118

Osanai, T., Kanesaki, Y., Nakano, T., Takahashi, H., Asayama, M., Shirai, M., Kanehisa, M., Suzuki, I., Murata, N., & Tanaka, K. (2005). Positive regulation of sugar catabolic pathways in the cyanobacterium *Synechocystis* sp. PCC 6803 by the group 2 σ factor SigE. *Journal of Biological Chemistry*, *280*(35), 30653–30659. https://doi.org/10.1074/jbc.M505043200

Otero, A., & Vincenzini, M. (2003). Extracellular polysaccharide synthesis by *Nostoc* strains as affected by N source and light intensity. *Journal of Biotechnology*, *102*(2), 143–152. https://doi.org/10.1016/S0168-1656(03)00022-1

Otero, A., & Vincenzini, M. (2004). *Nostoc* (Cyanophyceae) goes nude: extracellular polysaccharides serve as a sink for reducing power under unbalanced C/N metabolism. *Journal of Phycology*, *40*(1), 74–81. https://doi.org/10.1111/j.0022-3646.2003.03-067.x

Ou, Y., Xu, S., Zhu, D., & Yang, X. (2014). Molecular mechanisms of exopolysaccharide from *Aphanothece halaphytica* (EPSAH) induced apoptosis in HeLa cells. *PLoS ONE*, *9*(1), e87223.

Ozturk, S., & Aslim, B. (2010). Modification of exopolysaccharide composition and production by three cyanobacterial isolates under salt stress. *Environmental Science and Pollution Research*, *17*(3), 595–602. https://doi.org/10.1007/s11356-009-0233-2

Paiment, A., Hocking, J., & Whitfield, C. (2002). Impact of phosphorylation of specific residues in the tyrosine autokinase, Wzc, on its activity in assembly of group 1 capsules in *Escherichia coli*. *Journal of Bacteriology*, *184*(23), 6437–6447. https://doi.org/10.1128/JB.184.23.6437-6447.2002

Patel, S., & Goyal, A. (2013). Current and prospective insights on food and pharmaceutical applications of spirulina. *Current Trends in Biotechnology and Pharmacy*, *7*(2), 681–695.

Pengelly, J. J. L. (2008) Molecular characterisation of membrane transporters associated with saxitoxin biosynthesis in cyanobacteria (Doctoral thesis, University of New South Wales, Australia). Retrieved from http://unsworks.unsw.edu.au/fapi/datastream/unsworks:4309/SOURCE1?view=true

Pereira, S. B., Mota, R., Vieira, C. P., Vieira, J., & Tamagnini, P. (2015). Phylum-wide analysis of genes/proteins related to the last steps of assembly and export of extracellular polymeric substances (EPS) in cyanobacteria. *Scientific Reports*, *5*(July), 1–16. https://doi.org/10.1038/srep14835

Pereira, S., Micheletti, E., Zille, A., Santos, A., Moradas-Ferreira, P., Tamagnini, P., & De Philippis, R. (2011). Using extracellular polymeric substances (EPS)-producing cyanobacteria for the bioremediation of heavy metals: do cations compete for the EPS functional groups and also accumulate inside the cell?. *Microbiology*, *157*(2), 451–458. https://doi.org/10.1099/mic.0.041038-0

Pereira, S., Zille, A., Micheletti, E., Moradas-Ferreira, P., De Philippis, R., & Tamagnini, P. (2009). Complexity of cyanobacterial exopolysaccharides: Composition, structures, inducing factors and putative genes involved in their biosynthesis and assembly. *FEMS Microbiology Reviews*, *33*(5), 917–941. https://doi.org/10.1111/j.1574-6976.2009.00183.x

Planchon, M., Jittawuttipoka, T., Cassier-Chauvat, C., Guyot, F., Chauvat, F., & Spalla, O. (2013). Influence of exopolysaccharides on the electrophoretic properties of the model cyanobacterium *Synechocystis*. *Colloids and Surfaces B: Biointerfaces*, *110*, 171–177. https://doi.org/10.1016/j.colsurfb.2013.03.057

Pugh, N., Ross, S. A., ElSohly, H. N., ElSohly, M. A., & Pasco, D. S. (2001). Isolation of three high molecular weight polysaccharide preparations with potent immunostimulatory activity from *Spirulina platensis*, *Aphanizomenon flos-aquae* and *Chlorella pyrenoidosa*. *Planta Medica*, *67*(08), 737–742. https://doi.org/10.1055/s-2001-18358

Raven, J. A., Giordano, M., Beardall, J., & Maberly, S. C. (2012). Algal evolution in relation to atmospheric CO_2: carboxylases, carbon-concentrating mechanisms and carbon oxidation cycles. *Philosophical Transactions of the Royal Society of London. Series B, Biological Sciences*, *367*(1588), 493–507. https://doi.org/10.1098/rstb.2011.0212

Rehm, B. H. A. (2010). Bacterial polymers: Biosynthesis, modifications and applications. *Nature Reviews Microbiology*, *8*(8), 578–592. https://doi.org/10.1038/nrmicro2354

Rippka, R., Deruelles, J., & Waterbury, J. B. (1979). Generic assignments, strain histories and properties of pure cultures of cyanobacteria. *Journal of General Microbiology*, *111*(1), 1–61. https://doi.org/10.1099/00221287-111-1-1

Rossi, F., Mugnai, G., & De Philippis, R. (2018). Complex role of the polymeric matrix in biological soil crusts. *Plant and Soil*, *429*(1), 19–34. https://doi.org/10.1007/s11104-017-3441-4

Rossi, F., & Philippis, R. De. (2016). The Physiology of Microalgae. In M. A. Borowitzka, J. Beardall and J. A. Raven (Eds.). *The Physiology of Microalgae*. Switzerland: Springer International. https://doi.org/10.1007/978-3-319-24945-2

Sagan, L. (1967). On the origin of mitosing cells. *Journal of Theoretical Biology*, *14*(3), 225-IN6. https://doi.org/10.1016/0022-5193(67)90079-3

Saito, M. A. (2009). Biogeochemistry: Less nickel for more oxygen. *Nature*, *458*(7239), 714–715. https://doi.org/10.1038/458714a

Savage, D. F., Afonso, B., Chen, A. H., & Silver, P. A. (2010). Spatially ordered dynamics of the bacterial carbon fixation machinery. *Science*, *327*(5970), 1258–1261. https://doi.org/10.1126/science.1186090

Savakis, P., & Hellingwerf, K. J. (2015). Engineering cyanobacteria for direct biofuel production from CO_2. *Current Opinion in Biotechnology*, *33*, 8–14. https://doi.org/10.1016/j.copbio.2014.09.007

Schmid, J. (2018). Recent insights in microbial exopolysaccharide biosynthesis and engineering strategies. *Current Opinion in Biotechnology*, *53*, 130–136. https://doi.org/10.1016/j.copbio.2018.01.005

Schmid, J., Sieber, V., & Rehm, B. (2015). Bacterial exopolysaccharides: biosynthesis pathways and engineering strategies. *Frontiers in Microbiology*, *6*, 496. https://doi.org/10.3389/fmicb.2015.00496

Schopf, J. W. (2002). The fossil record: Tracing the roots of the cyanobacterial lineage. In B. A. Whitton and M. Potts (Eds.). *The Ecology of Cyanobacteria: Their Diversity in Time and Space* (pp. 13-35). Dordrecht: Springer. https://doi.org/10.1007/0-306-46855-7_2

Schwab, C., Walter, J., Tannock, G. W., Vogel, R. F., & Gänzle, M. G. (2007). Sucrose utilization and impact of sucrose on glycosyltransferase expression in *Lactobacillus reuteri*. *Systematic and Applied Microbiology*, *30*(6), 433–443. https://doi.org/10.1016/j.syapm.2007.03.007

Scott, M., McCollum, C., Vasil'ev, S., Crozier, C., Espie, G. S., Krol, M., Huner, N. P. A., & Bruce, D. (2006). Mechanism of the down regulation of photosynthesis by blue light in the cyanobacterium *Synechocystis* sp. PCC 6803. *Biochemistry*, *45*(29), 8952–8958. https://doi.org/10.1021/bi060767p

Seliktar, D. (2012). Designing cell-compatible hydrogels for biomedical applications. *Science*, *336*(6085), 1124–1128. https://doi.org/10.1126/science.1214804

Shah, V., Garg, N., & Madamwar, D. (1999). Exopolysaccharide production by a marine cyanobacterium *Cyanothece* sp. *Applied Biochemistry and Biotechnology*, *82*(2), 81–90. https://doi.org/10.1385/ABAB:82:2:81

Shibata, M., Katoh, H., Sonoda, M., Ohkawa, H., Shimoyama, M., Fukuzawa, H., Kaplan, A., & Ogawa, T. (2002). Genes essential to sodium-dependent bicarbonate transport in cyanobacteria: Function and phylogenetic analysis. *Journal of Biological Chemistry*, *277*(21), 18658–18664. https://doi.org/10.1074/jbc.M112468200

Singh, S., Kant, C., Yadav, R. K., Reddy, Y. P., & Abraham, G. (2019). Chapter 17 - Cyanobacterial exopolysaccharides: Composition, biosynthesis, and biotechnological applications. In A. K. Mishra, D. N. Tiwari, & A. N. B. T.-C. Rai (Eds.). Academic Press, pp. 347–358. https://doi.org/https://doi.org/10.1016/B978-0-12-814667-5.00017-9

Song, X., Diao, J., Yao, J., Cui, J., Sun, T., Chen, L., & Zhang, W. (2021). Engineering a central carbon metabolism pathway to increase the intracellular Acetyl-CoA pool in *Synechocystis* sp. PCC 6803 grown under photomixotrophic conditions. *ACS Synthetic Biology*, *10*(4), 836–846. https://doi.org/10.1021/acssynbio.0c00629

Soo, R. M., Hemp, J., Parks, D. H., Fischer, W. W., & Hugenholtz, P. (2017). On the origins of oxygenic photosynthesis and aerobic respiration in Cyanobacteria. *Science*, *355*(6332), 1436–1440. https://doi.org/10.1126/science.aal3794

Srikanth, R., Reddy, C. H. S. S. S., Siddartha, G., Ramaiah, M. J., & Uppuluri, K. B. (2015). Review on production, characterization and applications of microbial levan. *Carbohydrate Polymers*, *120*, 102–114. https://doi.org/10.1016/j.carbpol.2014.12.003

Standish, A. J., & Morona, R. (2014). The role of bacterial protein tyrosine phosphatases in the regulation of the biosynthesis of secreted polysaccharides. *Antioxidants and Redox Signaling*, *20*(14), 2274–2289. https://doi.org/10.1089/ars.2013.5726

Su, C., Chi, Z., & Lu, W. (2007). Optimization of medium and cultivation conditions for enhanced exopolysaccharide yield by marine *Cyanothece* sp. 113. *Chinese Journal of Oceanology and Limnology*, *25*(4), 411–417. https://doi.org/10.1007/s00343-007-0411-3

Su, J., Jia, S., Chen, X., & Yu, H. (2008). Morphology, cell growth, and polysaccharide production of *Nostoc flagelliforme* in liquid suspension culture at different agitation rates. *Journal of Applied Phycology*, *20*(3), 213–217. https://doi.org/10.1007/s10811-007-9221-4

Sutherland, I. W. (2001). Biofilm exopolysaccharides: A strong and sticky framework. *Microbiology*, *147*(1), 3–9. https://doi.org/10.1099/00221287-147-1-3

Thiel, K., Patrikainen, P., Nagy, C., Fitzpatrick, D., Pope, N., Aro, E.-M., & Kallio, P. (2019). Redirecting photosynthetic electron flux in the cyanobacterium *Synechocystis* sp. PCC 6803 by the deletion of flavodiiron protein Flv3. *Microbial Cell Factories*, *18*(1), 189. https://doi.org/10.1186/s12934-019-1238-2

Thiel, K., Vuorio, E., Aro, E.-M., & Kallio, P. T. (2017). The effect of enhanced acetate influx on *Synechocystis* sp. PCC 6803 metabolism. *Microbial Cell Factories*, *16*(1), 21. https://doi.org/10.1186/s12934-017-0640-x

Trabelsi, L., Ben Ouada, H., Bacha, H., & Ghoul, M. (2009). Combined effect of temperature and light intensity on growth and extracellular polymeric substance production by the cyanobacterium *Arthrospira platensis*. *Journal of Applied Phycology*, *21*(4), 405–412. https://doi.org/10.1007/s10811-008-9383-8

van der Woude, A. D., Angermayr, S. A., Puthan Veetil, V., Osnato, A., & Hellingwerf, K. J. (2014). Carbon sink removal: Increased photosynthetic production of lactic acid by

Synechocystis sp. PCC 6803 in a glycogen storage mutant. *Journal of Biotechnology*, *184*, 100–102. https://doi.org/10.1016/j.jbiotec.2014.04.029

Vasudevan, R., Gale, G. A. R., Schiavon, A. A., Puzorjov, A., Malin, J., Gillespie, M. D., Vavitsas, K., Zulkower, V., Wang, B., Howe, C. J., Lea-Smith, D. J., & McCormick, A. J. (2019). CyanoGate: A modular cloning suite for engineering cyanobacteria based on the plant MoClo Syntax. *Plant Physiology*, *180*(1), 39–55. https://doi.org/10.1104/pp.18.01401

Vavitsas, K., Crozet, P., Vinde, M. H., Davies, F., Lemaire, S. D., & Vickers, C. E. (2019). The synthetic biology toolkit for photosynthetic microorganisms. *Plant Physiology*, *181*(1), 14–27. https://doi.org/10.1104/pp.19.00345

Vavitsas, K., Kugler, A., Satta, A., Hatzinikolaou, D.G., Lindblad, P., Fewer, D.P., Lindberg, P., Toivari, M. & Stensjö, K. (2021). Doing synthetic biology with photosynthetic microorganisms. *Physiologia Plantarum*, Accepted Author Manuscript. https://doi.org/10.1111/ppl.13455

Vijay, D., Akhtar, M. K., & Hess, W. R. (2019). Genetic and metabolic advances in the engineering of cyanobacteria. *Current Opinion in Biotechnology*, *59*(August), 150–156. https://doi.org/10.1016/j.copbio.2019.05.012

Wendt, K. E., Ungerer, J., Cobb, R. E., Zhao, H., & Pakrasi, H. B. (2016). CRISPR/Cas9 mediated targeted mutagenesis of the fast growing cyanobacterium *Synechococcus elongatus* UTEX 2973. *Microbial Cell Factories*, *15*(1), 115. https://doi.org/10.1186/s12934-016-0514-7

Whitfield, C. (2006). Biosynthesis and assembly of capsular polysaccharides in *Escherichia coli*. *Annual Review of Biochemistry*, *75*, 39–68. https://doi.org/10.1146/annurev.biochem.75.103004.142545

Whitfield, C., & Stephen Trent, M. (2014). Biosynthesis and export of bacterial lipopolysaccharides. *Annual Review of Biochemistry*, *83*, 99–128. https://doi.org/10.1146/annurev-biochem-060713-035600

Whitfield, C., Wear, S. S., & Sande, C. (2020). Assembly of bacterial capsular polysaccharides and exopolysaccharides. *Annual Review of Microbiology*, *74*(1), 521–543. https://doi.org/10.1146/annurev-micro-011420-075607

Whitney, J. C., & Howell, P. L. (2013). Synthase-dependent exopolysaccharide secretion in Gram-negative bacteria. *Trends in Microbiology*, *21*(2), 63–72. https://doi.org/10.1016/j.tim.2012.10.001

Whitton, B.A. (2012). Ecology of cyanobacteria: Their diversity in space and time. In B. A. Whitton (Ed.). *Ecology of Cyanobacteria II*. Netherlands: Springer. https://doi.org/10.1007/978-94-007-3855-3

Wilde, A., & Mullineaux, C. W. (2015). Motility in cyanobacteria: Polysaccharide tracks and Type IV pilus motors. *Molecular Microbiology*, *98*(6), 998–1001. https://doi.org/10.1111/mmi.13242

Woese, C. R. (1987). Bacterial evolution. *Microbiological Reviews*, *51*(2), 221–271.

Xiong, W., Cano, M., Wang, B., Douchi, D., & Yu, J. (2017). The plasticity of cyanobacterial carbon metabolism. *Current Opinion in Chemical Biology*, *41*, 12–19. https://doi.org/10.1016/j.cbpa.2017.09.004

Xu, H., Jiang, H., Yu, G., & Yang, L. (2014). Towards understanding the role of extracellular polymeric substances in cyanobacterial *Microcystis* aggregation and mucilaginous bloom formation. *Chemosphere*, *117*(1), 815–822. https://doi.org/10.1016/j.chemosphere.2014.10.061

Xu, L., & Zhang, J. (2016). Bacterial glucans: production, properties, and applications. *Applied Microbiology and Biotechnology*, *100*(21), 9023–9036. https://doi.org/10.1007/s00253-016-7836-6

Yao, L., Cengic, I., Anfelt, J., & Hudson, E. P. (2016). Multiple gene repression in cyanobacteria using CRISPRi. *ACS synthetic biology,* *5*(3), 207–212. https://doi.org/10.1021/acssynbio.5b00264

Yoshimura, H., Kotake, T., Aohara, T., Tsumuraya, Y., Ikeuchi, M., & Ohmori, M. (2012). The role of extracellular polysaccharides produced by the terrestrial cyanobacterium *Nostoc* sp. strain HK-01 in NaCl tolerance. *Journal of Applied Phycology*, *24*(2), 237–243. https://doi.org/10.1007/s10811-011-9672-5

Yoshimura, H., Okamoto, S., Tsumuraya, Y., & Ohmori, M. (2007). Group 3 sigma factor gene, *sigJ*, a key regulator of desiccation tolerance, regulates the synthesis of extracellular polysaccharide in cyanobacterium *Anabaena* sp. strain PCC 7120. *DNA Research*, *14*(1), 13–24. https://doi.org/10.1093/dnares/dsm003

Yu, H., Jia, S., & Dai, Y. (2010). Accumulation of exopolysaccharides in liquid suspension culture of *Nostoc flagelliforme* cells. *Applied Biochemistry and Biotechnology*, *160*(2), 552–560. https://doi.org/10.1007/s12010-008-8428-4

Yu, J., Liberton, M., Cliften, P. F., Head, R. D., Jacobs, J. M., Smith, R. D., Koppenaal, D. W., Brand, J. J., & Pakrasi, H. B. (2015). *Synechococcus elongatus* UTEX 2973, a fast growing cyanobacterial chassis for biosynthesis using light and CO_2. *Scientific Reports*, *5*(1), 8132. https://doi.org/10.1038/srep08132

Yue, S. J., Jia, S. R., Yao, J., & Dai, Y. J. (2012). Nutritional analysis of the wild and liquid suspension cultured *Nostoc flagelliforme* and antitumor effects of the extracellular polysaccharides. *Advanced Materials Research*, 345, 177–182. https://doi.org/10.4028/www.scientific.net/AMR.345.177

Zeidan, A. A., Poulsen, V. K., Janzen, T., Buldo, P., Derkx, P. M. F., Øregaard, G., & Neves, A. R. (2017). Polysaccharide production by lactic acid bacteria: from genes to industrial applications. *FEMS Microbiology Reviews*, *41*(Supp_1), S168–S200. https://doi.org/10.1093/femsre/fux017

CHAPTER II

The role of the tyrosine kinase Wzc (Sll0923) and the phosphatase Wzb (Slr0328) in the production of extracellular polymeric substances (EPS) by *Synechocystis* PCC 6803

Work published in: Pereira, S.B.*, **SANTOS, M.***, Leite, J.P., Flores, C., Eisfeld, C., Büttel, Z., Mota, R., Rossi, F., De Philippis, R., Gales, L., Morais-Cabral, J.H. & Tamagnini, P. (2019). The role ofthe tyrosine kinase Wzc (Sll0923) and the phosphatase Wzb (Slr0328) in the production of extracellular polymeric substances (EPS) by *Synechocystis* PCC 6803. *Microbiologyopen* 8: e00753. https://doi.org/10.1002/mbo3.753.
*These authors contribute equally to this work

Received: 6 June 2018 | Revised: 21 September 2018 | Accepted: 22 September 2018

DOI: 10.1002/mbo3.753

ORIGINAL ARTICLE

WILEY MicrobiologyOpen Open Access

The role of the tyrosine kinase Wzc (Sll0923) and the phosphatase Wzb (Slr0328) in the production of extracellular polymeric substances (EPS) by *Synechocystis* PCC 6803

Sara B. Pereira[1,2*] | Marina Santos[1,2,3*] | José P. Leite[1,2,3] | Carlos Flores[1,2,3] | Carina Eisfeld[1,2] | Zsófia Büttel[2] | Rita Mota[1,2] | Federico Rossi[4] | Roberto De Philippis[4] | Luís Gales[1,2,3] | João H. Morais-Cabral[1,2] | Paula Tamagnini[1,2,5]

[1]i3S - Instituto de Investigação e Inovação em Saúde, Universidade do Porto, Porto, Portugal

[2]IBMC - Instituto de Biologia Molecular e Celular, Universidade do Porto, Porto, Portugal

[3]ICBAS – Instituto de Ciências Biomédicas Abel Salazar, Porto, Portugal

[4]Department of Agrifood Production and Environmental Sciences, University of Florence, Florence, Italy

[5]Faculdade de Ciências, Departamento de Biologia, Universidade do Porto, Porto, Portugal

Correspondence
Paula Tamagnini, i3S - Instituto de Investigação e Inovação em Saúde, Universidade do Porto, Porto, Portugal.
Email: pmtamagn@ibmc.up.pt

Present Address
Carina Eisfeld, Department of Water Management, Delft University of Technology, Delft, The Netherlands

Zsófia Büttel, Molecular Microbiology, Groningen Biomolecular Sciences and Biotechnology Institute, University of Groningen, Groningen, The Netherlands

Funding information
Norte Portugal Regional Operational Programme (NORTE 2020), Grant/Award Number: NORTE-01-0145-FEDER-000008 and NORTE-01-0145-FEDER-000012; FCT - Fundação para a Ciência e a Tecnologia/ Ministério da Ciência, Tecnologia e Ensino Superior, Grant/Award Number: PTDC/BIA-MIC/28779/2017, SFRH/BD/119920/2016, SFRH/BD/84914/2012 and SFRH/BD/99715/2014; FEDER - Fundo Europeu de Desenvolvimento Regional funds through the COMPETE 2020 - Operational Programme for Competitiveness and Internationalisation (POCI), Grant/Award Number: POCI-01-0145-FEDER-007274

Abstract

Many cyanobacteria produce extracellular polymeric substances (EPS) mainly composed of heteropolysaccharides with unique characteristics that make them suitable for biotechnological applications. However, manipulation/optimization of EPS biosynthesis/characteristics is hindered by a poor understanding of the production pathways and the differences between bacterial species. In this work, genes putatively related to different pathways of cyanobacterial EPS polymerization, assembly, and export were targeted for deletion or truncation in the unicellular *Synechocystis* sp. PCC 6803. No evident phenotypic changes were observed for some mutants in genes occurring in multiple copies in *Synechocystis* genome, namely Δ*wzy* (Δ*sll0737*), Δ*wzx* (Δ*sll5049*), Δ*kpsM* (Δ*slr2107*), and Δ*kpsM*Δ*wzy* (Δ*slr2107*Δ*sll0737*), strongly suggesting functional redundancy. In contrast, Δ*wzc* (Δ*sll0923*) and Δ*wzb* (Δ*slr0328*) influenced both the amount and composition of the EPS, establishing that Wzc participates in the production of capsular (CPS) and released (RPS) polysaccharides, and Wzb affects RPS production. The structure of Wzb was solved (2.28 Å), revealing structural differences relative to other phosphatases involved in EPS production and suggesting a different substrate recognition mechanism. In addition, Wzc showed the ATPase and autokinase activities typical of bacterial tyrosine kinases. Most importantly, Wzb was able to dephosphorylate Wzc in vitro, suggesting that tyrosine phosphorylation/dephosphorylation plays a role in cyanobacterial EPS production.

KEYWORDS
cyanobacteria, extracellular polymeric substances, *Synechocystis*, Wzb, Wzc

[a]These authors contributed equally to this work.

1 | INTRODUCTION

Polysaccharide-based biopolymers can provide a diverse and powerful platform to deliver a wide range of biological and functional properties to the industrial toolbox. However, and despite the overwhelming diversity of polymers synthesized by microorganisms, bacterial polysaccharides are still underrepresented in the market (Roca, Alves, Freitas, & Reis, 2015). Most cyanobacterial strains produce extracellular polymeric substances (EPS), mainly composed of heteropolysaccharides that can remain attached to the cell surface (CPS—capsular polysaccharides) or be released into the environment (RPS—released polysaccharides) (Pereira et al., 2009; Rossi & De Philippis, 2016). The distinctive features of the cyanobacterial EPS, including their strong anionic nature, presence of sulfate groups, high variety of possible structural conformations, and amphiphilic behavior, make these polymers suitable for biotechnological and biomedical applications such as flocculating, gelifying, emulsifying, or suspending agents, rheology modifiers, therapeutic or drug delivery agents (Leite et al., 2017; Pereira et al., 2009). The faster growth and easier genetic manipulation of cyanobacteria compared to algae and plants, and the low-cost biomass production (owing to their photosynthetic metabolism) are additional competitive advantages for the implementation of cyanobacteria as cost-effective cell factories for the production of these biopolymers. For this purpose, a deeper knowledge on the cyanobacterial EPS biosynthetic pathways is required to optimize the production and engineer structural and compositional variants tailored for a given application.

The mechanisms involved in EPS production seem to be relatively conserved throughout bacteria, with the polymerization, assembly, and export of the polymers usually following one of three main mechanisms, namely the Wzy-, ABC transporter-, or synthase-dependent pathways (Schmid, Sieber, & Rehm, 2015). However, in a phylum-wide analysis, we showed that most cyanobacteria harbor gene-encoding proteins related to the three pathways but often not the complete set defining a single pathway (Pereira, Mota, Vieira, Vieira, & Tamagnini, 2015), implying a more complex scenario than that observed for other bacteria. This complexity is also evident in the physical organization of the genes, with multiple copies scattered throughout the genomes, either isolated or in small clusters (Pereira et al., 2015, 2009). In particular, this analysis revealed that *Synechocystis* sp. PCC 6803 (hereafter *Synechocystis*) possesses the genes related to the Wzy- and/or ABC transporter-dependent pathways, whereas those related to the synthase-dependent pathway are mostly absent (Pereira et al., 2015). Mutational analyses showed that the ORFs *slr0977*, *slr0982*, *sll0574*, and *sll0575* putatively encoding ABC transporter components (TCDB: 3.A.1.103.5) operate in *Synechocystis*' EPS production (Fisher, Allen, Luo, & Curtiss, 2013). Likewise, *sll0923* and *sll1581*, encoding homologs of the polysaccharide copolymerase (PCP) Wzc (TCDB: 8.A.3) and outer membrane polysaccharide export (OPX) Wza (TCDB: 1.B.18) of the Wzy-dependent pathway, were also shown to be involved (Jittawuttipoka et al., 2013).

In bacteria, Wzc and Wza form a complex that spans the periplasmic space and promotes the export of EPS polymer. Wzc undergoes a phospholyation/dephosphorylation cycle that affects its oligomerization state and is dependent on the phosphatase activity of another protein, Wzb (Cuthbertson, Mainprize, Naismith, & Whitfield, 2009). The *Synechocystis*' Wzc homolog, Sll0923, possesses a C-terminal cytoplasmic domain harboring the Walker A, A', and B ATP-binding motifs and Y-rich region present in other Wzc proteins and characteristic of bacterial tyrosine kinases (BY-kinases) (Mijakovic, Grangeasse, & Turgay, 2016; Morona, Purins, Tocilj, Matte, & Cygler, 2009; Pereira et al., 2015; Pereira, Mota, Santos, Philippis, & Tamagnini, 2013; Standish & Morona, 2014). In addition, Sll0328 was identified as a low molecular weight protein tyrosine phosphatase (LMW-PTP; EC: 3.1.3.48) (Mukhopadhyay & Kennelly, 2011) and Wzb homolog. Altogether, this raises the possibility that EPS production is at least partially controlled by a tyrosine phosphoregulatory mechanism, similar to that observed in other organisms (Grangeasse, Cozzone, Deutscher, & Mijakovic, 2007; Mijakovic et al., 2016; Standish & Morona, 2014).

In this work, aiming at elucidating the process of EPS production in cyanobacteria, we generated an array of *Synechocystis*' mutants and characterized them in terms of growth, amount of EPS produced, and polymer composition. The results obtained demonstrate that Wzc (Sll0923) and Wzb (Sll0328) are involved in the production of EPS, influencing both the amount and the composition of polymer(s). The absence of both Wzc and Wzb seems to redirect RPS production toward an alternative route. We clarified the roles of both proteins through biochemical and structural analysis, providing the first insights into the molecular mechanisms of EPS production in this cyanobacterium.

2 | MATERIALS AND METHODS

2.1 | Organisms and growth conditions

The cyanobacterium *Synechocystis* sp. PCC 6803 (Pasteur Culture Collection) and mutant strains (Supporting Information Table S1) were cultured in BG11 medium (Stanier, Kunisawa, Mandel, & Cohen-Bazire, 1971) at 30°C, under a 12-hr light (50 µmol photons m^{-1} s^{-2})/12-hr dark regime and orbital agitation (150 rpm). For solid medium, BG11 was supplemented with 1.5% agar noble (Difco), 0.3% sodium thiosulfate, and 10 mM TES-KOH buffer (pH 8.2). For the selection and maintenance of mutants, BG11 medium was supplemented with kanamycin (Km, up to 700 µg/ml), spectinomycin (Sm, up to 50 µg/ml), and/or chloramphenicol (Cm, up to 25 µg/ml). The *Escherichia coli* strains used were cultured at 37°C in LB medium (Bertani, 1951) supplemented with Amp (100 µg/ml), Km (25 µg/ml), and/or Cm (25 µg/ml).

2.2 | Cyanobacterial DNA extraction and recovery

Cyanobacterial genomic DNA was extracted using the Maxwell® 16 System (Promega) except to use in Southern blot, for which the phenol/chloroform method previously described (Tamagnini, Troshina, Oxelfelt, Salema, & Lindblad, 1997) was preferred. Agarose gel electrophoresis was performed by standard protocols (Sambrook & Russell, 2001), and the DNA fragments were isolated from gels, enzymatic, or PCR reactions using the NZYGelpure purification kit (NZYTech).

2.3 | Plasmid construction for *Synechocystis* transformation

Plasmid pDsll0923::Km^r was kindly provided by F. Chauvat (Jittawuttipoka et al., 2013). The *Synechocystis* chromosomal regions flanking *wzy* (*sll0737*), *wzx* (*sll5049*), *kpsM* (*slr2107*), *wzb* (*slr0328*), or the last 78 bp of *wzc* (*sll0923*) were amplified by PCR using the specific oligonucleotide primers (Supporting Information Appendix S1 and Supporting Information Table S2). An overlapping region containing an *Xma*I restriction site was included in primers 5I and 3I for cloning purposes. For each gene, the purified PCR fragments were fused by "overlap-PCR" (Supporting Information Appendix S1). The resulting products were purified and cloned into the vector pGEM-T® Easy (Promega), originating pGDsll0737, pGDsll5049, pGDslr2107, pGDslr0328, and pGDsll0923$_{Trunc}$. A selection cassette containing the *nptII* gene (conferring resistance to neomycin and kanamycin) was amplified from pKm.1 using the primer pair Km.KmScFwd/KmRev (Pinto et al., 2015) (Supporting Information Appendix S1 and Supporting Information Table S2) and digested with *Xma*I (Thermo Scientific). Subsequently, the purified selection cassette was cloned in the *Xma*I restriction site of the plasmids using the T4 DNA ligase (Thermo Scientific) to form pGDsll0737.Km, pGDsll5049.Km, pGDslr2107.Km, pGDslr0328.Km, or pGDsll0923$_{Trunc}$.Km, respectively. The cassette containing the *aadA* gene (conferring resistance to streptomycin and spectinomycin) was obtained by digesting the plasmid pSEVA481 (Silva-Rocha et al., 2013) with *Psh*AI and *Swa*I, and the cassette was cloned in the *Xma*I/*Sma*I site of pGDslr0328 and pGDsll0727 to form plasmids pGDslr0328.Sm and pGDsll0727.Sm.

For mutants' complementation, the shuttle vector pSEVA351 (Silva-Rocha et al., 2013) was used. A fragment covering *wzc* and its native promoter (P$_{wzc}$) and RBS (−230 to +123, with +1 corresponding to transcriptional start site (Kopf et al., 2014)) was amplified using primer pair sll0923_compF1/sll0923_compR1 (Supporting Information Appendix S1 and Supporting Information Table S2). The purified product was cloned in pGEM-T® Easy after A-tailing and subsequently digested with *Xba*I and *Spe*I. The resultant DNA fragment was cloned into pSEVA351 previously digested with *Xba*I and *Spe*I, originating plasmid pS351sll0923. To obtain plasmid pS351sll0923$_{Trunc,}$ a similar procedure was used but the PCR was performed using primer pair sll0923_compF1/Sll0923.RTrunc (Supporting Information Appendix S1 and Supporting Information Table S2), and the digested fragment was cloned into the *Xba*I site of pSEVA351. Since *wzb* is part of a four gene operon (slr0326-slr0329) (Kopf et al., 2014), a different approach was used. The P$_{rnpB}$ promoter (Huang, Camsund, Lindblad, & Heidorn, 2010) was obtained by digesting the BioBrick vector pSB1C3 with *Xba*I and *Spe*I and subsequently cloned in pSEVA351 previously digested with the same enzymes, originating plasmid pS351P$_{rnpB}$. *wzb* was amplified using primer pair slr0328_compF/slr0328_compR, incorporating the synthetic RBS BBa_B0030 (Supporting Information Appendix S1 and Supporting Information Table S2). The purified product was cloned in pGEM-T® Easy after A-tailing, digested with *Xba*I and *Spe*I and subsequently cloned in the *Spe*I site of pS351P$_{rnpB}$ generating plasmid pS351slr0328.

All constructs were verified by sequencing (StabVida) before transformation of *Synechocystis*.

2.4 | Generation of *Synechocystis* mutants

Synechocystis was transformed with integrative plasmids using the procedure described previously (Williams, 1988). Briefly, *Synechocystis* cultures were grown until OD$_{730}$ around 0.5, cells were harvested by centrifugation and resuspended in one-tenth volume of BG11. One hundred microliter of cells were incubated with 6–20 μg/ml plasmid DNA for 5 hr before spread onto Immobilon™-NC membranes (0.45 μm pore size, Millipore) resting on solid BG11 plates at 30°C under continuous light. After 24 hr, the membranes were transferred to selective plates containing 10 μg/ml of kanamycin or 2.5 μg/ml of spectinomycin. Transformants were observed after 1–2 weeks. For complete segregation, colonies were grown at increasing antibiotic concentrations. Nonintegrative plasmids were transformed into *Synechocystis* by electroporation, as previously described (Chiaramonte, Giacometti, & Bergantino, 1999; Ludwig, Heimbucher, Gregor, Czerny, & Schmetterer, 2008). In this case, cells were washed with HEPES buffer, 1 mM pH 7.5. Afterwards, cells were resuspended in 1 ml HEPES and 60 μl were mixed with 1 μg of DNA and electroporated with a Bio-Rad Gene Pulser™, at a capacitor of 25 μF. The resistor used was 400 Ω for time constant of 9 ms with an electric field of 12 kV/cm. Immediately after the electric pulse, the cells were resuspended in 1 ml BG11 and spread onto the Immobilon™-NC membranes as described above. After 24 hr, the membranes were transferred to selective plates containing 10 μg/ml of chloramphenicol before grown at increasing antibiotic concentrations.

2.5 | Southern blots

Southern blots were performed using genomic DNA of the wild type and mutants digested with *Bam*HI (Δ*wzy* and Δ*kpsM*Δ*wzy*), *Eco*RI (Δ*kpsM* and Δ*kpsM*Δ*wzy*), *Ava*II (Δ*wzx*), *Nco*I (Δ*wzc*, *wzc*$_{Trunc}$ and Δ*wzc*Δ*wzb*), and/or *Mfe*I (Δ*wzb* and Δ*wzc*Δ*wzb*) (Thermo Scientific). The DNA fragments were separated by electrophoresis on a 1% agarose gel and blotted onto Amersham Hybond™-N membrane

(GE Healthcare). Probes were amplified by PCR and labeled using the primers indicated in Supporting Information Table S2 and DIG DNA labeling kit (Roche Diagnostics GmbH) according to the manufacturer's instructions. Hybridization was done overnight at 60°C (Δ*wzc*, and Δ*wzc*Δ*wzb*) or 65°C (Δ*wzy*, Δ*wzx*, Δ*kpsM*, Δ*kpsM*Δ*wzy*, Δ*wzb*, Δ*wzc*Δ*wzb*, and wzc_{Trunc}), and digoxigenin-labeled probes were detected by chemiluminescence using CPD-star (Roche Diagnostics GmbH) in a Chemi DocTM XRS+Imager (Bio-Rad).

2.6 | Transcription analysis

For RNA extraction, 100 ml of culture of *Synechocystis* sp. PCC 6803 wild type, Δ*wzy* (Δ*sll0737*), Δ*wzx* (Δ*sll5049*), or Δ*kpsM* (Δ*slr2107*) mutants (at $OD_{730nm} \approx 1$) were collected 6 hr into the light phase. RNA extraction, quantification, quality/integrity assessment were carried out as previously described (Pinto, Pacheco, Ferreira, Moradas-Ferreira, & Tamagnini, 2012). The absence of genomic DNA contamination was checked by PCR using primers for *rnpB* amplification and the following profile: 5 min at 95°C followed by 30 cycles of 30 s at 95°C, 30 s at 56°C, and 30 s at 72°C, and a final extension at 72°C for 7 min. After synthesis with random primers as described previously (Pinto et al., 2012), cDNAs were used as template in PCR amplifications with the oligonucleotide primers listed in Supporting Information Table S2. The PCR profile used was: 5 min at 95°C followed by 30 cycles of 40 s at 95°C, 40 s at 54°C, and 40 s at 72°C, and a final extension at 72°C for 7 min. A control PCR was performed for *rnpB* amplification as described above. Band intensities were estimated by ImageJ software (Schneider, Rasband, & Eliceiri, 2012).

2.7 | Growth measurements

Growth measurements were performed by monitoring the Optical Density (OD) at 730 nm (Anderson & McIntosh, 1991) using a Shimadzu UVmini-1240 (Shimadzu Corporation) and determining the chlorophyll *a* content as described previously (Meeks & Castenholz, 1971). Data were statistically analyzed as described below.

2.8 | Analysis of total carbohydrates, RPS and CPS

Total carbohydrates and RPS contents were determined as described previously (Mota et al., 2013). For the quantification of CPS, 5 ml of dialyzed cultures was centrifuged at 3,857 *g* for 15 min at room temperature, resuspended in water, and boiled for 15 min at 10°C to detach the CPS from the cells' surface. After new centrifugation as described above, CPS were quantified from the supernatants using the phenol-sulfuric acid method (Dubois, Gilles, Hamilton, Rebers, & Smith, 1956). Total carbohydrate, RPS, and CPS were expressed as mg per L of culture or normalized by optical density. Data were statistically analyzed as described below.

To determine the RPS' monosaccharidic composition, dialyzed cultures were centrifuged at 3,857 *g* for 10 min at room temperature to remove the cells and the supernatant was further centrifuged at 75,000 *g* for 1 hr 30 min at 15°C to remove LPS prior to lyophilization. 2–5 mg of isolated RPS was hydrolyzed with 1 ml of 2 M trifluoroacetic acid (TFA) at 120°C for 1 hr. Samples were analyzed by ion exchange chromatography using a Dionex ICS-2500 ion chromatograph with an ED50 pulsed amperometric detector using a gold working electrode (Dionex) and a Carbopac PA1 column (Dionex). The eluents used were (A) MilliQ-grade water, (B) 0.185 M sodium hydroxide solution, and (C) 0.488 M sodium acetate solution. The gradient consisted of a first stage with 84% solution A, 15% solution B, and 1% solution C (for 7 min); a second stage with 50% solution B and 50% solution C (for 9 min); and a final stage with 84% solution A, 15% solution B, and 1% solution C (for 14 min). The flow rate was 1 ml/min.

2.9 | LPS extraction and analysis

LPS extraction was performed according to (Simkovsky et al., 2012) with some modifications. Briefly, 25 ml of samples was collected by centrifugation at 3,857 *g* for 15 min at room temperature, washed once in BG11, and incubated on ice for 30 min in stripping buffer (sucrose 15% (w/v), Tris-HCl 50 mM, and Na_2EDTA 25 mM). After centrifugation at 3,802 *g* for 10 min at 4°C, the supernatant was transferred to a new tube and centrifuged at 16,170 *g* for 2 min at 4°C to remove minor cell contaminants. The supernatant was collected and centrifuged at 75,000 *g* for 90 min at 18°C. The pellet was resuspended in 100 µl of 10 mM Tris-HCl, pH 8.0. Protease digested LPS samples were analyzed in a 12% SDS-PAGE gel (Bio-Rad Laboratories) and stained using Pro-Q® Emerald 300 Lipopolysaccharide Gel Stain Kit (Molecular Probes, Inc.) according to the manufacturer's instructions.

2.10 | Transmission electron microscopy (TEM)

Cells were fixed before centrifugation and processed as described previously (Seabra, Santos, Pereira, Moradas-Ferreira, & Tamagnini, 2009), except that samples were embedded in EMBed-812 resin and sections were examined using a JEM-1400Plus (Jeol Ltd., Inc.). Negative staining was performed on cells mounted on formvar/carbon film-coated mesh nickel grids (Electron Microscopy Sciences) with 1% Ruthenium Red.

2.11 | Expression and purification of Wzb and Wzc

To overexpress N-terminal his-tagged Wzb (His6-Wzb, 18.9 kDa) and Wzc (His6-Wzc, 84.9 kDa), the genes were amplified from *Synechocystis* genomic DNA using the oligonucleotide pairs Ovslr0328F/Ovslr0328R or OvSll0923F/OvSll0923R, respectively (Supporting Information Table S2). The products obtained were digested with *Shp*I/*Pst*I or *Bam*HI/*Pst*I, respectively, and cloned into pQE-30 (QIAGEN). After confirming by sequencing (StabVida) that no mutations had been introduced, the constructs were introduced into M15 (pREP4) cells (QIAGEN). Transformed *E. coli* cells were grown in LB medium supplemented with 100 µg/ml of ampicillin

and 25 µg/ml of kanamycin, at 37°C, until an optical density at 600 nm of 0.6 for Wzb or 0.7–0.9 for Wzc. To express His6-Wzb, cells were induced for 1 hr at 37°C with 0.5 mM IPTG and lysed in a Branson sonifier 250 (Duty cycle 50%, output 5, 3 × 10 s) in Wzb lysis buffer (50 mM HEPES pH 8.0, 300 mM NaCl, 20 mM imidazole, 0.5% Triton X-100, 0.2 mg/ml lysozyme, 10 µg/ml DNase, 1 mM $MgCl_2$, and 1 mM phenylmethylsulfonyl fluoride—PMSF). After centrifugation at 35,000 *g* for 30 min at 4°C, His6-Wzb was purified using HisTrap affinity columns (GE Healthcare). Samples were loaded in Wzb-binding buffer (50 mM HEPES pH 8.0, 300 mM NaCl, 20 mM imidazole, 0.5% Triton X-100), and bound proteins were eluted using a step gradient in which imidazole increased up to 500 mM. Samples were concentrated and diafiltered with HEPES 50 mM pH 8.0 or further purified by size exclusion chromatography (SEC), using a Superpose12 10/300 column (GE healthcare) and Wzb SEC buffer (50 mM HEPES pH 8.0 and 100 mM NaCl). For His6-Wzc, cultures were subjected to a 30-min cold shock before induction with 0.5 mM IPTG and incubation at 20°C overnight. Cells were disrupted using a French Press (Thermo Electron Corporation) at 30 Kpsi in Wzc lysis buffer (50 mM HEPES pH 8.0, 100 mM NaCl, 0.2 mg/ml lysozyme, 10 µg/ml DNase, 1 mM $MgCl_2$, and 1 mM PMSF). After centrifugation at 30,000 *g* for 30 min at 4°C to remove cell debris, the membrane fraction was collected at 200,000 *g* for 1 hr 10 min at 4°C and resuspended in Wzc buffer A (50 mM HEPES pH 8.0, 100 mM NaCl). Triton X-100 was added to a final concentration of 10%, and samples were incubated for 1 hr at 4°C with orbital shaking to maximize protein solubilization. His6-Wzc was purified as described above, except that the composition of the Wzc binding buffer was 50 mM HEPES pH 8.0, 0.10 M NaCl, 20 mM imidazole, and 0.2% Triton X-100. Pooled fractions containing His6-Wzc were concentrated and dialyzed (Dialysis Membrane, 25 kDa MWCO,Spectra/Por) against buffer A supplemented with 1 mM *n*-Dodecyl-b-maltoside (DDM) ON at 4°C. Protein was further purified by SEC using a HiPrep 16/60 Sephacryl S-300 High Resolution column (GE healthcare) with Wzc SEC buffer (50 mM HEPES pH 8.0, 100 mM NaCl, 1 mM DDM, and 2.5% glycerol). The concentrations of the purified His-tagged protein solutions were determined by BCA colorimetric assay (Thermo Scientific) using bovine serum albumin as standard.

2.12 | Wzb phosphatase activity assay

The phosphatase activity of His6-Wzb was determined by continuously monitoring, at 405 nm, the formation of *p*-nitrophenol (pNP) from *p*-nitrophenyl phosphate (pNPP), at 30°C, in a Shimadzu UV-2401 PC (Shimadzu Corporation). 1 ml of reaction mixture contained 100 mM sodium citrate buffer, pH 6.5, 1 mM EDTA, 0.1% (vol/vol) β-mercaptoethanol, and 10 mM of pNPP. Reactions were initiated by adding 0.2 or 0.5 µg of purified His6-Wzb. The concentration of pNP formed was estimated using a molar extinction coefficient of 18,000 M^{-1} cm^{-1} (Ferreira et al., 2007; Preneta et al., 2002). Data were statistically analyzed as described below.

2.13 | Wzb crystallization, data collection, and processing

For the initial screening, His6-Wzb aliquots at 10 mg/ml were used. The screening was performed in 24-well sitting-drop vapor diffusion plates at 20°C with several commercially available kits. A single hit was obtained with MembFac (Hampton Research) condition #22. After optimization with solutions with varying pH and precipitant concentrations, the best diffracting crystals appeared between pH 6.2 and 7.0 and 1 M of ammonium sulfate. Crystals were subjected to a glycerol gradient up to 30% prior to being flash frozen in liquid nitrogen. A data set of a single diffracting crystal to 2.28 Å was determined at the ID23–2 beamline of the European Synchrotron Radiation Facility (λ = 0.873 Å; Grenoble, France). Diffraction images were processed with the XDS Program Package (Kabsch, 1993), and the diffraction intensities converted to structure factors in the CCP4 format (Bailey, 1994). A random 5% sample of the reflection data was flagged for R-free calculations (Brunger, 1992) during model building and refinement. A summary of the data collection and refinement statistics is presented in Table 2. Molecular replacement phases were generated with PhaserMR (McCoy et al., 2007), using as initial model the protein tyrosine phosphatase from *Entamoeba histolytica* (PDB entry 3IDO; (Linford et al., 2014)). The final models were obtained after further cycles of refinement and manual model building, carried out with PHENIX (Adams et al., 2010) and Coot (Emsley, Lohkamp, Scott, & Cowtan, 2010), respectively. Protein structure figures were generated with PyMol (Schrödinger, 2010).

2.14 | Phylogenetic analysis of Wzb

Synechocystis' Wzb sequence was used as query in blast searches against the PDB database (Jan 2017; https://www.rcsb.org/) (Berman et al., 2000) to retrieve homologs with 3D crystal structures available, using a significance cutoff of e-05. Sequences were aligned in MEGA6 (Tamura et al., 2013) using the ClustalW algorithm, and the phylogenetic tree was constructed in the same software by maximum likelihood, using the Jones-Taylor-Thornton (JTT) substitution model and a bootstrap of 500. A three-dimensional protein structure alignment was performed using representative LMW-PTP sequences from the eukaryote *E. histolytica* (PDB: 3ido; UniProt:C4LSE7), the Gram-negative bacteria *E. coli* (PDB: 2wja; UniProt:Q9X4B8) and the Gram-positive bacteria *Staphylococcus aureus* (PDB: 3rof; UniProt: P0C5D2), and the root mean square deviation (RMSD) was calculated as previously described (Krissinel & Henrick, 2004).

2.15 | Dephosphorylation of Wzc by Wzb

The dephosphorylation reaction was monitored by Western immunoblot analysis. For that, 1 µg of both His6-Wzc and His6-Wzb was incubated in 20 µl of reaction buffer (100 mM sodium citrate, pH 6.5, and 1 mM EDTA) at 30°C for 0, 1, 2, 4, 6, 12, or 24 hr. Reactions were terminated by adding SDS-PAGE sample buffer. Samples were

heated at 95°C for 5 min, separated on 4%–15% SDS-PAGE gels (Bio-Rad), and transferred onto nitrocellulose membranes as previously described (Leitao, Oxelfelt, Oliveira, Moradas-Ferreira, & Tamagnini, 2005). Membranes were probed with either monoclonal anti-phosphotyrosine antibody (PT-66; Sigma) diluted 1:2,000, or 6x-His Epitope Tag Antibody (Thermo Scientific) diluted 1:1,000. Membranes were then incubated with goat anti-mouse IgG-HRP (Santa Cruz Biotechnology) at a dilution of 1:5,000. Immunodetection was performed using the ECL™ Western blotting detection reagents (GE healthcare) or the WesternBright™ Quantum (Advansta) and a Chemi DocTM XRS+Imager (Bio-Rad). The relative signal intensity of the bands obtained by immunodetection was quantified using the Image Lab software (Bio-Rad). Data were statistically analyzed as described below.

2.16 | Wzc ATPase activity

The ATPase activity of His6-Wzc was determined using the ENLITEN® ATP Assay System Bioluminescence Detection Kit for ATP Measurement (Promega). Samples were incubated in 25 mM Tris-HCl pH 7.0, 1 mM DTT, and 5 mM $MgCl_2$ at 30°C for 45 min before reading luminescence using a Synergy™ 2 Multi-Mode Microplate Reader and Gen5™ software (BioTek) with an integration time of 10 s. When necessary, His6-Wzc and His6-Wzc were inactivated by incubation at 95°C for 5 min before adding ATP. Data were statistically analyzed as described below.

2.17 | Wzc autokinase activity

The autokinase activity of His6-Wzc was evaluated using everted membrane vesicles overexpressing the protein. For that, *E. coli* M15 (pREP4) cells harboring pQE-30::His6-Wzc or empty pQE-30 were grown as described above. Everted membrane vesicles were prepared from the *E. coli* cells following the protocol previously described (Rosen, 1986), except that buffer B contained 150 mM KCl instead of choline chloride and 1 mM PMSF. Isolated vesicles were incubated in dephosphorylation buffer with purified His6-Wzb using a total protein ratio of 20:1 for 0 or 6 hr. Subsequently, the dephosphorylation buffer and excess of His6-Wzb were removed by dialyzing against kinase buffer (100 mM Tris-HCl pH 8.0, 200 mM KCl, 1 mM $MgCl_2$) using membranes with a cutoff of 25 kDa (Spectra/Por®; Spectrum Labs) for a minimum of 16 hr at 4°C. Dephosphorylated vesicles were incubated in kinase buffer supplemented or not with 200 μM ATP for 0 hr, 10 min, 30 min, or 6 hr. The kinase reaction was monitored by Western immunoblot, and statistical analyses were performed as described below.

2.18 | Analysis of Wzc phosphorylation

Protein bands were excised from stained gels, and samples were processed for mass spectrometry analysis as previously described (Gomes et al., 2013; Osório & Reis, 2013). Briefly, protein spots were sequentially washed with ultrapure water, 50% acetonitrile in 50 mM ammonium bicarbonate (ABC) followed by dehydration with 100% acetonitrile. Afterward, protein spots were reduced with 25 mM dithiothreitol in 50 mM ABC, at 56°C for 20 min and alkylated with 55 mM iodoacetamide in 50 mM ABC, for 20 min at room temperature in the dark, followed by the above described washing/dehydration procedures. In-gel protein enzymatic digestion was performed using trypsin in the presence of 0.01% surfactant (Promega) for 3 hr at 37°C. Resulting peptides were extracted from gel plugs with 2.5% TFA for 15 min at 1,400 rpm (Thermomixer, Eppendorf), dried under vacuum (SpeedVac, Thermo Scientific), and resuspended in 0.1% TFA.

Protein identification was performed by MALDI mass spectrometry (4800 Plus MALDI TOF/TOF Analyzer; SCIEX). Protein digests were purified by reversed-phase C18 chromatography (ZipTips, Millipore) following manufacturer's instructions and eluted in the MALDI sample plate using the MALDI matrix alpha-Cyano-4-hydroxycinnamic acid (CHCA) as elution solution at 8 mg/ml in 50% ACN, 0.1% TFA, 6 mM ammonium phosphate. Peptide mass spectra were acquired in reflector positive mode in the mass range of *m/z* 700–5,000. Relevant peptide peaks were selected for MS/MS sequencing. Proteins were identified by Peptide Mass Fingerprint (PMF) approach with the Mascot software (v2.5.1, Matrix Science) using the UniProt protein sequence database for the taxonomic selection *Synechocystis* (2017_01 release). MS/MS phosphopeptide sequencing followed by Mascot analysis was performed for phosphorylation site determination. The protein search settings were cysteine carbamidomethylation (constant modification), methionine oxidation, and tyrosine phosphorylation (variable modifications), up to two missed trypsin cleavages, and maximum error tolerance of 10 ppm (MS)/0.5 Da (MS/MS). Protein scores >51 were considered significant ($p < 0.05$).

2.19 | Statistical analysis

Data were statistically analyzed in GraphPad Prism v7 (GraphPad Software) using a one-way analysis of variance (ANOVA), followed by Tukey's multiple comparisons.

3 | RESULTS

3.1 | Wzc and Wzb play a role in *Synechocystis*' EPS production

To unveil the key players in cyanobacterial EPS biosynthesis, we have used *Synechocystis* sp. PCC 6803 and deleted gene-encoding proteins putatively involved in the Wzy- and ABC transporter-dependent pathways. For this purpose, the genes were partially replaced with an antibiotic resistance cassette using double homologous recombination. The first fully segregated mutants obtained, namely Δ*wzy* (Δ*sll0737*—encoding the polymerase), Δ*wzx* (Δ*sll5049*—flippase), Δ*kpsM* (Δ*slr2107*—ABC transporter component), and Δ*kpsM*Δ*wzy* (Δ*slr2107*Δ*sll0737*), did not show any obvious phenotype in terms of growth, total carbohydrates, RPS,

and CPS content (Supporting Information Figures S1–S5). We also confirmed by RT-PCR that all the putative copies of *wzy* (*sll0737*, *slr0728*, *slr1515*, *sll5074*, and *slr1074*), *wzx* (*sll5049*, *slr0488*, *slr0896*, and *slr1543*), and *kpsM* (*slr2107*, *slr0977*, and *sll0564*) (see Pereira et al., 2015; Kopf et al., 2014) were transcribed under standard laboratory conditions (Supporting Information Figure S6). Subsequently, we generated Δ*wzc* (Δ*sll0923*), Δ*wzb* (Δ*slr0328*), Δ*wzc*Δ*wzb* (Δ*sll0923*Δ*slr0328*), and wzc_{Trunc} mutants. The last strain possesses a truncated Wzc, lacking the last 25 amino acids that constitute the C-terminal Y-rich region, where autophosphorylation and dephosphorylation by Wzb are expected to occur. Although a Δ*wzc* mutant strain was already described, we generated a Δ*wzc* in our *Synechocystis* strain using the construct kindly provided by Jittawuttipoka et al. (2013) to avoid phenotypic changes arising from the use of different *Synechocystis* substrains (Trautmann, Voß, Wilde, Al-Babili, & Hess, 2012). In all cases, the mutant strains were fully segregated (Supporting Information Figure S7) and did not display significant growth differences compared to the wild type (Figures 1 and 2), indicating that the targeted genes are not essential in standard laboratory conditions. With the exception of wzc_{Trunc}, the chlorophyll *a* content showed a linear correlation with OD values, proving to be a good estimation of cell density/number (Figures 1 and 2). The amount of total carbohydrates, RPS, and CPS produced per liter of culture was measured and normalized by the OD value and chlorophyll *a* content. These two approaches lead to congruent results and; therefore, only the production per OD value is shown (Figures 1c,d,e and 2c,d,e). Statistical analyses are presented for the last time point,

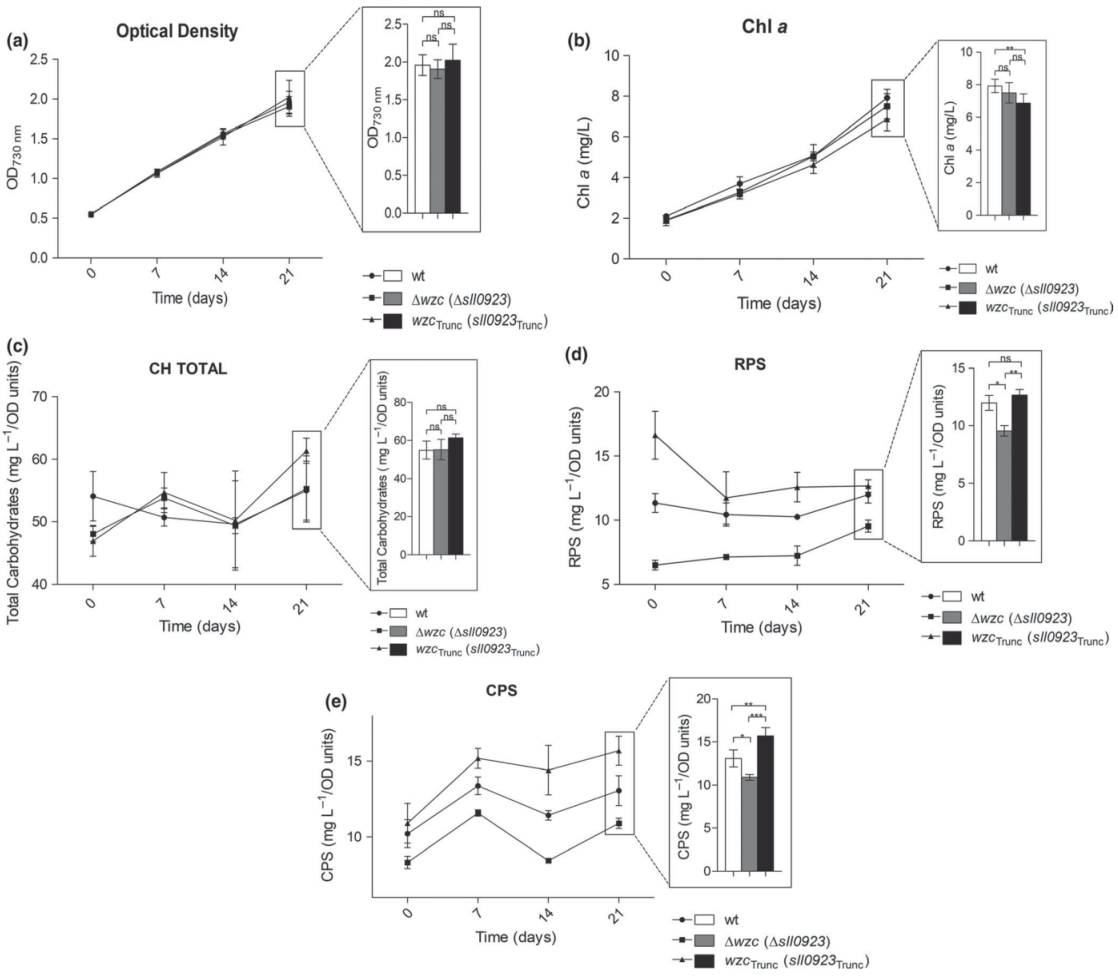

FIGURE 1 Characterization of *Synechocystis* sp. PCC 6803 wild type and Δ*wzc* and wzc_{Trunc} mutants in terms of growth ([a] optical density at λ = 730 nm [OD_{730nm}] and [b] μg of chlorophyll *a* per ml of culture [Chl *a*]), and production of (c) total carbohydrates, (d) released polysaccharides (RPS), and (e) capsular polysaccharides (CPS) expressed as mg per $OD730_{nm}$ units. Experiments were performed in triplicate. Data are means ± *SD*. Statistical analysis performed using one-way analysis of variance (ANOVA), followed by Tukey's multiple comparisons, is presented for the last time point. Significant differences are identified: *($p \leq 0.05$), **($p \leq 0.01$), ***($p \leq 0.001$). Ns: no significant differences

as the differences accumulate with the increase of the cell density of the cultures. The four mutants showed different amounts of CPS and/or RPS compared to the wild type, even if none of the mutations abolished CPS and/or RPS production. Δ*wzc* showed an approximately 20% and 17% decrease in the amount of RPS (Figure 1d) and CPS (Figure 1e), respectively, confirming the role of Wzc in the production of these polymers (Jittawuttipoka et al., 2013). These authors reported a higher decrease in CPS and RPS production (about 50%). The difference to the amounts reported here is likely related to the *Synechocystis* genetic background used to generate the mutants (Trautmann et al., 2012), the growth conditions (e.g. cultivation of cells in medium with Na_2CO_3 by Jittawuttipoka et al., 2013), and the experimental design (e.g. time course of the experiment and normalization of the data by amount of protein by Jittawuttipoka et al., 2013). Δ*wzb* exhibited 35% less RPS (Figure 2d) but no significant changes in the amount of CPS could be observed (Figure 2e), indicating that Wzb is only involved in RPS production. The double mutant Δ*wzc*Δ*wzb* exhibited 18% decrease in CPS (Figure 2e) and a 23% increase of RPS (Figure 2d). The decrease of CPS displayed by the double mutant and the single mutant Δ*wzc* is consistent with the hypothesis that Wzb does not play a role in the regulation of CPS production. In contrast, the higher amount of RPS produced by the double mutant suggests that, in the absence of both proteins, the RPS production is likely to be diverted to an alternative route. Interestingly, the wzc_{Trunc} mutant produced the same amount of RPS and 19% more CPS compared to the wild type (Figure 1d,e), suggesting that the C-terminal Y-rich region of this protein is only functionally relevant in the regulation of CPS production. The apparently contradictory outcomes of the Δ*wzb* and wzc_{Trunc} mutants have two

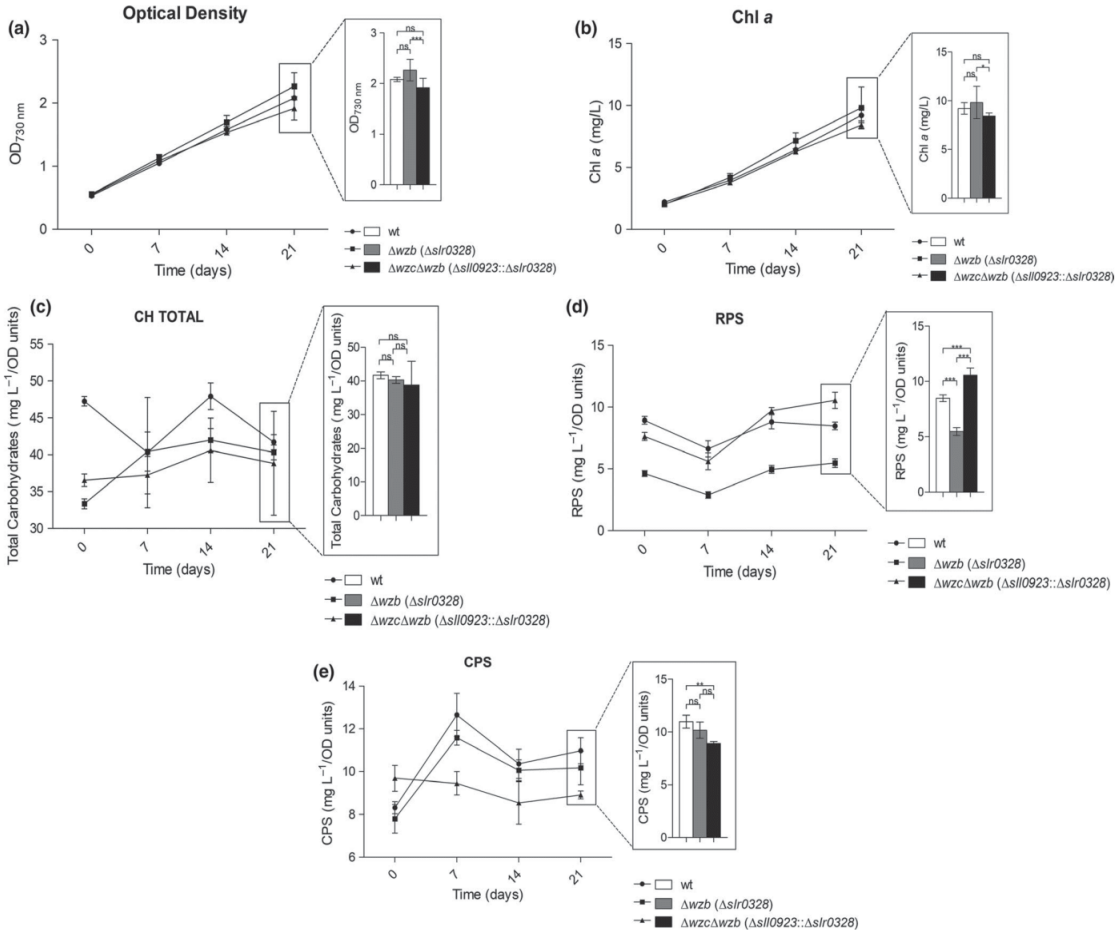

FIGURE 2 Characterization of *Synechocystis* sp. PCC 6803 wild type and Δ*wzb* and Δ*wzc*Δ*wzb* in terms of growth ([a] optical density at λ = 730 nm [OD_{730nm}] and [b] µg of chlorophyll *a* per ml of culture [Chl *a*]), and production of (c) total carbohydrates, (d) released polysaccharides (RPS), and (e) capsular polysaccharides (CPS) expressed as mg per $OD730_{nm}$ units. Experiments were performed in triplicate. Data are means ± *SD*. Statistical analysis performed using one-way analysis of variance (ANOVA), followed by Tukey's multiple comparisons, is presented for the last time point. Significant differences are identified: *($p \leq 0.05$), **($p \leq 0.01$), ***($p \leq 0.001$). Ns: no significant differences

TABLE 1 Monosaccharidic composition of the released polysaccharides extracted from *Synechocystis* sp. PCC 6803 wild type, Δ*wzc*, Δ*wzb*, Δ*wzc*Δ*wzb*, and wzc_{Trunc}

	Wild type		Δ*wzc*		Δ*wzb*		Δ*wzc*Δ*wzb*		wzc_{Trunc}	
Monosaccharide[a]	Mean[a]	*SD* (*n* = 3)	Mean[a]	*SD* (*n* = 3)	Mean[a]	*SD* (*n* = 3)	Mean[a]	*SD* (*n* = 3)	Mean[a]	*SD* (*n* = 3
Glucose	17.50	3.21	6.85	0.82	5.20	1.30	9.98	0.31	10.38	1.78
Mannose	10.17	2.66	7.19	1.95	2.52	1.02	7.13	2.80	5.06	0.18
Galactose	11.90	0.99	4.30	1.89	1.16	0.27	3.55	3.26	3.58	0.93
Fructose	np		np		np		Tr[b]		2.36	0.55
Fucose	8.23	0.70	5.14	1.18	1.84	0.25	4.64	1.76	3.60	0.13
Ribose	4.23	1.84	Tr[b]		np		Tr[b]		Tr[b]	
Rhamnose	6.19	2.55	50.51	8.47	88.60	3.34	48.32	11.47	57.81	5.30
Xylose	2.52	0.59	2.15	0.30	Tr[b]		2.10	0.45	Tr[b]	
Arabinose	7.74	5.17	6.93	2.78	Tr[b]		4.61	6.19	3.58	1.11
Glucuronic acid	np		np		np		7.38	2.64	Tr[b]	
Galacturonic acid	12.37	2.85	2.02	1.05	np		np		2.15	0.67
Glucosamine	7.46	1.70	1.87	0.67	np		Tr[b]		2.19	0.41
Galactosamine	15.14	2.20	13.36	1.56	np		10.74	1.78	7.31	2.84

Notes. Differences discussed in the text are highlighted in gray.
Np: not present.
[a]Mean expressed in Mol % of each monosaccharide. Sums may not be exactly 100% due to rounding. [b]Tr: traces <1%.

possible explanations: (a) Wzb is not involved in the dephosphorylation of the C-terminal Y-rich region of Wzc; or (b) the absence of Wzb affects the phosphorylation/dephosphorylation cycles of Wzc, altering RPS production, and this effect is not replicated when the Y-rich region of Wzc is truncated. To ensure that the observed phenotypes were not due to polar effects, the deletion mutants were complemented by the addition of *wzb* or *wzc* in *trans* restoring EPS production. This was done using the replicative vector pSEVA351 (Silva-Rocha et al., 2013) harboring the native *wzc* or the *wzb*.

Despite the changes observed for RPS and CPS in the mutants, the amount of total carbohydrates did not vary significantly (Figures 1c and 2c), consistent with an intracellular accumulation of the polysaccharides.

It has been previously shown for other bacteria that the assembly of EPS and other surface polysaccharides, such as the O-antigen of LPS and S-layer glycans, follows similar mechanisms that may be functionally connected (Babu et al., 2011; Ristl et al., 2011; Simkovsky et al., 2012; Whitfield & Trent, 2014). However, for *Synechocystis*, no obvious differences were observed for the LPS profile and the cells' surface ultrastructure comparing the wild type and the mutants (Supporting Information Figures S8 and S9). The monosaccharidic composition of the RPS produced by the different strains was also evaluated. A considerable increase in the percentage of rhamnose was observed in all mutants (Table 1). In addition, the RPS produced by *Δwzb* are composed by a smaller number of different monosaccharides. These results highlight that the differences induced by these mutations are not limited to the amount of the polymer but extend to their composition.

3.2 | Wzb has a classical LMW-PTP conformation

To better define the functional role of *Synechocystis*' Wzb in the production of EPS, we overexpressed this protein in *E. coli* and performed its purification. The presence of recombinant protein was confirmed by SDS-PAGE/Western blot (Supporting Information Figure S10).

The Wzb protein was crystallized and analyzed through X-ray diffraction. Data collection and refinement statistics are shown in Table 2. One monomer was present in the asymmetric unit, with the crystal lattice belonging to the $P3_12$ 1 space group. *Synechocystis*' Wzb displays the structure of a low molecular weight protein tyrosine phosphatase (LMW-PTP) (Figure 3). The PTPases signature motif, the PTP loop, with the characteristic sequence $C(X)_5R(S/T)$ (cysteine 7 to serine 14) is located between the C-terminus of the β1 strand and the N-terminus of the α1 helix, at the N-terminus side of the protein (Zhang, 1998). As in other LMW-PTP proteins, the PTP loop is preceded by a valine residue (V6) (Kolmodin & Aqvist, 2001; Mukhopadhyay & Kennelly, 2011). Opposite and topping this loop, there is the DPYY loop, which contains the functionally essential aspartate residue (D124). Together, the DPYY and PTP loops constitute the enzyme´s active site (Standish & Morona, 2014; Zhang, 1998). The tyrosine residues of the DPYY loop form one of the walls of the active site pocket, with a histidine (H45) delineating the other side of the substrate entry site.

A sequence alignment was performed, and a phylogenetic tree was constructed to assess sequence similarities and conservation of residues with other LMW-PTP with solved structures. *Synechocystis*' Wzb was shown to be more closely related to the

TABLE 2 Crystallographic data collection, processing, and structure refinement statistics for Wzb

Data collection	
Space group	$P3_12\ 1$
Unit cell dimensions	
a (Å)	73.41
b (Å)	73.41
c (Å)	68.07
$\alpha = \beta$ (°)	90
γ (°)	120
Resolution range (Å)	46.46–2.28 (2.36–2.28)
No. of unique reflections	10,021 (959)
Multiplicity (overall/last shell)	6.7 (7.2)
R_{merge} (%; overall/last shell)[a]	12.1 (83.6)
Completeness (%; overall/last shell)	100.0 (100.0)
$I/s(I)$ (overall/last shell)	8.2 (2.0)
Mathews coefficient (Å^3/Da)	2.80
Solvent content (%)	56.09
Structure refinement	
R_{factor}[b]/R_{free} (%)	22.4/25.3
No. of unique reflections (working/test set)	9,979 (973)
Total number of atoms	821
Clashscore	13.99
Average B-factor (Å^2)	34.68
Average protein B-factor (Å^2)	34.65
Average water B-factor (Å^2)	39.60
R.m.s. deviations from standard geometry	
Bonds (Å)	0.007
Angles (°)	1.00
Ramachandran plot statistics	
Most favored regions (%)	93.67
Allowed regions (%)	6.33
Outliers (%)	0.00

[a]$R_{merge} = \Sigma|I - \langle I\rangle|/\Sigma\langle I\rangle$, where I is the observed intensity and $\langle I\rangle$ is the average intensity of multiple observations of symmetry-related positions. [b]$R_{factor} = \Sigma||F_o|-|F_c||/\Sigma|F_o|$, where $|F_o|$ and $|F_c|$ are observed and calculated structure factor amplitudes, respectively.

LMW-PTP of the unicellular eukaryote *E. histolytica* than of the LMW-PTPs of other bacteria (Supporting Information Figure S11). Likewise, a three dimensional protein structure alignment revealed that the structure of Wzb is highly identical to that of the other LMW-PTPs, being more closely related to that of *E. histolytica* (PDB entry 3ido) (Linford et al., 2014), followed by *S. aureus* (Gram-positive; PDB entry 3rof) (Vega et al., 2011) and *E. coli* (Gram-negative; PDB entry 2wja) (Hagelueken, Huang, Mainprize, Whitfield, & Naismith, 2009), with root mean square deviation (RMSD) values (Å) of 1.04, 1.37, and 1.54, respectively, and an average of 95 superimposable residues.

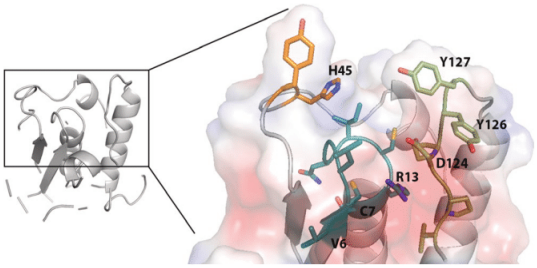

FIGURE 3 Structure of Wzb from *Synechocystis* sp. PCC 6803. A close view of the active site with surface representation is shown. The protein backbone is represented in gray; the active site residues are in stick representation, with oxygen in red, nitrogen in blue, and sulfur in yellow; the PTP, DPYY, and histidine 45-containing loops are represented in teal, light green, and orange, respectively. Relevant residues are labeled: valine (V) 6, cysteine (C) 7, arginine (R) 13, histidine (H) 45, aspartate (D) 124, tyrosine (Y) 126, and tyrosine (Y) 127. Representations made with Pymol (Schrödinger, 2010)

3.3 | Wzc is a substrate of the Wzb phosphatase

Our phenotypic characterization of the *Δwzb* and wzc_{Trunc} mutants raised the possibility that Wzb does not dephosphorylate Wzc. To solve this question, we first used a p-nitrophenyl phosphate hydrolysis assay to confirm that Wzb functions as a phosphatase (Figure 4), in agreement with our structural analysis (Figure 3) and previous data (Mukhopadhyay & Kennelly, 2011). We then asked whether *Synechocystis*' Wzc is a substrate for Wzb. Importantly, mass spectrometry analysis of purified Wzc expressed in *E. coli* and solubilized with detergent revealed the presence of phosphorylated tyrosine residues. In particular, the C-terminal Y-rich peptide—$_{740}$YYNNRYYDR$_{748}$—shows the presence of a phosphorylation in Y745 and a double phosphorylation at either the Y741 + Y746 pair or at Y745 + Y746 (Supporting Information Figure S12). We used this characteristic of Wzc and incubated the protein with Wzb, assessing the membrane protein phosphorylation load at different time points. In the presence of Wzb, a time-dependent dephosphorylation of Wzc was observed, with the signal of the anti-phophotyrosine antibody decreasing significantly after 2-hr incubation (Figure 5). By MS/MS analysis, we determined that Y745 is one of the residues that undergoes dephosphorylation, with the signal decreasing significantly after incubation of Wzb. In contrast, no Wzc dephosphorylation occurred in the absence of Wzb (Figure 5).These results clearly establish that Wzb is able to interact *in vitro* with the C-terminal Y-rich tail of Wzc, suggesting that in the cell, the phosphorylation state of Wzc is dependent on the activity of Wzb.

3.4 | Wzc has ATPase and autokinase activity

It was previously suggested that Wzc is a BY-kinase (Mijakovic et al., 2016; Pereira et al., 2013, 2015). To demonstrate that this protein functions as a kinase, we investigated its ability to hydrolyze

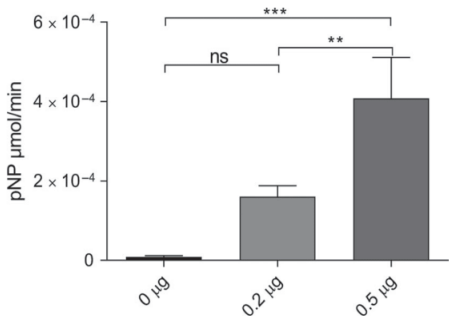

FIGURE 4 His6-Wzb phosphatase activity, expressed in µmoles per minute of p-nitrophenol (pNP), using two different amounts of protein and 10 mM of p-nitrophenyl phosphate (pNPP) substrate at pH 6.5. Experiments were performed in triplicate. Data are mean ± *SD*. Statistical analysis was performed using one-way analysis of variance (ANOVA), followed by Tukey's multiple comparisons. Statistically significant differences are identified: **($p \leq 0.01$) and ***($p \leq 0.001$). Ns: no significant differences

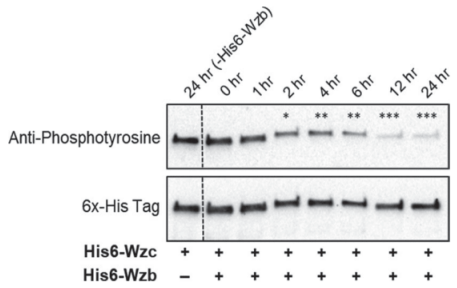

FIGURE 5 *In vitro* dephosphorylation of His6-Wzc by His6-Wzb for 0–24 hr. Samples were analyzed by Western blot using an anti-phosphotyrosine antibody. Subsequently, membranes were stripped and reprobed with a 6x-His epitope tag antibody (loading control). Lanes 24 hr (-His6-Wzb) refer to samples in which His6-Wzc was incubated in the absence of His6-Wzb (control). Experiments were performed in triplicate. Statistical analysis was performed using one-way analysis of variance (ANOVA), followed by Tukey's multiple comparisons. Significant intensity differences between 0 hr and other time points are identified: *($p \leq 0.05$), **($p \leq 0.01$), ***($p < 0.001$). Ns: no significant differences

ATP. ATPase activity was evaluated using a bioluminescence assay in which the signal intensity is proportional to the ATP concentration. A significant reduction of the signal intensity was observed for the reactions containing either Wzc or both Wzc and Wzb, compared to those in which Wzc was previously heat inactivated (Figure 6a). These results provide evidence that Wzc is capable of ATP binding and hydrolysis and that the presence of Wzb does not significantly impair this activity. To determine whether Wzc also displays autokinase activity, we tested its ability to autophosphorylate in the presence of ATP. For this, we used everted membrane vesicles (EMVs) of *E. coli* overexpressing *Synechocystis*' Wzc, which were pre-incubated with Wzb to generate dephosphorylated Wzc. To take into account possible differences in the amount of protein loaded, the signal obtained for the anti-phosphotyrosine antibody was normalized by that obtained for the 6x-His epitope tag antibody. The results revealed an ATP-dependent increase in the level of phosphorylated Y residues of Wzc over time (Figure 6b). To confirm that the immunoblot signal was due to the *Synechocystis*' Wzc and not the native *E. coli* Wzc, EMVs isolated from cells transformed with the empty pQE-30 vector were also included in the assay. Altogether, the ATPase activity and the increase in phosphorylation strongly suggest autokinase activity.

4 | DISCUSSION

The results obtained in this work clearly show that *Synechocystis*' Wzc and Wzb are involved in the production of EPS. Importantly, the amount of total carbohydrates did not vary in Δ*wzc* and Δ*wzb*, consistent with an intracellular accumulation of the polysaccharides and supporting the idea that these proteins are mainly involved in the later steps of polymer assembly and export. Neither Wzc nor Wzb are essential for EPS production, as the polymer(s) is still produced in their absence. This is consistent with the hypothesis of functional redundancy, either owing to the existence of multiple copies for some of the EPS-related genes/proteins and/or a crosstalk between the components of the different assembly and export pathways (Pereira et al., 2015). This hypothesis also helps to explain the lack of phenotypes for Δ*wzy* (Δ*sll0737*), Δ*wzx* (Δ*sll5049*), Δ*kpsM* (Δ*slr2107*), and Δ*kpsM*Δ*wzy* (Δ*slr2107*Δ*sll0737*).

We have established that the Wzb phosphatase has a classical LMW-PTPs conformation and that Wzc has the functional properties of a BY-kinase, showing ATPase and autophosphorylation activity. We also provide evidence that Wzc is a substrate of Wzb and that the Wzb-mediated dephosphorylation occurs at the C-terminal Y-rich loop of Wzc. These findings fit well with the previously proposed roles for the two proteins and strongly indicate that tyrosine phosphorylation of Wzc and its dephosphorylation by Wzb is a mechanism of regulation of EPS production. Two features of the Wzb structure are particularly relevant for its functional properties: (a) it possesses the second Y of the DPYY motif (Y127) that is absent in most prokaryotic LMW-PTPs (Bohmer, Szedlacsek, Tabernero, Ostman, & Hertog, 2013; Lescop et al., 2006; Standish & Morona, 2014). While the first tyrosine usually interacts with the aromatic ring of the substrate, being crucial for the interaction between LMW-PTPs and the BY-kinases (Lescop et al., 2006; Standish & Morona, 2014), the second tyrosine seems to play a role in substrate specificity (Bucciantini et al., 1999; Raugei, Ramponi, & Chiarugi, 2002). (b) *Synechocystis*' Wzb possesses an aromatic residue—histidine (H45)—in the catalytic site instead of the hydrophobic leucine that occupies this position in most prokaryotic LMW-PTPs (Lescop et al., 2006; Linford et al., 2014). Based on these characteristics, *Synechocystis* Wzb can be classified as a class I or eukaryotic-like LMW-PTP and is therefore likely to present a substrate recognition mechanism different from that of *E. coli* Wzb, a class II or prokaryotic-like LMW-PTPs (Lescop et al., 2006). These differences may contribute to the higher substrate affinity of the

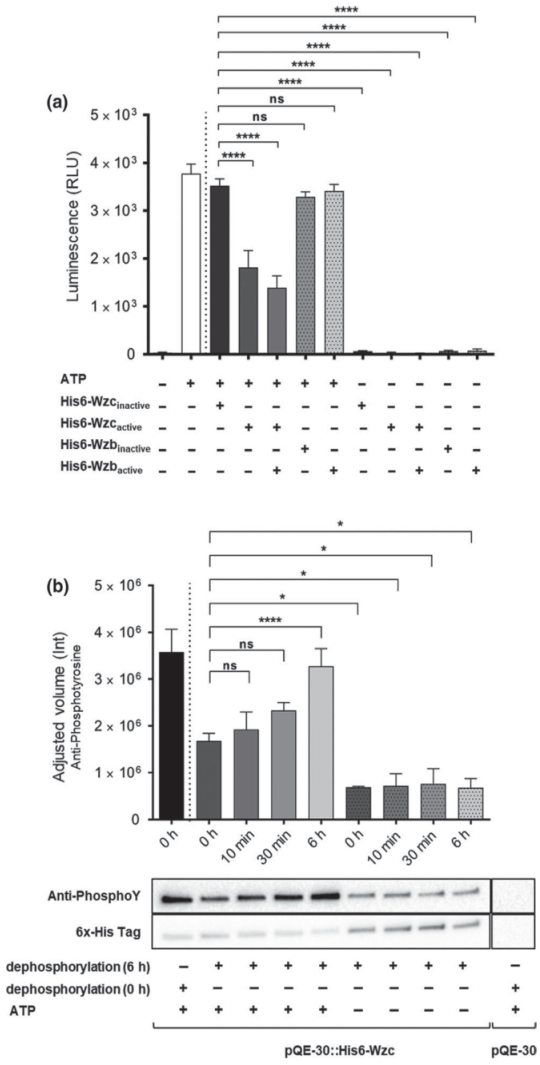

FIGURE 6 *In vitro* evaluation of His6-Wzc ATPase (a) and autokinase (b) activities. (a) The ATPase activity was measured using the luciferase assay, being the intensity of the emitted light (Relative Luminescence Unit—RLU) proportional to the ATP concentration in the samples. The presence/absence of ATP, active His6-Wzc, His6-Wzc inactivated by heat, His6-Wzb and/or Wzb inactivated by heat is indicated below. (b) To evaluate the autokinase activity, everted membrane vesicles of *Escherichia coli* cells containing pQE-30::His6-Wzc or pQE-30 were isolated, dephosphorylated for 0 or 6 hr with His6-Wzb, and dialyzed to remove the dephosphorylation buffer and most of the phosphatase, before incubation with or without 200 μM ATP for 0 hr, 10 min, 30 min, or 6 hr. The time of dephosphorylation and the presence/absence ATP is indicated below. Samples were analyzed by Western blot using an anti-phosphotyrosine antibody. Subsequently, membranes were stripped and reprobed with a 6*x*-His epitope tag antibody (loading control). The ratio between the two signals (adjusted volume) is shown. Experiments were performed in triplicate. Data are means ± *SD*. Statistical analysis was performed using one-way analysis of variance (ANOVA), followed by Tukey's multiple comparisons. Statistically significant differences between inactivated Wzc in the presence of ATP (a) or dephosphorylation for 6 hr followed by incubation with ATP for 0 hr (b) and other conditions are identified: *($p \leq 0.05$), **($p \leq 0.01$), ***($p \leq 0.001$), ****($p \leq 0.0001$). Ns: no significant differences

Synechocystis' Wzb compared to the *E. coli* homolog using pNPP as substrate (Lescop et al., 2006; Mukhopadhyay & Kennelly, 2011) and to the ability of *Synechocystis*' Wzb to dephosphorylate other substrates (Mukhopadhyay & Kennelly, 2011). In addition, since most of the phosphatases involved in the biosynthesis of capsules and/or EPS are class II LMW-PTPs, it is likely that the structural features of *Synechocystis*' Wzb reflect differences in EPS production.

Strikingly, although our results indicate that Wzb regulates the function of Wzc through dephosphorylation, the two proteins appear to have different roles in EPS production. Wzc plays a role in both CPS and RPS production, as shown here and previously (Jittawuttipoka et al., 2013), while Wzb participates in RPS production only. Our wzc_{Trunc} mutant, which lacks the protein region where Wzb acts, provides some insights into these differences. The phenotype of wzc_{Trunc}, together with the results obtained for Δ*wzc* and Δ*wzb*, supports previous indications that the production of CPS and RPS is, at least, divergent processes (Micheletti et al., 2008), relying on different proteins and/or different contributions of the same proteins (Jittawuttipoka et al., 2013). For example, it is possible that the assembly and export of CPS and RPS are regulated by different signals involving the Y-rich region of Wzc. This is true for *E. coli* K30 capsule (CPS-like) and K-12 colanic acid (RPS-like), with the production of the capsule depending on Wzc undergoing cycles of phosphorylation/dephosphorylation while the production of colanic acid being negatively regulated by phosphorylated Wzc (Paiment, Hocking, & Whitfield, 2002). However, it is important to keep in mind that the C-terminal Y-rich region is not universally present in the Wzc proteins of EPS-producing bacteria, including *Xanthomonas campestris*' GumC (Cuthbertson et al., 2009) and the Wzc homologs of the highly efficient EPS producer *Cyanothece* sp. CCY 0110 (Pereira et al., 2013).

In addition, our results show that Wzc and Wzb influence EPS composition. Three factors are likely to contribute to the monosaccharidic differences observed for the RPS of the mutants versus wild type: (a) *Synechocystis*' Wzc and Wzb interact with other proteins that may directly or indirectly affect monosaccharide and/or sugar nucleotide metabolism (Mukhopadhyay & Kennelly, 2011; Sato et al., 2007). In particular, Wzb substrates include proteins involved in the photosynthetic process (Mukhopadhyay & Kennelly, 2011) and changes in Wzb activity will likely affect central carbon metabolism. It is therefore not surprising that the RPS of Δ*wzb* displays the highest number of differences relative to wild type composition; (b) mutations may lead to differences in the affinity of the periplasm–spanning complex for monosaccharides. This explanation has been suggested for a mutant in the ATP-binding component (KpsT; Sll0982) of an EPS-related ABC transporter that also produces EPS enriched in rhamnose (Fisher et al., 2013). (c) The increase in the

rhamnose content may be related to the genomic context of *wzc*, since this gene is present in the vicinity of *slr0985* that encodes one of the enzymes involved in the dTDP-L-rhamnose biosynthesis, the dTDP-4-dehydrorhamnose 3,5-epimerase. Interestingly, the same is observed for *kpsT* (*sll0982*) and its cognate permease component *KpsM* (*sll0977*). In bacteria, L-rhamnose is a rare sugar that is most frequently found in the EPS and O-antigen of LPS and this genetic organization is not uncommon (Boels et al., 2004) (Giraud & Naismith, 2000; Roca et al., 2015). Further studies are necessary to discern the mechanistic role of Wzb and Wzc on the composition of EPS.

Overall, the results obtained in this study emphasize the complexity of EPS production in cyanobacteria, supporting previous hypothesis of functional redundancy and crosstalk between different pathways, and provide novel data on the specific function of two proteins—Wzc and Wzb—in *Synechocystis*. These findings provide a robust basis for future studies aiming at further elucidate cyanobacterial EPS production with the ultimate goal of establishing these organisms as sustainable platforms for the production of large amounts of these polymers and/or polymers with the desired characteristics for the industrial toolbox.

ACKNOWLEDGMENTS

This work was financed by FEDER—Fundo Europeu de Desenvolvimento Regional funds through the COMPETE 2020—Operational Programme for Competitiveness and Internationalisation (POCI); projects NORTE-01-0145-FEDER-000012—Structured Programme on Bioengineering Therapies for Infectious Diseases and Tissue Regeneration and NORTE-01-0145-FEDER-000008—Porto Neurosciences and Neurologic Disease Research Initiative at i3S, supported by Norte Portugal Regional Operational Programme (NORTE 2020), under the PORTUGAL 2020 Partnership Agreement; and by Portuguese funds through FCT—Fundação para a Ciência e a Tecnologia/Ministério da Ciência, Tecnologia e Ensino Superior in the framework of the project "Institute for Research and Innovation in Health Sciences" (POCI-01-0145-FEDER-007274 and PTDC/BIA-MIC/28779/2017) and grants SFRH/BD/119920/2016 (MS), SFRH/BD/99715/2014 (CF), and SFRH/BD/129921/2017 (JPL). The authors thank F. Chauvat and the Commissariat à l'Energie Atomique (CEA), Direction des Sciences du Vivant, for providing the cassette for the deletion of the *Synechocystis sll0923*, the staff of the European Synchrotron Radiation Facility (Grenoble, France) and SOLEIL (Essonne, France) synchrotrons, Filipe Pinto, Frederico Silva, Hugo Osório, and Joana Furtado for their technical assistance.

CONFLICT OF INTEREST

The authors declare that they have no conflict of interest.

AUTHORS CONTRIBUTION

SBP, MS, JMC, LG, and PT designed the research; SBP, MS, JPL, CF, ZB, CE, and FR performed research; SBP, MS, JPL, RM, RDP, LG, JMC, and PT analyzed and interpreted data; SBP, MS, JMC, and PT wrote the manuscript.

ETHICS STATEMENT

None required.

DATA ACCESSIBILITY

The atomic coordinates of Wzb have been deposited in the Protein Data Bank, www.pdb.org (PDB ID 5O7B). All data supporting this study are provided as Supporting Information Appendix S1 accompanying this paper.

ORCID

Sara B. Pereira http://orcid.org/0000-0003-3284-8092

Paula Tamagnini http://orcid.org/0000-0003-4396-2122

REFERENCES

Adams, P. D., Afonine, P. V., Bunkoczi, G., Chen, V. B., Davis, I. W., Echols, N., … Zwart, P. H. (2010). PHENIX: A comprehensive Python-based system for macromolecular structure solution. *Acta Crystallographica, Section D: Biological Crystallography*, *66*, 213–221.

Anderson, S. L., & McIntosh, L. (1991). Light-activated heterotrophic growth of the cyanobacterium *Synechocystis* sp. strain PCC 6803: A blue-light-requiring process. *Journal of Bacteriology*, *173*, 2761–2767. https://doi.org/10.1128/jb.173.9.2761-2767.1991

Babu, M., Diaz-Mejia, J. J., Vlasblom, J., Gagarinova, A., Phanse, S., Graham, C., … Emili, A. (2011). Genetic interaction maps in *Escherichia coli* reveal functional crosstalk among cell envelope biogenesis pathways. *PLoS Genetics*, *7*, e1002377. https://doi.org/10.1371/journal.pgen.1002377

Bailey, S. (1994). The Ccp4 suite - programs for protein crystallography. *Acta Crystallographica, Section D: Biological Crystallography*, *50*, 760–763. https://doi.org/10.1107/S0907444994003112

Berman, H. M., Westbrook, J., Feng, Z., Gilliland, G., Bhat, T. N., Weissig, H., … Bourne, P. E. (2000). The Protein Data Bank. *Nucleic Acids Research*, *28*, 235-242.

Bertani, G. (1951). Studies on lysogenesis. I. The mode of phage liberation by lysogenic *Escherichia coli*. *Journal of Bacteriology*, *62*, 293–300.

Boels, I. C., Beerthuyzen, M. M., Kosters, M. H. W., Van Kaauwen, M. P. W., Kleerebezem, M., & de Vos, W. M. (2004). Identification and functional characterization of the *Lactococcus lactis* rfb operon, required for dTDP-rhamnose biosynthesis. *Journal of Bacteriology*, *186*, 1239–1248. https://doi.org/10.1128/JB.186.5.1239-1248.2004

Bohmer, F., Szedlacsek, S., Tabernero, L., Ostman, A., & den Hertog, J. (2013). Protein tyrosine phosphatase structure-function relationships in regulation and pathogenesis. *FEBS Journal*, *280*, 413–431. https://doi.org/10.1111/j.1742-4658.2012.08655.x

Brunger, A. T. (1992). Free R-value - a novel statistical quantity for assessing the accuracy of crystal-structures. *Nature*, *355*, 472–475. https://doi.org/10.1038/355472a0

Bucciantini, M., Chiarugi, P., Cirri, P., Taddei, L., Stefani, M., Raugei, G., … Ramponi, G. (1999). The low Mr phosphotyrosine protein phosphatase behaves differently when phosphorylated at Tyr131 or Tyr132 by Src kinase. *FEBS Letters*, *456*, 73–78. https://doi.org/10.1016/s0014-5793(99)00828-5

Chiaramonte, S., Giacometti, G. M., & Bergantino, E. (1999). Construction and characterization of a functional

mutant of *Synechocystis* 6803 harbouring a eukaryotic PSII-H subunit. *European Journal of Biochemistry*, *260*, 833–843. https://doi.org/10.1046/j.1432-1327.1999.00226.x

Cuthbertson, L., Mainprize, I. L., Naismith, J. H., & Whitfield, C. (2009). Pivotal roles of the outer membrane polysaccharide export and polysaccharide copolymerase protein families in export of extracellular polysaccharides in gram-negative bacteria. *Microbiology and Molecular Biology Reviews*, *73*, 155–177. https://doi.org/10.1128/mmbr.00024-08

Dubois, M., Gilles, K. A., Hamilton, J. K., Rebers, P. A., & Smith, F. (1956). Colorimetric method for determination of sugars and related substances. *Analytical Chemistry*, *28*, 350–356. https://doi.org/10.1021/ac60111a017

Emsley, P., Lohkamp, B., Scott, W. G., & Cowtan, K. (2010). Features and development of coot. *Acta Crystallographica, Section D: Biological Crystallography*, *66*, 486–501.

Ferreira, A. S., Leitao, J. H., Sousa, S. A., Cosme, A. M., Sa-Correia, I., & Moreira, L. M. (2007). Functional analysis of *Burkholderia cepacia* genes *bceD* and *bceF*, encoding a phosphotyrosine phosphatase and a tyrosine autokinase, respectively: Role in exopolysaccharide biosynthesis and biofilm formation. *Applied and Environment Microbiology*, *73*, 524–534. https://doi.org/10.1128/aem.01450-06

Fisher, M. L., Allen, R., Luo, Y., & Curtiss, R. III (2013). Export of extracellular polysaccharides modulates adherence of the cyanobacterium *Synechocystis*. *PLoS One*, *8*, e74514. https://doi.org/10.1371/journal.pone.0074514

Giraud, M.-F., & Naismith, J. H. (2000). The rhamnose pathway. *Current Opinion in Structural Biology*, *10*, 687–696. https://doi.org/10.1016/s0959-440x(00)00145-7

Gomes, C., Almeida, A., Ferreira, J. A., Silva, L., Santos-Sousa, H., Pinto-de-Sousa, J., … Osório, H. (2013). Glycoproteomic analysis of serum from patients with gastric precancerous lesions. *Journal of Proteome Research*, *12*, 1454–1466. https://doi.org/10.1021/pr301112x

Grangeasse, C., Cozzone, A. J., Deutscher, J., & Mijakovic, I. (2007). Tyrosine phosphorylation: An emerging regulatory device of bacterial physiology. *Trends in Biochemical Sciences*, *32*, 86–94. https://doi.org/10.1016/j.tibs.2006.12.004

Hagelueken, G., Huang, H., Mainprize, I. L., Whitfield, C., & Naismith, J. H. (2009). Crystal structures of Wzb of *Escherichia coli* and CpsB of *Streptococcus pneumoniae*, representatives of two families of tyrosine phosphatases that regulate capsule assembly. *Journal of Molecular Biology*, *392*, 678–688. https://doi.org/10.1016/j.jmb.2009.07.026

Huang, H. H., Camsund, D., Lindblad, P., & Heidorn, T. (2010). Design and characterization of molecular tools for a Synthetic Biology approach towards developing cyanobacterial biotechnology. *Nucleic Acids Research*, *38*, 2577–2593. https://doi.org/10.1093/nar/gkq164

Jittawuttipoka, T., Planchon, M., Spalla, O., Benzerara, K., Guyot, F., Cassier-Chauvat, C., & Chauvat, F. (2013). Multidisciplinary evidences that *Synechocystis* PCC6803 exopolysaccharides operate in cell sedimentation and protection against salt and metal stresses. *PLoS One*, *8*, e55564. https://doi.org/10.1371/journal.pone.0055564

Kabsch, W. (1993). Automatic processing of rotation diffraction data from crystals of initially unknown symmetry and cell constants. *Journal of Applied Crystallography*, *26*, 795–800. https://doi.org/10.1107/S0021889893005588

Kolmodin, K., & Aqvist, J. (2001). The catalytic mechanism of protein tyrosine phosphatases revisited. *FEBS Letters*, *498*, 208–213. https://doi.org/10.1016/S0014-5793(01)02479-6

Kopf, M., Klähn, S., Scholz, I., Matthiessen, J. K. F., Hess, W. R., & Voß, B. (2014). Comparative analysis of the primary transcriptome of *Synechocystis* sp. PCC 6803. *DNA Research*, *21*, 527–539. https://doi.org/10.1093/dnares/dsu018

Krissinel, E., & Henrick, K. (2004). Secondary-structure matching (SSM), a new tool for fast protein structure alignment in three dimensions. *Acta Crystallographica. Section D, Biological Crystallography*, *60*, 2256–2268. https://doi.org/10.1107/S0907444904026460

Leitao, E., Oxelfelt, F., Oliveira, P., Moradas-Ferreira, P., & Tamagnini, P. (2005). Analysis of the *hupSL* operon of the nonheterocystous cyanobacterium *Lyngbya majuscula* CCAP 1446/4: Regulation of transcription and expression under a light-dark regimen. *Applied and Environment Microbiology*, *71*, 4567–4576. https://doi.org/10.1128/aem.71.8.4567-4576.2005

Leite, J. P., Mota, R., Durão, J., Neves, S. C., Barrias, C. C., Tamagnini, P., & Gales, L. (2017). Cyanobacterium-derived extracellular carbohydrate polymer for the controlled delivery of functional proteins. *Macromolecular Bioscience*, *17*, 1600206. https://doi.org/10.1002/mabi.201600206

Lescop, E., Hu, Y., Xu, H., Hu, W., Chen, J., Xia, B., & Jin, C. (2006). The solution structure of Escherichia coli Wzb reveals a novel substrate recognition mechanism of prokaryotic low molecular weight protein-tyrosine phosphatases. *Journal of Biological Chemistry*, *281*, 19570–19577. https://doi.org/10.1074/jbc.m601263200

Linford, A. S., Jiang, N. M., Edwards, T. E., Sherman, N. E., Van Voorhis, W. C., Stewart, L. J., … Petri, W. A. Jr (2014). Crystal structure and putative substrate identification for the *Entamoeba histolytica* low molecular weight tyrosine phosphatase. *Molecular and Biochemical Parasitology*, *193*, 33–44. https://doi.org/10.1016/j.molbiopara.2014.01.003

Ludwig, A., Heimbucher, T., Gregor, W., Czerny, T., & Schmetterer, G. (2008). Transformation and gene replacement in the facultatively chemoheterotrophic, unicellular cyanobacterium *Synechocystis* sp. PCC6714 by electroporation. *Applied Microbiology and Biotechnology*, *78*, 729–735. https://doi.org/10.1007/s00253-008-1356-y

McCoy, A. J., Grosse-Kunstleve, R. W., Adams, P. D., Winn, M. D., Storoni, L. C., & Read, R. J. (2007). Phaser crystallographic software. *Journal of Applied Crystallography*, *40*, 658–674.

Meeks, J. C., & Castenholz, R. W. (1971). Growth and photosynthesis in an extreme thermophile, *Synechococcus lividus* (Cyanophyta). *Archives of Microbiology*, *78*, 25–41. https://doi.org/10.1007/BF00409086

Micheletti, E., Pereira, S., Mannelli, F., Moradas-Ferreira, P., Tamagnini, P., & De Philippis, R. (2008). Sheathless mutant of cyanobacterium *Gloeothece* sp. strain PCC 6909 with increased capacity to remove copper ions from aqueous solutions. *Applied and Environment Microbiology*, *74*, 2797–2804. https://doi.org/10.1128/aem.02212-07

Mijakovic, I., Grangeasse, C., & Turgay, K. (2016). Exploring the diversity of protein modifications: Special bacterial phosphorylation systems. *FEMS Microbiology Reviews*, *40*, 398–417. https://doi.org/10.1093/femsre/fuw003

Morona, R., Purins, L., Tocilj, A., Matte, A., & Cygler, M. (2009). Sequence-structure relationships in polysaccharide co-polymerase (PCP) proteins. *Trends in Biochemical Sciences*, *34*, 78–84. https://doi.org/10.1016/j.tibs.2008.11.001

Mota, R., Guimaraes, R., Buttel, Z., Rossi, F., Colica, G., Silva, C. J., … Tamagnini, P. (2013). Production and characterization of extracellular carbohydrate polymer from *Cyanothece* sp. CCY 0110. *Carbohydrate Polymers*, *92*, 1408–1415. https://doi.org/10.1016/j.carbpol.2012.10.070

Mukhopadhyay, A., & Kennelly, P. J. (2011). A low molecular weight protein tyrosine phosphatase from *Synechocystis* sp. strain PCC 6803: Enzymatic characterization and identification of its potential substrates. *The Journal of Biochemistry*, *149*(5), 551–562. https://doi.org/10.1093/jb/mvr014

Osório, H., & Reis, C. A. (2013). Mass spectrometry methods for studying glycosylation in cancer. In R. Matthiesen (Ed.), *Mass spectrometry data analysis in proteomics* (pp. 301–316). Totowa, NJ: Humana Press.

Paiment, A., Hocking, J., & Whitfield, C. (2002). Impact of phosphorylation of specific residues in the tyrosine autokinase, Wzc, on its activity in assembly of group 1 capsules in *Escherichia coli*. *Journal of Bacteriology*, *184*, 6437–6447. https://doi.org/10.1128/JB.184.23.6437-6447.2002

Pereira, S. B., Mota, R., Santos, C. L., De Philippis, R., & Tamagnini, P. (2013). Assembly and export of extracellular polymeric substances (EPS) in cyanobacteria: A phylogenomic approach. In F. Chauvat, & C. Cassier-Chauvat (Eds.), *Advances in botanical research: Genomics of cyanobacteria* (pp. 235–279). San Diego, CA: Academic Press.

Pereira, S. B., Mota, R., Vieira, C. P., Vieira, J., & Tamagnini, P. (2015). Phylum-wide analysis of genes/proteins related to the last steps of assembly and export of extracellular polymeric substances (EPS) in cyanobacteria. *Scientific Reports*, *5*, 14835. https://doi.org/10.1038/srep14835

Pereira, S., Zille, A., Micheletti, E., Moradas-Ferreira, P., De Philippis, R., & Tamagnini, P. (2009). Complexity of cyanobacterial exopolysaccharides: Composition, structures, inducing factors and putative genes involved in their biosynthesis and assembly. *FEMS Microbiology Reviews*, *33*, 917–941. https://doi.org/10.1111/j.1574-6976.2009.00183.x

Pinto, F., Pacheco, C. C., Ferreira, D., Moradas-Ferreira, P., & Tamagnini, P. (2012). Selection of suitable reference genes for RT-qPCR analyses in cyanobacteria. *PLoS One*, *7*, e34983. https://doi.org/10.1371/journal.pone.0034983

Pinto, F., Pacheco, C. C., Oliveira, P., Montagud, A., Landels, A., Couto, N., … Tamagnini, P. (2015). Improving a *Synechocystis*-based photoautotrophic chassis through systematic genome mapping and validation of neutral sites. *DNA Research*, *22*, 425–437. https://doi.org/10.1093/dnares/dsv024

Preneta, R., Jarraud, S., Vincent, C., Doublet, P., Duclos, B., Etienne, J., & Cozzone, A. J. (2002). Isolation and characterization of a protein-tyrosine kinase and a phosphotyrosine-protein phosphatase from *Klebsiella pneumoniae*. *Comparative Biochemistry and Physiology Part B: Biochemistry and Molecular Biology*, *131*, 103–112. https://doi.org/10.1016/s1096-4959(01)00490-0

Raugei, G., Ramponi, G., & Chiarugi, P. (2002). Low molecular weight protein tyrosine phosphatases: Small, but smart. *Cellular and Molecular Life Sciences*, *59*, 941–949. https://doi.org/10.1007/s00018-002-8481-z

Ristl, R., Steiner, K., Zarschler, K., Zayni, S., Messner, P., & Schaffer, C. (2011). The S-layer glycome-adding to the sugar coat of bacteria. *International Journal of Microbiology*, *2011*, 127870. https://doi.org/10.1155/2011/127870

Roca, C., Alves, V. D., Freitas, F., & Reis, M. A. (2015). Polysaccharides enriched in rare sugars: Bacterial sources, production and applications. *Frontiers in Microbiology*, *6*, 288.

Rosen, B. P. (1986). Ion extrusion systems in *Escherichia coli*. *Methods in Enzymology*, *125*, 328–336. https://doi.org/10.1016/s0076-6879(86)25028-4

Rossi, F., & De Philippis, R. (2016).Exocellular polysaccharides in microalgae and cyanobacteria: chemical features, role and enzymes and genes involved in their biosynthesis. In M. A. Borowitzka, J. Beardall, & J. A. Raven (Eds.), *The physiology of microalgae* (pp. 565–590). Cham, Switzerland: Springer International Publishing.

Sambrook, J., & Russell, D. W. (2001). *Molecular cloning: A laboratory manual*. New York, NY: Cold Spring Harbor Laboratory Press.

Sato, S., Shimoda, Y., Muraki, A., Kohara, M., Nakamura, Y., & Tabata, S. (2007). A large-scale protein-protein interaction analysis in *Synechocystis* sp. PCC6803. *DNA Research*, *14*, 207–216. https://doi.org/10.1093/dnares/dsm021

Schmid, J., Sieber, V., & Rehm, B. (2015). Bacterial exopolysaccharides: Biosynthesis pathways and engineering strategies. *Frontiers in Microbiology*, *6*, 496. https://doi.org/10.3389/fmicb.2015.00496

Schneider, C. A., Rasband, W. S., & Eliceiri, K. W. (2012). NIH Image to ImageJ: 25 years of Image analysis. *Nature Methods*, *9*, 671–675. https://doi.org/10.1038/nmeth.2089

Schrödinger, L. (2010). *The PyMOL molecular graphics system, version 1.3r1*.

Seabra, R., Santos, A., Pereira, S., Moradas-Ferreira, P., & Tamagnini, P. (2009). Immunolocalization of the uptake hydrogenase in the marine cyanobacterium *Lyngbya majuscula* CCAP 1446/4 and two *Nostoc* strains. *FEMS Microbiology Letters*, *292*, 57–62.

R., Martínez-García, E., Calles, B., Chavarría, M., Arce-Rodríguez, A., Silva-Rocha de las Heras, A., …deLorenzo, V. (2013). The Standard European Vector Architecture (SEVA): A coherent platform for the analysis and deployment of complex prokaryotic phenotypes. *Nucleic Acids Research*, *41*, D666–D675. https://doi.org/10.1093/nar/gks1119

Simkovsky, R., Daniels, E. F., Tang, K., Huynh, S. C., Golden, S. S., & Brahamsha, B. (2012). Impairment of O-antigen production confers resistance to grazing in a model amoeba-cyanobacterium predator-prey system. *Proceedings of the National Academy of Sciences*, *109*, 16678–16683. https://doi.org/10.1073/pnas.1214904109

Standish, A. J., & Morona, R. (2014). The role of bacterial protein tyrosine phosphatases in the regulation of the biosynthesis of secreted polysaccharides. *Antioxidants and Redox Signaling*, *20*, 2274–2289. https://doi.org/10.1089/ars.2013.5726

Stanier, R. Y., Kunisawa, R., Mandel, M., & Cohen-Bazire, G. (1971). Purification and properties of unicellular blue-green algae (order Chroococcales). *Bacteriological Reviews*, *35*, 171–205.

Tamagnini, P., Troshina, O., Oxelfelt, F., Salema, R., & Lindblad, P. (1997). Hydrogenases in *Nostoc* sp. Strain PCC 73102, a strain lacking a bidirectional enzyme. *Applied and Environment Microbiology*, *63*, 1801–1807.

Tamura, K., Stecher, G., Peterson, D., Filipski, A., & Kumar, S. (2013). MEGA6: Molecular Evolutionary Genetics Analysis Version 6.0. *Molecular Biology and Evolution*, *30*, 2725-2729.

Trautmann, D., Voß, B., Wilde, A., Al-Babili, S., & Hess, W. R. (2012). Microevolution in Cyanobacteria: Re-sequencing a Motile Substrain of *Synechocystis* sp. PCC 6803. *DNA Research*, *19*, 435–448. https://doi.org/10.1093/dnares/dss024

Vega, C., Chou, S., Engel, K., Harrell, M. E., Rajagopal, L., & Grundner, C. (2011). Structure and substrate recognition of the *Staphylococcus aureus* protein tyrosine phosphatase PtpA. *Journal of Molecular Biology*, *413*, 24–31. https://doi.org/10.1016/j.jmb.2011.08.015

Whitfield, C., & Trent, M. S. (2014). Biosynthesis and export of bacterial lipopolysaccharides. *Annual Review of Biochemistry*, *83*, 99–128. https://doi.org/10.1146/annurev-biochem-060713-035600

Williams, J. G. K. (1988). Construction of specific mutations in photosystem II photosynthetic reaction center by genetic engineering methods in Synechocystis 6803. In L. Packer, & A. N. Glazer (Eds.), (pp. 766–778). San Diego, CA: Academic Press.

Zhang, Z. Y. (1998). Protein-tyrosine phosphatases: Biological function, structural characteristics, and mechanism of catalysis. *Critical Reviews in Biochemistry and Molecular Biology*, *33*, 1–52. https://doi.org/10.1080/10409239891204161

SUPPORTING INFORMATION

Additional supporting information may be found online in the Supporting Information section at the end of the article.

How to cite this article: Pereira SB, Santos M, Leite JP, et al. The role of the tyrosine kinase Wzc (Sll0923) and the phosphatase Wzb (Slr0328) in the production of extracellular polymeric substances (EPS) by *Synechocystis* PCC 6803. *MicrobiologyOpen*. 2019;8:e753. https://doi.org/10.1002/mbo3.753

Supporting information

The tyrosine kinase Wzc (Sll0923) and the phosphatase Wzb (Slr0328) play a role in the production of extracellular polymeric substances (EPS) in *Synechocystis* PCC 6803

Sara B. Pereira,[1,2†] Marina Santos,[1,2,3†] José P. Leite,[1,2,3] Carlos Flores,[1,2,3] Carina Eisfeld,[1,2‡] Zsófia Büttel,[2§] Rita Mota,[1,2,3] Federico Rossi,[4] Roberto De Philippis,[4] Luís Gales,[1,2,3] João H. Morais-Cabral,[1,2] and Paula Tamagnini[1,2,5*]

[1]i3S - Instituto de Investigação e Inovação em Saúde, Universidade do Porto, Porto Portugal.

[2]IBMC - Instituto de Biologia Molecular e Celular, Universidade do Porto, Porto, Portugal.

[3]ICBAS – Instituto de Ciências Biomédicas Abel Salazar, Porto, Portugal.

[4]Department of Agrifood Production and Environmental Sciences, University of Florence, Florence, Italy.

[5]Faculdade de Ciências, Departamento de Biologia, Universidade do Porto, Porto, Portugal.

[*]For correspondence. E-mail pmtamagn@ibmc.up.pt; Tel. +351 220 408 800.

[†]These authors contributed equally to this work.

[‡]Present address: Department of Water Management, Delft University of Technology, Delft, The Netherlands.

[§]Present address: Molecular Microbiology, Groningen Biomolecular Sciences and Biotechnology Institute, University of Groningen, Groningen, The Netherlands.

PCR protocols

Construction of pGDsll0727, pGDsll5049, pGDslr2107, pGDslr0328 and *pGDsll0923*$_{Trunc}$

For the amplification of *sll0727*, *sll5049*, *slr2107* and *slr0328* flanking regions, each PCR reaction mixture (50 µL) contained 1.5 u of *Pfu* DNA polymerase (Thermo Scientific), 1x reaction buffer, 250 µM of each deoxyribonucleotide triphosphate, 200 nM of each primer (primer pairs 5O/5I or 3O/3I), and 7 ng of *Synechocystis* genomic DNA. For the amplification of *sll0923*$_{Trunc}$ flanking regions, each PCR reaction mixture (50 µL) contained 1x Accuzyme reaction mix (Bioline), 200 nM of each primer (primer pairs 5O/5I or 3O/3I), and 12.6 ng of *Synechocystis* genomic DNA. The PCR profile was: 1 min at 94°C followed by 35 cycles of 30 s at 94°C, 45 s at 52°C (*sll0737*) or 48ºC (*sll5049* and *slr2107*) and 90 s at 72°C, and a final extension at 72°C for 7 min. For *slr0328*, the PCR profile was: 3 min at 94°C followed by 40 cycles of 1 min at 94°C, 1min at 48°C and 1min at 72°C, and a final extension at 72°C for 7 min. For *pGDsll0923*$_{Trunc}$ the PCR profile was: 1 min at 95°C followed by 35 cycles of 15 s at 95°C, 15 s at 52°C and 2 min at 72°C, and a final extension at 72°C for 7 min.

For the Overlap PCR, each reaction mixture (50 µL) contained 1.25 u of GoTaq® Flexi DNA polymerase (Promega), 1x Green GoTaq® Flexi Buffer, 1.5 µM $MgSO_4$, 250 µM of each deoxyribonucleotide triphosphate, 125 nM of each outer primer (5O and 3O), and 80 ng of each purified DNA fragment. The PCR profile used for *sll0737* and *sll5049* was: 5 min at 95°C, 10 cycles of 30 s at 95°C, 45 s at 48°C and 90 s at 72°C, followed by 30 cycles of 30 s 95°C 45 s at 55°C and 90 s at 72°C and a final extension at 72°C for 7 min. The PCR profile for *slr2107* was: 5 min at 95°C followed by 40 cycles of 30 s at 95 °C, 45 s at 55 °C and 90 s at 72 °C, and a final extension at 72 °C for 7 min. The PCR profile for *slr0328* was: 5 min at 94°C, followed by 40 cycles of 1 min at 94°C, 110 s at 56°C and 110 s at 72°C and a final extension at 72 °C for 7 min.

The PCR profile for *sll0923*$_{Trunc}$ was: 5 min at 95°C, followed by 10 cycles of 30 s at 95°C, 45 s at 48°C and 2 min at 72°C, 30 cycles of 30 s at 95°C, 45 s at 56°C and 2 min at 72°C and a final extension at 72 °C for 7 min.

Amplification Km resistance cassette from pKm.1

The PCR reaction mixture (50 µL) contained 1.25 u of *Pfu* polymerase (Thermo Scientific), 1x reaction buffer, 250 µM of each deoxyribonucleotide triphosphate, 200 nM of each primer and 10 ng of template DNA. The PCR profile was: 1 min at 95°C followed by 35 cycles of 60 s at 94°C, 45 s at 52°C and 3 min at 72°C, and a final extension at 72°C for 7 min.

Construction of pS351sll0923

For the amplification of a fragment covering *wzc* and its native promoter (P_{wzc}) and RBS, each PCR reaction mixture (20 µL) contained 0.4 u of *Phusion* DNA polymerase (Thermo Scientific), 1x *Phusion* HF reaction buffer, 200 µM of each deoxyribonucleotide triphosphate, 500 nM of each primer and 15 ng of *Synechocystis* genomic DNA. The PCR profile was: 30 s at 98°C followed by 35 cycles of 20 s at 98°C, 40 s at 68°C and 50 s at 72°C, and a final extension at 72°C for 10 s.

Construction of pS351sll0923$_{Trunc}$

For the amplification of a fragment covering *wzc*$_{Trunc}$ and its native promoter (P_{wzc}) and RBS, each PCR reaction mixture (50 µL) contained 1 u of *Phusion* DNA polymerase (Thermo Scientific), 1x *Phusion* HF reaction buffer, 200 µM of each deoxyribonucleotide triphosphate, 250 nM of each primer and 15 ng of *Synechocystis* genomic DNA. The PCR

profile was: 30 s at 98°C followed by 35 cycles of 10 s at 98°C, 30 s at 62°C and 90 s at 72°C, and a final extension at 72°C for 10 s.

Construction of pS351slr0328

For the amplification of a fragment covering *wzb* and incorporating the synthetic RBS BBa_B0030, each PCR reaction mixture (20 µL) contained 0.4 u of *Phusion* DNA polymerase (Thermo Scientific), 1x *Phusion* HF reaction buffer, 200 µM of each deoxyribonucleotide triphosphate, 500 nM of each primer and 15 ng of *Synechocystis* genomic DNA. The PCR profile was: 30 s at 98°C followed by 35 cycles of 20 s at 98°C, 40 s at 68°C and 15 s at 72°C, and a final extension at 72°C for 10 s.

Table S1. List of organisms and plasmids used/generated in this work.

Organism name/Genotype	**Description**	**Source**
Escherichia coli DH5α	Transformation/cloning strain.	Invitrogen
Escherichia coli XL1-Blue	Transformation/cloning strain.	Agilent
Escherichia coli M15 (pREP4)	Protein overexpression/purification strain.	QIAGEN
Synechocystis sp. PCC 6803	Wild type strain.	Pasteur Culture Collection
Δ*wzy*	*Synechocystis* mutant with *sll0727* replaced by a Km resistance cassette.	This work
Δ*wzx*	*Synechocystis* mutant with *sll5049* replaced by a Km resistance cassette.	This work
Δ*kpsM*	*Synechocystis* mutant with *slr2107* replaced by a Km resistance cassette.	This work
Δ*kpsM*Δ*wzy*	*Synechocystis* mutant with *slr2107* and *sll0727* replaced by a Km or a Sm/Sp cassettes, respectively.	This work
Δ*wzc*	*Synechocystis* mutant with *sll0923* replaced by a Km resistance cassette.	This work
Δ*wzb*	*Synechocystis* mutant with *slr0328* replaced by a Km resistance cassette.	This work
Δ*wzc*Δ*wzb*	*Synechocystis* mutant with *sll0923* and *slr0328* replaced by a Km or a Sm/Sp cassettes, respectively.	This work
Δ*wzb* pS351slr0328	*Synechocystis* Δ*wzb* mutant complemented with the replicative plasmid pS351sll0923.	This work
Δ*wzc* pS351sll0923	*Synechocystis* Δ*wzc* mutant complemented with the replicative plasmid pS351sll0923.	This work
Wzc_{trunc}	*Synechocystis* mutant with *sll0923* replaced by a truncated form of the gene (from 1 to 2196 bp) and a Km resistance cassette.	This work

Δ*wzc* pS351sll0923$_{Trunc}$	*Synechocystis* Δ*wzc* mutant complemented with the replicative plasmid pS351sll0923$_{Trun}$.	This work

Plasmid	**Description**	**Source**
pGEM®-T easy	T/A cloning vector.	Promega
pSEVA351	Replicative shuttle vector for *Synechocystis* transformation.	SEVA-DB (Silva-Rocha *et al.*, 2013)
pSEVA481	Source of the Sm resistance cassette.	SEVA-DB (Silva-Rocha *et al.*, 2013)
pKm.1	pGEM-T easy with the Km resistance cassette.	(Pinto *et al.*, 2015)
pGDsll0727	pGEM-T easy with *sll0727* and its flanking sequences, where the *sll0727* coding sequence (from 14 to 2475 bp) was replaced by a *Xma*I site.	This work
pGDsll0727.Km	pGDsll0727 with a Km resistance cassette inserted into the *Xma*I site.	This work
pGDsll0727.Sm	pGDsll0727 with a Sm/Sp resistance cassette inserted into the *Sma*I site.	This work
pGDsll0549	pGEM-T easy with *sll5049* and its flanking sequences, where the *sll5049* coding sequence (from 145 to 1310 bp) was replaced by a *Xma*I site.	This work
pGDsll0549.Km	pGDsll0549 with a Km resistance cassette inserted into the *Xma*I site.	This work
pGDslr2107	pGEM-T easy with *slr2107* and its flanking sequences, where the *slr2107* coding sequence (from 52 to 821 bp) was replaced by a *Xma*I site.	This work
pGDslr2107.Km	pGDslr2107 with a Km resistance cassette inserted into the *Xma*I site.	This work
pGDslr0328	pGEM-T easy with *slr0328* and its flanking sequences, where the *slr0328* coding sequence (from 214 to 383 bp) was replaced by a *Xma*I site.	This work

pGDslr0328.Km	pGDslr0328 with a Km resistance cassette inserted into the *Xma*I site.	This work
pGDslr0328.Sm	pGDslr0328 with a Sm/Sp resistance cassette inserted into the *Xma*I site.	This work
pDsll0923::Km^r	pDsll0923 with a Km resistance cassette inserted into a *SmaI* site.	(Jittawuttipoka *et al.*, 2013)
pGDsll0923$_{Trunc}$	pGEM-T easy with *sll0923* (from 1461 to 2193 bp) and its flanking sequence, where the last 78 bp of *sll0923* were replaced by a *Xma*I site.	This work
pGDsll0923$_{Trunc}$.Km	pGDsll0923$_{Trunc}$ with a Km resistance cassette inserted into the *Xma*I site.	This work
pSB1C3	Source of the promoter of *rnpB* (P_{rnpB}).	Registry of Standard Biological Parts (http://parts.igem.org).
pS351P_{rnpB}	pSEVA351 with P_{rnpB}.	This work
pS351slr0328	pSEVA351 with slr0328 downstream the synthetic RBS BBa_B0030, under the control of P_{rnpB}.	This work
pS351sll0923	pSEVA351 with *sll0923* downstream its native RBS and under the control of its native promoter P_{wzc} (-230 to +123).	This work
pS351sll0923$_{Trunc}$	pSEVA351 with a truncated *sll0923* (from 1 to 2196 bp) downstream its native RBS and under the control of P_{wzc}.	This work
pQE-30::His6-Wzc	pQE-30 with *sll0923* with 6xHis tag coding sequence at 5'.	This work
pQE-30::His6-Wzc$_{trunc}$	pQE-30 with a truncated *sll0923* (from 1 to 2196 bp) with 6xHis tag coding sequence at 5'.	This work

Table S2. Oligonucleotides used in this work.

Name	Sequence (5'-3')	Purpose	Reference
sll0737.5O	TGTTGAGGTGGAAGCAGCGGAGCCCAAAGG		This work
sll0737.5I	GAACCAAGTTACCAGCCCGGGAATCGGCGGCC ATACTGGGCAATACTCACAGG		This work
sll0737.3I	TATGGCCGCCGATTCCCGGGCTGGTAACTTGG TTCCCGTTTATGTTGCCTTCCC		This work
sll0737.3O	CTTCCTCTGCATACTGCCCAGCGGGAACAC		This work
sll5049.5O	TTGCCGAGTTTCGCCGAAGGTTTACCG		This work
sll5049.5I	ATCGGTAAACCCAGTCCCGGGTACCAACGCCA TCAGGCCAAACATTTCCG		This work
sll5049.3I	CCTGATGGCGTTGGTACCCGGGACTGGGTTTA CCGATTGAAGCGTTATGG		This work
sll5049.3O	TCAACACTATTGGGCACAAGGGAGACTTGGG		This work
slr2107.5O	CGCAGGCAATTGAAGATATAAAGTGGTGGATT CAAC		This work
slr2107.5I	ACGGCATCGCCAAACCCGGGACGACTCTCCGG CGTATAAACAATGACTGGTTGCG	Amplification of flanking region; 5I and 3I: overlap PCR	This work
slr2107.3I	TACGCCGGAGAGTCGTCCCGGGTTTGGCGATG CCGTTTATTGTTGAG		This work
slr2107.3O	CAATCTCCGCAAACGCCACCACATCCTCAAAT CG		This work
slr0328.5O	CACTTCCTTTGCCGTCAAAGTTGCTTCCAT		This work
slr0328.5I	CTCAAAACCAGCCTGCCCGGGCTGTCTAGCTC TTCCCTGCACCCGATAA		This work
slr0328.3I	GGGAAGAGCTAGACAGCCCGGGCAGGCTGGT TTTGAGCATGTGATTGATT		This work
slr0328.3O	CCGTAGGGTTTGGGCAGAAGCATGTTGCT		This work
sll0923.5O	GAGAGCTAGTCAGCACCACACCATCCT		This work
sll0923.5I	CTGTGCTCCCGATCCCGGGTTATTAGCCGGAC GTAGAAGTGATAGCATTGG		This work
sll0923.3I	ACGTCCGGCTAATAACCCGGGATCGGGAGCAC AGAACCCCACCTTGCGG		This work
sll0923.3O	CGGCGAGATTTAGACTTGCCTTGGCTAGA		This work

Km.KmScFwd	CTGACCCCGGGTGAATGTCAGCTACTGG	Amplification of Km resistance cassette	(Pinto *et al.*, 2015)
KmRev	CAAACCCGGGCGATTTACTTTTCGACCTC		(Pinto *et al.*, 2015)
sll0923_compF1	TCTAGAGGTTCTGCGTTAGCATCACA	Amplification of *wzc* or wzc_{Trunc}, native promoter and RBS	This work
sll0923_compR1	GCACTAGTCGATTAGCTCAGTTGGTAGA	Amplification of *wzc*, native promoter and RBS	This work
sll0923.RTrunc	GCACTAGTCTAGCCGGACGTAGAAGTGATA	Amplification of wzc_{Trunc}, native promoter and RBS	This work
slr0328_compF	GTTTCTTCGAATTCGCGGCCGCTTCTAGAGATTAAAGAGGAGAAAACTAGATGAAATTGTTATTTGTTTG	Amplification of *wzb* introducing B0030	This work
slr0328_compR	GTTTCTTCCTGCAGCGGCCGCTACTAGTACTAATTAACCAATTCCTTGC	Amplification of *wzb*	This work
sll0738F	GCTTGGTTTTGGCTACTGATCCT		This work
sll0738R	GGCGTAAACTATCCCAGCATC		This work
sll5048F	CAGCCTCTACCTAAACCTGGA		This work
sll5048R	GAATCGCCAAATCCGTTCCT		This work
slr2108F	CGGTAGTGATGTGGTGCTGT		This work
slr2108R	GCCGTTTCACAAATGCGAGT	Amplification of Southern blot probes	This work
sll0923F_SB	CCGCTAAATCCAAAGGCGA		This work
sll0923R_SB	CCCAGGCAGACAATTAGGAT		This work
sll0923F2_SB	CTGAAGCCAGTAGCAGCCAAC		This work
sll0923R2_SB	CGCTCTACCAACTGAGCTAATC		This work
slr0328F_SB	CCATTGCCATCCTGGTCTA		This work
slr0328R_SB	CCACATGGTAGCTGGAAGTA		This work
Ovslr0328F	TTTTGGCATGCAAATTGTTATTTGTTTGTTTAGG	*wzb* amplification	This work
Ovslr0328R	CAACCTGCAGCTAATTAACCAATTCCTTGCCC		This work
OvSll0923F	CAAGGGATCCACCTACAGTTACCCAGAATTG	*wzc* amplification	This work
OvSll0923R	CTCCTGCAGCTAATTGTCTGCCTGGGCA		This work

sll0737F(Ra)	CGGTTAGTTCCCCTTCATCCACT		This work
sll0737RO	GGGTAAACCACAGCAAAAGACTAA		This work
slr1515F	GGCAGTGTGCTCCATCGTTT		This work
slr1515R	CCGAAATGCACCAGTAGGCAA		This work
slr0728F	GCAACTCAATACCCTAGCTTGGC		This work
slr0728R	GGAGGAAGATTGAAGCGGTTAC		This work
sll5047F	TGTGACCGATAGCCTCTGGA		This work
sll5047R	CTGATTTCGTGCCTGCCCTA		This work
slr1074F	TGGCTACATTCTGGCTCTGC		This work
slr1074R	CCGTCTTGTAAAGGCGATGC		This work
sll5049F(Ra)	CCATTCGTGGCACCATTTGGACT		This work
sll5049RI	GCCGTGTTGAGAAAACTAGGCT		This work
slr1543F	TATGGGTGGCGGGACTAAGA	RT-PCR	This work
slr1543R	CCCAATAGCCAGCCCAAGAT		This work
slr0896F	TTTGGCACAAACCCCTCCAT		This work
slr0896R	ACCAATACTCACCAAGGCCG		This work
slr0488F	AAACCGTTACCACCCTGGTC		This work
slr0488R	GCGACCCCTAAACCCAGAAT		This work
slr2107F(Ra)	GACCCATCGTCAATCGCAAC		This work
slr2107RO	CCGTCACAATCGGTGGCAAA		This work
slr0977F	CGCACGGAGCGTCAGTATT		This work
slr0977RO	CCGCAAACACCAGAATGGGAT		This work
sll0574F	CGAAAGCACAACCAACCCAG		This work
sll0574R	GCCATTACCCCTATTGGCGA		This work

Underlined base pairs correspond to restriction sites.

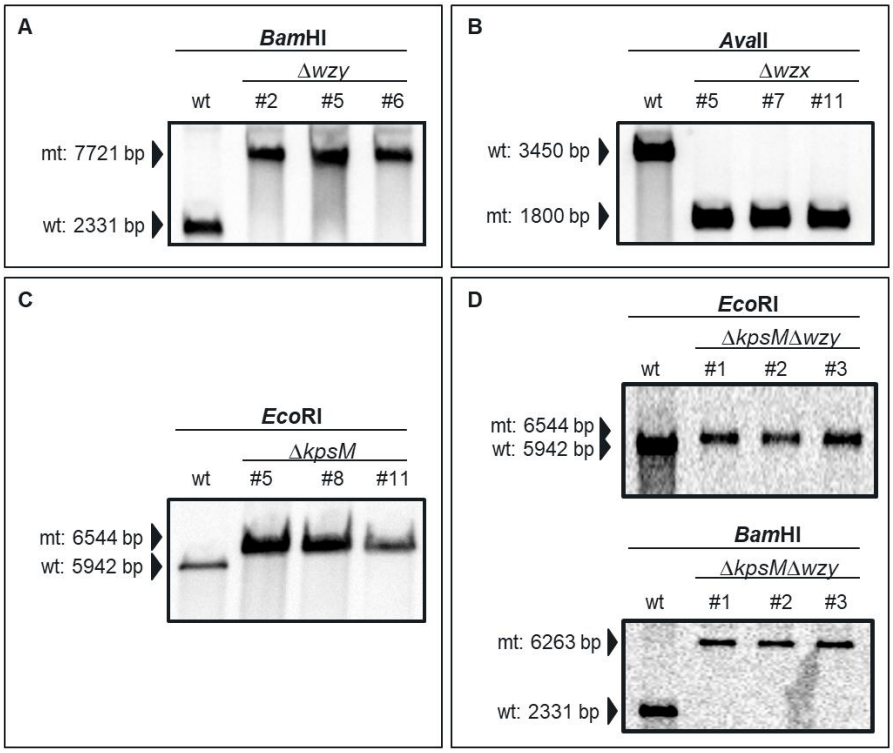

Fig. S1. Southern blot analysis confirming the segregation of the *Synechocystis* sp. PCC 6803 mutants (A) Δ*wzy*, (B) Δ*wzx*, (C) Δ*kpsM* and (D) Δ*kpsM*Δ*wzy* (Δ*kpsM* segregation – upper blot; Δ*wzy* segregation – lower blot). The DNAs were digested with the endonuclease indicated. A dioxigenin labeled probe covering the 3' flanking region of *wzy*, *wzx* or *kpsM*, repectively was used. The sizes of the DNA fragments are indicated. wt – wild type; # clone tested.

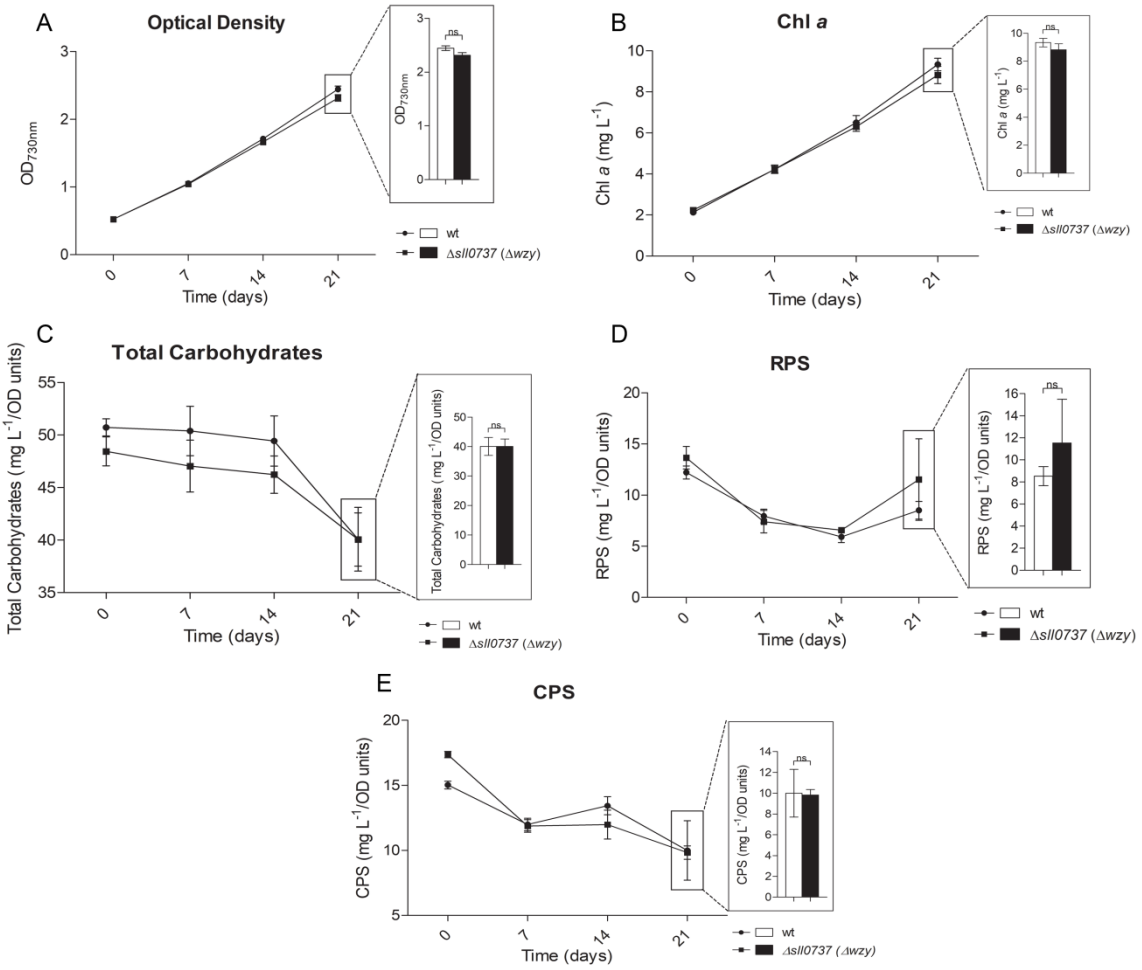

Fig. S2. Characterization of *Synechocystis* sp. PCC 6803 wild type and Δ*wzy* mutant in terms of growth [(A) optical density at λ=730nm (OD_{730nm}) and (B) µg of chlorophyll *a* per mL of culture (Chl *a*)], and production of (C) total carbohydrates, (D) released polysaccharides (RPS) and (E) capsular polysaccharides (CPS) expressed as mg per $OD730_{nm}$ units. Cells were grown in BG11 medium at 30 ºC, under a 12 h light (50 µE m^{-2} s^{-1})/12 h dark regimen at 150 rpm. Experiments were performed in triplicate. Data are means ± SD. Statistical analysis performed using one-way analysis of variance (ANOVA), followed by Tukey's multiple comparisons is presented for the last time point. Ns: no significant differences.

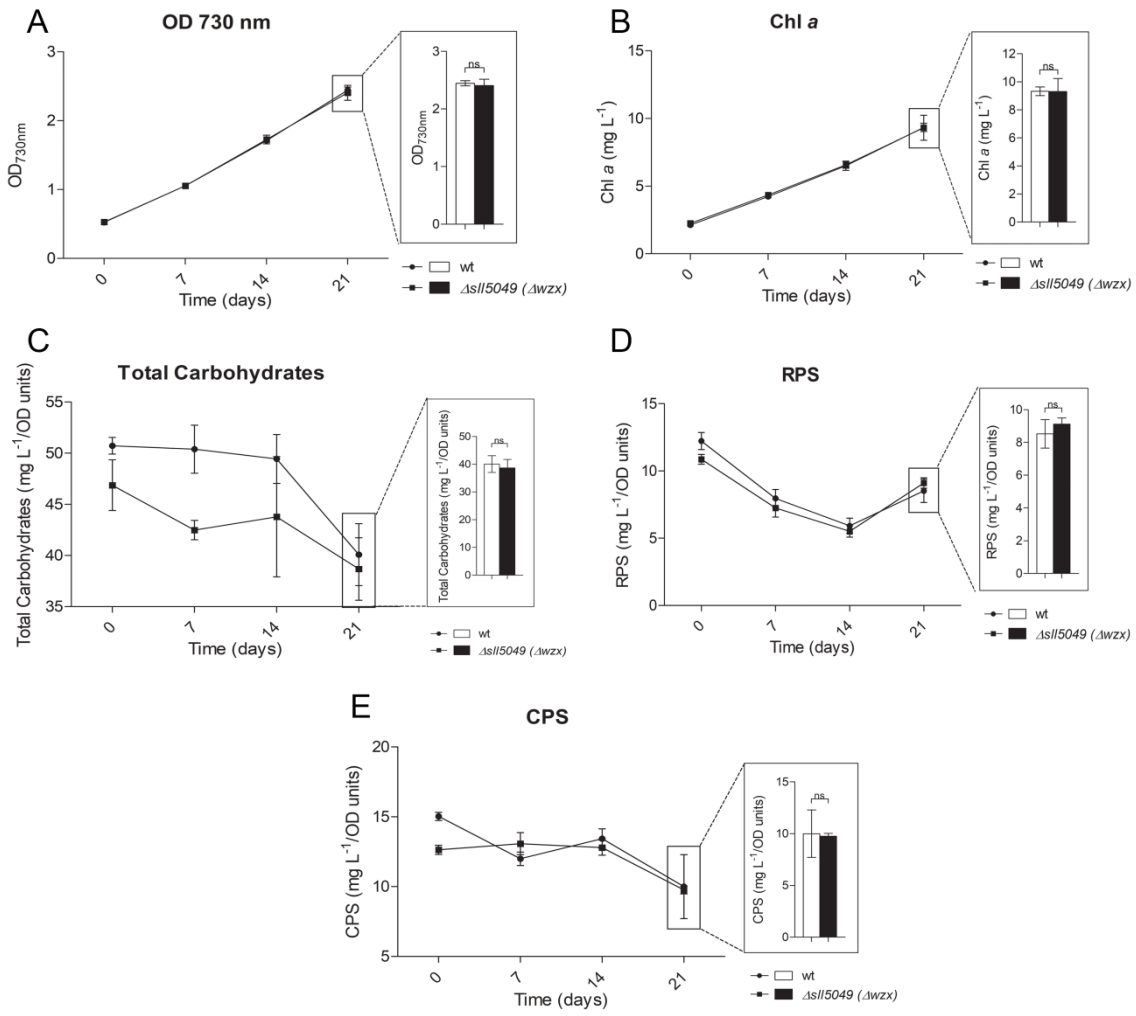

Fig. S3. Characterization of *Synechocystis* sp. PCC 6803 wild type and Δ*wzx* mutant in terms of growth [(A) optical density at λ=730nm (OD_{730nm}) and (B) µg of chlorophyll *a* per mL of culture (Chl *a*)], and production of (C) total carbohydrates, (D) released polysaccharides (RPS) and (E) capsular polysaccharides (CPS) expressed as mg per $OD730_{nm}$ units. Cells were grown in BG11 medium at 30 ºC, under a 12 h light (50 µE m^{-2} s^{-1})/12 h dark regimen at 150 rpm. Experiments were performed in triplicate. Data are means ± SD. Statistical analysis performed using one-way analysis of variance (ANOVA), followed by Tukey's multiple comparisons is presented for the last time point. Ns: no significant differences.

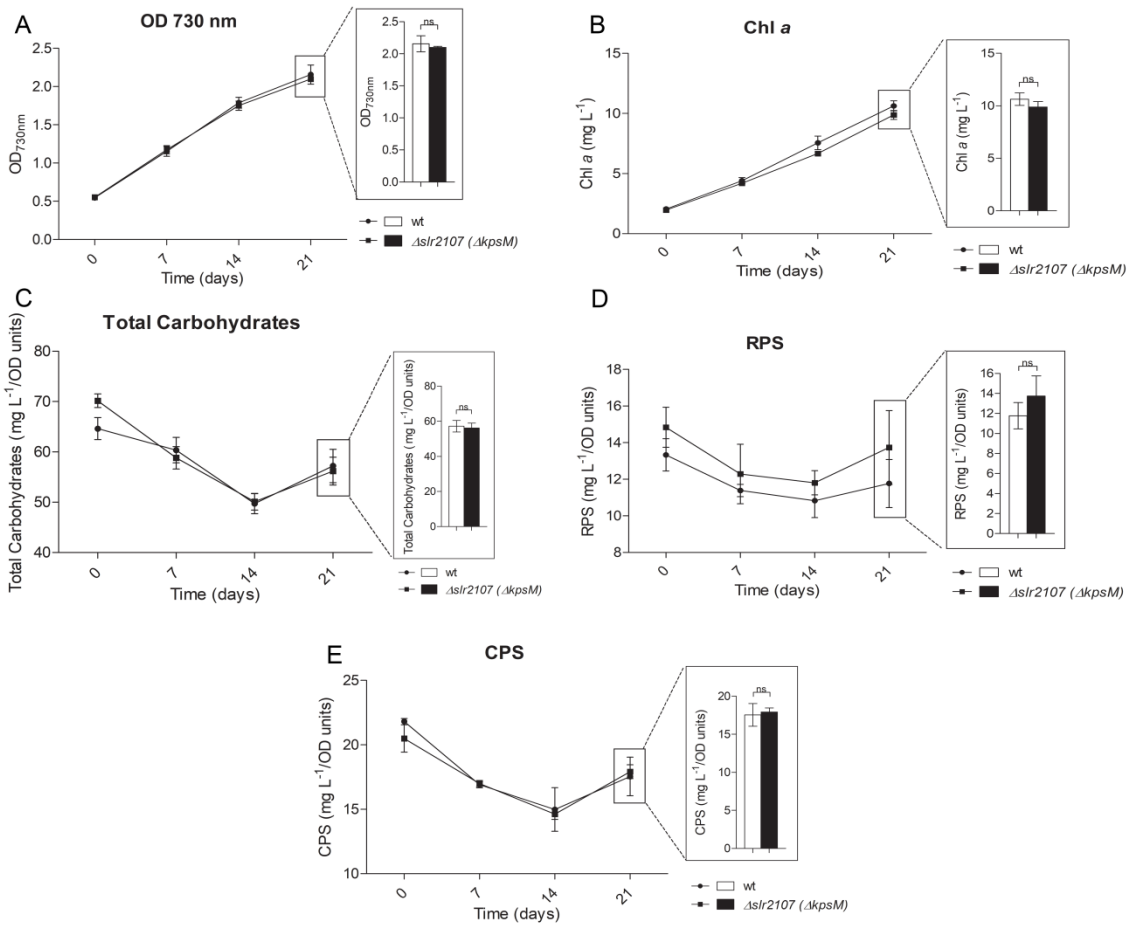

Fig. S4. Characterization of *Synechocystis* sp. PCC 6803 wild type and Δ*kpsM* mutant in terms of growth [(A) optical density at λ=730nm (OD_{730nm}) and (B) µg of chlorophyll *a* per mL of culture (Chl *a*)], and production of (C) total carbohydrates, (D) released polysaccharides (RPS) and (E) capsular polysaccharides (CPS) expressed as mg per $OD730_{nm}$ units. Cells were grown in BG11 medium at 30 ºC, under a 12 h light (50 µE m^{-2} s^{-1})/12 h dark regimen at 150 rpm. Experiments were performed in triplicate. Data are means ± SD. Statistical analysis performed using one-way analysis of variance (ANOVA), followed by Tukey's multiple comparisons is presented for the last time point. Ns: no significant differences.

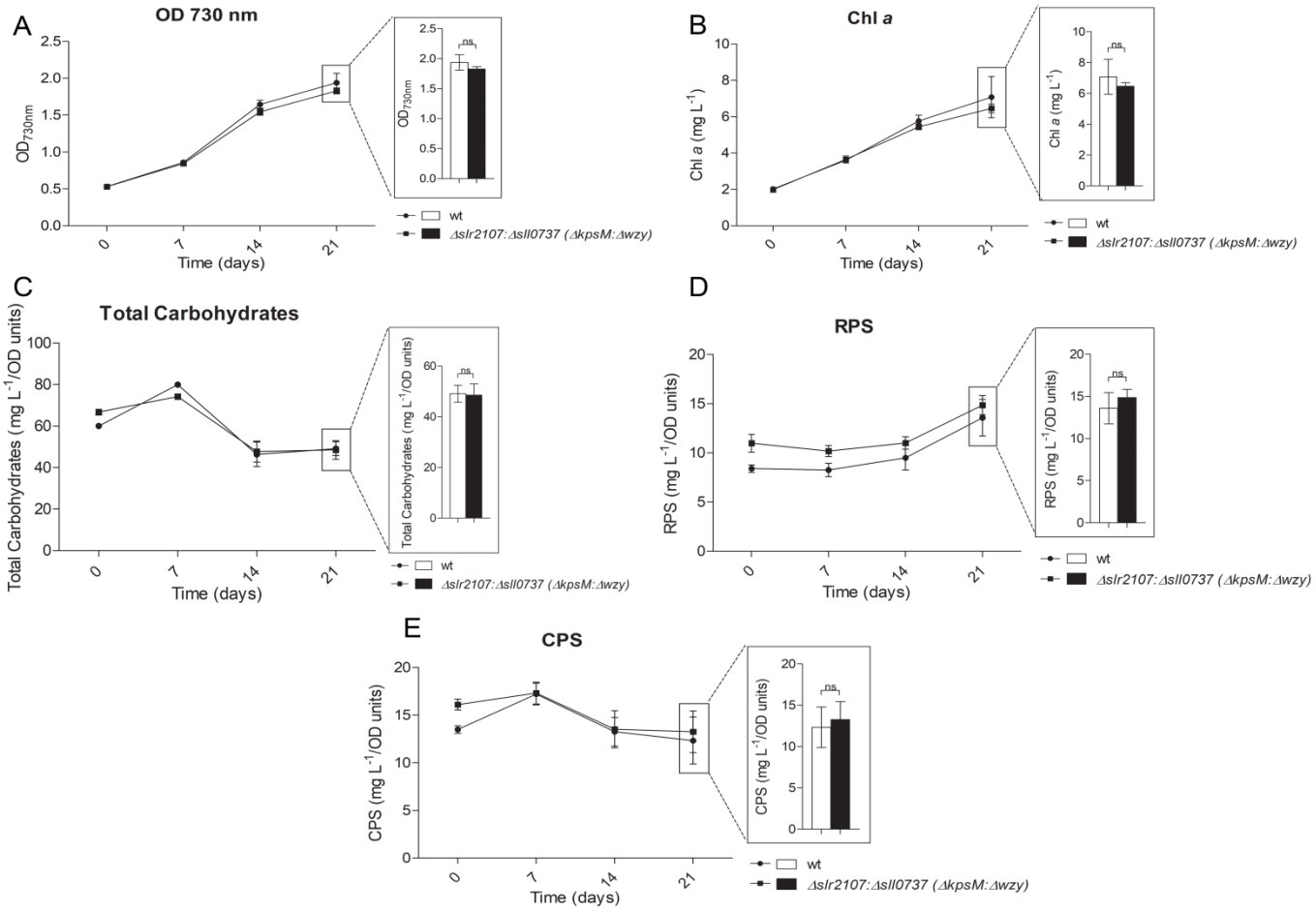

Fig. S5. Characterization of *Synechocystis* sp. PCC 6803 wild type and Δ*kpsM*Δ*wzy* mutant in terms of growth [(A) optical density at λ=730nm (OD_{730nm}) and (B) µg of chlorophyll *a* per mL of culture (Chl *a*)], and production of (C) total carbohydrates, (D) released polysaccharides (RPS) and (E) capsular polysaccharides (CPS) expressed as mg per $OD730_{nm}$ units. Cells were grown in BG11 medium at 30ºC, under a 12 h light (50 µE m^{-2} s^{-1})/12 h dark regimen at 150 rpm. Experiments were performed in triplicate. Data are means ± SD. Statistical analysis performed using one-way analysis of variance (ANOVA), followed by Tukey's multiple comparisons is presented for the last time point. Ns: no significant differences.

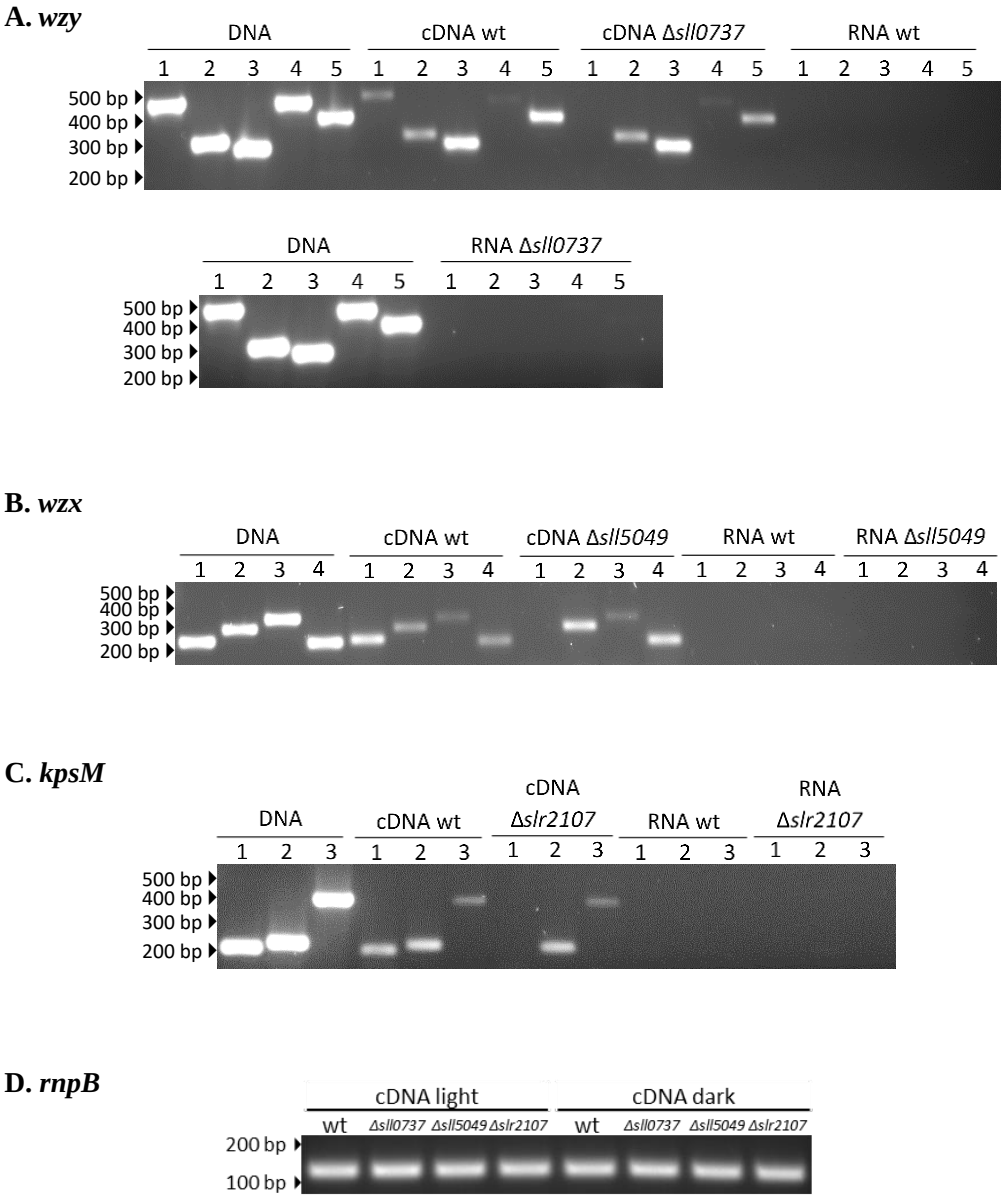

Fig. S6. Transcription profiles, evaluated by RT-PCR, of the putative *wzy* (A), *wzx* (B) and *kpsM* (C) gene copies in *Synechocystis* sp. PCC 6803 wild type (wt) and Δ*wzy* (Δ*sll0737*), Δ*wzx* (Δ*sll5049*) and Δ*kpsM* (Δ*slr2107*) mutants, respectively. Samples for RNA extraction were collected 6h into the light period of the 12h light (50 μE m^{-2} s^{-1}) / 12h dark growth regimen at 30ºC. The cDNAs were produced with random primers and used in PCR amplifications with specific primer pairs. Expected size of PCR products: *wzy*: 1 – *sll0737* (465 bp); 2 – *slr0728* (288 bp); 3 – *slr1515* (256 bp); 4 – *sll5074* (440 bp); 5 – *slr1074* (368 bp); *wzx*: 1 – *sll5049* (223 bp); 2 – *slr0488* (274 bp); 3 – *slr0896* (323 bp); 4- *slr1543* (208

bp); *kpsM*: 1 – *slr2107* (203 bp); 2 – *slr0977* (220 bp); 3 – *sll0564* (396 bp). RT-PCR controls were performed using RNA from *Synechocystis* wild-type and mutants as template. Amplification of the housekeeping gene *rnpb* was used as positive control (D) (Pinto *et al.*, 2012).

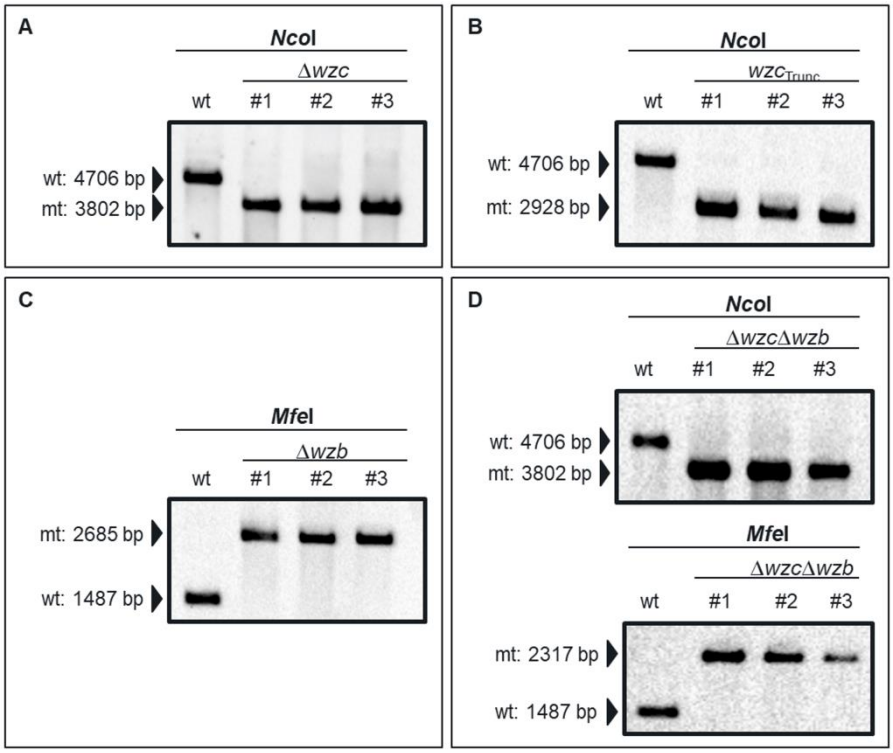

Fig. S7. Southern blot analysis confirming the segregation of the *Synechocystis* sp. PCC 6803 mutants (A) Δ*wzc*, (B) *wzc*$_{\text{Trunc,}}$ (C) Δ*wzb* and (D) Δ*wzc*Δ*wzb* (Δ*wzc* segregation – upper blot; Δ*wzb* segregation – lower blot). The DNAs were digested with the endonuclease indicated. A dioxigenin labeled probe covering the 5′ or 3' flanking region of *wzb* or *wzc*, repectively was used. The sizes of the DNA fragments are indicated. wt – wild type; # clone tested.

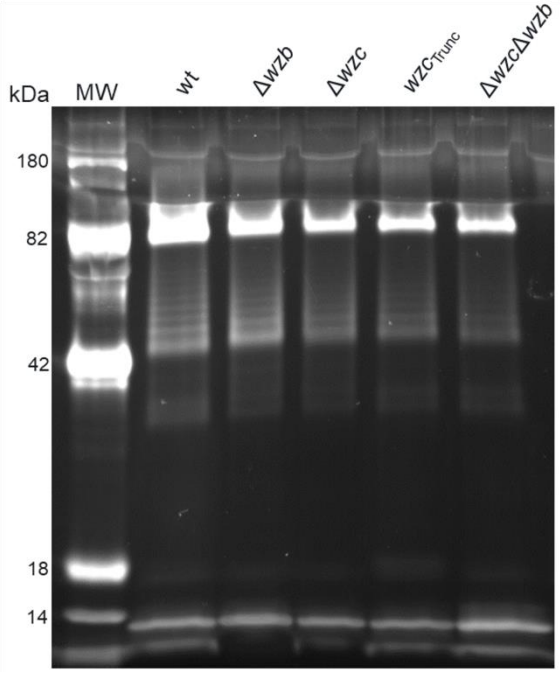

Fig. S8. Analysis of outer membrane preparations from *Synechocystis* sp. PCC 6803 wild type (wt) and the Δ*wzb*, Δ*wzc*, Δ*wzc*$_{trunc,}$ and Δ*wzc*Δ*wzb* mutants. Samples were resolved in Tris-glycine 12 % SDS gels and visualized using the Pro-Q® Emerald 300 Lipopolysaccharide Gel Stain Kit. LPSst: 0,5 µg of smooth LPS standard from *E. coli* serotype 055:B5 (control); MW: CandyCane™ glycoprotein molecular weight standards.

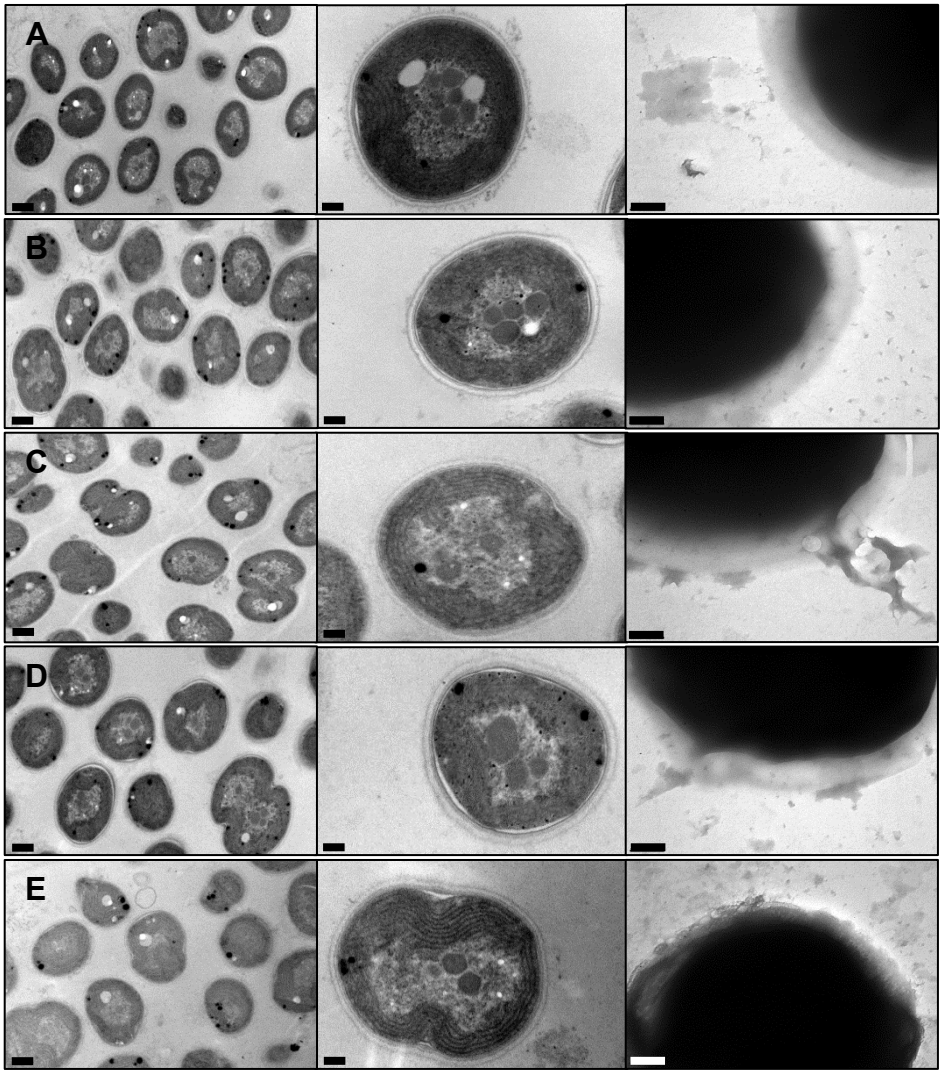

Fig. S9. Transmission electron micrographs of *Synechocystis* sp. PCC 6803 (A) wild type, (B) Δ*wzc*, (C) wzc_{trunc}, (D) Δ*wzb*, and (E) Δ*wzc*Δ*wzb*. Right panel – ruthenium red negatively stained cells. Size bars: left panel - 0.5 µm; middle and right panel - 0.2 µm.

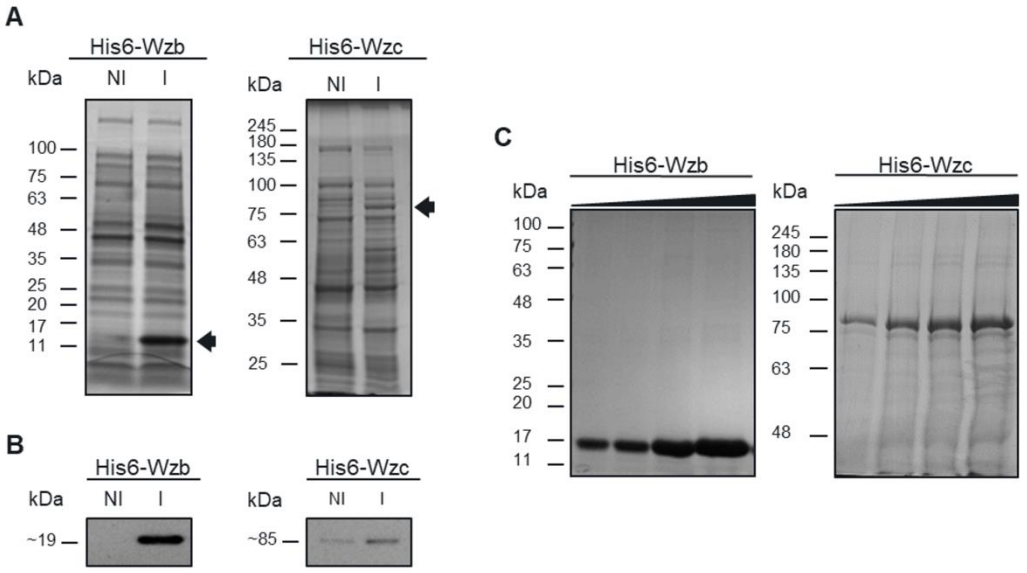

Fig. S10. Overexpression and purification of *Synechocystis* sp. PCC 6803 His6-Wzc and His6-Wzb. (A) SDS-PAGE analysis of crude cell extracts of *E. coli* M15(pREP) cells harboring plasmid pQE-30 encoding the His6-Wzc or His6-Wzb. Arrow heads indicate the target overexpressed protein. NI – non-induced cells, I – induced cells (IPTG). (B) Western blot analysis of His6-Wzc or His6-Wzb using a 6x-His epitope tag antibody. (C) SDS-Page analysis of increasing amounts of purified His6-Wzb (0.75, 1.5, 7.5 and 15 µg) and His6-Wzc (3.0, 6.0, 9.0 and 12.0 µg). Molecular mass standards are indicated on the left.

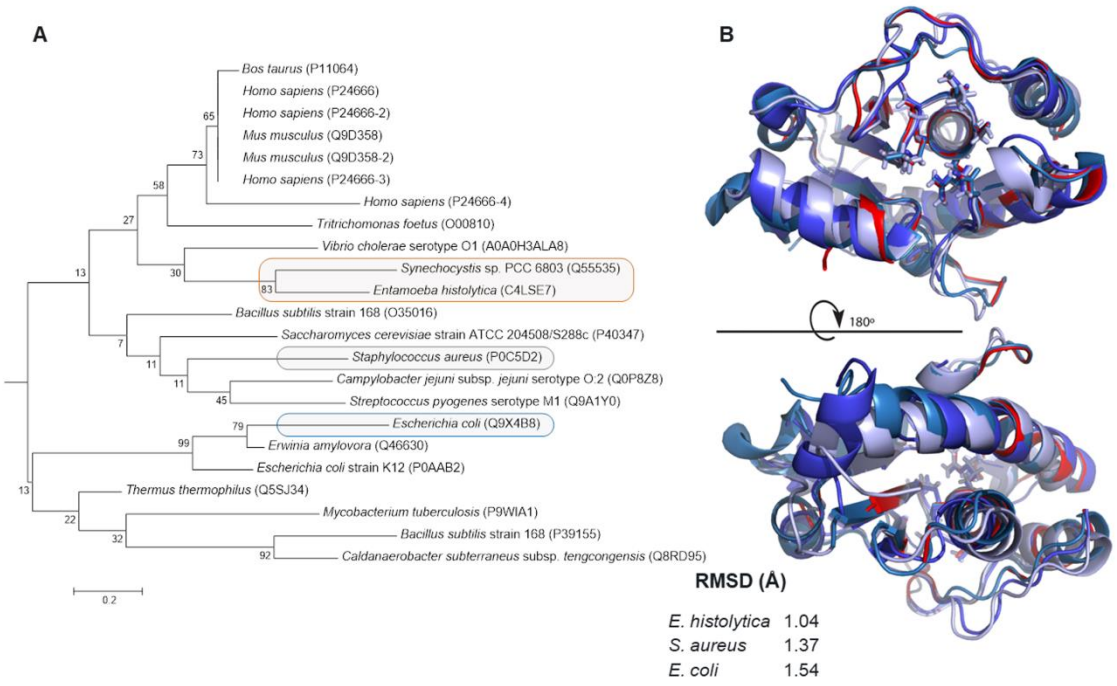

Fig. S11. Phylogenetical relationships and structural alignment and of *Synechocystis* sp. PCC 6803 Wzb. (A) Phylogenetic tree of Wzb and available homologs, as defined by Blast searches, with available crystal structure in PDB. Sequences are identified by the name of the organism and the UniProt entry within brackets. Sequences selected for the structural alignment are highlighted. (B) Structural alignment of Wzb (red) against LMW-PTP from *E. coli* (PDB: 2wja; UniProt: Q9X4B8; dark purple), *S. aureus* (PDB: 3rof; UniProt: P0C5D2; light purple) and *E. histolytica* (PDB: 3ido; UniProt:C4LSE7; blue). An overall structural similarity is visible, including active site superposition, as indicated by root mean square deviation (RMSD) values (Å): 1.54, 1.04 and 1.37 for Wzb against homolog from *E. coli*, *E. histolytica* and *S. aureus*, respectively (protein backbone in cartoon representation and catalytic residues in stick representation).

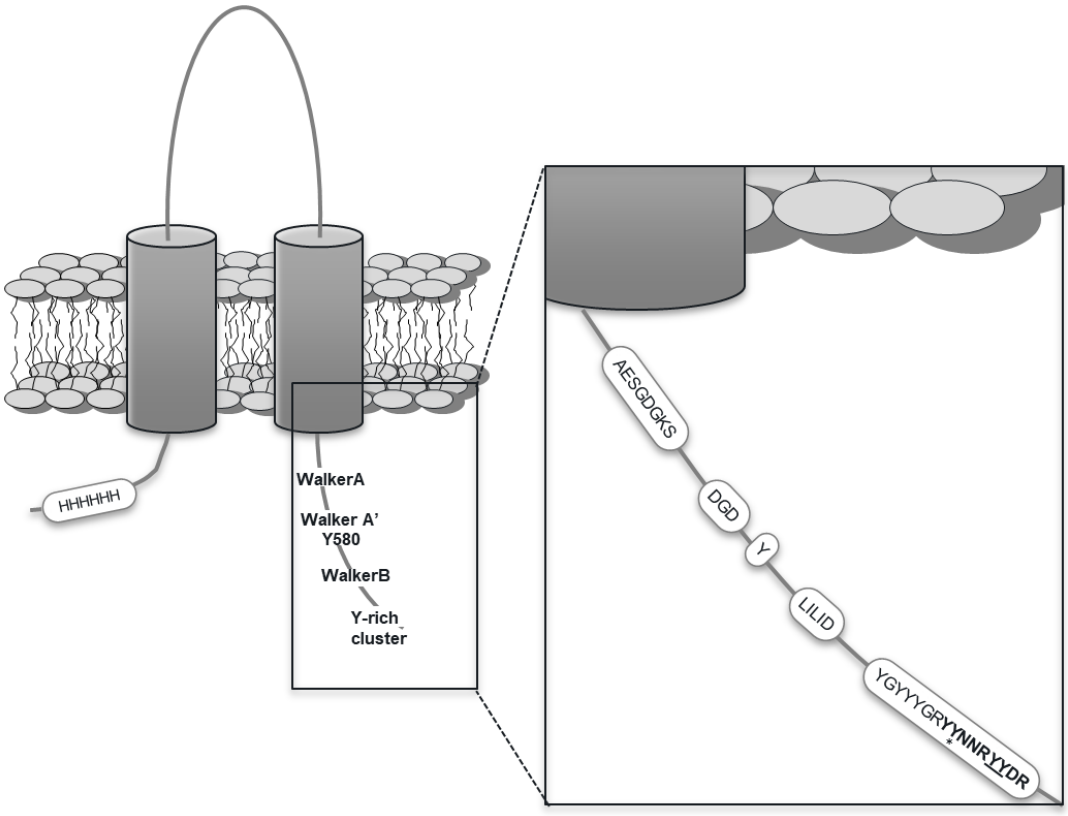

Fig. S12. Predicted topology of the Wzc protein according to the Phyre[2] database. The His6-tag on the N-terminal sequence is depicted. The C-terminal citoplasmic domain contains a canonical Walker A, Walker A', conserved tyrosine (Y) at position 580, Walker B and a C-terminal tyrosine rich cluster. The results from His6-Wzc MS/MS confirmed the phosphorylation of the C-terminal residues Y745 and Y746 (underlined). Residue Y741 (marked with an *) may also be phosphorylated, but further evidence is needed.

References

Jittawuttipoka, T., M. Planchon, O. Spalla, K. Benzerara, F. Guyot, C. Cassier-Chauvat & F. Chauvat, (2013) Multidisciplinary Evidences that *Synechocystis* PCC6803 Exopolysaccharides Operate in Cell Sedimentation and Protection against Salt and Metal Stresses. *PLoS One* **8**: e55564.

Pinto, F., C.C. Pacheco, D. Ferreira, P. Moradas-Ferreira & P. Tamagnini, (2012) Selection of suitable reference genes for RT-qPCR analyses in cyanobacteria. *PLoS One* **7**: e34983.

Pinto, F., C.C. Pacheco, P. Oliveira, A. Montagud, A. Landels, N. Couto, P.C. Wright, J.F. Urchueguía & P. Tamagnini, (2015) Improving a *Synechocystis*-based photoautotrophic chassis through systematic genome mapping and validation of neutral sites. *DNA Res.* **22**: 425-437.

Silva-Rocha, R., E. Martínez-García, B. Calles, M. Chavarría, A. Arce-Rodríguez, A. de las Heras, A.D. Páez-Espino, G. Durante-Rodríguez, J. Kim, P.I. Nikel, R. Platero & V. de Lorenzo, (2013) The Standard European Vector Architecture (SEVA): a coherent platform for the analysis and deployment of complex prokaryotic phenotypes. *Nucleic Acids Res.* **41**: D666-D675.

CHAPTER III

Absence of KpsM (Slr0977) impairs the secretion of extracellular polymeric substances (EPS) and impacts carbon fluxes in *Synechocystis* sp. PCC 6803

Work published in: **SANTOS, M.**, Pereira, S.B., Flores, C., Príncipe, C., Couto, N., Karunakaran, E., Cravo, S.M., Oliveira, P. & Tamagnini. P. (2021). Absence of KpsM (Slr0977) impairs the secretion of extracellular polymeric substances (EPS) and impacts carbon fluxes in *Synechocystis* sp. PCC 6803. *mSphere* 6: e00003–21. https://doi.org/10.1128/mSphere.00003-21.

AMERICAN SOCIETY FOR MICROBIOLOGY | mSphere®

RESEARCH ARTICLE
Molecular Biology and Physiology

Absence of KpsM (Slr0977) Impairs the Secretion of Extracellular Polymeric Substances (EPS) and Impacts Carbon Fluxes in *Synechocystis* sp. PCC 6803

Marina Santos,[a,b,c] Sara B. Pereira,[a,b] Carlos Flores,[a,b] Catarina Príncipe,[a,b,d] Narciso Couto,[e] Esther Karunakaran,[e] Sara M. Cravo,[f,g] Paulo Oliveira,[a,b,d] Paula Tamagnini[a,b,d]

[a]i3S-Instituto de Investigação e Inovação em Saúde, Universidade do Porto, Porto, Portugal
[b]IBMC-Instituto de Biologia Celular e Molecular, Universidade do Porto, Porto, Portugal
[c]Programa Doutoral em Biologia Molecular e Celular (MCbiology), Instituto de Ciências Biomédicas Abel Salazar (ICBAS), Universidade do Porto, Porto, Portugal
[d]Departamento de Biologia, Faculdade de Ciências, Universidade do Porto, Porto, Portugal
[e]Department of Chemical and Biological Engineering, University of Sheffield, Sheffield, United Kingdom
[f]Interdisciplinary Centre of Marine and Environmental Research (CIIMAR), Matosinhos, Portugal
[g]Laboratório de Química Orgânica, Departamento de Ciências Químicas, Faculdade de Farmácia, Universidade do Porto, Porto, Portugal

ABSTRACT Many cyanobacteria produce extracellular polymeric substances (EPS), composed mainly of heteropolysaccharides, that play a variety of physiological roles, being crucial for cell protection, motility, and biofilm formation. However, due to their complexity, the EPS biosynthetic pathways as well as their assembly and export mechanisms are still far from being fully understood. Here, we show that the absence of a putative EPS-related protein, KpsM (Slr0977), has a pleiotropic effect on *Synechocystis* sp. strain PCC 6803 physiology, with a strong impact on the export of EPS and carbon fluxes. The *kpsM* mutant exhibits a significant reduction of released polysaccharides and a smaller decrease of capsular polysaccharides, but it accumulates more polyhydroxybutyrate (PHB) than the wild type. In addition, this strain shows a light/cell density-dependent clumping phenotype and exhibits an altered protein secretion capacity. Furthermore, the most important structural component of pili, the protein PilA, was found to have a modified glycosylation pattern in the mutant compared to the wild type. Proteomic and transcriptomic analyses revealed significant changes in the mechanisms of energy production and conversion, namely, photosynthesis, oxidative phosphorylation, and carbon metabolism, in response to the inactivation of *slr0977*. Overall, this work shows for the first time that cells with impaired EPS secretion undergo transcriptomic and proteomic adjustments, highlighting the importance of EPS as a major carbon sink in cyanobacteria. The accumulation of PHB in cells of the mutant, without affecting significantly its fitness/growth rate, points to its possible use as a chassis for the production of compounds of interest.

IMPORTANCE Most cyanobacteria produce extracellular polymeric substances (EPS) that fulfill different biological roles depending on the strain/environmental conditions. The interest in the cyanobacterial EPS synthesis/export pathways has been increasing, not only to optimize EPS production but also to efficiently redirect carbon flux toward the production of other compounds, allowing the implementation of industrial systems based on cyanobacterial cell factories. Here, we show that a *Synechocystis kpsM* (*slr0977*) mutant secretes less EPS than the wild type, accumulating more carbon intracellularly, as polyhydroxybutyrate. Further characterization showed a light/cell density-dependent clumping phenotype, altered protein secretion, and modified glycosylation of PilA. The proteome and transcriptome of the mutant revealed significant changes, namely, in photosynthesis and carbon metabolism.

Citation Santos M, Pereira SB, Flores C, Príncipe C, Couto N, Karunakaran E, Cravo SM, Oliveira P, Tamagnini P. 2021. Absence of KpsM (Slr0977) impairs the secretion of extracellular polymeric substances (EPS) and impacts carbon fluxes in *Synechocystis* sp. PCC 6803. mSphere 6:e00003-21. https://doi.org/10.1128/mSphere.00003-21.

Editor Yonghua Li-Beisson, Aix-Marseille University

Address correspondence to Paula Tamagnini, pmtamagn@ibmc.up.pt.

Received 8 January 2021
Accepted 8 January 2021
Published 27 January 2021

Altogether, this work provides a comprehensive overview of the impact of *kpsM* disruption on *Synechocystis* physiology, highlighting the importance of EPS as a carbon sink and showing how cells adapt when their secretion is impaired, and the redirection of the carbon fluxes.

KEYWORDS *Synechocystis*, carbon fluxes, cyanobacteria, extracellular polymeric substances, polyhydroxybutyrate, secretion

Most cyanobacterial strains produce extracellular polymeric substances (EPS), composed mainly of polysaccharides, that can either remain associated with the cell surface (capsules, sheaths, or slime) or be released to the extracellular medium, referred to as released polysaccharides (RPS) (1). Over the last 2 decades, a variety of functions have been assigned to these EPS, namely, cell protection, adherence, formation of biofilms, sequestration of nutrients, and motility (2–7). Furthermore, the cyanobacterial extracellular polymers possess unique features compared to their bacterial counterparts, such as the diversity of constituent monomers (up to 13), including uronic acids (up to 2), amino sugars, and deoxysugars, and the presence of sulfate groups and peptides that may contribute to their biological activity (1, 8, 9). Overall, these characteristics make them attractive candidates for biotechnological/biomedical applications ranging from their use as gelling or emulsifying agents to their use in drug delivery and as therapeutic agents (10–14).

Consequently, there is increasing interest in understanding the cyanobacterial EPS biosynthetic pathways, not only to optimize production yields but also to engineer polymer variants tailored for a specific application (9). However, when the main purpose is to potentiate the use of cyanobacteria as "cell factories," the highly energy-consuming process of EPS production can strongly impair productivity. Thus, comprehensive knowledge of their pathways is also required to efficiently redirect the carbon flux toward the production of other compounds of interest (15, 16).

The final steps of EPS assembly and export are mostly conserved throughout bacteria, following one of three major mechanisms: the ABC transporter-, the Wzy-, or the synthase-dependent pathway (17–19). The ABC transporter-dependent pathway translocates the fully polymerized polysaccharide to the periplasm using a two-protein complex, composed of the transport permease KpsM and the ATP binding component KpsT. The Wzy-dependent pathway relies on Wzx to translocate the oligosaccharide lipid-linked repeat units to the periplasm, where polymerization is performed by Wzy. For both pathways, export to the extracellular space occurs through the action of a polysaccharide copolymerase (KpsE and Wzc) and outer membrane polysaccharide export (KpsD and Wza) (17, 20–22). For the production of alginate, the synthase-dependent pathway requires a synthase, Alg8, to simultaneously polymerize and export the polymer across the plasma membrane to the periplasmic site (18, 23).

A cyanobacterial phylum-wide analysis disclosed the presence of genes encoding proteins from the three pathways (mainly from the first two ones) but often not the complete gene set that defines a single pathway (24). This complexity is also evident in the physical organization of EPS-related genes in cyanobacteria, with multiple copies scattered throughout the genomes, either isolated or in small clusters (8, 24), suggesting a more intricate mechanism for EPS production/regulation in cyanobacteria. Previous works, based mainly on the generation and characterization of knockout mutants of the model cyanobacterium *Synechocystis* sp. strain PCC 6803 (here *Synechocystis*), have confirmed the involvement of homologues of key proteins from both the ABC transporter- and Wzy-dependent pathways in cyanobacterial EPS production. Regarding the ABC transporter-dependent pathway, mutants in *Synechocystis* *slr0977* (*kpsM*), *sll0574* (*kpsM*), *slr0982* (*kpsT*), and *sll0575* (*kpsT*) produce EPS with monosaccharidic compositions different from that of the wild type (3). Slr0977 and Sll0574 have the Pfam domains typical of bacterial KpsM and Wzm, which are part of the EPS or O-antigen (OAg) ABC transporters, respectively (24). Due to the homology with

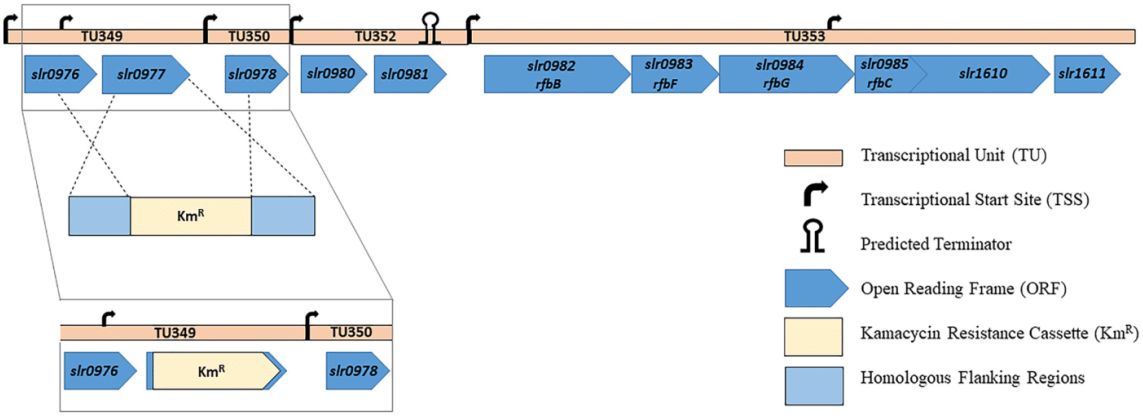

FIG 1 Schematic representation of the *slr0977* (*kpsM*) genomic context in *Synechocystis* sp. PCC 6803 and the generation of the *slr0977* knockout mutant by double homologous recombination. *slr0982*, *slr0983*, *slr0984*, and *slr0985* are annotated as *rfbBFG* and *rfbC*, while *slr1610* is annotated as encoding a methyltransferase (3). The remaining ORFs encode hypothetical proteins of unknown function. The transcriptional unit and transcription start site are annotated according to Kopf et al. (27). The predicted terminator was found using the FindTerm algorithm (Softberry); the insertion of the antibiotic cassette did not alter the prediction.

Escherichia coli, *slr0977* (previously referred to as *rfbA*) was designated *wzm* (3). However, the absence of Slr0977 did not result in changes in the lipopolysaccharide (LPS) profile of *Synechocystis* (3), suggesting that this protein is a KpsM homologue. Regarding the mutants of putative Wzy-dependent components, *wza* (*sll1581*), *wzb* (*slr0328*), and *wzc* (*sll0923*) mutants were also shown to be involved in EPS production, exhibiting less capsular polysaccharide (CPS), less released polysaccharide (RPS), or less of both, respectively (25, 26). Until now, none of the generated mutants exhibited a substantial decrease in RPS production, and a *wzc*:*wzb* double mutant exhibited a decrease in CPS and an increase in RPS, suggesting that in the absence of the two proteins, RPS production is likely to be diverted to an alternative route (26). Altogether, these results support the involvement of different players and possibly cross talk between homologues of the different canonical bacterial pathways.

In this work, and in order to pursue the unraveling of cyanobacterial EPS assembly and export pathways, a *Synechocystis slr0977* (*kpsM*) knockout mutant was generated and extensively characterized. This gene was targeted, taking into account its relevant genomic location (within a cluster of genes related to sugar metabolism) and previous observations that the absence of *slr0977* leads to EPS with altered composition (3). The *kpsM* mutant was characterized in terms of growth/fitness, EPS production, protein secretion, and cell envelope ultrastructure. In addition, and to achieve a comprehensive overview, the transcriptomes and proteomes of the *kpsM* mutant and the wild type were assessed.

RESULTS

In the present work, an *slr0977* (*kpsM*) *Synechocystis* knockout mutant was generated and extensively characterized. This open reading frame (ORF) is located in a genomic locus containing 11 genes in which about half are putatively related to sugar metabolism (for details, see Fig. 1). The disruption of *kpsM*, which encodes a putative transport permease of the ABC transporter, was achieved via double homologous recombination by partially replacing the gene (749 bp out of 831 bp) with a kanamycin (Km) resistance cassette. The complete segregation of the mutant was confirmed by PCR and Southern blotting (see Fig. S1 in the supplemental material).

The *Synechocystis kpsM* mutant exhibits a light-dependent clumping phenotype and produces less EPS than the wild type. The *kpsM* mutant was initially characterized in terms of growth/fitness. Under the conditions tested (12 h of light at 50 μE m^{-2} s^{-1}/12 h of dark, at 30°C and 150 rpm), the mutant strain did not show any significant

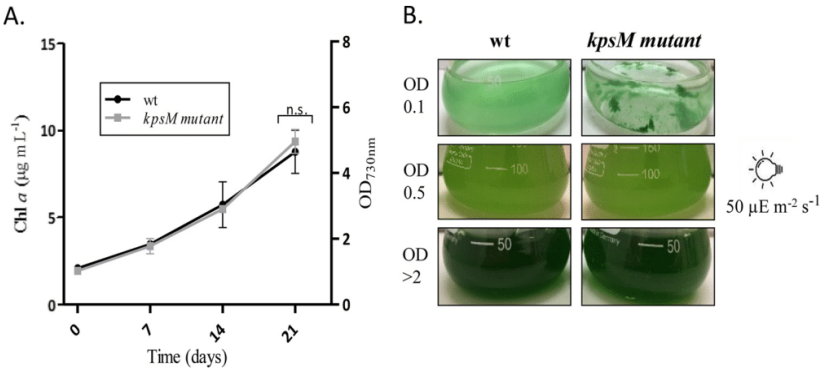

FIG 2 Growth curves of *Synechocystis* sp. PCC 6803 wild-type (wt) and *kpsM* mutant strains (A) and the respective phenotypes showing the clumping of the mutant cells at lower cell densities (B). Cells were grown in BG11 medium at 30°C under a 12-h light (50 μE m^{-2} s^{-1})/12-h dark regimen, with orbital shaking at 150 rpm. Growth experiments were performed in triplicate, and statistical analysis is presented for the last time point (n.s., not significant[*P* value of >0.05]). Chl *a*, chlorophyll *a*.

growth differences compared to the wild type (Fig. 2A). However, at lower cell densities (optical density [OD] of <0.5), it displayed a clumping phenotype that faded with culture growth (Fig. 2B). Interestingly, this phenotype was not observed when cultures were grown at a lower light intensity (20 μE m^{-2} s^{-1}) but was always visible for cultures grown at a higher light intensity (100 μE m^{-2} s^{-1}). Gradual bleaching was also observed for the mutant cells exposed to 100 μE m^{-2} s^{-1} (data not shown).

The total carbohydrate contents were similar for the wild type and the *kpsM* mutant (Fig. 3A). However, the mutant showed 20% less capsular polysaccharide (CPS) (Fig. 3B) and released 50% less RPS than the wild type after 21 days of cultivation (Fig. 3C). Statistical analyses are presented for the last time point, as the differences accumulate with cell density (at this time point, the cultures no longer exhibit the initial clumping phenotype). The smaller amount of RPS secreted by the mutant, without a significant change in the total carbohydrate content, suggests a possible accumulation of carbon intracellularly.

To ensure that the observed phenotype was not due to polar effects, the knockout mutant was complemented in *trans* using the replicative vector pSEVA351 containing the native *kpsM* gene under the control of the *psbA2** promoter. The complementation restored EPS production, reaching even higher levels of CPS and RPS than the wild type (Fig. S2).

The *kpsM* mutant accumulates more polyhydroxybutyrate. To evaluate if the *kpsM* knockout mutant accumulates carbon intracellularly, the amount of carbon storage compounds was determined. Regarding glycogen, no significant differences were found between the mutant and the wild type/complemented mutant (Fig. 4A), representing about 4% of the dry-cell weight. In contrast, the *kpsM* mutant accumulates approximately 30% more polyhydroxybutyrate (PHB) than the wild type/complemented mutant (Fig. 4B). The PHB content represents about 1% of the dry-cell weight for the wild type. Moreover, cultivation under conditions that potentiate the accumulation of PHB (nitrate-free medium [$BG11_0$]) (28) led to an increase in the PHB content in both the *kpsM* mutant and the wild type (Fig. S3).

The extracellular medium of the *kpsM* mutant contains fewer carotenoids. While performing the RPS quantification, a clearly visible difference between the colors of the cell-free media from the wild type and the *kpsM* mutant was observed (Fig. 5B). Therefore, the pigment contents in the extracellular media of both cultures were analyzed. The absorption spectra of the concentrated samples showed the characteristic peaks of carotenoids for both strains although with a significantly higher content for the wild type (Fig. 5A), with the intracellular content not varying considerably (Fig. S4).

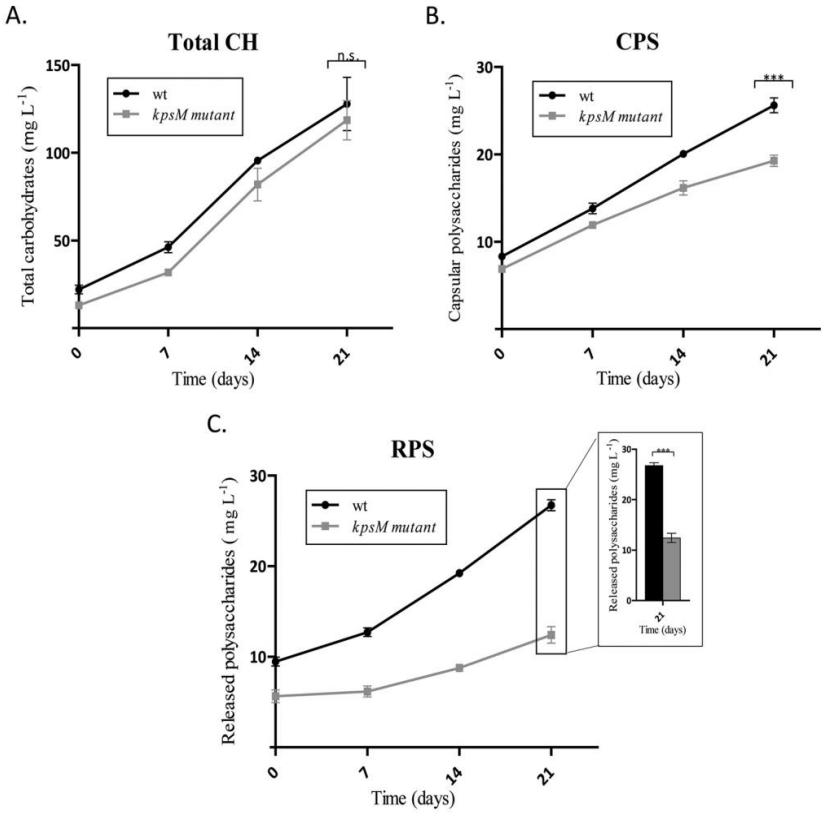

FIG 3 Total carbohydrates (Total CH) (A), capsular polysaccharides (CPS) (B), and released polysaccharides (RPS) (C) of *Synechocystis* sp. PCC 6803 wild-type (wt) and *kpsM* mutant strains, expressed as milligrams of carbohydrates per liter of culture. Cells were grown in BG11 medium at 30°C under a 12-h light (50 μE m^{-2} s^{-1})/12-h dark regimen, with orbital shaking at 150 rpm. Experiments were performed in triplicate, and statistical analysis is presented for the last time point (***, *P* value of ≤0.001).

For the complemented mutant, the intracellular and extracellular carotenoid contents are slightly higher than those of the wild type (Fig. S4). As carotenoids are lipophilic molecules and, thus, embedded in lipid structures, the presence of lipopolysaccharides (LPS) was also investigated. However, no significant differences were observed in terms of the LPS profile (Fig. 5C).

The *kpsM* mutant has altered protein secretion. Taking into consideration the differences observed due to the amount of carotenoids, further characterization of the extracellular media was undertaken. First, the exoproteomes of the wild type, the *kpsM* mutant, and the complemented strain were analyzed to unveil possible alterations in protein secretion. The *kpsM* mutant releases more proteins into the medium than the wild type (Fig. 6A). In addition, although the in-gel profiles of the exoproteomes of the three strains were overall similar, it was possible to observe a strong band with a molecular mass of approximately 22 kDa for the wild type and a similar but weaker band for the complemented mutant, while a band with a molecular mass of approximately 17 kDa was observed for the *kpsM* mutant (Fig. 6A). These proteins were identified by mass spectrometry and contained peptides corresponding to the pilus component PilA. We hypothesized that the molecular mass shift observed for the *kpsM* mutant could be due to alterations in posttranslational modifications of PilA, namely, glycosylation. To validate this, the exoproteome samples were stained with a glycoprotein staining kit (Pierce). The band identified in the wild type and the complemented

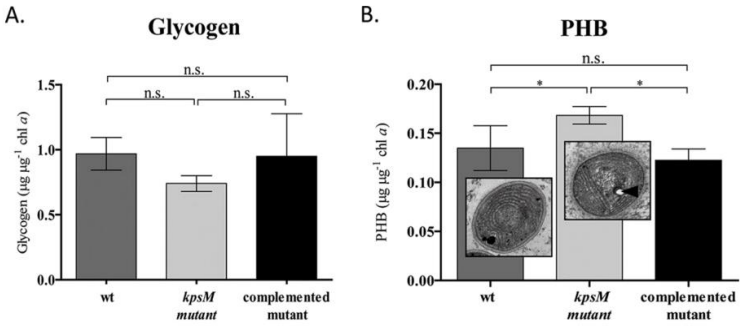

FIG 4 Quantification of glycogen and polyhydroxybutyrate (PHB) in *Synechocystis* sp. PCC 6803 wild-type (wt), *kpsM* mutant, and complemented mutant strains. (A) Glycogen quantification performed by the phenol-sulfuric acid assay and normalized by chlorophyll *a*. (B) PHB content determined by HPLC and normalized by chlorophyll *a*. The TEM micrographs show the ultrastructure of *Synechocystis* wild-type and *kpsM* mutant cells, with the arrowhead indicating the intracellular accumulation of PHB in the *kpsM* mutant. Cells were grown in BG11 medium at 30°C under a 12-h light (50 μE m^{-2} s^{-1})/12-h dark regimen, with orbital shaking at 150 rpm. Experiments were performed in triplicate, and statistical analysis is presented (n.s., not significant [*P* value of >0.05]; *, *P* value of ≤0.05).

mutant as PilA was glycosylated, while differential glycosylation occurred in the region of the PilA-corresponding band in the *kpsM* mutant (Fig. 6B). In addition, the intracellular and outer membrane proteome profiles of the wild type and the *kpsM* mutant were also analyzed. Overall, these profiles were similar between the two strains (Fig. S5), with no significant differences observed.

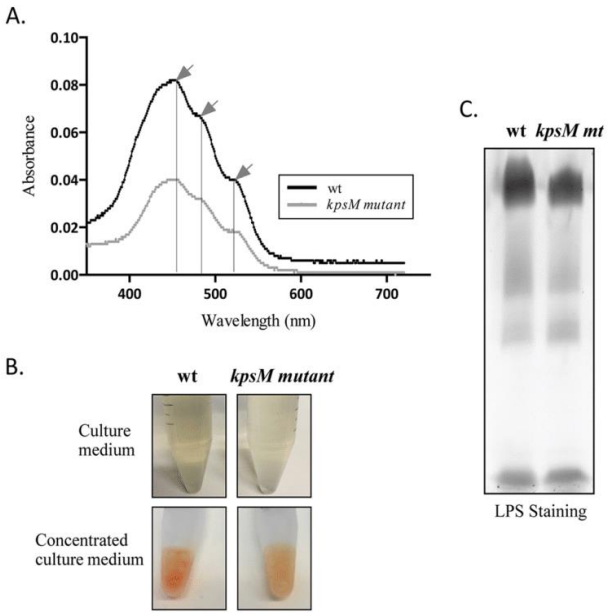

FIG 5 Analysis of the extracellular medium from *Synechocystis* sp. PCC 6803 wild-type (wt) and *kpsM* mutant cultures. (A) Absorption spectra of concentrated medium, with arrows indicating the characteristic carotenoid peaks (at 460, 487, and 521 nm). (B) *Synechocystis* wild-type and *kpsM* mutant culture media exhibiting different orange color intensities due to the amounts of carotenoids. (C) Analysis of the lipopolysaccharides (LPS) in the extracellular culture medium of *Synechocystis* wild-type and *kpsM* mutant (*mt*) strains by SDS-polyacrylamide gel electrophoresis followed by staining with Pro-Q Emerald 300 lipopolysaccharide.

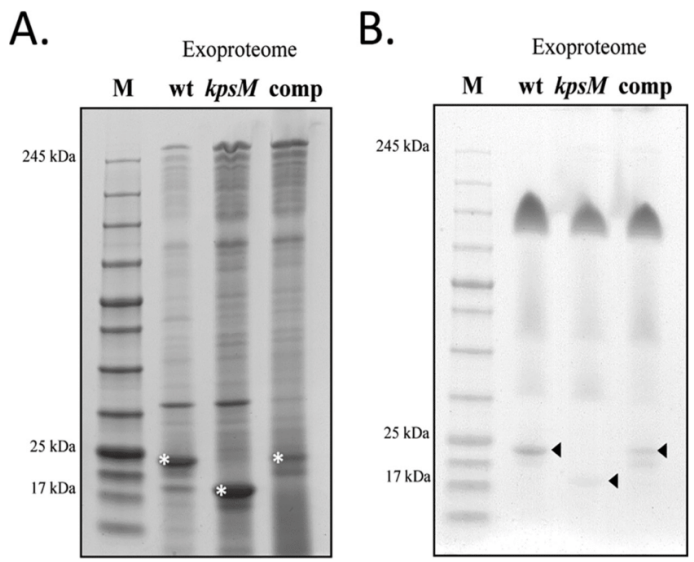

FIG 6 Exoproteomes of *Synechocystis* sp. PCC 6803 wild-type (wt), *kpsM* mutant, and complemented mutant strains. (A) Analysis of the proteins separated by SDS-PAGE and stained with Roti-Blue. Bands highlighted with an asterisk were observed across at least three biological replicates and excised for protein identification. (B) Analysis of the glycoproteins by SDS-PAGE followed by staining with a glycoprotein staining kit (Pierce). Arrowheads indicate glycosylation differences in the PilA component. Sample loading was normalized to each culture cell density (OD_{730}), volume of cell-free medium concentrated, and concentration factor. M, NZYColour protein marker II (NZYTech).

Absence of KpsM has a pleiotropic effect on *Synechocystis* homeostasis. To obtain an overview of the metabolic changes associated with the absence of KpsM in *Synechocystis*, in particular in carbon-related metabolic pathways, two different high-throughput analyses were performed, namely, (i) whole-transcriptome analysis by RNA sequencing (RNA-seq) (Fig. 7) and (ii) isobaric tags for relative and absolute quantification (iTRAQ)-based quantitative proteomic analysis (Fig. 8). The genes and proteins referred to throughout this section are listed in Tables 1 and 2, respectively. The full lists of gene transcripts and proteins showing significant fold changes between the *kpsM* mutant and the wild type are available in Tables S1 and S2 in the supplemental material, respectively.

Regarding RNA sequencing, approximately 700 genes (out of the 3,636 identified and quantified, representing a coverage of 85.12%) were significantly differentially expressed (*P* value of <0.05) in the *kpsM* mutant compared to the wild type. Of those, 406 were downregulated, while 297 were upregulated. The highest percentage (43%) belongs to the "unknown" and "hypothetical" categories, consistent with the fact that nearly half of the *Synechocystis* genome is still annotated as hypothetical. The other most represented functional groups include the broad-range category "other signaling and cellular processes" and "transporters" (Fig. 7A). Moreover, it is important to highlight the considerable changes observed in the levels of transcripts related to the mechanisms of energy production and conversion, including "photosynthesis," "carbon metabolism," and "oxidative phosphorylation." In addition, "translation" and "photosynthesis" were two of the functional categories with the highest numbers of downregulated genes (Fig. 7B), indicating a strong effect of the absence of KpsM on the translational mechanisms and significant changes in the photosynthetic machinery of the mutant. In agreement, several *psb* genes (encoding components of photosystem II) were downregulated, whereas a number of those coding for photosystem I constituents, *psa*, were upregulated in the *kpsM* mutant. Notably, inactivation of *kpsM* also affects the transcript levels of genes putatively related to the Wzy-dependent pathway

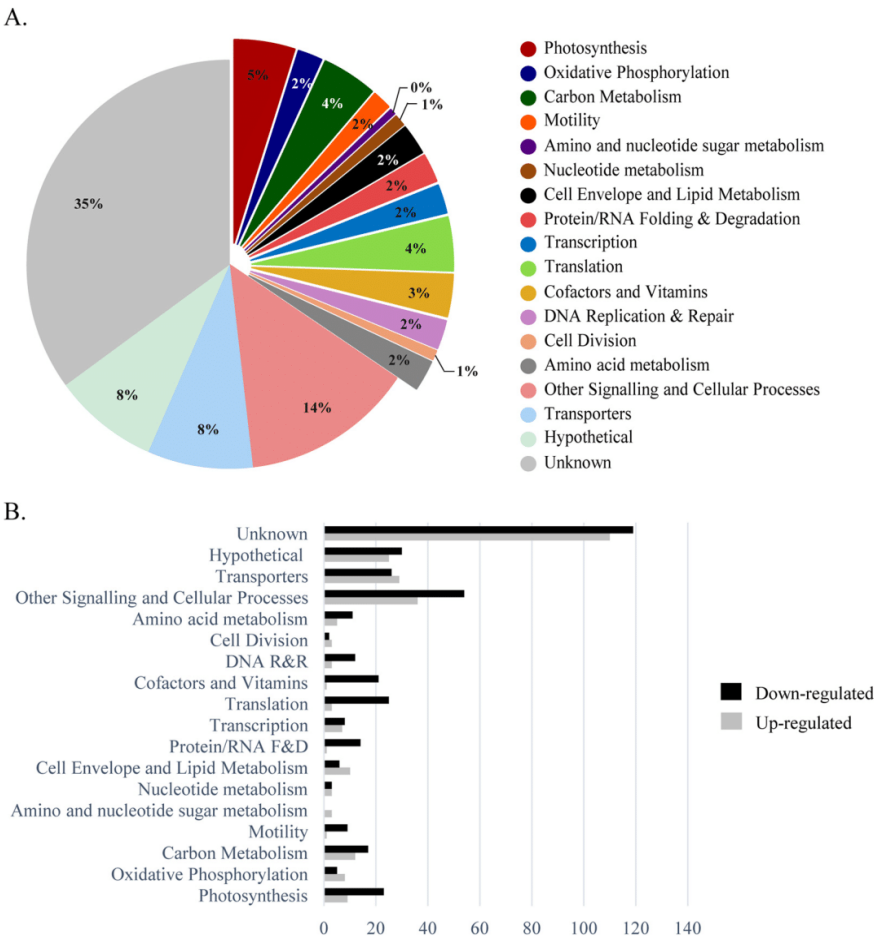

FIG 7 Functional groups of genes with transcript levels with significant fold changes in the *Synechocystis kpsM* mutant versus the wild type. (A) Distribution by functional category of the genes identified and quantified with significant fold changes in the RNA-seq analysis. (B) Number of genes up- or downregulated in the *kpsM* mutant compared to the wild type by functional category. See the annotated list of genes in Table S3 in the supplemental material. Functional categories were assigned based on information available at the CyanoBase and KEGG databases. R&R, replication and repair; F&D, folding and degradation.

of EPS assembly and export, with upregulations of 1.8- and 2.0-fold of *wza* and *wzc*, respectively, and a downregulation of 2.7-fold of *wzb* (gene encoding a low-molecular-weight phosphatase). In addition, genes encoding proteins related to the cell surface/cell wall, namely, the *pil* components (*pilA*, *pilN*, *pilO*, and *pilT*) involved in pilus biogenesis and motility, were downregulated, while the *mur* genes, associated with peptidoglycan biosynthesis, were upregulated.

Regarding the main players in oxidative phosphorylation, the transcript levels of NADH dehydrogenase and ATPase subunits (f, g, i, and d) were significantly higher in the mutant (Table 1). Furthermore, *zwf* (*slr1843*), encoding the key player in the oxidative pentose phosphate pathway (OxPPP), glucose-6-phosphate dehydrogenase, was upregulated 1.4-fold in the mutant. In agreement, an upregulation of ~2-fold of the transcript levels of the gene encoding sigma factor E was also observed.

The iTRAQ-based quantitative proteome analysis led to the identification and quantification of 1,675 proteins (coverage, 47.7%). Statistically significant fold changes (*P*

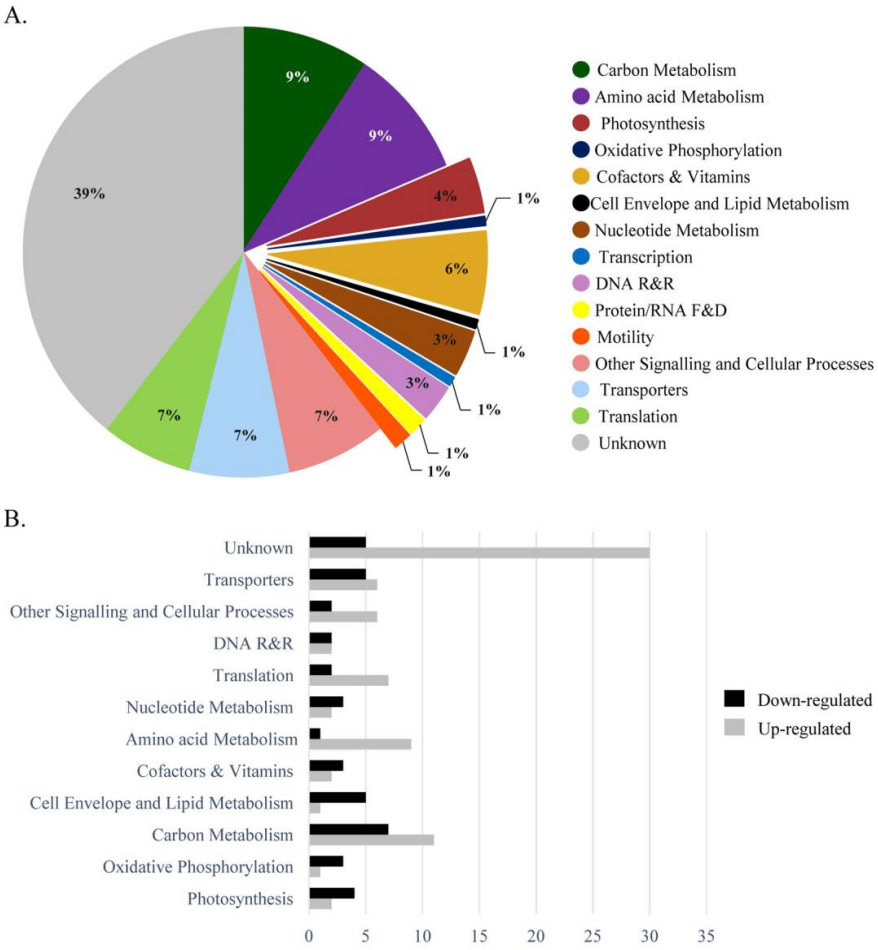

FIG 8 Functional groups of proteins with significant fold changes in the *Synechocystis kpsM* mutant versus the wild type. (A) Distribution by functional category of the proteins identified and quantified by iTRAQ analysis. (B) Number of proteins by functional category with significantly higher or lower abundances in the *kpsM* mutant than in the wild type. See the annotated list of proteins in Table S4 in the supplemental material. Functional categories were assigned based on information available at the CyanoBase and KEGG databases.

value of <0.05) were found for 150 proteins. Of these, the levels of 79 were significantly higher whereas those of 71 were significantly lower in the mutant than in the wild type. The distribution of these proteins by functional category is similar to that observed for the gene transcripts, with "unknown" being the most represented, comprising 38 and 41% of the proteins with higher and lower abundances, respectively. Other strongly represented functional categories included "carbon metabolism," "nucleotide metabolism," "transporters," "other signaling and cellular processes," and "translation" (Fig. 8A). The distribution by functional category of the proteins displaying higher or lower abundances in the mutant is shown in Fig. 8B. Notably, phasin (PhaP), which accumulates together with PHB granules, was found to be more abundant in the mutant (3.1-fold), in agreement with the mutant accumulating more PHB than the wild type. The absence of KpsM also led to an increase of 2.7-fold in the abundance of the S-layer protein Sll1951 in the mutant. In addition, the d subunit of the ATP synthase (Sll1325) was 1.5-fold more abundant in the mutant than in the wild type, in agreement with the results obtained by RNA sequencing. Furthermore, two

TABLE 1 Distribution by functional category of the genes presented in Results, quantified in the RNA-seq analysis with significant fold changes in mRNA transcript levels in the *Synechocystis kpsM* mutant versus the wild type

Functional category and ORF	Gene ID(s)	Description	Fold change (mutant/wt)
Photosynthesis			
ssr2831	*psaE*	Photosystem I reaction center subunit IV	1.8
sll1194	*psbU*	Photosystem II 12-kDa extrinsic protein	−1.6
ssr0390	*psaK1*	Photosystem I reaction center subunit X	1.7
ssr3451	*psbE*	Cytochrome b_{559} alpha subunit	−1.6
sml0008	*psaJ*	Photosystem I reaction center subunit IX	1.7
sll0629	*psaK*	Photosystem I subunit X	1.6
sll0427	*psbO*	Photosystem II manganese-stabilizing polypeptide	−1.5
smr0004	*psaI*	Photosystem I subunit VIII	1.6
	psbZ	Photosystem II	−1.5
sll0819	*psaF*	Photosystem I reaction center subunit III (PSI-F)	1.4
sll1867	*psbA3*	Photosystem II D1 protein	−2.1
smr0008	*psbJ*	Photosystem II PsbJ protein	−2.0
ssl0563	*psaC*	Photosystem I subunit VII	−1.3
smr0005	*psaM*	Photosystem I PsaM subunit	1.4
Oxidative phosphorylation			
sll1324	*atpF*	ATP synthase subunit b	2.2
sll1323	*atpG*	ATP synthase subunit b′	2.2
sll0223	*ndhB*	NAD(P)H dehydrogenase I subunit 2	1.5
sll1322	*atpI*	ATP synthase subunit a	1.7
sll1325	*atpD*	ATP synthase d subunit	1.8
sll0522	*ndhE*	NADH dehydrogenase subunit 4L	−1.7
slr0851	*ndh*	NADH dehydrogenase	1.4
Carbon metabolism			
slr1945	*pgm*	2,3-Bisphosphoglycerate-independent phosphoglycerate mutase	1.6
slr1843	*zwf*	Glucose-6-phosphate 1-dehydrogenase	1.4
Motility			
slr1276		Type IV pilus assembly protein PilO	−1.7
slr1275		Type IV pilus assembly protein PilN	−1.8
sll1694	*hofG*	General secretion pathway protein G	−1.5
sll1533	*pilT*	Twitching motility protein	−1.8
sll1291		Twitching motility two-component system response regulator PilG	2.0
Amino sugar and nucleotide sugar metabolism			
slr0017	*murA*	UDP-*N*-Acetylglucosamine 1-carboxyvinyltransferase	2.8
slr1746	*murI*	Glutamate racemase	3.0
slr1423	*murC*	UDP-*N*-Acetylmuramate-alanine ligase	2.2
Transcription			
sll1689	*sigE*; *rpoD*	Sigma factor E	1.8
Amino acid metabolism			
slr0528	*murE*	UDP-MurNAc-tripeptide synthetase	1.7
Transporters			
sll0923	*epsB*; *wzc*	Exopolysaccharide export protein	2.0
sll1581	*gumB*	Polysaccharide biosynthesis/export	1.8
Other signaling and cellular processes			
slr0328	*wzb*	Low-mol-wt protein-tyrosine phosphatase	−2.7

proteins involved in carotenoid biosynthesis were found at lower abundances in the mutant than in the wild type. These proteins were the β-carotene ketolase CrtO (Slr0088) (1.3-fold less abundant) and the carotenoid phi-ring synthase Sll0254 (1.7-fold less abundant). Additionally, the orange carotenoid binding protein (OCP) was found at a higher abundance in the mutant than in the wild type (1.4-fold).

TABLE 2 Distribution by functional category of the proteins presented in Results, quantified by iTRAQ analysis with significant fold changes in the *Synechocystis kpsM* mutant versus the wild type

Functional category and protein name (alternative name[s])	UniProt accession no.	Description[a]	Fold change (mutant/wt)
Oxidative phosphorylation			
Sll1325 (AtpH; AtpD)	P27180	ATP synthase d subunit	1.5
Carbon metabolism			
Ssl2501 (PhaP)	P73545	Phasin (GA13)	3.1
Sll1070 (TktA)	P73282	Transketolase (EC 2.2.1.1)	1.4
Slr1945 (Gpml; Pgm)	P74507	iPGM (EC 5.4.2.12)	1.3
Slr0752 (Eno)	P77972	Enolase (EC 4.2.1.11) (2-phospho-D-glycerate hydrolyase) (2-phosphoglycerate dehydratase)	1.2
Cell envelope and lipid metabolism			
Sll1951	P73817	S-layer protein (HLP)	2.7
Cofactors and vitamin metabolism			
Slr1055 (ChlH)	P73020	Mg-chelatase subunit ChlH (anti-sigma factor E)	−1.3
Other signaling and cellular processes			
Slr1963	P74102	OCP	1.4
Slr0088 (CrtO)	Q55808	β-Carotene ketolase	−1.3
Sll0254	P73872	Carotenoid phi-ring synthase	−1.7

[a]iPGM, 2,3-bisphosphoglycerate-independent phosphoglycerate mutase; HLP, hemolysin-like protein; OCP, orange carotenoid binding protein.

Regarding carbon metabolism, we observed increases in the levels of the enzymes involved in the sugar catabolic pathways, namely, the transketolase TktA (Sll1070), the phosphoglycerate mutase Pgm (Slr1945), and the enolase Eno (Slr0752) (Table 2). Relevantly, a smaller amount of the anti-sigma factor E enzyme ChlH (Slr1055) (29) was observed in the mutant than in the wild type, whereas the levels of SigE did not change significantly.

Previous studies found that the correlation between transcriptomes and proteomes across large data sets was somewhat modest (30). Nevertheless, it was also described that the cellular processes/functional categories identified by the transcriptomic and proteomic analyses can be very similar (30, 31), which is in agreement with our data sets.

Due to the observed differences in the transcriptomic and proteomic data regarding photosynthetic mechanisms and cell wall/surface components between the *kpsM* mutant and the wild type, the O_2 evolution/consumption rates and the cell envelope ultrastructures of the two strains were evaluated. The mutant showed a similar O_2 evolution rate during the light period and a higher O_2 consumption rate during the dark period (Fig. 9).

Furthermore, no noticeable differences were observed for the cell envelope, except for a small but significant difference in the peptidoglycan thickness (mutant, 6.48 $\pm$ 1.7 nm; wild type, 7.53 $\pm$ 1.6 nm) (Fig. 10).

DISCUSSION

The thorough characterization of the *Synechocystis slr0977* (*kpsM*) knockout mutant performed here shows that the absence of the putative transport permease has a pleiotropic effect on a variety of cellular processes. Although a *Synechocystis slr0977* mutant was generated previously by Fisher et al. (3), we chose to generate a mutant using the Kazusa substrain (32) to allow direct comparison with several EPS-related mutants previously generated in our laboratory (26). In agreement with the results obtained by Fisher et al. (3), no significant growth differences were observed between the *kpsM* mutant and the wild type, and the presence of a flocculent phenotype was also noticed, suggesting a light-sensitive phenotype. In addition to the previously reported differences in the EPS monosaccharidic composition (3), our results clearly show that

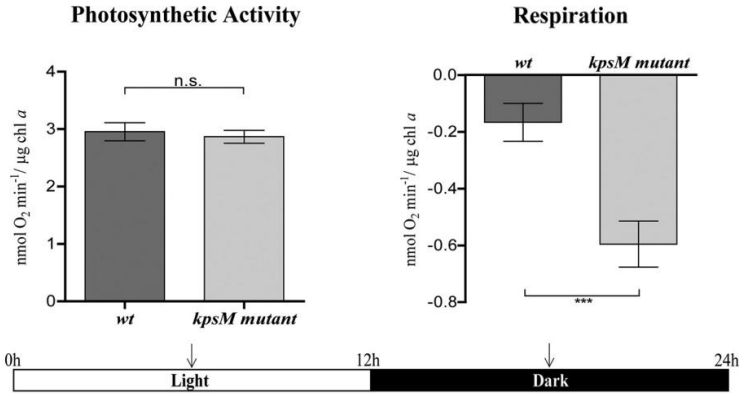

FIG 9 Oxygen evolution and consumption rates by *Synechocystis* sp. PCC 6803 wild-type (wt) and *kpsM* mutant strains. Photosynthetic activity was measured in the middle of the light period, and respiration was measured in the middle of the dark period (arrows) of the 12-h light/12-h dark growth regimen as described in Materials and Methods (*, *P* value of ≤0.05; **, *P* value of ≤0.01).

the absence of KpsM leads to an overall reduction of EPS production, with the mutant having a significant reduction of RPS (50% after 21 days of culture) and a less pronounced decrease of CPS (about 20%). Complementation of the mutant with native *kpsM* (*kpsM* mutant::p351slr0977) restored EPS production to levels that even surpassed the ones of the wild type (see Fig. S2 in the supplemental material), with this most likely being due to the use of a medium-strength promoter, *psbA2** (33) instead of the native one. Interestingly, another *Synechocystis* mutant generated in our laboratory in another putative *kpsM* homologue (*slr2107*) shows no differences regarding EPS production compared to the wild type (26), suggesting that, at least under the conditions tested, Slr2107 does not play a major role in EPS production. Interestingly, the

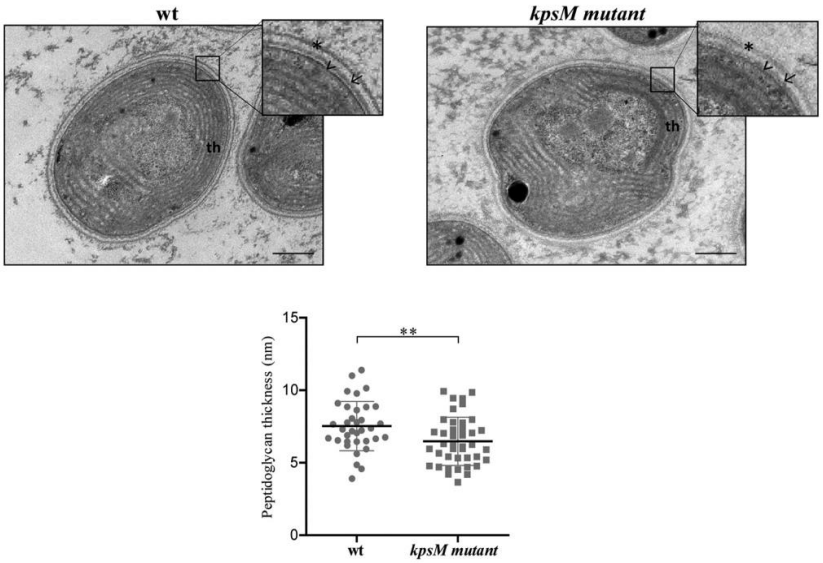

FIG 10 Ultrastructure of *Synechocystis* sp. PCC 6803 wild-type (wt) and *kpsM* mutant cells. The inset panels show details of the cell walls. Asterisk, S layer; arrow, outer membrane; arrowhead, peptidoglycan; th, thylakoids. Bars, 100 nm. The measurements of peptidoglycan thickness are presented below the micrographs (**, *P* value of ≤0.01).

EPS produced by the triple mutant (*slr0977* [*kpsM*] *sll0574* [*kpsM*] *sll0575* [*kpsT*]) generated by Fisher et al. has a composition similar to that of the wild type, leading the authors to hypothesize the use of different transport components or an alternative route (3). Previous works in *Synechocystis* demonstrated that the putative Wzy-dependent components Wza, Wzb, and Wzc are also involved in EPS production (25, 26). The deletion of *wza* results in a substantial decrease in CPS, with no effect on RPS production, while the deletion of *wzb* results in a decrease in RPS only, and the deletion of *wzc* decreases the amounts of both RPS and CPS produced. However, different *Synechocystis* substrains and culture conditions were used in the two studies, not allowing a direct comparison of the results. Since the *Synechocystis* substrain and the experimental design used here were the same as the ones used previously by Pereira et al. (26), we can infer that deletion of *kpsM* results in one of the most significant reductions of the amount of RPS reported to date.

In other bacteria, in the Wzy-dependent pathway, Wzc undergoes a phosphorylation/dephosphorylation cycle that affects its oligomerization state and is dependent on the phosphatase activity of Wzb (34). Recently, Pereira et al. (26) also showed that in *Synechocystis*, and at least *in vitro*, Wzc is a substrate of Wzb, suggesting a possible regulatory role for the low-molecular-weight phosphatase Wzb. In agreement, the transcriptomic data obtained here show the upregulation of *wza* and *wzc* and the downregulation of *wzb* in the *Synechocystis kpsM* mutant, although no significant differences were observed regarding the abundances of the corresponding proteins. These results reinforce the indirect role of *wzb* in cyanobacteria as in other bacteria. The transcriptional response of these putative Wzy-dependent components raises the hypothesis that the mutant attempts to balance the absence of *kpsM* either by using a distinct export route or even by using other components, as the two canonical bacterial pathways might not function as separate entities in *Synechocystis*/cyanobacteria.

Our results also showed that in the *kpsM* mutant, the decrease of EPS goes together with the intracellular accumulation of carbon in the form of the storage compound polyhydroxybutyrate (PHB). Supporting this result, the phasin PhaP, a protein that is known to accumulate on the surface of PHB granules (35), was found in a higher abundance in the mutant than in the wild type. Previous work suggested that the accumulation of PHB is a direct result of glycogen turnover during nitrogen depletion in *Synechocystis* (36–38). It is important to highlight that the culture conditions used throughout this study are always those of nitrogen sufficiency and that the *kpsM* mutant does not show a statistically significant decrease in glycogen accumulation compared to the wild type; therefore, it is not possible to make the same inference from our work. Interestingly, the level of EPS produced by the *Synechocystis* wild-type strain ($\sim$6 μg μg^{-1} chlorophyll *a*) is approximately 6-fold higher than that of the most commonly abundant intracellular carbon storage compound, glycogen ($\sim$1 μg μg^{-1} chlorophyll *a*) (Fig. 2B and C and Fig. 3A). This oftentimes-overlooked fact suggests that EPS can act as an effective carbon sink in cyanobacteria. Lau et al. (39) previously reported that the main driving force for the synthesis of PHB in *Synechocystis* is the total flux of carbon. In agreement, the *kpsM* mutant shows differences in sugar metabolism/catabolism pathways compared to the wild type, including the upregulation of *sigE* and the lower abundance of the anti-sigma factor E enzyme ChlH. SigE was previously described as a positive transcriptional regulator of sugar catabolic pathways in *Synechocystis* (36, 40–42), with its activity being inhibited by ChlH (29). The results of RNA sequencing and iTRAQ analyses also showed that players involved in sugar catabolic pathways, including glycolysis and the oxidative pentose phosphate pathway (OxPPP), are present in higher abundances in the mutant (Tables 1 and 2). Among these is the upregulated phosphoglycerate mutase Pgm (Slr1945), operating at the beginning of lower glycolysis. Recently, this protein was proposed to play a key role in the regulation of cyanobacterial carbon storage metabolism (43). It was suggested that the higher carbon flux through lower glycolysis results in higher pyruvate levels, thereby increasing the amount of PHB (43). Similarly, Lau et al. (39) had suggested that

an increment of sugar catabolism pathways likely results in a higher abundance of cellular metabolites that can be used as precursors for the synthesis of PHB. Moreover, other players involved in sugar catabolism uncovered by our transcriptomic and proteomic analyses comprise the OxPPP key component *zwf*, the transketolase TktA, and a second protein involved in lower glycolysis, the enolase Eno. These results are in agreement with those described previously by Tokumaru et al. (42), who reported the upregulation of players involved in sugar catabolism in a *Synechocystis* SigE overexpression mutant.

The high numbers of changes observed in the transcriptome and proteome of the *kpsM* mutant related to central energy and carbon metabolism seem to be correlated with a higher respiratory (O_2 consumption) rate. However, the growth rates are similar between the mutant and the wild type, suggesting that the differences observed do not affect growth under standard laboratory conditions and thus suggesting that these physiological adjustments do not impact biomass formation.

The smaller amount of carotenoids present in the extracellular medium of the *kpsM* mutant and the lower levels of the β-carotene ketolase CrtO (Slr0088) and the carotenoid phi-ring synthase Sll0254 point toward an impairment in the carotenoid biosynthetic pathways. These results, together with the smaller amount of RPS, may explain the observed light-dependent clumping phenotype observed for the mutant. This mechanism provides self-shading for the cells, which may attenuate the absence of protection conferred by the carotenoids and extracellular polysaccharides (1, 44, 45). Furthermore, Slr1963 (encoding the orange carotenoid binding protein [OCP]) is more abundant in the mutant, suggesting a photoprotective mechanism in the *kpsM* mutant since it was previously described that OCP is an essential player in the stress response to high-light conditions by interacting with the phycobilisome by increasing energy dissipation in the form of heat, thereby decreasing the amount of energy arriving at the reaction centers and preventing an excess of reactive oxygen species (ROS) (46–48). Moreover, in other bacteria, biosynthesis and accumulation of PHB can be used as a mechanism to maintain the redox equilibrium in the cell by allowing the elimination of excess acetyl-CoA and reducing equivalents (49). Thus, the accumulation of PHB in the *kpsM* mutant could be another strategy to relieve oxidative stress, in parallel with the increase in the level of OCP and the clumping observed at low cell densities.

In line with results obtained by Fisher et al. (3), no differences were observed between the LPS profiles of the mutant and the wild type, supporting that disruption of *kpsM* does not alter the structure of the O-antigen (OAg) and thus solidifying the role of KpsM as an extracellular polysaccharide transporter. On the other hand, the higher accumulation of proteins in the extracellular medium of the mutant indicates that in the absence of KpsM, the protein secretion capacity is affected. Moreover, the glycosylation pattern of the pilus component PilA present in the exoproteome is altered. Gonçalves et al. (50) reported differential pilin glycosylation in the PilA1 component of knockout mutants lacking proteins associated with the TolC-dependent secretion mechanisms. Gonçalves et al. (50) suggest that the deleted proteins could be involved in the processing and/or secretion of different extracellular proteins, thus affecting PilA1. In the case of the *kpsM* mutant, differences in the PilA glycosylation profile may be related to the role of KpsM in polysaccharide transport. Relevantly, differences in the transcripts levels of *pil* components and the *mur* genes and the higher abundance of the S-layer protein Sll1951 did not result in noticeable alterations of the cell envelope of the mutant compared to the wild type, except for a minor difference in peptidoglycan thickness. In agreement, previous work reported that a high rate of turnover of peptidoglycan components occurred when cells were light sensitive and, thus, more susceptible to photodamage (51, 52).

Overall, our transcriptomic and proteomic data indicate alterations in the mechanisms of energy production and conversion in the *kpsM* mutant compared to the wild type. Both approaches resulted in the identification of altered levels of transcripts and

proteins belonging to the same functional categories, highlighting a number of key metabolic processes affected by the disruption of *kpsM*, namely, photosynthesis, oxidative phosphorylation, and carbon metabolism. In conclusion, we provide evidence of (i) the involvement of *Synechocystis* KpsM (Slr0977) in EPS export; (ii) the broad transcriptomic, proteomic, and, ultimately, physiological adaptation of *Synechocystis* cells to the absence of KpsM; and (iii) how a mutant impaired in the export of polysaccharides can redirect carbon flux toward the production of other carbon-based compounds, in particular PHB. Furthermore, in addition to the biological roles already described for cyanobacterial extracellular polysaccharides, the present work emphasizes the importance of cyanobacterial EPS as a carbon sink and shows how cells metabolically adapt when their secretion is impaired. Due to its fitness and accumulation of PHB, the *kpsM* mutant can also be used as a platform/chassis for the production of carbon-based compounds or other compounds of interest.

MATERIALS AND METHODS

Bacterial strains and culture conditions. The cyanobacterium *Synechocystis* sp. PCC 6803 substrain Kazusa (Pasteur Culture Collection) used in this work is nonmotile and glucose tolerant (32, 53). *Synechocystis* wild-type and mutant strains (see Table S3 in the supplemental material) (58) were cultured in BG11 medium (54) at 30°C under a 12-h light (50 μmol photons m^{-1} s^{-2})/12-h dark regime with orbital agitation (150 rpm). For solid medium, BG11 medium was supplemented with 1.5% Noble agar (Difco), 0.3% sodium thiosulfate, and 10 mM TES [*N*-tris(hydroxymethyl)methyl-2-aminoethanesulfonic acid]-potassium hydroxide (KOH) buffer (pH 8.2). For the selection and maintenance of mutants, BG11 medium was supplemented with kanamycin (Km) (up to 700 μg ml^{-1}), streptomycin (Sm) (up to 25 μg ml^{-1}), and/or chloramphenicol (Cm) (up to 25 μg ml^{-1}). The *E. coli* strains used were cultured at 37°C in LB medium supplemented with ampicillin (100 μg ml^{-1}), Km (25 μg ml^{-1}), and/or Cm (25 μg ml^{-1}).

Cyanobacterial DNA extraction and recovery. Cyanobacterial genomic DNA was extracted using the Maxwell 16 system (Promega). For use in Southern blot analysis, the phenol-chloroform method described previously (55) was preferred. Agarose gel electrophoresis was performed according to standard protocols (56), and the DNA fragments were isolated from gels, enzymatic assay mixtures, or PCR mixtures using the NZYGelpure purification kit (NZYTech).

Plasmid construction for *Synechocystis* transformation. The *Synechocystis* chromosomal regions flanking *kpsM* (*slr0977*) were amplified by PCR using specific oligonucleotides (Table S4). An overlapping region containing an XmaI restriction site was included in primers 5I and 3I for cloning purposes. For each gene, the purified PCR fragments were fused by "overlap PCR." The resulting products were purified and cloned into the vector pGEM-T Easy (Promega), creating plasmid pGDslr0977. A selection cassette containing the *nptII* gene (conferring resistance to neomycin and kanamycin) was amplified from pKm.1 using the primer pair Km.KmScFwd/KmRev (57) (Table S4) and digested with XmaI (Thermo Scientific). Subsequently, the purified selection cassette was cloned into the XmaI restriction site of the plasmids using the T4 DNA ligase (Thermo Scientific) to form pGDslr0977.Km.

The cassette containing the *aadA* gene (conferring resistance to streptomycin and spectinomycin) was obtained by digesting the plasmid pSEVA481 (57) with PshAI and SwaI, and the cassette was cloned in the XmaI/SmaI site of pGDslr0977 to form plasmid pGDslr0977.Sm.

For mutant complementation, the shuttle vector pSEVA351 (57) was used. A fragment covering the whole *kpsM* gene was amplified using primer pair slr0977Fwd_comp/sll0977Rev_comp (Table S2), purified from the gel, and digested with XbaI and PstI. The P_{psbA2*} promoter (33) and the synthetic ribosome binding site (RBS) BBa_B0030 were purified from the gel after digestion of plasmid $pSBA2P_{psbA2*}$::B0030 with EcoRI and SpeI. The purified products were simultaneously cloned into pSEVA351 previously digested with EcoRI and PstI, creating plasmid $pS351P_{psbA2*}$::B0030.*slr0977*. All constructs were verified by sequencing (StabVida) before transformation into *Synechocystis*.

Generation of the *Synechocystis* sp. PCC 6803 mutants. *Synechocystis* was transformed with integrative plasmids using a procedure described previously (59). Briefly, *Synechocystis* cultures were grown until the optical density at 730 nm (OD_{730}) reached ~0.5, and cells were harvested by centrifugation and suspended in a 1/10 volume of BG11 medium. Five hundred microliters of cells was incubated with 10 μg ml^{-1} plasmid DNA for 5 h before spreading them onto Immobilon-NC membranes (0.45-μm pore size; Millipore) resting on solid BG11 plates; plates were kept at 30°C under continuous light for 24 h. Membranes were transferred to selective plates containing 10 μg ml^{-1} of kanamycin. Transformants were observed after 1 to 2 weeks. For complete segregation, colonies were grown with increasing antibiotic concentrations. Nonintegrative plasmids were transferred to *Synechocystis* by electroporation, as described previously (33). Briefly, cells were washed with 1 mM HEPES buffer (pH 7.5). Afterwards, cells were resuspended in 1 ml HEPES, and 60 μl was mixed with 1 μg of DNA and electroporated with a Bio-Rad Gene Pulser instrument at a capacitance of 25 μF. The resistor used was 400 Ω for a time constant of 9 ms with an electric field of 12 kV cm^{-1}. Immediately after the electric pulse, the cells were suspended in 1 ml BG11 medium and spread onto the Immobilon-NC membranes as described above. After 24 h, the membranes were transferred to selective plates containing 2.5 μg ml^{-1} of chloramphenicol before being grown with increasing antibiotic concentrations.

Southern blotting. Southern blot analyses were performed using genomic DNAs of the wild type and *kpsM* mutant clones digested with SpeI. DNA fragments were separated by electrophoresis on a 1% agarose gel and blotted onto an Amersham Hybond-N membrane (GE Healthcare). Probes were amplified by PCR and labeled using the primers indicated in Table S2 with the digoxigenin (DIG) DNA labeling kit (Roche Diagnostics GmbH) according to the manufacturer's instructions. Hybridization was done overnight at 56°C, and digoxigenin-labeled probes were detected by chemiluminescence using CPD-star (Roche Diagnostics GmbH) in a Chemi Doc XRS$^+$ imager (Bio-Rad).

Growth assessment. Growth measurements were performed by monitoring the OD at 730 nm (60) using a Shimadzu UVmini-1240 instrument (Shimadzu Corporation) and determining the chlorophyll *a* content as described previously (61). All experiments were performed with three technical and three biological triplicates. Data were statistically analyzed as described below.

Determination of total carbohydrate content, RPS, and CPS. Total carbohydrate and RPS contents were determined as described previously (62). For CPS quantification, the procedure was performed as described previously (26). Briefly, 5 ml of dialyzed cultures was centrifuged at 3,857 × *g* for 15 min at room temperature, suspended in water, and boiled for 15 min at 100°C to detach the CPS from the cells' surface. After new centrifugation as described above, CPS were quantified from the supernatants using the phenol-sulfuric acid method (63). Total carbohydrate, RPS, and CPS were expressed as milligrams per liter of culture or normalized by the chlorophyll *a* content. All experiments were performed with three technical and three biological triplicates. Data were statistically analyzed as described below.

Glycogen quantification. Cells were collected at an OD_{730} of 1.5 and washed twice with BG11 medium. Glycogen was extracted as described previously (64, 65). Briefly, the pellet was suspended in ~100 μl of double-distilled water (ddH_2O), and 400 μl of 30% KOH was added. The mixture was incubated at 100°C for 90 min and then quickly cooled on ice. Six hundred microliters of ice-cold absolute ethanol was added, and the mixture was incubated on ice for 2 h and centrifuged for 5 min at maximum speed at 4°C. The supernatant was discarded, and the isolated glycogen isolated in the pellet was stored. Pellets were washed twice with 500 μl of ice-cold ethanol and dried at 60°C. Glycogen quantification was performed using the phenol-sulfuric acid assay (63).

PHB quantification. The PHB content was determined as described previously (37). Roughly 100 ml of cells was harvested and centrifuged at 4,000 × *g* for 10 min at 25°C. The resulting pellet was dried overnight at 80°C. About 30 mg of dried cells was boiled with 1 ml of H_2SO_4 at 100°C for 1 h to convert PHB to crotonic acid. After cooling, 100 μl was diluted with 900 μl of 0.014 M H_2SO_4, and the samples were centrifuged to remove cell debris for 10 min at 10,000 × *g*. Five hundred microliters of the supernatant was transferred to 500 μl of 0.014 M H_2SO_4. After an additional centrifugation step (the same conditions as the ones described above), the supernatant was used for high-performance liquid chromatography (HPLC) analysis. Commercially available crotonic acid was used as a standard with a conversion ratio of 0.893 (37). For the HPLC analysis, an ACE-C_{18} column (150- by 4.6-mm internal diameter [ID] with a particle size of 5 μm) (Advanced Chromatography Technologies Ltd.) was used. The HPLC system was equipped with a Shimadzu LC-20AD pump, a Shimadzu DGV-20A5 degasser, a Rheodyne 7725i injector fitted with a 100-μl loop, and an SPD-M20A diode array detection (DAD) detector. Data acquisition was performed using Shimadzu LCMS Lab Solutions software, version 3.50 SP2. The mobile phase composition was 20 mM phosphate buffer (NaH_2PO_4) (pH 2.5) and acetonitrile (95:5, vol/vol). All HPLC-grade solvents were purchased from Merck Life Science SLU. The flow rate was 0.85 ml min^{-1}, and the UV detection wavelength was 210 nm. Analyses were performed at 30°C in an isocratic mode. Crotonic acid was purchased from Merck Life Science SLU, and serial dilutions were prepared in 0.014 M H_2SO_4 (0.1, 0.5, 1, 5, 10, 50, and 100 μM) to obtain the standard curve (retention time = 11.4 min; $y = 123{,}225x + 152{,}755$; $R^2 = 0.999$). All samples were injected in duplicate.

Outer membrane isolation and lipopolysaccharide staining. Outer membranes were isolated as described previously by Simkovsky et al. (66). The pellet was suspended in 100 μl of 10 mM Tris-HCl (pH 8.0). Protease-digested samples were separated by electrophoresis on 12% SDS-PAGE gels (Bio-Rad), and lipopolysaccharide (LPS) was stained using a Pro-Q Emerald 300 lipopolysaccharide gel stain kit (Molecular Probes), according to the manufacturer's instructions.

Analysis of extracellular medium. The medium from the *Synechocystis* wild-type and *kpsM* mutant cultures was isolated according to methods described previously by Oliveira et al. (67). Briefly, 100 ml of cultures was collected at an OD_{730} of ~1.5 by centrifugation (4,000 × *g*). The supernatant was filtered through a 0.2-μm-pore-size filter and further concentrated by centrifugation with Amicon Ultra-15 centrifugal filter units (Merck Millipore) with a nominal molecular weight limit of 3 kDa. Concentrated exoproteome samples were then saved at −20°C until further analysis. Analysis of the exoproteomes was performed using concentrated medium samples. Exoproteome samples were separated by electrophoresis on 4-to-15% gradient SDS-polyacrylamide gels (Bio-Rad) and visualized with either Roti-Blue (Roth) or a glycoprotein staining kit (Pierce). Samples were normalized to the culture cell density (OD_{730}), volume of cell-free culture medium concentrated, and concentration factor. Stained bands or gel regions observed consistently across at least three biological replicates were further excised and processed for mass spectrometry analysis as described previously (68, 69). Samples were reduced, alkylated, and further trypsin digested for obtaining the mass spectra by using a liquid chromatography-mass spectrometry (LC-MS) Orbitrap instrument. Protein identification was performed using the UniProt protein sequence database for the taxonomic selection *Synechocystis* (2017_01 release). Quantification of protein abundance was performed using the LFQ (label-free quantification) approach. For pigment analysis, absorption spectra in the visible light range (between 350 and 750 nm) were collected from concentrated exoproteome samples diluted 1:100 on a Shimadzu UV-2401 PC spectrophotometer (Shimadzu

Corporation). For LPS detection, concentrated medium samples were separated by gel electrophoresis on 4 to 15% SDS-polyacrylamide gels (Bio-Rad), which were stained as mentioned above.

Total protein and outer membrane protein profile analyses and iTRAQ experiments. For total protein isolation, cells were harvested by centrifugation at 3,857 × *g* for 10 min at room temperature and washed in phosphate buffer (50 mM K_2HPO_4, 50 mM KH_2PO_4 [pH 6.9]). Cells were suspended in protein extraction buffer (50 mM Tris-HCl, 1 mM EDTA, 0.5% Triton X-100, 10% glycerol, 2 mM dithiothreitol [DTT], and 1 tablet of cOmplete EDTA-free protease inhibitor cocktail [Roche] per 10 ml of buffer), and proteins were extracted by mechanical cell disruption using a FastPrepR-24 cell disruptor, with an output of 6.5 m/s and 5 cycles of 30 s (MP Biomedicals), using glass beads (425 to 600 μm; Sigma-Aldrich), followed by centrifugation at 16,100 × *g* for 15 min at 4°C. Outer membranes were isolated as described above (see "Outer membrane isolation and lipopolysaccharide staining"). Protein preparations were stored at −80°C until further use. The protein concentration was determined using the bicinchoninic acid (BCA) protein assay kit (Pierce Biotechnology) and the iMark microplate absorbance reader (Bio-Rad) according to the manufacturers' instructions. Samples were separated by electrophoresis as described above (see "Analysis of extracellular medium"). The proteomes of *Synechocystis* wild-type and *kpsM* mutant strains were analyzed by 8-plex isobaric tags for relative and absolute quantification (iTRAQ), using three biological replicates. A detailed description of the procedure can be found in Text S1 in the supplemental material. Descriptions of the proteins identified and their distributions into functional categories were based on data from the CyanoBase (http://genome.microbedb.jp/cyanobase) (70), UniProt (http://www.uniprot.org/), and KEGG (Kyoto Encyclopedia of Genes and Genomes) (http://www.genome.jp/kegg/) databases and complemented with the information available in the literature.

RNA extraction and RNA sequencing. For RNA extraction, the TRIzol reagent (Ambion) was used in combination with the PureLink RNA minikit (Ambion). Briefly, cells were disrupted in TRIzol containing 0.2 g of 0.2-mm-diameter glass beads (acid washed; Sigma) using a FastPrepH-24 instrument (MP Biomedicals), and the following extraction steps were performed according to the manufacturer's instructions. DNase treatment was performed according to the on-column PureLink DNase treatment protocol (Life Technologies/Invitrogen). RNA was quantified on a NanoDrop ND-1000 spectrophotometer (NanoDrop Technologies, Inc.), and the quality and integrity were checked using the Experion RNA StdSens analysis kit (Bio-Rad).

The transcriptomes of the *Synechocystis* wild-type and *kpsM* mutant strains were analyzed by RNA sequencing (RNA-seq), using three biological replicates. RNA-seq data were generated by Novogene. A total amount of 3 to 5 μg RNA per sample was used as the input material for the RNA sample preparations. A detailed description of the procedure can be found in Text S1. The distribution of the identified proteins into functional categories was performed as described above.

O_2 evolution measurements (photosynthetic activity and respiration). O_2 evolution was measured using a Clark-type O_2 electrode (Oxygraph; Hansatech Ltd.). Calibration was performed using sodium bisulfite and air-saturated water at 30°C. Assays were carried out using 1 ml of culture (previously centrifuged at 3,500 × *g* for 90 s to remove the medium/extracellular polysaccharides and resuspended in BG11 medium), at 30°C and 100 rpm. The O_2 net evolution of cells collected in the middle of the light period of the 12-h light/12-h dark growth regimen was assessed under standard growth irradiance of 50 μE m^{-2} s^{-1}. Respiration was also assessed but in samples collected in the middle of the dark period.

Transmission electron microscopy. Cells were fixed directly in culture medium with final concentrations of 2.5% glutaraldehyde and 2% paraformaldehyde in 0.05 M sodium cacodylate buffer (pH 7.2) (overnight), washed three times in double-strength buffer followed by postfixation with 2% osmium tetroxide in 0.1 M sodium cacodylate buffer (pH 7.2) (overnight), and washed again in the same buffer. The samples were further processed as described previously (71), except that samples were embedded in EMBed-812 resin (Electron Microscopy Sciences) and sections were examined using a JEM-1400Plus instrument (JEOL Ltd., Inc.). For peptidoglycan thickness measurements, 35 and 41 transmission electron microscopy (TEM) micrographs of the wild type and the *kpsM* mutant were used, respectively. Peptidoglycan thickness was measured in four points of the cell whenever possible.

Statistical analysis. Data were statistically analyzed with GraphPad Prism v5 (GraphPad Software) using analysis of variance (ANOVA), followed by Tukey's multiple-comparison test, or using the *t* test.

Data availability. New RNAseq data provided in this paper have been deposited in the Gene Expression Omnibus (GEO) under accession no. GSE165073.

SUPPLEMENTAL MATERIAL

Supplemental material is available online only.

TEXT S1, DOCX file, 0.03 MB.

FIG S1, TIF file, 0.04 MB.

FIG S2, TIF file, 0.04 MB.

FIG S3, TIF file, 0.04 MB.

FIG S4, TIF file, 0.1 MB.

FIG S5, TIF file, 0.1 MB.

TABLE S1, DOCX file, 0.1 MB.

TABLE S2, DOCX file, 0.03 MB.

TABLE S3, DOCX file, 0.01 MB.

TABLE S4, DOCX file, 0.01 MB.

ACKNOWLEDGMENTS

This work was financed by FEDER-Fundo Europeu de Desenvolvimento Regional funds through the COMPETE 2020-Operacional Programme for Competitiveness and Internationalisation (POCI), Portugal 2020, and by Portuguese funds through the Fundação para a Ciência e a Tecnologia (FCT)/Ministério da Ciência, Tecnologia e Ensino Superior, in the framework of project POCI-01-0145-FEDER-028779, and partially supported by national funds through the FCT within the scope of UIDB/04423/2020 and UIDP/04423/2020 and under project PTDC/SAU-PUB/28736/2017 (reference POCI-01-0145-FEDER-028736), cofinanced by COMPETE 2020, Portugal 2020, and the European Union through the ERDF and by FCT through national funds. We also greatly acknowledge FCT for fellowship SFRH/BD/119920/2016 (M.S.), contract DL57/2016/CP1327/CT0007 (S.B.P.), and FCT investigator grant IF/00256/2015 (P.O.). N.C. and E.K. acknowledge a BBSRC award to the University of Sheffield (BB/M012166/1). We acknowledge the support of the i3S Scientific Platform Histology and Electron Microscopy (HEMS), a member of the national infrastructure PPBI-Portuguese Platform of Bioimaging (PPBI-POCI-01-0145-FEDER-022122), and the i3S Proteomics Scientific Platform with the assistance of Hugo Osório. This work had support from the Portuguese Mass Spectrometry Network, integrated in the National Roadmap of Research Infrastructures of Strategic Relevance (ROTEIRO/0028/2013; LISBOA-01-0145-FEDER-022125). We have no conflict of interest to declare.

REFERENCES

1. Rossi F, De Philippis R. 2016. Exocellular polysaccharides in microalgae and cyanobacteria: chemical features, role and enzymes and genes involved in their biosynthesis, p 565–590. *In* Borowitzka MA, Beardall J, Raven JA (ed), The physiology of microalgae. Springer, Cham, Switzerland.
2. Chen L-Z, Wang G-H, Hong S, Liu A, Li C, Liu Y-D. 2009. UV-B induced oxidative damage and protective role of exopolysaccharides in desert cyanobacterium *Microcoleus vaginatus*. J Integr Plant Biol 51:194–200. https://doi.org/10.1111/j.1744-7909.2008.00784.x.
3. Fisher ML, Allen R, Luo Y, Curtiss R, III. 2013. Export of extracellular polysaccharides modulates adherence of the cyanobacterium *Synechocystis*. PLoS One 8:e74514. https://doi.org/10.1371/journal.pone.0074514.
4. Khayatan B, Meeks JC, Risser DD. 2015. Evidence that a modified type IV pilus like system powers gliding motility and polysaccharide secretion in filamentous cyanobacteria. Mol Microbiol 98:1021–1036. https://doi.org/10.1111/mmi.13205.
5. Wilde A, Mullineaux CW. 2015. Motility in cyanobacteria: polysaccharide tracks and type IV pilus motors. Mol Microbiol 98:998–1001. https://doi.org/10.1111/mmi.13242.
6. Kehr JC, Dittman E. 2015. Biosynthesis and function of extracellular glycans in cyanobacteria. Life (Basel) 5:164–180. https://doi.org/10.3390/life5010164.
7. Adessi A, Carvalho RC, De Philippis R, Branquinho C, Silva JM. 2018. Microbial extracellular polymeric substances improve water retention in dryland biological soil crusts. Soil Biol Biochem 116:67–69. https://doi.org/10.1016/j.soilbio.2017.10.002.
8. Pereira S, Zille A, Micheletti E, Moradas-Ferreira P, De Philippis R, Tamagnini P. 2009. Complexity of cyanobacterial exopolysaccharides: composition, structures, inducing factors and putative genes involved in their biosynthesis and assembly. FEMS Microbiol Rev 33:917–941. https://doi.org/10.1111/j.1574-6976.2009.00183.x.
9. Pereira SB, Sousa A, Santos M, Araújo M, Serôdio F, Granja PL, Tamagnini P. 2019. Strategies to obtain designer polymers based on cyanobacterial extracellular polymeric substances (EPS). Int J Mol Sci 20:5693. https://doi.org/10.3390/ijms20225693.
10. Chentir I, Hamdi M, Doumandji A, HadjSadok A, Ouada HB, Nasri M, Jridi M. 2017. Enhancement of extracellular polymeric substances (EPS) production in *Spirulina* (*Arthrospira* sp.) by two-step cultivation process and partial characterization of their polysaccharidic moiety. Int J Biol Macromol 105:1412–1420. https://doi.org/10.1016/j.ijbiomac.2017.07.009.
11. Leite JP, Mota R, Durao J, Neves SC, Barrias CC, Tamagnini P, Gales L. 2017. Cyanobacterium-derived extracellular carbohydrate polymer for the controlled delivery of functional proteins. Macromol Biosci 17:1600206. https://doi.org/10.1002/mabi.201600206.
12. Estevinho BN, Mota R, Leite JP, Tamagnini P, Gales L, Rocha F. 2019. Application of a cyanobacterial extracellular polymeric substance in the microencapsulation of vitamin B12. Powder Technol 343:644–651. https://doi.org/10.1016/j.powtec.2018.11.079.
13. Flores C, Lima RT, Adessi A, Sousa A, Pereira SB, Granja PL, De Philippis R, Soares P, Tamagnini P. 2019. Characterization and antitumor activity of the extracellular carbohydrate polymer from the cyanobacterium *Synechocystis* Δ*sigF* mutant. Int J Biol Macromol 136:1219–1227. https://doi.org/10.1016/j.ijbiomac.2019.06.152.
14. Mota R, Vidal R, Pandeirada C, Flores C, Adessi A, De Philippis R, Nunes C, Coimbra MA, Tamagnini P. 2020. Cyanoflan: a cyanobacterial sulfated carbohydrate polymer with emulsifying properties. Carbohydr Polym 229:115525. https://doi.org/10.1016/j.carbpol.2019.115525.
15. van der Woude AD, Angermayr SA, Puthan VV, Osnato A, Hellingwerf KJ. 2014. Carbon sink removal: increased photosynthetic production of lactic acid by *Synechocystis* sp. PCC6803 in a glycogen storage mutant. J Biotechnol 184:100–102. https://doi.org/10.1016/j.jbiotec.2014.04.029.
16. Katayama N, Iijima H, Osanai T. 2018. Production of bioplastic compounds by genetically manipulated and metabolic engineered cyanobacteria. Adv Exp Med Biol 1080:155–169. https://doi.org/10.1007/978-981-13-0854-3_7.
17. Islam ST, Lam JS. 2014. Synthesis of bacterial polysaccharides via the Wzx/Wzy dependent pathway. Can J Microbiol 60:697–716. https://doi.org/10.1139/cjm-2014-0595.
18. Whitfield C, Trent MS. 2014. Biosynthesis and export of bacterial lipopolysaccharides. Annu Rev Biochem 83:99–128. https://doi.org/10.1146/annurev-biochem-060713-035600.
19. Schmid J, Sieber V, Rehm B. 2015. Bacterial exopolysaccharides: biosynthesis pathways and engineering strategies. Front Microbiol 6:496. https://doi.org/10.3389/fmicb.2015.00496.
20. Cuthbertson L, Mainprize IL, Naismith JH, Whitfield C. 2009. Pivotal roles of the outer membrane polysaccharide export and polysaccharide copolymerase protein families in export of extracellular polysaccharides in Gram-negative bacteria. Microbiol Mol Biol Rev 73:155–177. https://doi.org/10.1128/MMBR.00024-08.
21. Cuthbertson L, Kos V, Whitfield C. 2010. ABC transporters involved in export of cell surface glycoconjugates. Microbiol Mol Biol Rev 74:341–362. https://doi.org/10.1128/MMBR.00009-10.
22. Whitfield C, Wear SS, Sande C. 2020. Assembly of bacterial capsular polysaccharides and exopolysaccharides. Annu Rev Microbiol 74:521–543. https://doi.org/10.1146/annurev-micro-011420-075607.
23. Whitney JC, Howell PL. 2013. Synthase-dependent exopolysaccharide

secretion in gram-negative bacteria. Trends Microbiol 21:63–72. https://doi.org/10.1016/j.tim.2012.10.001.
24. Pereira SB, Mota R, Vieira CP, Vieira J, Tamagnini P. 2015. Phylum-wide analysis of genes/proteins related to the last steps of assembly and export of extracellular polymeric substances (EPS) in cyanobacteria. Sci Rep 5:14835. https://doi.org/10.1038/srep14835.
25. Jittawuttipoka T, Planchon M, Spalla O, Benzerara K, Guyot F, Cassier-Chauvat C, Chauvat F. 2013. Multidisciplinary evidences that *Synechocystis* PCC 6803 exopolysaccharides operate in cell sedimentation and protection against salt and metal stresses. PLoS One 8:e55564. https://doi.org/10.1371/journal.pone.0055564.
26. Pereira SB, Santos M, Leite JP, Flores C, Eisfeld C, Büttel Z, Mota R, Rossi F, De Philippis R, Gales L, Morais-Cabral JH, Tamagnini P. 2019. The role of the tyrosine kinase Wzc (Sll0923) and the phosphatase Wzb (Slr0328) in the production of extracellular polymeric substances (EPS) by *Synechocystis* PCC 6803. Microbiologyopen 8:e00753. https://doi.org/10.1002/mbo3.753.
27. Kopf M, Klähn S, Scholz I, Matthiessen JKF, Hess WR, Voß B. 2014. Comparative analysis of the primary transcriptome of *Synechocystis* sp. PCC 6803. DNA Res 21:527–539. https://doi.org/10.1093/dnares/dsu018.
28. Wu Q, Huang H, Hu G, Chen J, Ho KP, Chen GQ. 2001. Production of poly-3-hydroxybutyrate by *Bacillus* sp. JMa5 cultivated in molasses media. Antonie Van Leeuwenhoek 80:111–118. https://doi.org/10.1023/A:1012222625201.
29. Osanai T, Imashimizu M, Seki A, Sato S, Tabata S, Imamura S, Asayama M, Ikeuchi M, Tanaka K. 2009. ChlH, the H subunit of the Mg-chelatase, is an anti-sigma factor for SigE in *Synechocystis* sp. PCC 6803. Proc Natl Acad Sci U S A 106:6860–6865. https://doi.org/10.1073/pnas.0810040106.
30. Huang S, Chen L, Te R, Qiao J, Wang J, Zhang W. 2013. Complementary iTRAQ proteomics and RNA-seq transcriptomics reveal multiple levels of regulation in response to nitrogen starvation in *Synechocystis* sp. PCC 6803. Mol Biosyst 9:2565–2574. https://doi.org/10.1039/c3mb70188c.
31. Qiao J, Huang S, Te R, Wang J, Chen L, Zhang W. 2013. Integrated proteomic and transcriptomic analysis reveals novel genes and regulatory mechanisms involved in salt stress responses in *Synechocystis* sp. PCC 6803. Appl Microbiol Biotechnol 97:8253–8264. https://doi.org/10.1007/s00253-013-5139-8.
32. Trautmann D, Voss B, Wilde A, Al-Babili S, Hess WR. 2012. Microevolution in cyanobacteria: re-sequencing a motile substrain of *Synechocystis* sp. PCC 6803. DNA Res 19:435–448. https://doi.org/10.1093/dnares/dss024.
33. Ferreira EA, Pacheco CC, Pinto F, Pereira J, Lamosa P, Oliveira P, Kirov B, Jaramillo A, Tamagnini P. 2018. Expanding the toolbox for *Synechocystis* sp. PCC 6803: validation of replicative vectors and characterization of a novel set of promoters. Synth Biol (Oxf) 3:ysy014. https://doi.org/10.1093/synbio/ysy014.
34. Mukhopadhyay A, Kennelly PJ. 2011. A low molecular weight protein tyrosine phosphatase from *Synechocystis* sp. strain PCC 6803: enzymatic characterization and identification of its potential substrates. J Biochem 149:551–562. https://doi.org/10.1093/jb/mvr014.
35. Dutt V, Srivastava S. 2018. Novel quantitative insights into carbon sources for synthesis of polyhydroxybutyrate in *Synechocystis* PCC 6803. Photosynth Res 136:303–314. https://doi.org/10.1007/s11120-017-0464-x.
36. Osanai T, Kanesaki Y, Nakano T, Takahashi H, Asayama M, Shirai M, Kanehisa M, Suzuki I, Murata N, Tanaka K. 2005. Positive regulation of sugar catabolic pathways in the cyanobacterium *Synechocystis* sp. PCC 6803 by the group 2 sigma factor SigE. J Biol Chem 280:30653–30659. https://doi.org/10.1074/jbc.M505043200.
37. Koch M, Doello S, Gutekunst K, Forchhammer K. 2019. PHB is produced from glycogen turn-over during nitrogen starvation in *Synechocystis* sp. PCC 6803. Int J Mol Sci 20:1942. https://doi.org/10.3390/ijms20081942.
38. Koch M, Berendzen KW, Forchhammer K. 2020. On the role and production of polyhydroxybutyrate (PHB) in the cyanobacterium *Synechocystis* sp. PCC 6803. Life (Basel) 10:47. https://doi.org/10.3390/life10040047.
39. Lau NS, Foong CP, Kurihara Y, Sudesh K, Matsui M. 2014. RNA-Seq analysis provides insights for understanding photoautotrophic polyhydroxyalkanoate production in recombinant *Synechocystis* sp. PLoS One 9:e86368. https://doi.org/10.1371/journal.pone.0086368.
40. Osanai T, Oikawa A, Azuma M, Tanaka K, Saito K, Yokota M, Ikeuchi M. 2011. Genetic engineering of group 2 sigma factor SigE widely activates expressions of sugar catabolic genes in *Synechocystis* species PCC 6803. J Biol Chem 286:30962–30971. https://doi.org/10.1074/jbc.M111.231183.
41. Osanai T, Numata K, Oikawa A, Kuwahara A, Iijima H, Doi Y, Tanaka K, Saito K, Hirai MY. 2013. Increased bioplastic production with an RNA polymerase sigma factor SigE during nitrogen starvation in *Synechocystis* sp. PCC 6803. DNA Res 20:525–535. https://doi.org/10.1093/dnares/dst028.
42. Tokumaru Y, Uebayashi K, Toyoshima M, Osanai T, Matsuda F, Shimizu H. 2018. Comparative targeted proteomics of the central metabolism and photosystems in SigE mutant strains of *Synechocystis* sp. PCC 6803. Molecules 23:1051. https://doi.org/10.3390/molecules23051051.
43. Orthwein T, Scholl J, Spät P, Lucius S, Koch M, Macek B, Hagemann M, Forchhammer K. 2020. The novel PII-interacting regulator PirC (Sll0944) identifies 3-phosphoglycerate mutase (PGAM) as central control point of carbon storage metabolism in cyanobacteria. bioRxiv https://doi.org/10.1101/2020.09.11.292599.
44. Kirilovsky D. 2010. The photoactive orange carotenoid protein and photoprotection in cyanobacteria. Adv Exp Med Biol 675:139–159. https://doi.org/10.1007/978-1-4419-1528-3_9.
45. Zhu Y, Graham JE, Ludwig M, Xiong W, Alvey RM, Shen G, Bryant DA. 2010. Roles of xanthophyll carotenoids in protection against photoinhibition and oxidative stress in the cyanobacterium *Synechococcus* sp. strain PCC 7002. Arch Biochem Biophys 504:86–99. https://doi.org/10.1016/j.abb.2010.07.007.
46. Kirilovsky D. 2007. Photoprotection in cyanobacteria: the orange carotenoid protein (OCP)-related non-photochemical-quenching mechanism. Photosynth Res 93:7–16. https://doi.org/10.1007/s11120-007-9168-y.
47. Kirilovsky D, Kerfeld CA. 2012. The orange carotenoid protein in photoprotection of photosystem II in cyanobacteria. Biochim Biophys Acta 1817:158–166. https://doi.org/10.1016/j.bbabio.2011.04.013.
48. Kirilovsky D, Kerfeld CA. 2016. Cyanobacterial photoprotection by the orange carotenoid protein. Nat Plants 2:16180. https://doi.org/10.1038/nplants.2016.180.
49. Batista MB, Teixeira CS, Sfeir M, Alves L, Valdameri G, Pedrosa FO, Sassaki GL, Steffens M, de Souza EM, Dixon R, Müller-Santos M. 2018. PHB biosynthesis counteracts redox stress in *Herbaspirillum seropedicae*. Front Microbiol 9:472. https://doi.org/10.3389/fmicb.2018.00472.
50. Gonçalves CF, Pacheco CC, Tamagnini P, Oliveira P. 2018. Identification of inner membrane translocase components of TolC-mediated secretion in the cyanobacterium *Synechocystis* sp. PCC 6803. Environ Microbiol 20:2354–2369. https://doi.org/10.1111/1462-2920.14095.
51. Huesgen PF, Miranda H, Lam X, Perthold M, Schuhmann H, Adamska I, Funk C. 2011. Recombinant Deg/HtrA proteases from *Synechocystis* sp. PCC 6803 differ in substrate specificity, biochemical characteristics and mechanism. Biochem J 435:733–742. https://doi.org/10.1042/BJ20102131.
52. Miranda H. 2011. Stress response in the cyanobacterium Synechocystis sp. PCC 6803. PhD dissertation. Department of Chemistry, Umeå University, Umeå, Sweden. http://urn.kb.se/resolve?urn=urn:nbn:se:umu:diva-43086.
53. Kanesaki Y, Shiwa Y, Tajima N, Suzuki M, Watanabe S, Sato N, Ikeuchi M, Yoshikawa H. 2012. Identification of substrain-specific mutations by massively parallel whole-genome resequencing of *Synechocystis* sp. PCC 6803. DNA Res 19:67–79. https://doi.org/10.1093/dnares/dsr042.
54. Stanier RY, Kunisawa R, Mandel M, Cohen-Bazire G. 1971. Purification and properties of unicellular blue-green algae (order Chroococcales). Bacteriol Rev 35:171–205. https://doi.org/10.1128/MMBR.35.2.171-205.1971.
55. Tamagnini P, Troshina O, Oxelfelt F, Salema R, Lindblad P. 1997. Hydrogenases in *Nostoc* sp. strain PCC 73102, a strain lacking a bidirectional enzyme. Appl Environ Microbiol 63:1801–1807. https://doi.org/10.1128/AEM.63.5.1801-1807.1997.
56. Sambrook J, Russell DW. 2001. Molecular cloning: a laboratory manual, 3rd ed. Cold Spring Harbor Laboratory Press, Cold Spring Harbor, NY.
57. Pinto F, Pacheco CC, Oliveira P, Montagud A, Landels A, Couto N, Wright PC, Urchueguía JF, Tamagnini P. 2015. Improving a *Synechocystis*-based photoautotrophic chassis through systematic genome mapping and validation of neutral sites. DNA Res 22:425–437. https://doi.org/10.1093/dnares/dsv024.
58. Silva-Rocha R, Martínez-García E, Calles B, Chavarría M, Arce-Rodríguez A, de las Heras A, Páez-Espino AD, Durante-Rodríguez G, Kim J, Nikel PI, Platero R, de Lorenzo V. 2013. The Standard European Vector Architecture (SEVA): a coherent platform for the analysis and deployment of complex prokaryotic phenotypes. Nucleic Acids Res 41:D666–D675. https://doi.org/10.1093/nar/gks1119.
59. Williams JGK. 1988. Construction of specific mutations in photosystem II photosynthetic reaction center by genetic engineering methods in *Synechocystis* 6803. Methods Enzymol 167:766–778. https://doi.org/10.1016/0076-6879(88)67088-1.
60. Anderson SL, McIntosh L. 1991. Light-activated heterotrophic growth of

the cyanobacterium *Synechocystis* sp. strain PCC 6803: a blue-light-requiring process. J Bacteriol 173:2761–2767. https://doi.org/10.1128/jb.173.9.2761-2767.1991.
61. Meeks JC, Castenholz RW. 1971. Growth and photosynthesis in an extreme thermophile, *Synechococcus lividus* (Cyanophyta). Arch Mikrobiol 78:25–41. https://doi.org/10.1007/BF00409086.
62. Mota R, Guimarães R, Buttel Z, Rossi F, Colica G, Silva CJ, Santos C, Gales L, Zille A, De Philippis R, Pereira SB, Tamagnini P. 2013. Production and characterization of extracellular carbohydrate polymer from *Cyanothece* sp. CCY 0110. Carbohydr Polym 92:1408–1415. https://doi.org/10.1016/j.carbpol.2012.10.070.
63. Dubois M, Gilles KA, Hamilton JK, Rebers PA, Smith F. 1956. Colorimetric method for determination of sugars and related substances. Anal Chem 28:350–356. https://doi.org/10.1021/ac60111a017.
64. Ernst A, Kirschenlohr H, Diez J, Böger P. 1984. Glycogen content and nitrogenase activity in *Anabaena variabilis*. Arch Microbiol 140:120–125. https://doi.org/10.1007/BF00454913.
65. Vidal R, Venegas-Calerón M. 2019. Simple, fast and accurate method for the determination of glycogen in the model unicellular cyanobacterium *Synechocystis* sp. PCC 6803. J Microbiol Methods 164:105686. https://doi.org/10.1016/j.mimet.2019.105686.
66. Simkovsky R, Daniels EF, Tang K, Huynh SC, Golden SS, Brahamsha B. 2012. Impairment of O-antigen production confers resistance to grazing in a model amoeba-cyanobacterium predator-prey system. Proc Natl Acad Sci U S A 109:16678–16683. https://doi.org/10.1073/pnas.1214904109.
67. Oliveira P, Martins NM, Santos M, Pinto F, Büttel Z, Couto NA, Wright PC, Tamagnini P. 2016. The versatile TolC-like Slr1270 in the cyanobacterium *Synechocystis* sp. PCC 6803. Environ Microbiol 18:486–502. https://doi.org/10.1111/1462-2920.13172.
68. Gomes C, Almeida A, Ferreira JA, Silva L, Santos-Sousa H, Pinto-de-Sousa J, Santos LL, Amado F, Schwientek T, Levery SB, Mandel U, Clausen H, David L, Reis CA, Osório H. 2013. Glycoproteomic analysis of serum from patients with gastric precancerous lesions. J Proteome Res 12:1454–1466. https://doi.org/10.1021/pr301112x.
69. Osório H, Reis CA. 2013. Mass spectrometry methods for studying glycosylation in cancer. Methods Mol Biol 1007:301–316. https://doi.org/10.1007/978-1-62703-392-3_13.
70. Fujisawa T, Narikawa R, Maeda S, Watanabe S, Kanesaki Y, Kobayashi K, Nomata J, Hanaoka M, Watanabe M, Ehira S, Suzuki E, Awai K, Nakamura Y. 2017. CyanoBase: a large-scale update on its 20th anniversary. Nucleic Acids Res 45:D551–D554. https://doi.org/10.1093/nar/gkw1131.
71. Seabra R, Santos A, Pereira S, Moradas-Ferreira P, Tamagnini P. 2009. Immunolocalization of the uptake hydrogenase in the marine cyanobacterium *Lyngbya majuscula* CCAP 1446/4 and two *Nostoc* strains. FEMS Microbiol Lett 292:57–62. https://doi.org/10.1111/j.1574-6968.2008.01471.x.

Supporting Information

Supporting Experimental Procedures

Detailed description of the RNA Sequencing experiment

The trancriptomes of *Synechocystis* wild type and *kpsM* mutant were analyzed by RNA sequencing, using three biological replicates. Cultures were grown in the conditions described at the Experimental procedures section until reaching an OD_{730nm} of 1.5. At that point, 100 ml of each culture was centrifuged at 3850 g for 5 min at room temperature, and cells were washed with sterile BG11 and pre-treated with RNAprotect Bacteria Reagent® (Qiagen) before saved at -80 ºC. After RNA extraction, a total amount of 1 µg RNA per sample was used as input material for the RNA sample preparations. Sequencing libraries were generated using NEBNext® Ultra TM RNA Library Prep Kit for Illumina® (NEB, USA) following manufacturer's recommendations and index codes were added to attribute sequences to each sample. Briefly, mRNA was purified from total RNA using poly-T oligo-attached magnetic beads. Fragmentation was carried out using divalent cations under elevated temperature in NEBNext First Strand Synthesis Reaction Buffer (5X). First strand cDNA was synthesized using random hexamer primer and M-MuLV Reverse Transcriptase (RNase H-). Second strand cDNA synthesis was subsequently performed using DNA Polymerase I and RNase H. Remaining overhangs were converted into blunt ends via exonuclease/polymerase activities. After adenylation of 3' ends of DNA fragments, NEBNext Adaptor with hairpin loop structure were ligated to prepare for hybridization. In order to select cDNA fragments of preferentially 150~200 bp in length, the library fragments were purified with AMPure XP system (Beckman Coulter, Beverly, USA). Then 3 µl USER Enzyme (NEB, USA) was used with size-selected, adaptorligated cDNA at 37 °C for 15 min followed by 5 min at 95 °C before PCR. Then PCR was performed with Phusion High-Fidelity DNA polymerase, Universal PCR primers and Index (X) Primer. At last, PCR products were purified (AMPure XP system) and library quality was assessed on the Agilent Bioanalyzer 2100 system. The clustering of the index-coded samples was performed on a cBot Cluster Generation System using PE Cluster Kit cBot-HS (Illumina) according to the manufacturer's instructions. After cluster generation, the library preparations were sequenced on an Illumina platform and paired-end reads were generated. Raw data (raw reads) of FASTQ format were firstly processed through in-house scripts. In this step, clean data (clean reads) were obtained by removing reads containing adapter and poly-N

sequences and reads with low quality from raw data. At the same time, Q20, Q30 and GC content of the clean data were calculated. All the downstream analyses were based on the clean data with high quality. Reference genome and gene model annotation files were downloaded from genome website browser (NCBI/UCSC/Ensembl) directly. Paired-end clean reads were mapped to the reference genome using HISAT2 software. HISAT2 uses a large set of small GFM indexes that collectively cover the whole genome. These small indexes (called local indexes), combined with several alignment strategies, enable rapid and accurate alignment of sequencing reads. HTSeq was used to count the read numbers mapped of each gene, including known and novel genes. And then RPKM of each gene was calculated based on the length of the gene and reads count mapped to this gene. RPKM, Reads Per Kilobase of exon model per Million mapped reads, considers the effect of sequencing depth and gene length for the reads count at the same time, and is currently the most commonly used method for estimating gene expression levels. Differential expression analysis between two conditions/groups (three biological replicates per condition) was performed using DESeq2 R package. DESeq2 provides statistical routines for determining differential expression in digital gene expression data using a model based on the negative binomial distribution. The resulting P values were adjusted using the Benjamini and Hochberg's approach for controlling the False Discovery Rate (FDR). Genes with an adjusted P value < 0.05 found by DESeq2 were assigned as differentially expressed.

Detailed description of iTRAQ experiment

The proteomes of Synechocystis wild type and *kpsM* mutant were analyzed by 8-plex isobaric tags for relative and absolute quantification (iTRAQ), using three biological replicates. Cultures were grown in the conditions described at the Experimental procedures section until reaching a OD_{730nm} of 1.5. At that point, 75 ml of each culture was centrifuged at 3850 g for 5 min at room temperature, and cells were washed with K phosphate buffer (50 mM K2HPO4, 50 mM KH2PO4, pH 6.9) before saved at -80 ºC. Cell pellets of WT (3 biological replicates) and *kpsM* mutant (3 biological replicates), were thawed and cells were re-suspended in 400 µL lysis buffer [200 mM triethylammonium bicarbonate (TEAB), 10 mM dithiothreitol (DTT), 1% (w/v) sodium deoxycholate, 0.1% (v/v) NP40 and 5 µL protease inhibitor cocktail set II, pH 8.5] and transferred to 2 mL LoBind microcentrifuge tubes (Eppendorf) containing ~400 mg of 200 µm Zirconium beads. Cell lysis was performed using a cell disruptor (Genie, VWR, UK) using 10 cycles of 60 s with a one minute cooling step on ice between cycles. Samples were centrifuged at 13,000 g for 10 min

at 4°C, and supernatants were transferred to clean microcentrifuge tubes. Remaining pellets were further resuspended in 200 µL of lysis buffer, and a further 5 cycles on the cell disruptor was used as before. Samples were centrifuged and supernatants were combined. The combined supernatants were further clarified by centrifugation at 13,000 g for 10 min at 4°C to ensure that any remaining cell debris was removed from the extracts. The clarified extracts were incubated with 2 µl of benzonase nuclease (Novagene) for 2 min on ice. Protein content in each extract was estimated using the modified Lowry spectrophotometric method as previously described [1]. The concentration of the protein extracts was evaluated by sodium dodecyl sulfate polyacrylamide gel [2] followed by silver staining [3]. Isobaric tags for relative and absolute quantitation (iTRAQ) 8-plex labelling was performed according to the manufacturer's protocol (8-plex iTRAQ reagent Multiplex kit, ABSciex, USA). Before labelling, samples were reduced, alkylated and digested as follows: 100 µg of proteins from each sample was first reduced with 2.5 µL of 10 mM Tris (2-carboxyethyl) phosphine hydrochloride and incubated at 60 °C for 1 h. Samples were then alkylated using 4.5 µL of 20 mM methyl methanethiosulfonate at room temperature for 30 min. Subsequently, proteins were digested with trypsin (Promega, UK) at a ratio of 1:20 (trypsin:protein) overnight at 37 °C. After digestion, biological replicates from each Synechocystis strain (WT and *kpsM* mutant) were labelled with a specific iTRAQ reagent. Labels 113, 114 and 115 were used to label the WT samples and labels 116, 117 and 118 were used to label the *kpsM* mutant samples. After 2 h incubation at room temperature, iTRAQ-labelled peptides were combined and concentrated using a vacuum concentrator (Eppendorf). iTRAQ-labelled peptides were off-line fractionated using a porous graphitic column (Hypercarb) with the following specifications: 7 µm particle size, 50 mm length, 2.1 mm diameter and 250 Å pore size (Thermo Fisher Scientific, Waltham, MA, USA) coupled with an UHPLC Ultimate 3000 RS (Thermo Fisher Scientific, Dionex, Hemel Hempstead, UK) at a flow rate of 0.2 mL min^{-1}. iTRAQ-labelled peptides were resuspended in 100 µL of buffer A [97% (v/v) HPLC water, 3% (v/v) HPLC acetonitrile, 0.1% (v/v) trifluoroacetic acid] and separated using a 86 minutes gradient starting with 2% buffer B [97% (v/v) HPLC acetonitrile, 3% (v/v) HPLC water, 0.1% (v/v) trifluoroacetic acid] for 5 min, 2–10% buffer B for 5 min, 10–60% buffer B for 50 min, 60–80% buffer B for 10 min, 80–90% buffer B for 1 min, 90% buffer B for 5 min and 90-2% buffer B for 1 min and 2% buffer B for 9 min. The chromatographic profile of the separated peptides was monitored at the wavelength of 240 nm using Chromeleon software (Thermo Fisher Scientific, Hemel, Hempstead, UK). Fractions were collected every 2 min from 10 min to 50 min (20 fractions). Collected

fractions were then dried in a vacuum concentrator and stored at −20 °C until further analysis.

Each fraction was resuspended in 10 µL reverse phase (RP) buffer A [97% (v/v) HPLC water, 3% (v/v) HPLC acetonitrile, 0.1% (v/v) formic acid] and combined to obtain 10 fractions for mass spectrometric analysis. Each fraction was run using a Q Exactive™ Hybrid Quadrupole-Orbitrap™ mass spectrometer (Thermo Scientific, Bremen, Germany) coupled with an online UHPLC Ultimate 3000 (Thermo Fisher Scientific, Dionex, Hemel Hempstead, UK). From each fraction, 4 µL were injected and peptides were separated using a PepMap RSLC C18 column with the following characteristics: 2 µm, 100 Å, 75 µm × 50 cm (Thermo Fisher Scientific, Hemel, Hempstead, UK) at a constant flow rate of 300 nL min^{-1}. A 135 min gradient was performed using RP buffer B [97% (v/v) HPLC acetonitrile, 3% (v/v) HPLC water, 0.1% (v/v) formic acid] as follows: 4% B for 0 min, 4% B for 5 min, 4–40% B for 100 min, 40–90% B for 1 min, 90% B for 14 min, 90–4% for 1 min and finally 4% of buffer B for 14 min. Mass spectrometry (MS) data was acquired using Xcalibur software v 4.0 (Thermo Scientific, Bremen, Germany) with the following settings. MS scans were acquired with 60,000 resolution, automatic gain control (AGC) target 3e6, maximum injection time (IT) 100 ms. The MS mass range was set to be in the range 100–1500 m/z. Tandem mass spectrometry (MS/MS) scans were acquired using high-energy collision dissociation (HCD), 30,000 resolution, AGC target 5e4, maximum IT 120 ms. In total, 15 MS/MS were acquired per MS scan using normalised collision energy (NCE) of 34% and isolation window of 1.2 m/z. The *Synechocystis* sp. PCC 6803 (taxon ID: 1111708) database containing 3507 proteins was downloaded from Uniprot (.fasta) and uploaded on MaxQuant software (version 1.5.4.1). The settings were as follows; for "type the experimental set" MS2 and 8-plex iTRAQ were selected with reporter mass tolerance of 0.01 Da. Enzymatic digestion with trypsin was specified and two missed cleavages were allowed per peptide. Oxidation of methionine and deamidation of asparagine and glutamine were selected as variable modifications and methylthio modification of cysteine was selected as the fixed modification. The false discovery rate (FDR) at the peptide spectrum match/protein level was set at 1%. The reporter ions intensities (113, 114, 115, 116, 117 and 118) were used for quantification purposes. Fold changes of the differentially abundant proteins were calculated using a published method [4] and using the ProteoSign, an online service.

References

[1] Bensadoun, A., and Weinstein, D. (1976) Assay of proteins in the presence of interfering materials. *Analytical Biochemistry* 70: 241−250.

[2] Laemmli, U.K. (1970) Cleavage of structural proteins during the assembly of the head of bacteriophage T4. *Nature* 227: 680–685.

[3] Couto, N., Barber, J., and Gaskell, S.J. (2011) Matrix-assisted laser desorption/ionization (MALDI) mass spectrometric response factors of peptides generated using different proteolytic enzymes. *Journal of Mass Spectrometry* 46: 1233−1240.

[4] Efstathiou, G., Antonakis, A.N., Pavlopoulos, G.A., Theodosiou, T., Divanach, P., Trudgian, D.C., Thomas, B., Papanikolaou, N., Aivaliotis, M., Acuto, O., and Iliopoulos, I. (2017) ProteoSign: an end-user online differential proteomics statistical analysis platform. *Nucleic Acids Research* 45: W300–W306.

[5] Trautner, C., and Vermaas, W.F.J. (2013) The *sll1951* gene encodes the surface layer protein of *Synechocystis* sp. Strain PCC 6803. *Journal of Bacteriology* 195: 5370–5380.

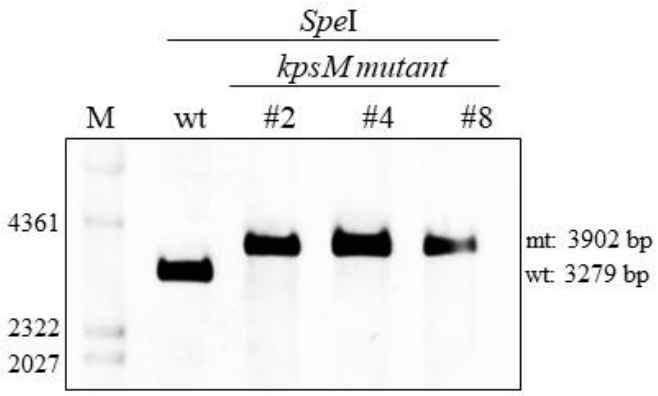

Figure S1. Southern blot analysis confirming the segregation of the *Synechocystis* sp. PCC 6803 *kpsM* mutant. The DNA was digested with the endonuclease *SpeI*. A dioxigenin labeled probe covering the 5' flanking region of kpsM was used (primers listed on Table S4). The sizes of the DNA fragments hybridizing with the probe are indicated. wt – wild type; # clone tested.

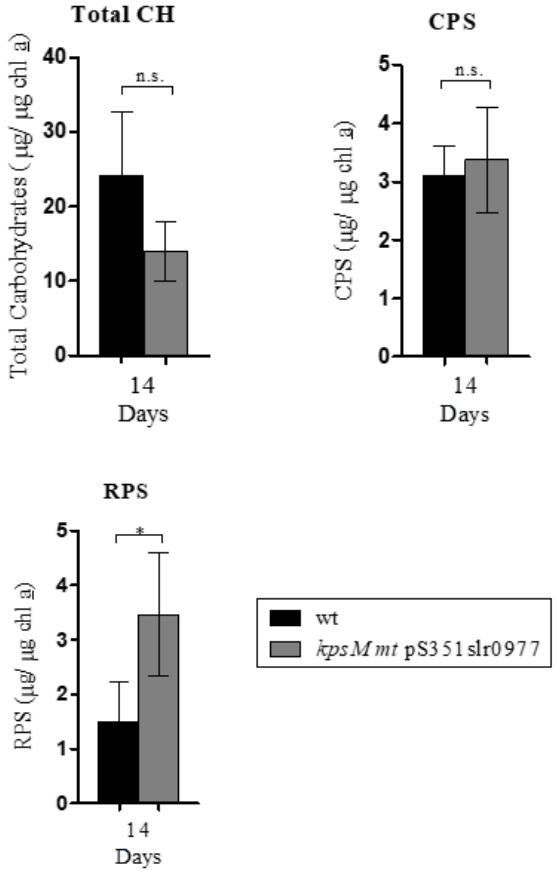

Figure S2. Total carbohydrates (Total CH), capsular (CPS) and released (RPS) polysaccharides of *Synechocystis* sp. PCC 6803 wild-type (wt) and *kpsM*

mutant:pS351slr0977 expressed as µg of carbohydrates per µg of chlorophyll *a* (chl *a*). Cells were grown in BG11 at 30 °C under a 12 h light (50 µE m^{-2} s^{-1})/12 h dark regimen, with orbital shaking at 150 r.p.m. Experiments were made in duplicate and the statistical analysis is presented (not significant (n.s.) p value > 0,05; * p value ≤ 0.05).

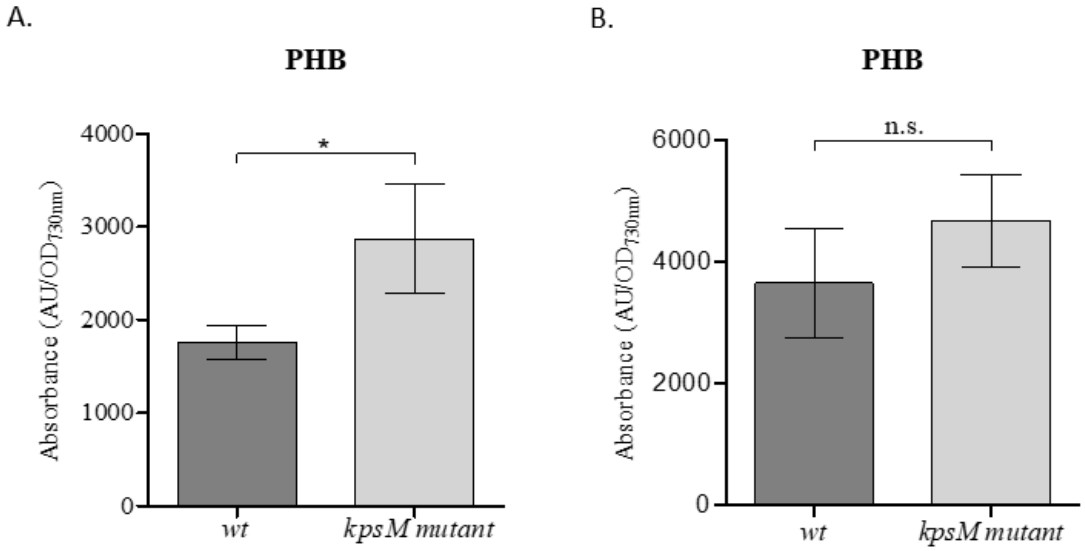

Figure S3. Quantification of PHB content of *Synechocystis* sp. PCC 6803 wild-type (wt) and *kpsM* mutant by Nile red-based fluorescence spectroscopy. A. Cells were grown in BG11 at 30 °C under a 12 h light (50 µE m−2 s−1)/12 h dark regimen, with orbital shaking at 150 r.p.m. B. Cells were cultured in $BG11_0$ at 30 °C under a 12 h light (50 µE m^{-2} s^{-1})/12 h dark regimen, with orbital shaking at 150 r.p.m for 5 days. Experiments were made in triplicate and the statistical analysis is presented (not significant (n.s.); p value > 0,05; * p value < 0.05).

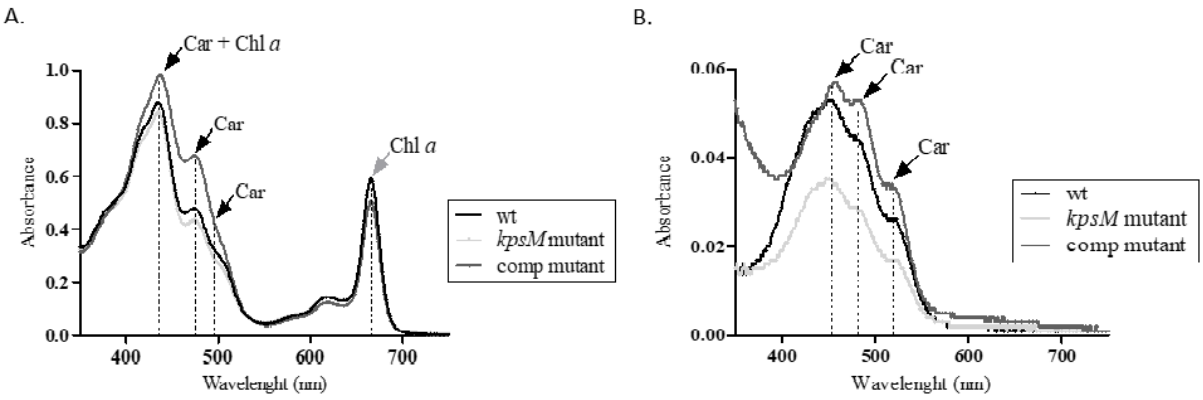

Figure S4. Analysis of the intracellular and extracellular medium carotenoids content of *Synechocystis* sp. PCC 6803 wild type (wt), *kpsM* mutant, and the complemented mutant (comp mutant). Absorption spectra of A. cell-free extracts (intracellular content) and B. concentrated medium. Black arrows arrows indicate the characteristic carotenoids peaks (at 460, 487 and 521 nm), while the grey arrow indicates the absorption peak of chlorophyll *a*. Car, carotenoids; Chl *a*, chlorophyll *a*.

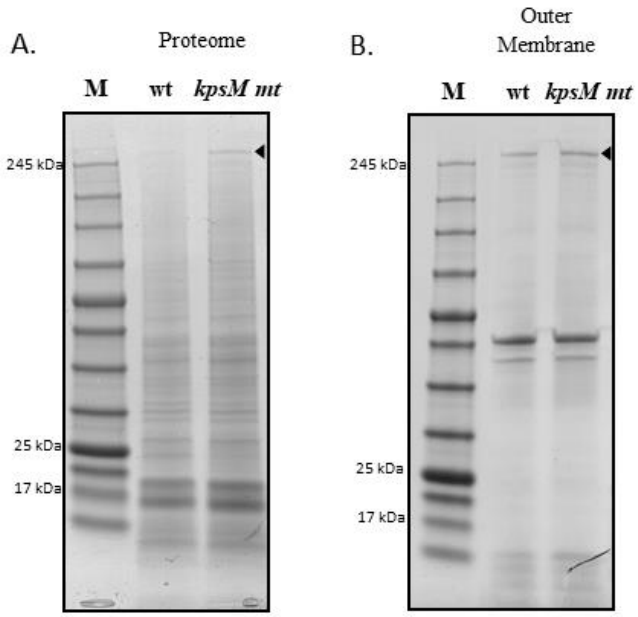

Figure S5. Total protein and outer membrane extracts of *Synechocystis* sp. PCC 6803 wild-type (wt) and *kpsM* mutant. Roti-Blue^{TM} stained 4-15% SDS-polyacrylamide gel of A. total protein extracts and B. outer membrane protein extracts. Sample loading was normalized to amount of protein. Arrowheads highlight bands corresponding to the S-layer protein component - Sll1951 [5]. M, NZYColour Protein Marker II (NZYTech).

Table S1. Distribution by functional categories of the genes quantified in the RNAseq analysis with significant fold changes in mRNA transcript levels in *Synechocystis kpsM* mutant vs. wild type.

ORF	Gene ID	Description	Fold Changes (mt:wt)
Photosynthesis			
slr0148	-	ferredoxin	-2,6
slr0750	*chlN*	light-independent protochlorophyllide reductase subunit	-3,0
sll0199	*petE*	Plastocyanin	-1,7
slr1828	*petF*	ferredoxin	2,1
sll0662	-	ferredoxin (bacterial type ferredoxin family)	-2,0
sll1584	-	ferredoxin like protein	-3,0
sll1317	*petA*	apocytochrome f, component of cytochrome b6/f complex	-2,2
ssr2831	*psaE*	Photosystem I reaction center subunit IV	1,8
slr0342	*petB*	cytochrome b6	-1,7
sll1194	*psbU*	photosystem II 12 kD extrinsic protein	-1,6
ssr0390	*psaK1*	photosystem I reaction center subunit X	1,7
ssr3451	*psbE*	cytochrome b559 alpha subunit	-1,6
slr0150	*petF*	ferredoxin	-1,9
slr0753	*p*	P protein	-1,9
slr1459	*apcF*	phycobilisome core component	-1,5
sll0550	*Dfa1*	Diflavin flavoprotein A1 (NADH:oxygen oxidoreductase)	-1,7
sml0008	*psaJ*	Photosystem I reaction center subunit IX	1,7
sll0629	*psaK*	photosystem I subunit X	1,6
sll0427	*psbO*	photosystem II manganese-stabilizing polypeptide	-1,5
ssl0453	*nblA*	phycobilisome degradation protein	-1,6
ssr2049	*bchB*	protochlorophillide reductase 57 kD subunit	-2,7
smr0004	*psaI*	photosystem I subunit VIII	1,6
slr2051	*cpcG; cpcG1*	Phycobilisome rod-core linker polypeptide	1,4
-	*psbZ*	photosystem II	-1,5
sll1513	*ccsA*	c-type cytochrome synthesis protein	-1,3
sll0819	*psaF*	Photosystem I reaction center subunit III (PSI-F)	1,4
sll1867	*psbA3*	photosystem II D1 protein	-2,1
ssr3383	*apcC*	Phycobilisome, allophycocyanin-associated	-1,5
smr0008	*psbJ*	photosystem II PsbJ protein	-2,0
ssl0563	*psaC*	photosystem I subunit VII	-1,3
sll1316	*petC*	plastoquinol--plastocyanin reductase	-1,4
smr0005	*psaM*	photosystem I PsaM subunit	1,4
Oxidative Phosphorylation			
sll1324	*atpF*	ATP synthase subunit b	2,2
sll1323	*atpG*	ATP synthase subunit b'	2,2
slr1137	*ctaD*	cytochrome c oxidase subunit I	-1,7
slr1136	*ctaC*	cytochrome c oxidase subunit II	-1,7
slr1233	*frdA*	Succinate dehydrogenase flavoprotein subunit	-1,4
sll0223	*ndhB*	NAD(P)H dehydrogenase I subunit 2	1,5
sll1322	*atpI*	ATP synthase subunit a	1,7
sll1325	*atpD*	ATP synthase d subunit	1,8

slr1138	*ctaE*	cytochrome c oxidase subunit III	-1,7
sll1899	*ctaB*	cytochrome c oxidase folding protein	1,4
sll0522	*ndhE*	NADH dehydrogenase subunit 4L	-1,7
sll0813	*ctaC*	cytochrome c oxidase subunit II	1,4
slr0851	*ndh*	NADH dehydrogenase	1,4
Carbon Metabolism			
sll1776	*deoC*	deoxyribose-phosphate aldolase	-3,5
slr0194	*rpiA*	Ribose-5-phosphate isomerase A	-2,5
slr0985	*rfbC*	dTDP-6-deoxy-L-mannose-dehydrogenase	2,8
slr0983	*rfbF*	glucose-1-phosphate cytidylyltransferase	2,1
slr0953	-	sucrose-6-phosphatase	-2,0
slr0301	*ppsA*	phosphoenolpyruvate synthase	-2,1
slr0984	*rfbG*	CDP-glucose 4,6-dehydratase	2,3
slr1349	*pgi*	glucose-6-phosphate isomerase	-1,7
slr0237	*glgX*	glycogen operon protein; GlgX	-1,6
sll1723	-	Probable glycosyltransferase	2,5
slr1945	*pgm*	2,3-bisphosphoglycerate-independent phosphoglycerate mutase	1,6
slr0288	*glnN*	glutamine synthetase	1,6
sll0745	*pfkA*	phosphofructokinase	-1,6
sll1664	-	probable glycosyl transferase	1,5
sll1023	*sucC*	succinate--CoA ligase	-1,9
sll1031	*ccmM*	carbon dioxide concentrating mechanism protein	-1,6
slr1830	*phbC*	polyhydroxyalkanoate synthase subunit PhaC	-1,7
slr0344	*rbfW*	Glycosyltransferase	-2,0
slr0943	*fda*	fructose-bisphosphate aldolase	-1,6
sll1231	*mtfB*	Mannosyltransferase B	-1,8
slr0606	-	Probable glycosyltansferase	1,4
slr1843	*zwf*	Glucose-6-phosphate 1-dehydrogenase	1,4
sll1535	*rfbP*	galactosyl-1-phosphate transferase	1,4
slr1050	-	dolichyl-phosphate-mannose-protein mannosyltransferase	-1,5
slr1513	-	Part of the SbtA/B Ci uptake system	-1,6
slr2132	*pta*	phosphotransacetylase	1,5
slr2116	*spsA*	spore coat polysaccharide biosynthesis protein	-1,6
slr0394	*pgk*	phosphoglycerate kinase	1,3
sll0920	*ppc*	phosphoenolpyruvate carboxylase	-1,4
Motility			
sll0043	-	Cyanobacterial hybrid kinase	-3,3
sll0041	-	Putative methyl-accepting chemotaxis protein	-2,1
slr1276	-	type IV pilus assembly protein PilO	-1,7
slr1275	-	type IV pilus assembly protein PilN	-1,8
sll1694	*hofG*	General secretion pathway protein G	-1,5
sll1533	*pilT*	twitching mobility protein	-1,8
sll1291	-	twitching motility two-component system response regulator PilG	2,0
slr1044	*mcpA*	Methyl-accepting chemotaxis protein	-1,5
sll1695	*hofG*	type IV pilus assembly protein PilA	-1,3
sll0039	-	CheY subfamily	-1,3
Amino Sugar and Nucleotide Sugar Metabolism			
slr0017	*murA*	UDP-N-acetylglucosamine 1-carboxyvinyltransferase	2,8

slr1746	*murI*	Glutamate racemase	3,0
slr1423	*murC*	UDP-N-acetylmuramate-alanine ligase	2,2
		Nucleotide Metabolism	
slr0597	*purH*	phosphoribosyl aminoimidazole carboxy formyl formyltransferase/inosinemonophosphate cyclohydrolase; PUR-H(J)	-1,6
sll0368	*pyrR*	Bifunctional protein PyrR [Includes: Pyrimidine operon regulatory protein; Uracil phosphoribosyltransferase (UPRTase)	1,6
slr0520	*purL*	phosphoribosyl formylglycinamidine synthase	1,7
sll1823	*purA*	Adenylosuccinate synthetase (AMPSase) (AdSS) (IMP--aspartate ligase)	-1,4
sll0646	*cyaA*	adenylate cyclase	-1,6
slr0379	-	dTMP kinase	1,7
Cell Envelope and Lipid Metabolism			
ssl1498	-		-5,2
slr1028	-	integrin alpha-subunit domain homologue	2,0
slr0993	*nlpD*	lipoprotein	2,1
slr0938	-	lipid II isoglutaminyl synthase	-2,1
ssl3177	*repA*	rare lipoprotein A	2,1
slr1744	*amiA*	N-acetylmuramoyl-L-alanine amidase	1,6
slr0883	*psr*	polyisoprenyl-teichoic acid--peptidoglycan teichoic acid transferase	1,8
sll0513	-	farnesyl-diphosphate farnesyltransferase	2,0
sll0083	*gmhA*	Phosphoheptose isomerase	1,6
sll1775	-	non-lysosomal glucosylceramidase	-1,6
slr0488	-	putative peptidoglycan lipid II flippase	1,8
sll1522	*pgsA*	CDP-diacylglycerol--glycerol-3-phosphate 3-phosphatidyltransferase	-1,7
slr0193	-	RNA-binding protein (involved in lipid peroxidation and change of degree of lipid unsaturation)	-1,3
slr0408	-	integrin alpha subunit domain homologue	1,3
slr1677	-	lipid-A-disaccharide synthase	-2,7
sll0914	-	lipid metabolic process	2,1
Protein / RNA Folding and Degradation			
slr0083	*crhR; deaD*	RNA helicase CrhR (mRNA degradation)	-2,8
slr0551	-	ribonuclease J	-2,0
slr1129	*rne*	ribonuclease E	-2,1
slr0165	*clpP3*	ATP-dependent Clp protease proteolytic subunit 3	-2,0
sll0430	*htpG*	Heat shock protein	-1,8
sll1679	*hhoA*	Putative serine protease	1,7
sll1463	*ftsH4*	ATP-dependent zinc metalloprotease FtsH 4	-1,5
slr0164	*clpR*	ATP-dependent Clp protease proteolytic subunit-like	-1,6
slr2076	*GroL1, Cpn60-1, GroEL1*	Chaperonin 1	-1,5
sll1043	*pnp*	polyribonucleotide nucleotidyltransferase	-1,5
ssr3307	*Ycf47*	preprotein translocase subunit SecG	-1,3
sll0535	*clpX*	ATP-dependent Clp protease ATP-binding subunit	-1,4
sll0416	*GroL2, Cpn60-2, GroEL2*	Chaperonin 2	-1,4
sll1910	*zam*	ribonuclease R	-1,5

sll0020	*clpC*	ATP-dependent Clp protease regulatory subunit	-1,4
Transcription			
slr1545	*sigG*	Sigma factor G	2,9
sll1961	-	GntR family transcriptional regulator	2,2
sll1742	*nusG*	transcription antitermination protein	-2,0
sll1689	*sigE; rpoD*	Sigma factor E	1,8
sll1818	*rpoA*	RNA polymerase alpha subunit	-2,0
slr1912	-	anti-sigma F factor antagonist	2,1
sll1789	*rpoC2*	RNA polymerase beta prime subunit	-1,6
slr1738	-	Fur family transcriptional regulator, peroxide stress response regulator	-1,7
sll1787	*rpoB*	RNA polymerase beta subunit	-1,8
slr0743	*nusA*	N utilization substance protein	-1,6
sll0306	*rpoD*	RNA polymerase sigma factor	-1,5
sll0856	*rpoE*	RNA polymerase sigma-E factor	1,8
sll0567	*fur*	ferric uptake regulation protein	1,5
slr0302	-	two-component sensor activity, regulation of transcription	-1,4
sll0998	-	LysR transcriptional regulator	1,4
Translation			
sll1799	*rplC*	50S ribosomal protein L3	-2,1
sll1101	*rpsJ*	30S ribosomal protein S10	-2,4
slr1795	*msrA*	peptide methionine sulfoxide reductase	-2,2
sll1743	*rplK*	50S ribosomal protein L11	-2,1
sll1866	-	L-threonylcarbamoyladenylate synthase	-2,2
ssl1426	*Rpl35*	50S ribosomal protein L35	-1,6
sll0947	*Hpf; lrtA*	Ribosome hibernation promotion factor (HPF) (Light-repressed protein A)	-1,6
-	*rpmG*	large subunit ribosomal protein L33	-1,7
sll1261	*tsf*	Elongation factor Ts (EF-Ts)	-1,7
sll1816	*rpsM; rps13*	30S ribosomal protein S13	-1,5
slr1031	*tyrS*	tyrosyl tRNA synthetase	-1,8
ssr1399	*rpsR; rps18*	30S ribosomal protein S18	-1,6
slr1550	*lysS*	lysyl-tRNA synthetase	-1,9
slr0923	-	Probable 30S ribosomal protein PSRP-3 (Ycf65-like protein)	-1,5
sll1810	*rplF; rpl6*	50S ribosomal protein L6	1,5
sll1821	*rplM; rpl13*	50S ribosomal protein L13	-1,6
ssr0482	*Rps16*	30S ribosomal protein S16	-1,4
sll0767	*rplT; rpl20*	50S ribosomal protein L20	-1,5
sll1817	*rpsK; rps11*	30S ribosomal protein S11	-1,5
sll1260	*rpsB; rps2*	30S ribosomal protein S2	-1,5
sll1822	*rpsI; rps9*	30S ribosomal protein S9	-1,4
sll0495	*asnS*	asparaginyl-tRNA synthetase	1,4
ssr1736	*Rps32*	50S ribosomal protein L32	-1,5
sll1097	*rpsG; rps7*	30S ribosomal protein S7	-1,5
slr0120	-	tRNA/rRNA methyltransferase	2,0
sll1740	*rplS; rpl19*	50S ribosomal protein L19	-1,3
slr1115	-	tRNA (cmo5U34)-methyltransferase	-1,7
slr0033	-	aspartyl-tRNA(Asn)/glutamyl-tRNA(Gln) amidotransferase subunit C	-1,3

Cofactors and Vitamins Metabolism			
slr1434	*pntB*	pyridine nucleotide transhydrogenase beta subunit	-2,9
slr0536	*hemE*	uroporphyrinogen decarboxylase	-1,9
slr1916	-	Probable esterase	-2,1
slr0506	*Por; pcr*	Light-dependent protochlorophyllide reductase (PCR) (NADPHprotochlorophyllide oxidoreductase) (LPOR) (POR)	-1,8
sll0898	-	thiamine phosphate phosphatase	-1,9
slr1882	-	riboflavin kinase	-1,9
sll1876	*hemN*	oxygen independent coprophorphyrinogen III oxidase	-1,8
slr1808	*hemA*	Glutamyl-tRNA reductase (GluTR)	-1,6
slr1518	*menA*	1,4-dihydroxy-2-naphtoic acid prenyltransferase	1,7
sll1282	*ribH*	riboflavin synthase beta subunit	-1,7
slr0902	*moaC*	molybdenum cofactor biosynthesis protein C	-2,2
sll0166	*hemD*	uroporphyrin-III synthase	-1,4
slr0749	*chlL*	light-independent protochlorophyllide reductase iron protein subunit	-1,6
slr0711	-	7-cyano-7-deazaguanine reductase	-1,5
slr0553	-	dephospho-CoA kinase	-1,7
slr0901	*moaA*	molybdenum cofactor biosynthesis protein A	-1,7
slr0427	-	nicotinamide-nucleotide amidase	-1,7
slr1784	*bvdR*	biliverdin reductase	-1,7
sll0603	*menD*	2-succinyl-6-hydroxy-2,4-cyclohexadiene-1-carboxylate synthase	-1,6
slr1780	-	Ycf54-like protein	-1,5
sll1415	-	NAD+ kinase	-1,4
slr0239	*cbiF*	precorrin methylase	-1,6
DNA Replication and Repair			
sll1772	*mutS*	DNA mismatch repair protein MutS	-2,8
slr1130	*rhnB*	ribonuclease HII	-2,4
sll1629	*phr*	DNA photolyase	-2,1
slr1822	*nth*	endonuclease III	-2,0
sll1429	-	similar to archaeal holliday junction resolvase and Mrr protein	1,9
slr1803	*mbpA*	adenine-specific DNA metylase	-2,0
slr0965	*dnaN*	DNA polymerase III beta subunit	-2,0
sll0729	-	modification methylase	-1,9
sll1143	*uvrD*	ATP-dependent DNA helicase	-1,5
slr1048	-	DNA repair protein SbcC/Rad50	-1,7
sll0569	*recA*	Protein RecA (Recombinase A)	1,3
slr0020	*recG*	DNA recombinase	-1,3
slr0181	-	DNA repair protein RecO	1,3
sll1099	*tufA*	elongation factor Tu	-1,4
sll0270	*priA*	primosomal protein N'	-1,6
Cell Division			
slr1604	-	cell division protein FtsH	-2,1
slr2073	-	cell division inhibitor SepF	1,6
slr0228	*ftsH*	cell division protein	-1,5
slr1267	*mrdB*	cell division protein FtsW	1,5
sll1632	-	cell division protein FtsQ	1,3
Amino Acid Metabolism			

slr0055	*trpG*	anthranilate synthase component II	-2,0
slr0543	*trpB*	tryptophan synthase beta subunit	-1,5
sll1760	*thrB*	homoserine kinase	1,9
slr0528	*murE*	UDP-MurNac-tripeptide synthetase	1,7
sll0228	-	arginase	-1,8
slr0827	*alr*	alanine racemase	1,4
slr0596	-	creatinine amidohydrolase	-1,6
sll1561	*putA*	delta-1-pyrroline-5-carboxylate dehydrogenase	-1,4
sll0892	*panD*	aspartate 1-decarboxylase	-1,5
slr1705	*aspA*	aspartoacylase	-1,6
slr0689	-	L-aspartate semialdehyde sulfurtransferase	1,4
sll0934	*ccmA*	Carboxysome formation protein	-1,4
sll0006	*aspC*	aspartate aminotransferase	-1,5
slr0549	*asd*	aspartate beta-semialdehyde dehydrogenese	-1,3
sll0402	*aspC*	aspartate aminotransferase	-1,4
slr2079	-	glutaminase	1,6
Other Signalling and Cellular Processes			
sll0042	*tar*	methyl-accepting chemotaxis protein II	-3,8
slr0121	-	beta-lactamase class A	3,2
slr0323	*ams1*	α-Mannosidase	-2,5
slr0474	*Rcp1*	response regulator	-2,8
slr1963	-	Orange carotenoid-binding protein (OCP)	-2,1
sll1566	*otsA*	glucosylglycerol-phosphate synthase	2,1
slr1805	-	two-component sensor histidine kinase	2,5
ssl0707	*glnB*	nitrogen regulatory protein P-II	1,9
slr1971	-	Zn-dependent protease	2,1
slr0242	*bcp*	bacterioferritin comigratory protein	-1,9
slr2089	*shc*	squalene-hopene-cyclase	-1,8
sll0005	-	aarF domain-containing kinase	-1,9
slr1269	*ggt*	gamma-glutamyltranspeptidase	2,1
sll0080	*argC*	N-acetyl-gamma-glutamyl-phosphate reductase	1,8
sll1226	*hoxH*	Oxireductase (hydrogen as donor), NIFe bidirectional hydrogenase	-1,8
slr0926	*ubiA*	4-hydroxybenzoate-octaprenyl transferase	-1,9
sll1678	-	spore maturation protein A	2,5
sll1786	*tatD*	DNase family protein	-1,7
slr1472	-	spoIIIJ-associated protein	-2,7
sll1454	*narB*	nitrate reductase	-2,3
sll1933	*dnaJ*	DnaJ protein	-2,1
slr1414	-	sensory transduction histidine kinase	-2,5
sll1677	-	spore maturation protein B	2,7
slr1348	*cysE*	serine acetyltransferase	-1,8
slr0841	-	heat shock protein HslJ	1,7
slr1950	-	cation-transporting ATPase	-1,6
sll1314	*dctP*	C4-dicarboxylase binding protein	2,1
slr0550	*dapA*	dihydrodipicolinate synthase	-1,8
sll1223	*hoxU*	hydrogenase subunit	-1,6
slr0077	*Csd; sufS*	Probable cysteine desulfurase	-1,9
ssl3335	*secE*	secretory protein; SecE	-1,6
slr0328	*wzb*	low molecular weight protein-tyrosine-phosphatase	-2,7
ssl2923	*vapC*	virulence associated protein C	-3,0

slr0742	-	ribosome maturation factor RimP	-1,7
slr0423	*rlpA*	rare lipoprotein A	2,0
sll1783	-	Monooxygenase (associated to polysaccharide processing)	2,0
sll1068	*acp*	acyl carrier protein	-2,2
slr1849	*merA*	mercuric reductase	-2,1
slr0605	-	Oxireductase (quinone as aceptor), putative glutathione S transferase	-1,6
sll1515	*gifB*	glutamine synthetase inactivating factor IF17	-2,1
slr1924	-	D-alanyl-D-alanine carboxypeptidase	-1,6
slr0484	-	sensory transduction histidine kinase	1,5
sll0474	-	sensory transduction histidine kinase	-2,0
sll2009	-	processing protease	-1,8
sll1224	*hoxY*	hydrogenase small subunit	-1,6
sll1825	-	aklaviketone reductase	1,6
slr1400	-	hybrid sensory kinase	1,5
sll1771	*pphA*	protein serin-threonin phosphatase	-1,5
sll0222	*phoA*	Alkaline phosphatase	-1,6
sll0337	*sphS*	regulation of the phosphate regulon	1,5
slr1728	*kdpA*	otassium-transporting ATPase A chain	2,1
slr1641	*clpB*	ClpB protein	-1,4
slr1594	-	PatA subfamily	1,8
sll1462	*hypE*	hydrogenase expression/formation protein	-1,6
sll1626	*lexA*	Transcription regulator LexA	1,6
slr1207	-	HlyD family secretion protein	1,5
slr1639	*smpB*	SsrA-binding protein	-1,6
sll1353	-	sensory transduction histidine kinase	-1,6
sll1283	*spoIID*	sporulation protein	1,5
slr1668	-	fimbrial chaperone protein	-1,7
sll1124	-	sensory transduction histidine kinase	-1,5
slr1516	*sobB*	superoxide dismutase	-1,4
sll0659	-	lycopene cyclase CruP	-1,7
slr0687	*pleD*	PleD gene product	1,8
slr0473	*phy*	phytochrome	-1,5
slr0457	*truB*	tRNA pseudouridine 55 synthase tRNA pseudouridine 55 synthase	-2,0
slr2135	*hupE*	hydrogenase accessory protein	1,7
sll1666	*dnaJ*	DnaJ protein	1,5
sll1187	*lgt*	prolipoprotein diacylglyceryl transferase	-1,4
sll0247	*isiA*	iron-stress chlorophyll-binding protein	1,7
ssl2922	*vapB*	virulence associated protein B	-3,1
slr0801	-	putative flavoprotein involved in K+ transport	1,7
slr0509	-	alkaline phosphatase like protein	1,5
sll1770	*spkI*	protein kinase activity, protein phosphorylation	-1,4
slr2123	-	D-isomer specific 2-hydroxyacid dehydrogenase family	-1,5
sll0330	*fabG*	3-ketoacyl-acyl carrier protein reductase	1,5
sll1929	*comEc*	competence protein ComEC	1,6
sll1475	-	sensory transduction histidine kinase	-1,7
slr0701	*merR*	mercuric resistance operon regulatory protein	1,9
sll0782	-	putative protein kinase	1,8
sll0260	-	putative hemolysin	1,4
slr1760	-	regulatory components of sensory transduction system	1,7

slr1983	-	two-component system, response regulator	-1,5
slr0095	-	O-methyltransferase	-1,6
sll0410	-	acyl-CoA thioester hydrolase	-1,4
slr0079	*gspE*	general secretion pathway protein E	-1,3
sll1394	*msrA*	peptide methionine sulfoxide reductase	-1,5
sll1468	*bhy*	b-carotene hydroxylase	1,4
slr0348	-	4-hydroxy-3-methylbut-2-en-1-yl diphosphate reductase	1,3
slr0659	*prlC*	oligopeptidase A	-1,3
Transporters			
sll1762	-	ABC amino acid transporter	1,5
slr1227	-	chloroplast import-associated channel IAP75	2,2
sll0224	-	-	3,0
sll0384	-	cobalt/nickel transport system permease	-3,2
sll0385	*cbiO*	ATP-binding protein of ABC transporter	-2,6
slr0797	-	cation-transporting ATPase	-2,5
slr0610	-	ABC-2 type transport system permease	-2,8
slr1319	-	iron-uptake system ATP-binding protein	2,5
sll0923	*epsB; wzc*	exopolysaccharide export protein	2,0
sll1087	-	sodium-coupled permease	2,0
sll0383	*cbiM*	cobalt/nickel transport system permease	-2,5
sll0108	-	putative ammonium transporter	2,0
sll1581	*gumB*	polysaccharide biosynthesis/export	1,8
slr1229	-	sulfate permease	-2,7
sll0382	-	nickel transport protein	-1,9
slr0982	*rfbB*	lipopolysaccharide transport system ATP-binding protein	1,9
sll1024	-	ion channel-forming bestrophin family protein	-2,5
sll1600	*mntB*	Mn transporter	-1,9
slr1113	-	ABC transporter	1,6
slr2107	-	probable polysaccharide ABC transporter permease protein	-2,5
slr0773	-	trk system potassium uptake protein	-1,8
sll0679	*sphX*	phosphate transport system substrate-binding protein	2,5
sll1864	-	chloride channel protein	-1,7
sll1482	-	ABC-transporter DevC homologue	-1,9
slr0677	*exbB*	biopolymer transport ExbB protein	1,5
slr0369	-	cation or drug efflux system protein	1,6
slr1295	*sufA*	iron transport protein	1,8
sll1017	-	putative ammonium transporter	2,4
sll1374	*melB*	melibiose carrier protein	1,6
sll0671	-	magnesium transporter	1,7
slr1457	*chrA*	chromate transport protein	-1,8
sll1845	-	translocator protein	1,7
sll1406	*fhuA*	ferrichrome-iron receptor	1,7
slr0354	-	ABC transporter	1,9
slr0044	*nrtD*	nitrate transport protein	-2,5
slr1270	*tolC*	outer membrane factor	1,4
slr0964	-	high-affinity iron transporter	-1,6
sll0985	-	moderate conductance mechanosensitive channel	-1,6
sll0616	*secA*	Protein translocase subunit SecA	-1,4
slr1200	*livH*	high-affinity branched-chain amino acid transport protein	1,7

slr0075	*Ycf16*	ABC transporter subunit	-1,6
slr1201	-	urea transport system permease protein	1,8
sll0834	-	low affinity sulfate transporter	-1,5
sll1586	-	translocation and assembly module TamB	1,4
slr2019	-	ABC transporter	-1,4
slr2131	-	cation or drug efflux system protein	1,4
slr0305	-	Putative membrane protein	-2,0
sll0374	*brag; livF*	High-affinity branched-chain amino acid transport ATP-binding protein	1,7
slr1647	-	putative ABC transport system permease protein	-1,7
sll0672	-	cation-transporting ATPase	-1,4
slr0625	-	glutamate:Na+ symporter	-1,5
slr0341	-	polar amino acid transport system substrate-binding protein	1,7
slr0513	*futA*	Iron uptake (photosystem II protection from ROS)	1,5
sll1053	-	Putative periplasmic adaptor protein (AcrA-like)	1,6
slr1454	*cysW*	sulfate transport system permease protein	-2,8
Hypothetical			
slr0554	-	-	2,7
slr1610	-	putative C-3 methyl transferase	2,9
sll1464	-	-	-2,5
sll1188	-	-	-2,7
slr1152	-	-	1,8
sll1505	-	-	-4,6
slr1542	-	2-C-methyl-D-erythritol 2,4-cyclodiphosphate synthase	-2,7
slr0967	-	-	2,1
slr1593	-	-	2,8
slr1649	-	-	-2,0
slr1104	-	-	-1,7
slr0483	-	-	1,7
slr0383	-	-	2,8
slr0755	-	-	-1,8
slr0769	-	-	1,6
sll0189	-	putative endonuclease	-1,9
sll0168	-	-	-1,7
sll0545	-	-	-1,9
sll0154	-	hypothetical 35.6 kD protein	1,5
sll0686	-	-	2,1
sll1526	-	-	1,7
ssl0331	-	-	-1,9
sll1355	-	-	1,5
sll1680	-	peptide-methionine (R)-S-oxide reductase	-1,5
slr0053	-	probable rRNA maturation factor	-1,6
slr0284	-	putative membrane protein	1,6
slr1241	-	-	-2,1
sll1232	-	-	-2,3
sll1103	-	-	1,6
slr1851	-	-	1,4
slr0359	-	-	-1,5
slr1102	-	-	-1,4
sll1433	-	-	-1,6

sll1738	-	-	-1,4
sll1924	-	-	1,5
slr0581	-	-	1,7
slr0021	-	putative protease	-1,6
slr0784	-	-	1,7
slr1261	-	-	-1,5
sll0141	-	-	1,5
sll1693	-	-	-1,4
slr1692	-	-	-1,5
sll0297	-	-	-1,4
sll1509	*ycf20*	-	1,6
sll1254	-	Hemolysin-like	1,4
sll0217	-	potential FMN-protein	1,4
ssr2998	-	-	-1,4
sll0424	-	-	-1,5
sll0036	-	-	1,4
slr0076	-	Fe-S cluster assembly protein SufD	-1,4
sll0536	-	-	1,6
slr0404	-	-	-1,3
sll0183	-	-	1,4
sll1504	-	-	-1,8
sll1534	-	-	-1,4
Unknown			
slr1546	-	Possible anti-sigma factor sigG	3,9
slr1816	-	-	-2,9
slr1218	-	-	4,3
slr1940		Protein putatively involved in extracellular connection structures	2,7
slr1547	-	-	2,8
ssr3465	-	-	2,4
sll1102	-	-	3,4
sll1722	-	-	3,1
slr0358	-	-	2,5
slr1772	-	-	-2,5
slr0243	-	-	-3,2
sll0781	-	-	2,5
slr1771	-	-	2,2
ssr2554	-	-	2,3
slr0976	-	-	2,1
sll1265	-	-	1,9
slr1178	-	-	2,4
sll1837	-	Periplasmic protein	2,1
ssr1853	-	-	2,3
sll1086	-	-	2,4
slr1966	-	-	2,4
slr1169	-	-	-3,3
sll1834	-	-	2,1
slr1815	-	-	-2,2
slr0334	-	-	-2,7
sll0710	-	-	-2,3
slr0061	-	-	-3,9

slr1236	-	-	1,8
slr0702	-	-	2,4
slr0376	-	Encoding gene is part of responsive operon to stress	2,0
sll0314		Lipoprotein (signaling)	1,8
sll1696	-	-	-2,6
sll1488	-	-	1,8
slr2126	-	-	-2,4
sll1550	-	-	2,1
slr0373	-	-	1,8
slr1258	-	-	1,8
sll0983	-	-	-2,0
slr0981	-	-	1,7
sll1507	-	-	1,7
slr0333	-	-	-2,2
ssr3000	-	-	-2,4
sll0031	-	-	2,0
slr0149	-	-	-2,0
sll0862	-	-	-1,7
slr1990	-	-	-1,9
ssl3291	-	-	1,9
slr2052	-	-	2,3
slr0145	-	-	-2,2
slr1262	-	-	-1,9
sll0044	-	-	-3,0
slr1415	-	-	-2,0
slr1601	-	-	1,8
slr1406	-	-	1,8
sll0630	-	-	1,7
sll1378	-	-	-2,0
slr1681	-	-	1,9
sll1766	-	-	-1,9
sll0180	-	-	1,6
slr0505	-	-	-2,1
slr1927	-	-	-1,7
sll0178	-	-	-1,7
slr2103	-	-	-2,1
slr1590	-	-	-1,6
slr1442	-	-	1,6
slr1222	-	-	-2,0
sll0350	-	-	2,0
sll0072	-	-	-2,4
sll1333	-	-	2,0
sll1336	-	-	-1,5
ssr0336	-	-	-2,1
slr0397	-	-	2,0
slr0287	-	-	-1,8
slr0731	-	-	-1,8
sll0756	-	-	-1,7
sll0846	-	-	-1,5
slr1413	-	-	-1,5
sll1757	-	-	-2,0
slr1866	-	-	-2,1

slr1391	-	-	-2,4
slr0338	-	-	1,6
sll1892	-	-	1,5
slr1240	-	-	-2,0
slr1378	-	-	-1,5
slr1634	-	-	1,6
slr0592	-	-	1,8
slr1173	-	-	1,5
ssr2781	-	-	-2,6
slr1541	-	-	-1,9
slr1928	-	-	-2,1
sll0253	-	-	-1,5
slr0060	-	-	-2,1
sll1036	-	-	-1,7
sll1222	-	-	-1,6
slr1852	-	-	1,7
sll1009	*frpC*	Protein with calcium ion binding motifs (Ironregulated protein)	1,4
sll1543	-	-	1,4
slr0978	-	-	1,5
slr1263	-	-	1,6
slr0300	-	-	-1,7
sll1873	-	-	-1,4
sll0319	-	-	1,7
slr1708	-	lysostaphin	1,5
sll1634	-	-	2,0
slr0643	-	-	-1,6
slr0238	-	-	-1,8
sll0839	-	-	-2,2
ssr1600	-	-	1,5
sll1752	-	-	1,7
sll0933	-	-	-1,5
sll0266	-	-	-1,6
sll1359	-	-	-1,8
sll0293	-	-	1,7
sll0943	-	-	2,2
ssr3304	-	-	1,6
slr1946	-	-	-1,4
sll0225	-	-	2,2
sll1917	-	oxygen-independent coproporphyrinogen-III oxidase-like protein	-1,9
slr0374	-	Possible aaa protease	1,5
slr1230	-	universal stress protein Slr1230-like	-1,9
sll1621	-	Putative peroxiredoxin	-1,4
ssr2153	-	-	1,6
slr1576	-	-	1,8
sll1119	-	-	1,7
sll0264	-	-	1,4
sll0863	-	-	-2,2
slr0244	-	-	-1,4
slr2018	-	-	-1,5
slr1638	-	-	-1,5

slr0889	-	uncharacterized protein slr0889 isoform X1	-1,6
sll0181	-	-	-1,8
slr0668	-	-	-1,9
sll0783	-	-	2,3
sll0556	-	-	-1,4
slr0819	*int*	apolipoprotein N-acyltransferase	-1,5
slr0888	-	-	-1,5
sll0294	-	-	1,8
slr0700	-	-	-2,0
ssr2315	-	-	-1,8
slr2124	-	short-chain alcohol dehydrogenase family	-1,6
slr1958	-	-	-1,5
sll0447	-	-	-1,9
sll0670	-	-	1,7
slr2027	-	-	-1,5
slr1770	-	-	1,5
ssr3570	-	-	-1,8
sll1751	-	-	-1,9
sll0008	-	-	-1,6
slr0552	-	-	-1,5
sll1913	-	-	-1,7
sll1049	-	-	1,5
sll1885	-	-	1,5
ssl1533	-	-	1,4
sll1959	*suhB*	extragenic suppressor	-1,8
ssl1046	-	-	1,8
ssl2138	-	-	-2,0
ssl2920	-	-	-3,2
sll1162	-	-	-2,5
slr0957	-	-	1,4
slr0109	-	-	-2,0
sll1106	-	-	-1,4
sll1131	-	-	1,7
slr0151	-	-	-1,4
slr2117	-	-	-2,1
sll1681	-	-	-1,5
sll0160	-	-	-1,6
ssr3467	-	-	1,6
slr1926	-	-	-1,3
sll0503	-	-	-1,6
sll0494	-	-	-1,7
slr0377	-	-	1,4
sll0543	-	-	1,5
slr1303	-	-	-1,8
slr0007	-	-	-1,4
slr1076	-	-	1,4
slr1095	-	-	1,5
slr1148	-	-	-2,1
sll1060	-	Membrane protein (UPF0182 protein)	-1,5
slr0587	-	-	-1,5
sll0944	-	-	1,4
ssr3129	-	-	1,4

sll0740	-	-	1,3
sll1516	-	-	-1,4
slr0038	-	-	1,4
slr1142	-	-	1,5
slr1110	-	-	-1,7
slr1484	-	-	2,8
slr1612	-	-	1,4
sll0471	-	-	-1,6
sll1726	-	-	1,9
sll0736	-	-	-1,9
sll1396	-	-	1,4
sll0442	-	-	-1,8
slr0309	-	P-methylase	1,4
sll0887	-	-	-1,4
sll2003	-	-	1,5
slr2127	-	-	-1,6
sll1334	-	-	1,4
sll0243	-	-	-1,3
sll1251	-	-	1,5
slr0363	-	-	1,7
ssl1263	-	-	-1,4
slr0147	-	-	-1,5
sll0525	-	-	-1,5
sll1832	-	-	1,5
sll1217	-	-	1,5
slr0119	*brkB*	serum resistance locus	-1,9
ssl2245	-	-	1,4
slr0666	-	-	1,3
sll0488	-	-	1,4
sll0481	-	-	1,6
ssr2087	-	-	1,6
slr1081	-	-	-1,4
slr1591	-	-	-1,6
sll1939	-	-	1,4
slr0656	-	-	-1,3
slr2141	-	-	1,5
sll0644	-	esterase	1,5
sll1089	-	-	1,4
sll0066	-	-	-1,6
slr1778	-	-	-1,5
sll0737	-	-	-1,4
sll1159	-	-	1,5
slr1087	-	-	1,4
slr0386	-	-	1,4
sll2015	-	-	1,4
slr1056	-	-	-1,4
slr0351	-	-	1,4
sll0446	-	-	-1,4

Table S2. Distribution by functional categories of the proteins quantified in the iTRAQ analysis with significant fold changes in *Synechocystis kpsM* mutant vs. wild type.

Protein Name	Uniprot ID	Description	Fold Change (mt:wt)
Photosynthesis			
Sll1796; PetJ	P46445	Cytochrome c6 (Cytochrome c553)	3,5
Ssl0020; Fed; PetF	P27320	Ferredoxin-1 (Ferredoxin I)	1,4
Slr0574; Cyp120; Cyp	Q59990	Putative cytochrome P450 120	-1,3
Slr0335; ApcE	Q55544	Phycobiliprotein	-1,4
Smr0007; PsbL	Q55354	Photosystem II reaction center protein L (PSII-L)	-1,6
Sml0008; PsaJ	Q55329	Photosystem I reaction center subunit IX	-1,7
Oxidative Phosphorylation			
Sll1325; AtpH; AtpD	P27180	ATP synthase d subunit	1,5
Carbon Metabolism			
Ssl2501; PhaP	P73545	Phasin (GA13)	3,1
Slr0009; CbbL; RbcL	P54205	Ribulose bisphosphate carboxylase large chain (RuBisCO large subunit)	1,6
Slr0435; AccB	Q55120	Biotin carboxyl carrier protein of acetyl-CoA carboxylase	1,5
Sll1841; OdhB	P74510	Dihydrolipoamide acetyltransferase component of pyruvate dehydrogenase complex	1,4
Slr0233	P52232	Thioredoxin-like protein	1,4
Sll1070; TktA	P73282	Transketolase (EC 2.2.1.1)	1,4
Slr1289; Icd	P80046	isocitrate dehydrogenase (NADP+)	1,3
Slr1945; GpmI; Pgm	P74507	2,3-bisphosphoglycerate-independent phosphoglycerate mutase (iPGM) (EC 5.4.2.12)	1,3
Slr1994; PhaB	P73826	Acetoacetyl-CoA reductase (EC 1.1.1.36)	1,3
Slr0752; Eno	P77972	Enolase (EC 4.2.1.11) (2-phospho-D-glycerate hydro-lyase) (2-phosphoglycerate dehydratase)	1,2
Sll0990; FrmA	P73138	S-(hydroxymethyl)glutathione dehydrogenase	1,2
Sll0861; MurQ	P73585	N-acetylmuramic acid 6-phosphate etherase (MurNAc-6-P etherase)	-1,2
Sll1383; SuhB	P74158	Inositol-1-monophosphatase (I-1-Pase) (IMPase) (Inositol-1-phosphatase) (EC 3.1.3.25)	-1,4
Slr1762	P73039	Phosphoglycolate phosphatase	-1,5
Cell Envelope and Lipid Metabolism			
Sll1951	P73817	S-layer protein (Hemolysin-like protein) (HLP)	2,7
Cofactors and Vitamins Metabolism			
Sll1282; RibH	P73527	6,7-dimethyl-8-ribityllumazine synthase (DMRL synthase) (LS) (Lumazine synthase)	1,8
Sll1341; Bfr	P24602	Bacterioferritin (BFR) (EC 1.16.3.1)	1,6
Slr1923	P74473	3,8-divinyl protochlorophyllide a 8-vinyl-reductase	-1,2
Slr1055; ChlH	P73020	Mg-chelatase subunit ChlH (Anti-sigma factor E)	-1,3
Sll0179; GltX	Q55778	Glutamate--tRNA ligase (EC 6.1.1.17) (Glutamyl-tRNA synthetase) (GluRS)	-1,4

Sll0250; CoaBC; Dfp	P73881	Coenzyme A biosynthesis bifunctional protein CoaBC (DNA/pantothenate metabolism flavoprotein) (Phosphopantothenoylcysteine synthetase/decarboxylase) (PPCS-PPCDC)	-1,4
Sll1184; PbsA1	P72849	Heme oxygenase 1 (EC 1.14.14.18)	-1,4
Slr0506; Por; Pcr	Q59987	Light-dependent protochlorophyllide reductase (PCR) (EC 1.3.1.33) (NADPH-protochlorophyllide oxidoreductase) (LPOR) (POR)	-1,5
Slr1649; CpcT	P74371	Chromophore lyase CpcT/CpeT	-1,5
Aminoacid Metabolism			
Slr0032; IlvE	P54691	Probable branched-chain-amino-acid aminotransferase (BCAT) (EC 2.6.1.42)	1,8
Slr0229; MmsB	Q55702	Uncharacterized oxidoreductase slr0229	1,5
Slr1022; ArgD	P73133	Acetylornithine aminotransferase (ACOAT) (EC 2.6.1.11)	1,3
Sll0585	Q55865	L-asparaginase	1,3
Sll1058; DapB	P72642	4-hydroxy-tetrahydrodipicolinate reductase (HTPA reductase) (EC 1.17.1.8)	1,3
Sll1750; UreC	P73061	Urease subunit alpha (EC 3.5.1.5) (Urea amidohydrolase subunit alpha)	1,3
Sll0109; AroH	Q55869	Chorismate mutase AroH (EC 5.4.99.5)	1,2
Sll1234; AhcY	P74008	Adenosylhomocysteinase (EC 3.3.1.1) (S-adenosyl-L-homocysteine hydrolase)	1,2
Sll1987; KatG	P73911	Catalase-peroxidase (CP) (EC 1.11.1.21)	1,2
Slr0662; SpeA1; SpeA	P74576	Biosynthetic arginine decarboxylase 1 (ADC 1) (EC 4.1.1.19)	-1,2
Slr1560; HisZ; HisS2	P74592	ATP phosphoribosyltransferase regulatory subunit	-1,2
Sll0712; CysM	P72662	Cysteine synthase	-1,2
Slr0738; TrpE	P20170	Anthranilate synthase component 1 (AS) (ASI) (EC 4.1.3.27)	-1,2
Slr1867; TrpD	P73617	Anthranilate phosphoribosyltransferase (EC 2.4.2.18)	-1,3
Nucleotide Metabolism			
Sll0744	Q55989	dihydroorotate dehydrogenase (fumarate)	1,3
Slr1239; PntA	P73496	Pyridine nucleotide transhydrogenase alpha subunit	1,3
Sll1815; Adk1	P73302	Adenylate kinase 1 (AK 1) (EC 2.7.4.3)	-1,4
Slr1256; UreA	P73796	Urease subunit gamma (EC 3.5.1.5) (Urea amidohydrolase subunit gamma)	-1,2
Sll0509	Q55478	Ap-4-A phosphorylase II	-1,3
Transcription			
Slr8026	Q6ZE66	MarR family transcriptional regulatory protein	-1,3
Translation			
Sll1807; RplX; Rpl24	P73309	50S ribosomal protein L24	1,7
Ssl3437; RpsQ; Rps17	P73311	30S ribosomal protein S17	1,5
Sll1767; RpsF; Rps6	P73636	30S ribosomal protein S6	1,5
Sll1822; RpsI; Rps9	P73293	30S ribosomal protein S9	1,4
Sll1816; RpsM; Rps13	P73299	30S ribosomal protein S13	1,3
Sll1464; SelO	P73436	Protein adenylyltransferase SelO (EC 2.7.7.-)	1,4

Slr0950	P74319	23S rRNA (cytidine1920-2'-O)/16S rRNA (cytidine1409-2'-O)-methyltransferase	1,3
Sll1098; FusB; Fus	P74228	Elongation factor G 2 (EF-G 2)	-1,2
Sll1110; PrfA	P74707	Peptide chain release factor 1 (RF-1)	-1,2
Sll1253; PcnB	P74081	A-adding tRNA nucleotidyltransferase (A-adding TNT) (EC 2.7.7.-) (A-adding enzyme)	-1,4
DNA Replication and Repair			
Slr1056	P73021	DNA replication and repair protein RecF	1,4
Sll0021; SbcD	Q55661	Nuclease SbcCD subunit D	1,4
Slr0417; GyrA	Q55738	DNA gyrase subunit A (EC 5.6.2.2)	-1,2
Slr0833; DnaB	Q55418	Replicative DNA helicase (EC 3.6.4.12)	-1,4
Protein / RNA Folding and Degradation			
Slr1377; LepB2	P73157	Probable signal peptidase I-2 (SPase I-2) (EC 3.4.21.89) (Leader peptidase I-2)	-1,5
Slr0228; FtsH2	Q55700	FtsH Protease (quality control of Photosystem II in the thylakoid membrane)	-1,4
Motility			
Slr0161; PilT	P74463	Twitching motility protein	-1,3
Slr1276; PilO	P74188	Type IV pilus assembly protein	-1,7
Other Signalling and Cellular Processes			
Sll1957; ArsA	P73808	Arsenical resistance operon repressor	2,2
Slr6037; ArsI2	Q6YRW7	Arsenate reductase - glutaredoxin-dependent family (use the GSH/glutaredoxin system)	2,1
Slr1198	P73348	Rehydrin	1,8
Sll0709; llaI.2	P72665	2nd component required for LlaI restriction activity	1,4
Slr0242; Bcp	P72697	Bacterioferritin comigratory protein	1,3
Slr1963	P74102	Orange carotenoid-binding protein (OCP)	1,4
Slr0088; CrtO	Q55808	B-carotene ketolase	-1,3
Slr1894	P73321	Starvation-inducible DNA-binding protein	-1,2
Slr1205	P73355	Ferredoxin component	-1,4
Slr0758; KaiC	P74646	Circadian clock protein kinase KaiC (EC 2.7.11.1)	-1,4
Sll0254	P73872	Carotenoid phi-ring synthase	-1,7
Transporters			
Sll1450; NrtA	P73452	Nitrate Transport 45kDa protein	1,9
Sll1017	P72935	Putative Ammonium Transporter	1,9
Slr0530	Q55472	Membrane bound sugar transport protein	1,7
Sll1270; GlnH; GlnP	P73544	Glutamine-binding periplasmic protein/glutamine transport system permease	1,4
Sll1180; HlyB	P74176	ABC transporter	1,2
Sll0108	P54147	Putative ammonium transporter	1,2
Slr1881; LivF	P73650	High-affinity branched-chain amino acid transport ATP-binding protein BraG	-1,2
Sll1614; Pma1	P37367	Cation-transporting ATPase pma1 (EC 7.2.2.-)	-1,2
Sll5052	Q6ZES8	Similar to Exopolysaccharide Export Protein	-1,3
Slr0074; Ycf24	Q55790	ABC Transporter Subunit	-1,3
Slr0625	Q55868	Glutamate: Na+ Symporter	-1,4
Unknown			
Slr1853	P73604		2,8

Ssl1046	P74772		2,1
Slr0168	Q55549		2,1
Sll0242	P73896		2,0
Ssr2406	P73506		1,8
Ssr2554	P73961		1,7
Sll5034	Q6ZEU6		1,7
Slr1519; HglK	P73963		1,7
Slr1752	P73459		1,6
Ssl2595	P73587		1,6
Ssr1407	P74775		1,6
Sll0781	Q55953		1,6
Sll1837	P73107	Periplasmic protein	1,5
Slr0545	Q55493	auxin-induced protein	1,5
Slr1618	P72896		1,4
Slr1576	P74609		1,4
Ssl0832	P74691		1,4
Sll1665	P72805		1,4
Ssl5113	Q6ZEL7		1,4
Slr1753	P73032		1,4
Slr1619	P72897		1,4
Slr0171; Ycf37	Q55551	Ycf37 gene product	1,4
Slr1194	P73342		1,3
Sll0737	O06944		1,3
Ssl2148	P74239		1,3
Sll1296	P73172	CheA like protein	1,3
Slr1437	P73503		1,3
Sll1150	P73793		1,3
Slr0650	Q55730		1,3
Slr1444	P73516		1,2
Slr6095	Q6YRQ9		-1,2
Sll8004	Q6ZE88		-1,2
Sll0487	Q55818		-1,2
Sll0877	P73552		-1,2
Slr1596; PcxA; CotA	P75028	Proton extrusion protein PcxA	-1,3
Sll1424	P73944		-1,3
Sll0396	Q55733	OmpR subfamily	-1,3
Sll8049	Q6ZE43	Type I site-specific deoxyribonuclease chain R	-1,3
Sll1526	P74360		-1,3
Sll1636; Fbp	P73050	Ferripyochelin binding protein	-1,3
Sll2002	P73680		-1,3
Sll0815	P74042		-1,3
Slr1306	P72844		-1,3
Sll1528	P74358		-1,3
Slr1103	P72747		-1,3
Sll0274	P74392		-1,3
Slr0865	P73759		-1,3
Sll0595	Q55853		-1,4
Slr0399; Ycf39	P74429	Ycf39 gene product	-1,5
Sll0529	Q55517		-1,5
Slr2080	P73905		-1,5
Slr5017	Q6ZEW3		-1,5

Sll1730	P73396		-1,5
Slr0937	P74302		-1,5
Slr0320	Q55524		-1,5
Slr6039	Q6YRW5		-1,6
Sll1396	P72619		-1,8
Ssl2733	P72616		-1,8
Sll1891	P74109	Secreted protein (related to stress conditions)	-2,1

Table S3. List of organisms and plasmids used/generated in this work.

Organism name/Genotype	**Description**	**Source**
Escherichia coli DH5α	Transformation/cloning strain.	Invitrogen
Escherichia coli XL1-Blue	Transformation/cloning strain.	Agilent
Synechocystis sp. PCC 6803	Wild type strain.	PCC
kpsM mutant	*Synechocystis* mutant with *slr0977* replaced by a Km resistance cassette.	This work
kpsM mutant pS351slr0977	*Synechocystis kpsM* mutant complemented with the replicative plasmid pS351slr0977.	This work
Plasmid	**Description**	**Source**
pGEM®-T easy	T/A cloning vector.	Promega
pSEVA351	Replicative shuttle vector for *Synechocystis* transformation.	SEVA-DB [58]
pSEVA481	Source of the Sm/Sp resistance cassette.	SEVA-DB
pKm.1	pGEM-T easy with the Km resistance cassette.	[57]
pGDslr0977	pGEM-T easy with *slr0977* and its flanking sequences, where the *slr0977* coding sequence was replaced by a *Xma*I site.	This work
pGDslr0977.Km	pGDslr0977 with a Km resistance cassette inserted into the *Xma*I site.	This work
pGDslr0977.Sm	pGDslr0977 with a Sm/Sp resistance cassette inserted into the *Sma*I site.	This work
pSBA2	Source of the promoter of *psbA2** (P_{psbA2*}) and the synthetic RBS BBa_B0030.	Registry of Standard Biological Parts (http://parts.igem.org).
pS351slr0977	pSEVA351 with *slr0977* downstream the synthetic RBS BBa_B0030, under the control of P_{psbA2*}.	This work

Table S4. Oligonucleotides used in this work.

Name	Sequence (5'-3')	Purpose	Reference
slr0977.5O	CGGATGCCACTATGCTTTTGAGTGATGAACC	Amplification of flanking region; 5I and 3I: overlap PCR	
slr0977.5I	CGTTCCATCTTACGCCCGGGAGAACTGATTATTGAAGCAGGACGCACGG*		
slr0977.3I	TCAATAATCAGTTCTCCCGGGCGTAAGATGGAACGCACCTTCGCTGATGT*		
slr0977.3O	GGATGGGGTCAGCCAGAAAATCTAACCAC		
Slr0977Fwd_comp	GTTTCTTCGAATTCGCGGCCGCTTCTAGAGATGAAAACTTCCCCCCCAGA	Amplification of *kpsM*	This work
Slr0977Rev_comp	GTTTCTTCCTGCAGCGGCCGCTACTAGTATTAAATCACATCAGCGAAGGTGC		
slr0978F_SB	CGTTGAGTGGAACCGTCGAAA	Southern Blot probe amplification	
slr0980R_SB	CGGACTTCCTCCACTAAATTCTC		
slr0977.5O.2	CTTGGCATCCACCAGGGTCA	*kpsM* segregation confirmation	
slr0977R	GTACCGCAATGTCCCGCCAA		
KmRFwd	CCAGTCATAGCCGAATAGCCTC		
KmRRev	GCATCGCCTTCTATCGCCTT		
Km.KmScFwd	CTGACCCCGGGTGAATGTCAGCTACTGG*	Amplification of the Km resistance cassette	[57]
KmRev	CAAACCCGGGCGATTTACTTTTCGACCTC*		

*Underlined base pairs correspond to restriction sites.

CHAPTER IV

CRISPRi as a tool to repress multiple copies of extracellular polymeric substances (EPS)-related genes in the cyanobacterium *Synechocystis* sp. PCC 6803

Work published in: **SANTOS, M.**, Pacheco, C.C., Yao, L., Hudson, E.P. & Tamagnini. P. (2021) CRSPRi as a tool to repress multiple copies of extracellular polymeric substances (EPS)-related genes in the cyanobacterium *Synechocystis* sp. PCC 6803. *Life*, 11:1198. https://doi.org/10.3390/life11111198

life

MDPI

Communication

CRISPRi as a Tool to Repress Multiple Copies of Extracellular Polymeric Substances (EPS)-Related Genes in the Cyanobacterium *Synechocystis* sp. PCC 6803

Marina Santos [1,2,3], Catarina C. Pacheco [1,2], Lun Yao [4,5,†], Elton P. Hudson [4,5] and Paula Tamagnini [1,2,6,*]

1 i3S-Instituto de Investigação e Inovação em Saúde, Universidade do Porto, 4000-008 Porto, Portugal; marina.santos@ibmc.up.pt (M.S.); cclopes@ibmc.up.pt (C.C.P.)
2 IBMC-Instituto de Biologia Molecular e Celular, Universidade do Porto, 4000-008 Porto, Portugal
3 Programa Doutoral em Biologia Molecular e Celular (MCbiology), Instituto de Ciências Biomédicas Abel Salazar (ICBAS), Universidade do Porto, 4000-008 Porto, Portugal
4 Science for Life Laboratory, KTH Royal Institute of Technology, 10004 Stockholm, Sweden; lunyao@kth.se (L.Y.); paul.hudson@scilifelab.se (E.P.H.)
5 Department of Protein Science, KTH Royal Institute of Technology, 10004 Stockholm, Sweden
6 Departamento de Biologia, Faculdade de Ciências, Universidade do Porto, 4000-008 Porto, Portugal
* Correspondence: pmtamagn@ibmc.up.pt; Tel.: +351-226074957
† Present Address: Dalian Institute of Chemical Physics, Dalian 116000, Shandong, China.

Abstract: The use of the versatile cyanobacterial extracellular polymeric substances (EPS) for biotechnological/biomedical applications implies an extensive knowledge of their biosynthetic pathways to improve/control polymer production yields and characteristics. The multiple copies of EPS-related genes, scattered throughout cyanobacterial genomes, adds another layer of complexity, making these studies challenging and time-consuming. Usually, this issue would be tackled by generating deletion mutants, a process that in cyanobacteria is also hindered by the polyploidy. Thus, the use of the CRISPRi multiplex system constitutes an efficient approach to addressing this redundancy. Here, three putative *Synechocystis* sp. PCC 6803 *kpsM* homologues (*slr0977*, *slr2107*, and *sll0574*) were repressed using this methodology. The characterization of the 3-sgRNA mutant in terms of fitness/growth and total carbohydrates, released and capsular polysaccharides, and its comparison with previously generated single knockout mutants pointed towards Slr0977 being the key KpsM player in *Synechocystis* EPS production. This work validates CRISPRi as a powerful tool to unravel cyanobacterial complex EPS biosynthetic pathways expediting this type of studies.

Keywords: CRISPRi; cyanobacteria; *Synechocystis*; extracellular polymeric substances (EPS); KpsM

Citation: Santos, M.; Pacheco, C.C.; Yao, L.; Hudson, E.P.; Tamagnini, P. CRISPRi as a Tool to Repress Multiple Copies of Extracellular Polymeric Substances (EPS)-Related Genes in the Cyanobacterium *Synechocystis* sp. PCC 6803. *Life* **2021**, *11*, 1198. https://doi.org/10.3390/life1111198

Academic Editors: Paul M. D'Agostino, Nádia Eusébio and Ângela Brito

Received: 18 October 2021
Accepted: 3 November 2021
Published: 6 November 2021

1. Introduction

Most of the cyanobacterial strains can produce extracellular polymeric substances (EPS), mainly composed of heteropolysaccharides, that can be released to the extracellular medium or remain associated to the cell surface as capsules, sheaths, or slime. [1,2]. These EPS are emerging as promising biomaterials for biotechnological and biomedical applications as they possess distinctive and advantageous characteristics compared to other natural and synthetic polymers [3–5]. In addition to the complexity/variety of polymers produced by cyanobacteria, their cultivation is inexpensive due to their photoautotrophic lifestyle, the growth rates are similar or higher than algae and plants, and often, the produced polymers can be easily functionalized and the producing strain engineered to obtain a product with the desired properties and/or enhanced performance [6]. However, this manipulation requires a comprehensive knowledge on the molecular mechanisms underlying EPS biosynthesis, assembly, and export. Such knowledge is therefore crucial to increase the production yields and to tailor polymer variants for a specific application. In addition, this knowledge can also aid efforts to redirect carbon fluxes from the high-energy-demanding

EPS production towards the production of target/value-added compounds, when using cyanobacteria as green cell factories [7,8].

The last steps of the EPS biosynthetic pathways are relatively conserved throughout bacteria and often follow one of three major pathways—Wzy-, ABC transporter- or Synthase-dependent—ending with an assembled polymer outside the cell wall [9]. Previously, by performing a phylum-wide analysis, we showed that most cyanobacteria harbor genes encoding proteins related to these pathways but often not a complete set defining one pathway, and the EPS-related genes are scattered throughout the genomes or organized in small clusters, often in multiple copies [1,10,11]. Up until now, the study of the putative EPS-related genes/proteins has been performed, by us and others, mainly through the generation and characterization of knockout mutants using the model cyanobacterium *Synechocystis* sp. PCC 6803 (hereafter *Synechocystis*). Previous works have confirmed the involvement of cyanobacterial homologues of key bacterial proteins belonging to both the ABC transporter- and Wzy-dependent pathways in EPS production. Regarding the Wzy-dependent pathway, knockout mutants of *wza* (*sll1581*), *wzb* (*slr0328*), and *wzc* (*sll0923*) exhibited fewer capsular polysaccharides (CPS), fewer released polysaccharides (RPS), or less of both, respectively [12,13]. Regarding the ABC transporter-dependent pathway, Fisher et al. reported knockout mutants of a putative transport permease (*slr0977* (*kpsM*)) and its associated ATP-binding module (*slr0982* (*kpsT*)), and a triple mutant (*slr0977* (*kpsM*) and the putative pair *sll0574* (*kpsM*)/*sll0575* (*kpsT*)) produced EPS with different monosaccharidic composition compared to the EPS produced by the wild-type [14]. While Fisher et al. [14] did not report on the amounts of EPS produced by these mutants, a recent extensive characterization of a *slr0977* (*kpsM*) mutant showed that the absence of Slr0977 resulted in a significant reduction of RPS (50%) and a smaller decrease of CPS (20%) [8]. In addition, a mutant lacking Slr2107 (another KpsM homologue) did not show significant differences in the total carbohydrates, RPS, and CPS compared to the wild-type [13]. Although one must bear in mind the growth conditions and the *Synechocystis* substrain used in those studies, disruption of *slr0977* (*kpsM*) is thus responsible for one of the most significant reductions in the amount of RPS reported to date.

Nevertheless, it is important to highlight that *kpsM* has three putative homologues in *Synechocystis*: *slr0977*, *slr2107*, and *sll0574* (Figure 1A), and it is necessary to clarify the role of the proteins, encoded by these genes, on EPS production. Traditionally, this would be tackled by generating a triple knockout mutant. However, the systematic knockout of multiple genes in *Synechocystis* is a time-consuming task due to its relatively slow growth rate compared to other bacteria, polyploidy [15], and the need to use different and increasing concentrations of antibiotics as selection markers. The use of a system such as CRISPR/Cas (clustered regularly interspaced short palindromic repeats/CRISPR associated nuclease) allows faster and easier gene editing, cleavage, or inactivation [16]. In addition, CRISPRi (interference), which relies on the use of a nuclease-deficient Cas9 (dCas9) and a single-guide RNA (sgRNA), enables targeted gene regulation as the dCas9-sgRNA complex blocks the RNA polymerase binding or the elongation, resulting in gene repression. The main advantage of CRISPRi over traditional gene knockouts is the ability to repress multiple genes simultaneously, as elegantly demonstrated in 2016 by Yao et al. [17] that reported the repression of up to four genes, providing the CRISPRi multiplex proof-of-concept for cyanobacteria.

In this work, to pursue the unravelling of cyanobacterial EPS assembly and export pathways, the CRISPRi system was employed as a tool for the multiplex repression of EPS-related genes in *Synechocystis*, namely for the three *kpsM* homologues (*slr0977*, *slr2107* and *sll0574*). The generated mutant was characterized in terms of growth and carbohydrate production, and its phenotype compared to the conventional single knockout mutants generated by double homologous recombination.

2. Experimental Section

To construct the strain that will serve as a control and genetic background for the CRISPRi experiments (*Syn* dCas9), *Synechocystis* sp. PCC 6803 (Pasteur Culture Collection), substrain Kazusa [18,19] was transformed with the pMD19T vector harboring the sequence encoding the dCas9 from *Streptococcus pyogenes* under the control of the constitutive promoter PpsbA2. This construct was integrated into the *psbA1* neutral site of the *Synechocystis* chromosome (Figure S1). For the simultaneous repression of the three putative *kpsM* homologues (*slr0977*, *slr2107*, and *sll0574*), an array of 3-sgRNAs was designed based on Larson et al. [20] and constructed as described [17]. Each 100 bp sgRNA unit comprised (i) its own promoter, (ii) the dCas9 binding handle and protospacer, and (iii) a terminator. The designed sgRNAs (Table 1) were evaluated for potential off-target binding sites using the CasOT software [21]. All the potential off-targets detected contained 6 or more mismatches compared to the sgRNA protospacer, including at least 1 in the 12 bp seed region (Table S1), so off-target binding was likely not significant. Therefore, these sgRNAs were expressed constitutively using the PL31 promoter (without a TetR repressor) and introduced into *Syn* dCas9 using a pLYK2-derived replicative plasmid (Table S2).

Table 1. Sequences of the three sgRNAs used in this study.

sgRNA Identifier/(Position) *	sgRNA Sequence Including PAM #
sll0574 (15)	GGGGACCAGTTCACCCTTGTCGG
slr0977 (16)	CCCCCAGAACTGATTATTGAAGCAGGAC
slr2107 (56)	CCCATGACTGGTTGCGATTGACGAT

* sgRNA nucleotide binding position counting from the start codon. # underlined nucleotides indicate the protospacer adjacent motif (PAM).

The multiplex repression of the *kpsM* homologues was quantified by RT-qPCR, assessing the expression of *slr0977*, *slr2107*, and *sll0574* in the 3-sgRNA *kpsM* mutant compared to the *Syn* dCas9. Sample collection (using three clones of the 3-sgRNA *kpsM* mutant), RNA extraction, cDNA synthesis, as well as the control measurements and PCRs were performed as previously described [22], except that three-fold standard dilutions of the cDNAs were made (1/3, 1/9, 1/27 and 1/81). The RT-qPCR reactions (10 µL) were setup as described by Pinto et al. [23] using the iTaq™ Universal SYBR® Green Supermix (Bio-Rad(Hercules, CA, USA)), 1 µL of template cDNA and the primers listed in Table S3. Validation of the reference genes (*rrn16S*, *petB*, and *rnpB*) and data analysis were performed using the Bio-Rad CFX Maestro™ 1.1 software. The single *sll0574* knockout mutant was generated via double homologous recombination, by partially replacing the gene with a kanamycin (Km) resistance cassette, as described by Santos et al. [8]. The mutants were characterized in terms of growth (absorbance and chlorophyll *a* content) and carbohydrate production (total carbohydrates, CPS, and RPS) using the phenol-sulfuric acid method [24], as described previously by Santos et al. [8]. Data were statistically analyzed with GraphPad Prism v5 (GraphPad Software) using analysis of variance (ANOVA), followed by Tukey's multiple-comparison test. For the qPCR data, analysis was performed using CFX Maestro Software (Bio-Rad) using analysis of variance (ANOVA).

3. Results & Discussion

Repression of Three kpsM Homologues in Synechocystis and Characterization of the 3-sgRNA Mutant

The *kpsM* homologues (*slr0977*, *slr2107*, and *sll0574*) were successfully repressed in the *Synechocystis* 3-sgRNA *kpsM* mutant compared to *Syn* dCas9 (control strain). The repression levels for the target genes were: ~60% for *slr0977*, ~70% for *slr2107*, and ~80% for *sll0574* (Figure 1B). Since the repression of *slr0977* was weaker compared to the other targets, the integrity of the sgRNAs in all clones was confirmed by sequencing. The repression level observed could be explained by *slr0977* being the second gene in its operon (Figure 1C). The *slr0977* predicted transcription start site (TSS) is 1175 bp upstream from the start codon [25]

and 1191 bp upstream from the sgRNA binding site (Figure 1C). As mentioned by Yao et al. [17], the blocking of transcription elongation may not be as efficient if the gene of interest is part of an operon with a distant TSS. Nevertheless, the repression levels obtained in this study are within those previously reported for other targets in *Synechocystis* [17,26,27]. On the one hand, it is also possible to purposefully design the sgRNA further from the TSS, resulting in lower repression of the target gene(s) and enabling fine-tuning gene expression, as demonstrated by Shabestary et al. [26]. On the other hand, a partial repression will allow to sustain cell viability, even when essential genes are targeted, allowing the identification of new phenotypes.

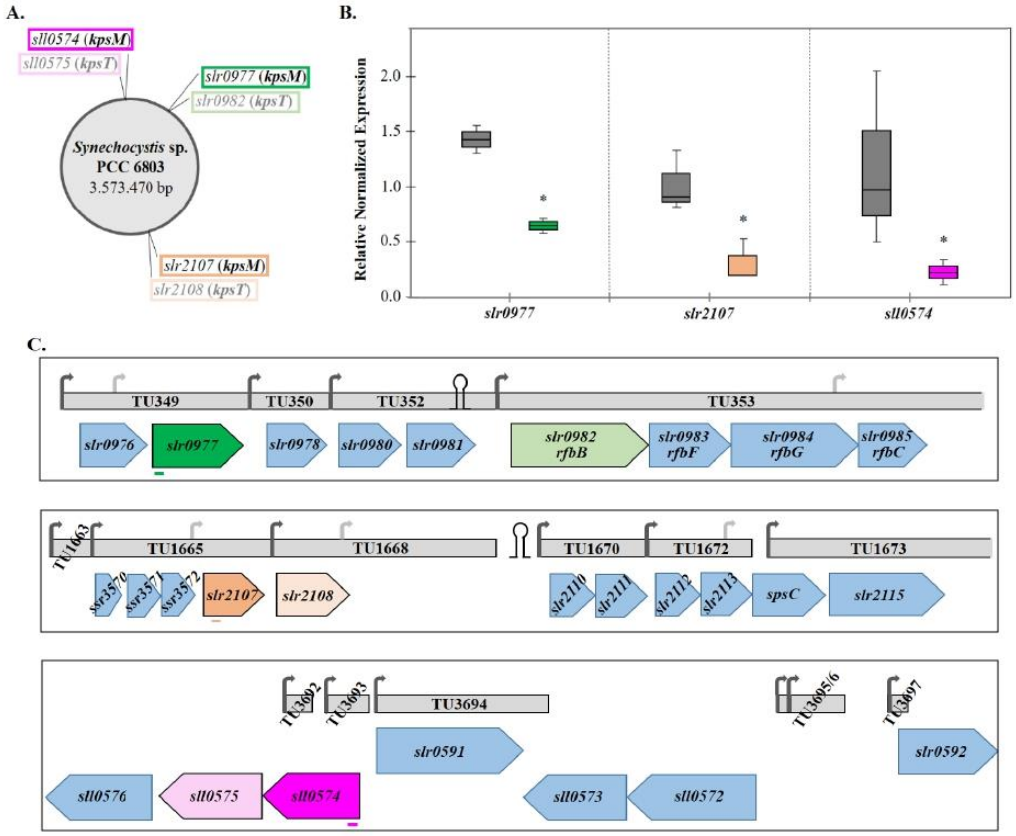

Figure 1. EPS-related genes in *Synechocystis* sp. PCC 6803 encoding a putative transport permease of the ABC transporter-dependent pathway. (**A**) Location of the putative homologues of *kpsM*/*kpsT* in *Synechocystis* chromosome (*kpsT* is the second component of the two-protein complex, and is responsible for ATP-binding). (**B**) CRISPRi multiplex repression of three *kpsM* homologues (*sll0574*, *slr0977*, and *slr2107*), evaluated by RT-qPCR. The catalytically dead Cas9 (dCas9) and the 3 single guide-RNAs were constitutively expressed from promoters PpsbA2 and PL31, respectively. Expression of the target genes in the 3-sgRNA mutant (*slr0977*: green; *slr2107*: orange; *sll0574*: pink) relative to *Synechocystis* wild-type harboring dCas9 (grey). Data from at least two biological replicates and three technical replicates were normalized against three reference genes (*rrn16S*, *rnpB*, and *petB*), the whiskers represent the minimum and maximum non-outlier values in the data set. * p-value ≤ 0.05. (**C**) Schematic representation of the genomic context of the three target genes. sgRNA binding sites are depicted as colored lines below the target gene. Neighboring genes are annotated according to information available at the CyanoBase and KEGG databases. The transcriptional unit and transcription start sites (arrows; light grey indicate internal TSSs) are annotated according to Kopf et al. [25]. The predicted terminators (loops) were found using the FindTerm algorithm (Softberry).

Subsequently, the 3-sgRNA *kpsM* mutant was characterized in terms of growth and carbohydrate production. Repression of the *kpsM* homologues did not significantly affect growth, compared to the *Syn* dCas9 (Figure 2A) and wild-type strains. However, similarly to the *slr0977* knockout mutant, the 3-sgRNA *kpsM* mutant displayed a clumping phenotype at low cell densities [8]. Regarding total carbohydrates, the 3-sgRNA *kpsM* mutant produced approximately the same amount as the *Syn* dCas9 strain (Figure 2B). However, it had approximately 20% less CPS and 40% less RPS at 21 days of cultivation (Figure 2C,D).

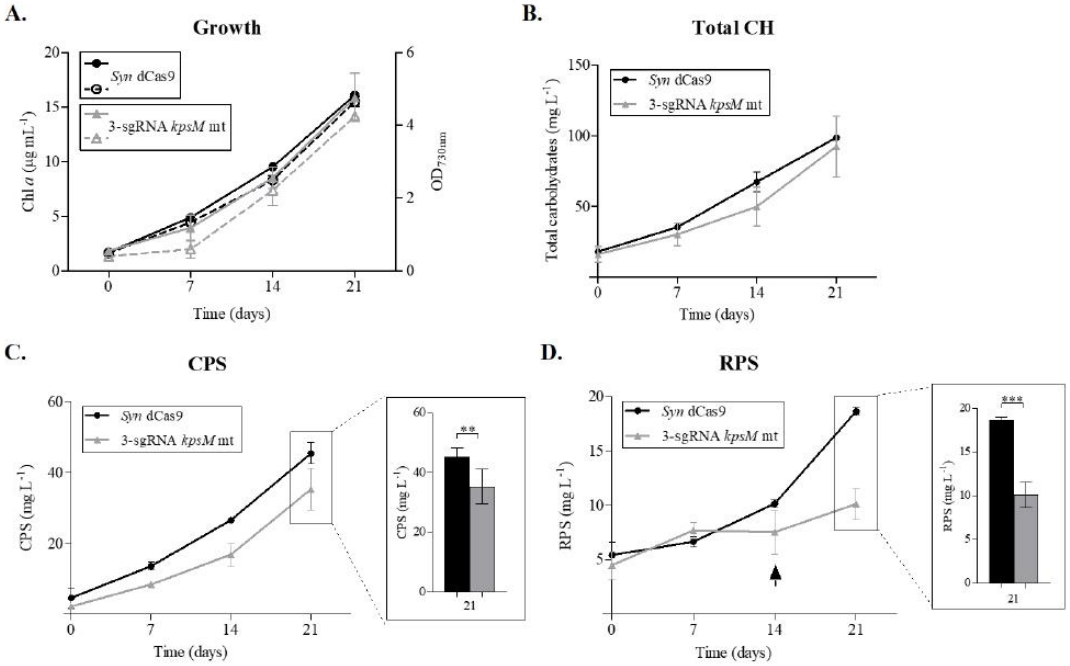

Figure 2. Growth curves and carbohydrate production by *Synechocystis* sp. PCC 6803 constitutively expressing the dead Cas 9 (*Syn* dCas9), and the 3 single guide-RNAs *kpsM* mutant targeting *sll0574*, *slr0977* and *slr2107* (3-sgRNA *kpsM* mt). Growth was monitored by measuring the optical density at 730 nm (full lines) and chlorophyll *a* (Chl *a*) (dashed lines) (**A**). Total carbohydrates (Total CH) (**B**), capsular polysaccharides (CPS) (**C**), and released polysaccharides (RPS) (**D**) were measured by the phenol-sulfuric acid method [24] and expressed as milligrams per liter of culture. The arrow indicates the point of divergence between the amount of RPS of *Syn* dCas9 and the 3-sgRNA *kpsM* mutant. Cells were grown in BG11 medium at 30 °C under a 12 h light (50 µE m^{-2} s^{-1})/12 h dark regimen, with orbital shaking at 150 rpm. Experiments were performed in triplicate, and statistical analysis is presented for the final time point (** *p-value* ≤ 0.01 *** *p*-value < 0.001).

This phenotype is very similar to the one observed for the *slr0977* single knockout mutant [8], suggesting that the protein encoded by *slr0977* could be the main KpsM homologue involved in RPS export, at least in the conditions tested. However, in the *slr0977* single mutant, at 21 days, the amount of RPS is 50% less compared to the wild-type [8], while in the 3-sgRNA *kpsM* mutant, this difference only reaches 40%. In addition, while the amount of RPS for the *slr0977* mutant is already reduced at the start of the experiment [8], in the 3-sgRNA *kpsM* mutant, this asymmetry is only noticeable after 14 days of cultivation (Figure 2D, arrow), which could be due to the weaker level of repression achieved for *slr0977* (60%). This reduction on RPS production occurs without a significant change in the amount of total carbohydrates. In the single *slr0977* mutant, this is associated with the intracellular accumulation of poly-hydroxybutyrate (PHB) [8], as it may happen in the 3-sgRNA *kpsM* mutant.

To our knowledge, no single mutant on the third *kpsM* homologue, *sll0574*, had been previously generated. Therefore, we generated a *sll0574* knockout mutant by partially

replacing the gene with a kanamycin (Km) resistance cassette via double homologous recombination (Table S2) and characterized it in terms of its growth and carbohydrate content. The *sll0574* mutant did not show any significant differences in growth, total carbohydrates, RPS, or CPS compared to the wild-type (Figure 3), as it was previously reported for the *slr2107* mutant [13]. CRISPRi mutants for each target gene were not generated, as the goal was to evaluate the effect of the simultaneous repression of the three *kpsM* homologues. Although each sgRNA could have off-target effects (detailed analysis in Table S1), Yao et al. have previously shown that the expression of dCas9 from various weak and moderate promoters with a non-targeting, "dummy" sgRNA does not significantly affect the growth of *Synechocystis* or its transcriptome, suggesting that off-target binding with phenotypical consequences is indeed infrequent [17,28]. A direct comparison between deletion and repression mutants is not straightforward; however, the phenotype shared by the 3-sgRNA *kpsM* and *slr0977* mutants, together with the absence of an EPS-related phenotype for the *slr2107* and *sll0574* single knockout mutants, further supports our hypothesis that Slr0977 is the key KpsM homologue involved in RPS export, at least under the conditions tested. In agreement, a comparative analysis of the transcriptomes of *Synechocystis* under ten different conditions [25] showed that *slr0977* was indeed the most expressed, while the *slr2107* transcript levels increased under specific stress conditions (low temperature and nitrogen depletion). In Kopf et al., no data were reported for *sll0574* (consistent with the low levels detected in our RT-qPCR experiment).

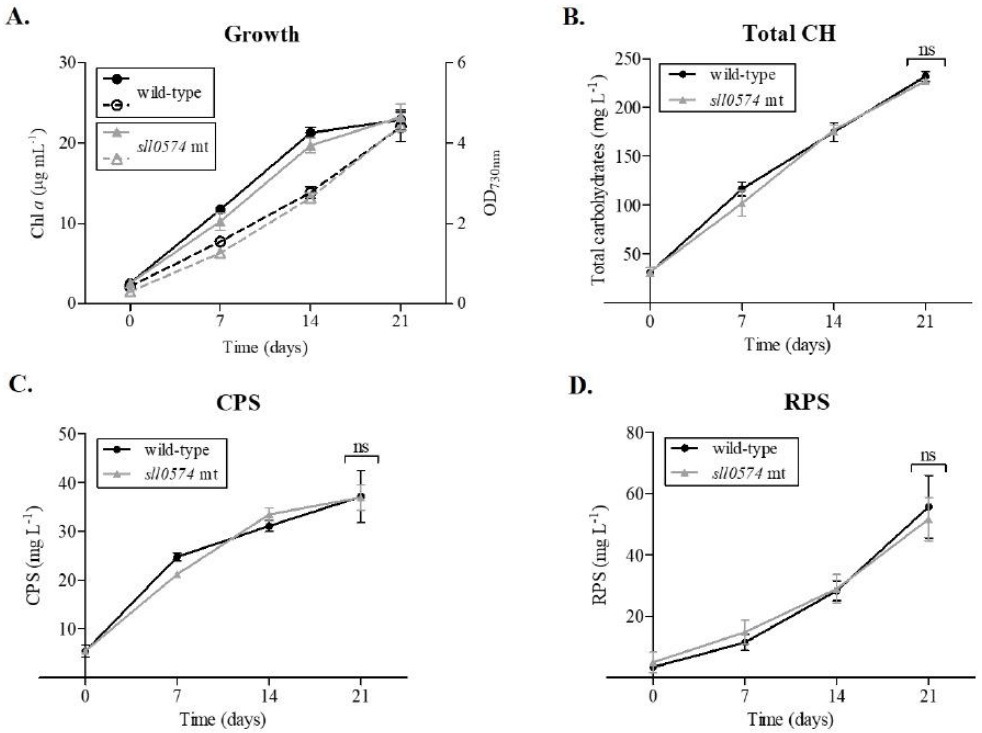

Figure 3. Growth curves and carbohydrate production by *Synechocystis* sp. PCC 6803 wild-type and the *kpsM sll0574* mutant (*sll0574* mt). Growth was monitored by measuring the optical density at 730 nm (full lines) and chlorophyll *a* (Chl *a*) (dashed lines) (**A**). Total carbohydrates (Total CH) (**B**), capsular polysaccharides (CPS) (**C**), and released polysaccharides (RPS) (**D**) were measured by the phenol-sulphuric acid method [24] and expressed as milligrams per liter of culture. Cells were grown in BG11 medium at 30 °C under a 12 h light (50 µE m^{-2} s^{-1})/12 h dark regimen, with orbital shaking at 150 rpm. Experiments were performed in triplicate, and statistical analysis is presented for the final time point (ns: not significant; *p*-value > 0.05).

4. Conclusions

In summary, the use of CRISPRi in multiplex to repress the three putative *kpsM* homologues in *Synechocystis* established a novel approach to tackle the redundancy of EPS-related genes. The use of this methodology not only expands the possibilities to study other putative redundant components, but also the simultaneous evaluation of homologues that in other bacteria are associated with the different pathways. As we expect that the cyanobacterial EPS biosynthetic pathways will diverge from the well-characterized bacterial ones, the use of CRISPRi will enable a faster screening of the role of the different players, allowing to piece together these molecular mechanisms. Although the use of CRISPRi in cyanobacteria is not yet widespread, this platform is certainly a powerful tool and will become more relevant as it is more frequently used.

Supplementary Materials: The following are available online at https://www.mdpi.com/article/10.3390/life11111198/s1: Figure S1: *Synechocystis* sp. PCC 6803 wild-type *slr1181* (*psbA1*) genomic context and confirmation of the *Syn* dCas9 mutant generation. Table S1: list of potential off-target binding sites for the three sgRNAs used in this work; Table S2: list of organisms and plasmids used/generated in this work; Table S3: primer nucleotide sequences and annealing temperatures (Ta) used in RT-qPCR; Table S4: Primer nucleotide sequences used to verify the segregation of the *Syn* dCas9 strain.

Author Contributions: Conceptualization, M.S., C.C.P., E.P.H. and P.T.; methodology, M.S., C.C.P. and L.Y.; validation, M.S. and C.C.P.; formal analysis, M.S. and C.C.P.; investigation, M.S., L.Y. and C.C.P.; resources, E.P.H. and P.T.; writing—original draft preparation, M.S., C.C.P. and P.T.; writing—review and editing, M.S., C.C.P., E.P.H. and P.T.; visualization, M.S., C.C.P. and P.T.; supervision, E.P.H. and P.T.; project administration, P.T.; funding acquisition, P.T. All authors have read and agreed to the published version of the manuscript.

Funding: This work was financed by FEDER-Fundo Europeu de Desenvolvimento Regional funds through the COMPETE 2020-Operacional Programme for Competitiveness and Internationalisation (POCI), Portugal 2020, and by Portuguese funds through the Fundação para a Ciência e a Tecnologia (FCT)/Ministério da Ciência, Tecnologia e Ensino Superior, in the framework of projects POCI-01-0145-FEDER-028779 (PTDC/BIA-MIC/28779/2017), and also supported by national funds through the FCT, I.P., under the projects UIDB/04293/2020 and UIDP/04293/2020. We also greatly acknowledge FCT for the PhD fellowship SFRH/BD/119920/2016 (M.S.) and the assistant researcher contract CEECIND/00259/2017 (C.C.P.).

Institutional Review Board Statement: Not applicable.

Informed Consent Statement: Not applicable.

Data Availability Statement: Not applicable.

Acknowledgments: The authors acknowledge the technical and scientific support of the i3S Scientific Platform "Cell Culture and Genotyping" in the real-time qPCR experiments.

Conflicts of Interest: The authors declare no conflict of interest.

References

1. Pereira, S.; Zille, A.; Micheletti, E.; Moradas-Ferreira, P.; De Philippis, R.; Tamagnini, P. Complexity of cyanobacterial exopolysaccharides: Composition, structures, inducing factors and putative genes involved in their biosynthesis and assembly. *FEMS Microbiol. Rev.* **2009**, *33*, 917–941. [CrossRef] [PubMed]
2. Rossi, F.; De Philippis, R. Exocellular polysaccharides in microalgae and cyanobacteria: Chemical features, role and enzymes and genes involved in their biosynthesis. In *The Physiology of Microalgae*, 1st ed.; Borowitzka, M.A., Beardall, J., Raven, J.A., Eds.; Springer: Cham, Switzerland, 2016; pp. 565–590.
3. Flores, C.; Lima, R.T.; Adessi, A.; Sousa, A.; Pereira, S.B.; Granja, P.L.; De Philippis, R.; Soares, P.; Tamagnini, P. Characterization and antitumor activity of the extracellular carbohydrate polymer from the cyanobacterium *Synechocystis* Δ*sigF* mutant. *Int. J. Biol. Macromol.* **2019**, *136*, 1219–1227. [CrossRef]
4. Costa, R.; Costa, L.; Rodrigues, I.; Meireles, C.; Soares, R.; Tamagnini, P.; Mota, R. Biocompatibility of the biopolymer Cyanoflan for applications in skin wound healing. *Mar. Drugs* **2021**, *19*, 147. [CrossRef]
5. Pierre, G.; Delattre, C.; Dubessay, P.; Jubeau, S.; Vialleix, C.; Cadoret, J.-P.; Probert, I.; Michaud, P. What is in store for EPS microalgae in the next decade? *Molecules* **2019**, *24*, 4296. [CrossRef] [PubMed]

6. Pereira, S.B.; Sousa, A.; Santos, M.; Araújo, M.; Serôdio, F.; Granja, P.L.; Tamagnini, P. Strategies to obtain designer polymers based on cyanobacterial extracellular polymeric substances (EPS). *Int. J. Mol. Sci.* **2019**, *20*, 5693. [CrossRef]
7. van der Woude, A.D.; Angermayr, S.A.; Puthan, V.V.; Osnato, A.; Hellingwerf, K.J. Carbon sink removal: Increased photosynthetic production of lactic acid by *Synechocystis* sp. PCC 6803 in a glycogen storage mutant. *J. Biotechnol.* **2014**, *184*, 100–102. [CrossRef]
8. Santos, M.; Pereira, S.B.; Flores, C.; Príncipe, C.; Couto, N.; Karunakaran, E.; Cravo, S.M.; Oliveira, P.; Tamagnini, P. Absence of KpsM (Slr0977) impairs the secretion of extracellular polymeric substances (EPS) and impacts carbon fluxes in *Synechocystis* sp. PCC 6803. *mSphere* **2021**, *6*, e00003-21. [CrossRef] [PubMed]
9. Whitfield, C.; Wear, S.S.; Sande, C. Assembly of bacterial capsular polysaccharides and exopolysaccharides. *Annu. Rev. Microbiol.* **2020**, *74*, 521–543. [CrossRef]
10. Pereira, S.B.; Mota, R.; Vieira, C.P.; Vieira, J.; Tamagnini, P. Phylum-wide analysis of genes/proteins related to the last steps of assembly and export of extracellular polymeric substances (EPS) in cyanobacteria. *Sci. Rep.* **2015**, *5*, 14835. [CrossRef]
11. Maeda, K.; Okuda, Y.; Enomoto, G.; Watanabe, S.; Ikeuchi, M. Biosynthesis of a sulfated exopolysaccharide, synechan, and bloom formation in the model cyanobacterium *Synechocystis* sp. strain PCC 6803. *eLife* **2021**, *10*, e66538. [CrossRef]
12. Jittawuttipoka, T.; Planchon, M.; Spalla, O.; Benzerara, K.; Guyot, F.; Cassier-Chauvat, C.; Chauvat, F. Multidisciplinary evidences that *Synechocystis* PCC 6803 exopolysaccharides operate in cell sedimentation and protection against salt and metal stresses. *PLoS ONE* **2013**, *8*, e55564. [CrossRef]
13. Pereira, S.B.; Santos, M.; Leite, J.P.; Flores, C.; Eisfeld, C.; Büttel, Z.; Mota, R.; Rossi, F.; De Philippis, R.; Gales, L.; et al. The role of the tyrosine kinase Wzc (Sll0923) and the phosphatase Wzb (Slr0328) in the production of extracellular polymeric substances (EPS) by *Synechocystis* PCC 6803. *Microbiologyopen* **2019**, *8*, e00753. [CrossRef]
14. Fisher, M.L.; Allen, R.; Luo, Y.; Curtiss, R., III. Export of extracellular polysaccharides modulates adherence of the cyanobacterium *Synechocystis*. *PLoS ONE* **2013**, *8*, e74514. [CrossRef]
15. Zerulla, K.; Ludt, K.; Soppa, J. The ploidy level of *Synechocystis* sp. PCC 6803 is highly variable and is influenced by growth phase and by chemical and physical external parameters. *Microbiology* **2016**, *162*, 730–739. [CrossRef] [PubMed]
16. Bikard, D.; Jiang, W.; Samai, P.; Hochschild, A.; Zhang, F.; Marraffini, L.A. Programmable repression and activation of bacterial gene expression using an engineered CRISPR-Cas system. *Nucleic Acids Res.* **2013**, *41*, 7429–7437. [CrossRef] [PubMed]
17. Yao, L.; Cengic, I.; Anfelt, J.; Hudson, E.P. Multiple gene repression in cyanobacteria using CRISPRi. *ACS Synth. Biol.* **2016**, *5*, 207–212. [CrossRef]
18. Trautmann, D.; Voss, B.; Wilde, A.; Al-Babili, S.; Hess, W.R. Microevolution in cyanobacteria: Re-sequencing a motile substrain of *Synechocystis* sp. PCC 6803. *DNA Res.* **2012**, *19*, 435–448. [CrossRef]
19. Kanesaki, Y.; Shiwa, Y.; Tajima, N.; Suzuki, M.; Watanabe, S.; Sato, N.; Ikeuchi, M.; Yoshikawa, H. Identification of substrain-specific mutations by massively parallel whole-genome resequencing of *Synechocystis* sp. PCC 6803. *DNA Res.* **2012**, *19*, 67–79. [CrossRef]
20. Larson, M.H.; Gilbert, L.A.; Wang, X.; Lim, W.A.; Weissman, J.S.; Qi, L.S. CRISPR interference (CRISPRi) for sequence-specific control of gene expression. *Nat. Protoc.* **2013**, *8*, 2180–2196. [CrossRef]
21. Xiao, A.; Cheng, Z.; Kong, L.; Zhu, Z.; Lin, S.; Gao, G.; Zhang, B. CasOT: A genome-wide Cas9/gRNA off-target searching tool. *Bioinformatics* **2014**, *30*, 1180–1182. [CrossRef]
22. Gonçalves, C.F.; Pacheco, C.C.; Tamagnini, P.; Oliveira, P. Identification of inner membrane translocase components of TolC-mediated secretion in the cyanobacterium *Synechocystis* sp. PCC 6803. *Environ. Microbiol.* **2018**, *20*, 2354–2369. [CrossRef] [PubMed]
23. Pinto, F.; Pacheco, C.C.; Ferreira, D.; Moradas-Ferreira, P.; Tamagnini, P. Selection of suitable reference genes for RT-qPCR analyses in cyanobacteria. *PLoS ONE* **2012**, *7*, e34983. [CrossRef] [PubMed]
24. Dubois, M.; Gilles, K.A.; Hamilton, J.K.; Rebers, P.A.; Smith, F. Colorimetric method for determination of sugars and related substances. *Anal. Chem.* **1956**, *28*, 350–356. [CrossRef]
25. Kopf, M.; Klähn, S.; Scholz, I.; Matthiessen, J.K.F.; Hess, W.R.; Voß, B. Comparative analysis of the primary transcriptome of *Synechocystis* sp. PCC 6803. *DNA Res.* **2014**, *21*, 527–539. [CrossRef]
26. Shabestary, K.; Anfelt, J.; Ljungqvist, E.; Jahn, M.; Yao, L.; Hudson, E.P. Targeted repression of essential genes to arrest growth and increase carbon partitioning and biofuel titers in cyanobacteria. *ACS Synth. Biol.* **2018**, *7*, 1669–1675. [CrossRef]
27. Kirtania, P.; Hódi, B.; Mallick, I.; Vass, I.Z.; Fehér, T.; Vass, I.; Kós, P.B. A single plasmid based CRISPR interference in *Synechocystis* 6803—A proof of concept. *PLoS ONE* **2019**, *14*, e0225375. [CrossRef]
28. Yao, L.; Shabestary, K.; Björk, S.M.; Asplund-Samuelsson, J.; Joensson, H.N.; Jahn, M.; Hudson, E.P. Pooled CRISPRi screening of the cyanobacterium *Synechocystis* sp PCC 6803 for enhanced industrial phenotypes. *Nat. Commun.* **2020**, *11*, 1666. [CrossRef]

life

MDPI

Supplementary Materials: CRISPRi as a Tool to Repress Multiple Copies of Extracellular Polymeric Substances (EPS)-Related Genes in the Cyanobacterium *Synechocystis* sp. PCC 6803

Marina Santos [1,2,3], Catarina C. Pacheco [1,2], Lun Yao [4,5,†], Elton P. Hudson [4,5] and Paula Tamagnini [1,2,6,*]

[1] i3S- Instituto de Investigação e Inovação em Saúde, Universidade do Porto, 4000-008 Porto, Portugal; marina.santos@ibmc.up.pt (M.S.); cclopes@ibmc.up.pt (C.C.P)
[2] IBMC- Instituto de Biologia Molecular e Celular, Universidade do Porto, 4000-008 Porto, Portugal
[3] Programa Doutoral em Biologia Molecular e Celular (MCbiology), Instituto de Ciências Biomédicas Abel Salazar (ICBAS), Universidade do Porto, 4000-008 Porto, Portugal
[4] Science for Life Laboratory, KTH Royal Institute of Technology, 10004 Stockholm, Sweden; lunyao@kth.se (L.Y.); paul.hudson@scilifelab.se (E.P.H)
[5] Department of Protein Science, KTH Royal Institute of Technology, 10004 Stockholm, Sweden
[6] Departamento de Biologia, Faculdade de Ciências, Universidade do Porto, 4000-008 Porto, Portugal
* Correspondence: pmtamagn@ibmc.up.pt, Tel.: +351 226074957
† Present Address: Dalian Institute of Chemical Physics, Dalian 116000, Shandong, China

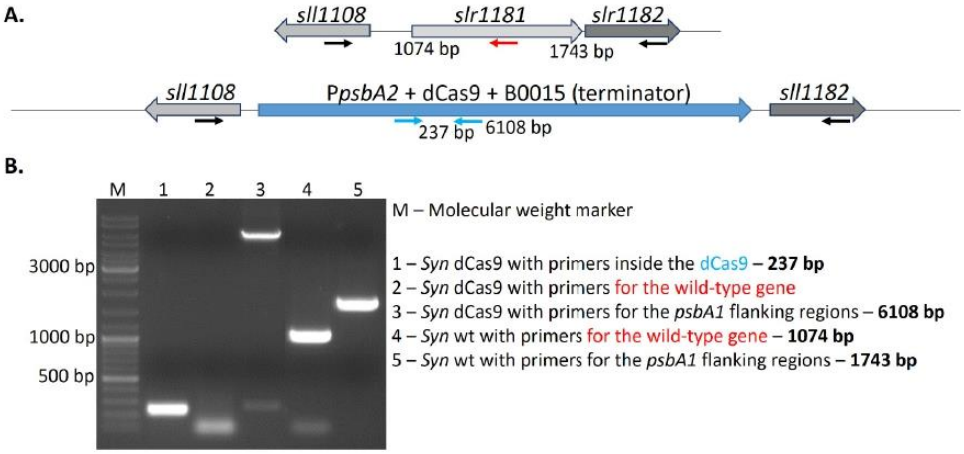

Figure S1. *Synechocystis* sp. PCC 6803 wild-type *slr1181* (*psbA1*) genomic context and confirmation of the *Syn* dCas9 mutant generation. (**A**) Schematic representation of the *slr1181* locus in the genome of *Synechocystis*. Arrowheads—oligonucleotides used to assess mutant identity and segregation (Table S4). (**B**) GreenSafe stained agarose gel showing PCR analyses to assess chromosome segregation of *Syn* dCas9 mutant. PCRs were carried out by using genomic DNA extracted from *Synechocystis* wild-type (*Syn* wt) (Lanes 4 and 5) or the *Syn* dCas9 mutant (Lanes 1,2 and 3) as template. M, GeneRuler DNA ladder mix (Thermo Scientific). The sizes in base-pairs (bp) of some of the GeneRuler DNA Ladder Mix fragments are shown for reference on the left.

Table S1. List of potential off-target binding sites for the three sgRNAs used in this work.

Target	Chromosome Location	Strand	Site	Mismatch (Mm) Type	All Mm	Target	Feature
slr0977	180238-180266	-	tTaaccagatcta_AATCAGcgCTGG	A212	13	*slr1414*	sensory transduction histidine kinase
	283005-283033	-	cggagcagatcAT_AATCctTTCTGG	A211	13	-	-
	307315-307343	+	GaCgaatgcCcAg_AAcCAGTgCTGG	A209	11	*slr1303*	unknown protein
	528989-529017	+	agaCacCaTtAcc_AATCAacTCTGG	A209	11	*slr1753*	unknown protein
	604729-604757	+	cTtaTctTcCtgT_AAaCAGTgCTGG	A208	10	-	-

	609572-609600	-	aTagctCcaCAtc_AAcCAGTTtTG G	A209	11	*slr1906*	unknown protein
	709902-709930	-	GaatctggTgAca_AAgaAGTTCTG G	A210	12	-	-
	714970-714998	-	caagaatcgCcca_AATCAGTTCaaG	A212	14	*sll1583*	DNA ligase
	804862-804890	+	tTttccCaTggca_AATCAtTTCTGc	A210	12	*sll1076*	Zinc exporter
	816533-816561	+	tggagGtcgtAgg_AAgCAGTgCTG G	A211	13	*sll1072*	unknown protein
	1479022-1479050	-	taataatcgttta_AAcCAtTTCTGG	A213	15	*slr1724*	unknown protein
	1643383-1643411	-	aattTGgcaCctT_AAcCAGTTCTtG	A209	11	-	-
	1724715-1724743	+	GcgtaGaTaCggc_AATCAGcaCTG G	A209	11	*sll1258*	unknown protein
	1887090-1887118	-	agCaatCagCtca_AAcCcGTTCTG G	A210	12	-	-
	2076362-2076390	+	taaCcatccaAcc_AgTCAGTgCTGG	A211	13	*sll1522*	CDP-diacylglycerol-glycerol-3-phosphate 3phosphatidyltransferase
	2228027-2228055	+	catCccCagggAa_AATtAGTTCgG G	A210	12	*slr1933*	dTDP-4-dehydrorhamnose 3,5-epimerase
	2438430-2438458	-	ccCagGggcaAtg_AATtAGTTtTG G	A210	12	*sll0319*	unknown protein
	2735371-2735399	+	ccCCatggcCgca_AcTCAGTTaTG G	A210	12	-	-
	2782435-2782463	-	tTttctaaTaAgT_AATCAaTTtTGG	A209	11	*slr0907*	unknown protein
	3142190-3142218	+	taaaactTTtcta_AATCAGTgCcGG	A211	13	*sll0045*	sucrose phosphate synthase
	3231946-3231974	-	tTaCccacTgcAa_AATCtGTTCcGG	A209	11	*slr0930*	unknown protein
	46664-46689	-	tgctCTatga_cCGATgGACGAT	A208	10	*slr1494*	ABC transporter
	312905-312930	-	AgaggattTg_GCGATcGcCGAT	A208	10	*slr1306*	unknown protein
	355492-355517	-	AaaAtccccg_GCGATcGcCGAT	A208	10	*slr0985*	dTDP-6-deoxy-L-mannose-dehydrogenase
	482785-482810	-	tTacCTtccT_GCcATTGACGgT	A206	8	-	-
	538261-538286	-	gacAtgGtcg_GCGATcGcCGAT	A208	10	*slr1760*	regulatory components of sensory transduction system
	674519-674544	-	gcaAaaaaTT_GCGgTTGACGAc	A207	9	*slr1379*	cytochrome oxidase d subunit I
	932640-932665	+	ATtAtTGcgg_GCctTTGACGAT	A205	7	*slr1829*	polyhydroxyalkanoate synthase subunit PhaE
	1458346-1458371	-	ccatCaccaT_GCGATTGACcAc	A208	10	*sll1614*	cation-transporting ATPase
	1586617-1586642	+	Aaattcaccg_GCaATTGACGAT	A109	10	*sll1425*	proline-tRNA ligase
	1763748-1763773	-	AgttCcaGcg_GCGATcGcCGAT	A207	9	*slr1962*	unknown protein
	1935017-1935042	-	cattgccaaa_GCcATTGACGcT	A210	12	*sll1091*	bacteriochlorophyll synthase subunit
	1944159-1944184	-	cgtttTtGca_cCGtTTGACGAT	A208	10	*slr1173*	unknown protein
	1960433-1960458	+	ATacCcaGTT_GgGgTTGACGAT	A204	6	*sll1564*	alpha-isopropylmalate synthase
	2154990-2155015	-	cccAtaacaa_GCGATcGgCGAT	A209	11	*sll0356*	5'-phosphoribosyl anthranilate isomerase
	2178468-2178493	+	catttTtcag_GCGATcGcCGAT	A209	11	-	-
slr2107	2400367-2400392	+	tccgCccaTg_GCGATcGgCGAT	A208	10	*sll0771*	glucose transport protein
	2431716-2431741	-	gccttcaacT_GgGtTTGACGAT	A209	11	*slr0346*	ribonuclease III
	2446056-2446081	+	ATattgtcaT_GgGATTGACaAT	A207	9	-	-
	2541513-2541538	+	gTttagtcTg_GCGATcGcCGAT	A208	10	*sll0415*	ABC transporter
	2572081-2572106	-	tgccgcccTg_GCGATcGcCGAT	A209	11	*sll0068*	unknown protein
	2574029-2574054	-	taaggTGccg_GCGATcGcCGAT	A208	10	*sll0067*	glutathione S-transferase
	2588466-2588491	+	gcattgGtca_cCGATTGACGcT	A209	11	*sll0058*	DnaK protein
	2597048-2597073	-	ActtgTccca_cCGATTGgCGAT	A208	10	*slr0067*	ATP-binding protein involved in chromosome partitioning
	2942897-2942922	+	ggGgCattTg_GCGATcGcCGAT	A207	9	-	-
	2947562-2947587	+	ATtgCcctca_GCGATTtACGcT	A207	9	*slr0615*	ATP-binding cassette, subfamily B, multidrug efflux pump
	3212295-3212320	+	tccAaattgg_GCGATcGgCGAT	A209	11	*slr0541*	unknown protein
	3395838-3395863	+	ATGgaaaaTg_GCGATTaACcAT	A206	8	*sll1477*	unknown protein
	3412312-3412337	-	caacaatGga_cCGATTGgCGAT	A209	11	*sll0736*	unknown protein
	3520784-3520809	+	gTacCcaccT_GCGATcGcCGAT	A207	9	*sll1110*	peptide chain release factor
	3537459-3537484	-	ggtAtTGacg_GCGATcGcCGAT	A207	9	*sll0578*	phosphoribosyl aminoimidazole carboxylase
	3556832-3556857	-	gactggcaaa_GCcATTGgCGAT	A210	12	*sll0564*	unknown protein

	80660-80683	+	cattcCCA_GTTCAgCtTTGT	A205	7	*sll1056*	phosphoribosylformyl glycinamidine synthetase II
	114355-114378	-	GGcaAttt_GTTCACCaaTGT	A205	7	*slr0729*	unknown protein
	135400-135423	-	GGGccggc_GTTtgCCCTTGT	A205	7	*slr0744*	initiation factor IF-2
	219419-219442	-	GccGctCg_GgTCACCCTgGT	A205	7	*sll1029*	carbon dioxide concentrating mechanism protein
	322713-322736	-	ttGGAaCg_GTTtACCCaTGT	A204	6	*slr0963*	ferredoxin-sulfite reductase
	529560-529583	+	tGGagtgg_cTTCACCCTaGT	A206	8	*slr1753*	unknown protein
	602477-602500	+	ccGcttCg_GTTaACCtTTGT	A206	8	*sll1932*	DnaK protein
	803137-803160	-	ctGGAgtg_cTTCACCCTgGT	A205	7	*slr1143*	unknown protein
	835311-835334	+	GcGGAtgc_cTTtACCCTTGT	A204	6	*sll1810*	50S ribosomal protein L6
	1177960-1177983	+	aacaAtat_tTTCACCCTTGa	A207	9	*slr1403*	integrin alpha- and beta4- subunit domain homologue
	1564393-1564416	-	atccACCA_GTTCACCgaTGT	A204	6	*slr2098*	hybrid sensory kinase
sll0574	1613993-1614016	+	caccAggc_GTTtAtCCTTGT	A207	9	*slr1521*	GTP-binding protein
	2332627-2332650	+	ttccttat_GTTCACCtTTGc	A208	10	*sll0158*	1,4-alpha-glucan branching enzyme
	2359738-2359761	-	GaGtcCag_GTTCACCCgTGa	A205	7	-	-
	2547462-2547485	+	cGaGgagA_GTTaACCaTTGT	A205	7	*sll0409*	o-succinylbenzoate synthase
	2813544-2813567	-	cctccCtg_GTTaACCaTTGT	A207	9	*sll0545*	unknown protein
	2842647-2842670	-	tcccAttg_GTTCACCaTTGa	A207	9	-	-
	3006504-3006527	-	aGacgaCc_GTaCcCCCTTGT	A206	8	*sll0290*	polyphosphate kinase
	3007775-3007798	+	cactAaag_GTTCcCCtTTGT	A207	9	*sll0289*	septum site-determining protein
	3157718-3157741	+	GaattagA_GTTaACCCaTGT	A206	8	*slr0033*	aspartyl-tRNA(Asn)/glutamyl-tRNA(Gln) amidotransferase subunit C
	3247855-3247878	+	GGcactaA_GTTCACCCcTGg	A205	7	-	-
	3433031-3433054	-	cttGgCtA_GTTaACCCTTtT	A205	7	-	-
	3476773-3476796	-	GGaGAagc_GTctACCCTTGT	A204	6	*slr1668*	unknown protein
	3521819-3521842	+	atGtttgA_GTTCAtCaTTGT	A206	8	*sll1109*	unknown protein

Table S2. List of organisms and plasmids used/generated in this work.

Organism Name/Genotype.	**Description**	**Source**
Escherichia coli DH5α	Transformation/cloning strain	Invitrogen
Escherichia coli XL1-Blue	Transformation/cloning strain	Agilent
Synechocystis sp. PCC 6803	Wild-type substrain Kasuza	Pasteur Culture Collection
sll0574 mutant	*Synechocystis* mutant with *sll0574* (from 46 to 764 bp) replaced by a Km resistance cassette	This work
Syn dCas9	Δ*psbA1*::P_{psbA2} dCas9 SpR	This work
3-sgRNA *kpsM* mutant	Δ*psbA1*::P_{psbA2} dCas9 SpR; pLY::P_{L31} sgRNA-sll0574_15 slr0977_16 slr2107_56 CmR	This work
Plasmid	**Description**	**Source**
pGEM®-T easy	T/A cloning vector	Promega
pKm.1	pGEM-T easy with the Km resistance cassette	Pinto *et al*, 2015
pGDsll0574	pGEM-T easy habouring *sll0574*'s flanking sequences for double homologous recombination, including a XmaI site in between	This work
pGDsll0574.Km	pGDsll0574 with a Km resistance cassette inserted into the XmaI site	This work
pMD19T_psbA1_P_{psbA2}_dCas9_B0015_SpR	Plasmid to transform the dCas9 into *Synechocystis*	Yao *et al*, 2016
pMD19T_slr0230_slr0231_P_{L31}_sgRNA NT1_B0015_KmR	Assembly plasmid for the sgRNA arrays	Yao *et al*, 2016
pLY KmR	Replicative vector for *Synechocystis*	Kindly provided by Paul Hudson's group
pLY CmR	Replicative vector for *Synechocystis*	This work
pLY::P_{L31}_sgRNA-sll0574_15 slr0977_16 slr2107_56 CmR	Replicative vector for *Synechocystis* transformation	This work

Table S3. Primer nucleotide sequences and annealing temperatures (T_a) used in RT-qPCR.

Gene	Primer Name	Primer Sequence (5′- 3′)	T_a (°C)	Source
sll0574	sll0574_RTq_Fwd	CCGGCACAATTTCGGATGG	56	This work
	sll0574_RTq_Rev	CCCTCTCCATGATCGTCGC		
slr2107	slr2107F(Ra)	GACCCATCGTCAATCGCAAC	56	This work
	slr2107RT	CACATCCTTCGCCACCAA		
slr0977	slr0977F	CGCACGGAGCGTCAGTATT	56	This work
	slr0977RO	CCGCAAACACCAGAATGGGAT		
rrn16Sa.b	BD16SF1	CACACTGGGACTGAGACAC	56	
	BD16SR1	CTGCTGGCACGGAGTTAG		
petB	SpetB1F	CCTTCGCCTCTGTCCAATAC	56	Pinto *et al*, 2012
	SpetB1R	TAGCATTACACCCACAACCC		
rnpB	rnpBF1	CGTTAGGATAGTGCCACAG	56	
	rnpBR1	CGCTCTTACCGCACCTTTG		

Table S4. Primer nucleotide sequences used to verify the segregation of the *Syn* dCas9 strain.

Primer Name	Primer Sequence (5′-3′)	Source
dCas9i_Fwd	GTTTTGCCAATCGCAATTTT	This work
dCas9i_Rev	CACGTGCCATTTCAATAACG	
psbA1_Rev	AACCAAGGAACCGTGCATAG	
FR_Fwd	GCCACAACCAGGCAGTATTT	
FR_Rev	CCAGGCAATCCACTGATTTT	

CHAPTER V

Generation and characterization of other EPS-related mutants

Generation and characterization of other EPS-related mutants

Following the work presented in the previous chapters (II, III and IV), some preliminary results regarding the generation and characterization of two other EPS-related mutants are described here.

1. The *wzy* (*slr1074*) mutant

Results published by Pereira, Santos, et al. (2019) (Chapter II) showed that a *Synechocystis* sp. PCC 6803 Δ*sll0737* mutant (one of the 5 putative *wzy* copies present in the *Synechocystis* genome), had no phenotypic changes concerning the EPS production, strongly suggesting functional redundancy. In the same publication, RT-PCR results also hinted that *slr1074* is one of the most expressed *wzy* homologues, in agreement with data previously published by Kopf et al. (2014). Thus, we also generated a *slr1074* (*wzy*) knockout mutant. This gene is located in the chromosome, near a cluster of genes annotated as involved in sugar-metabolism, such as the *rfb* genes (including *rfbC* – *slr0985*), and other genes that have experimentally been shown to affect EPS production and export, such as *sll0923* (*wzc*) and *slr0977* (*kpsM*) (Fisher et al., 2013; Jittawuttipoka et al., 2013; Pereira et al., 2019; Santos et al., 2021). The *slr1074* (*wzy*) mutant was generated by double homologous recombination, partially replacing the gene with a kanamycin (Km) resistance cassette, as previously described by Santos et al. (2021). The strains, plasmids and primers used for this purpose, and to check the segregation of the mutant are listed in Tables S1, S2 and S3, respectively). Full segregation of the *slr1074* (*wzy*) mutant was verified by PCR (Figure 1).

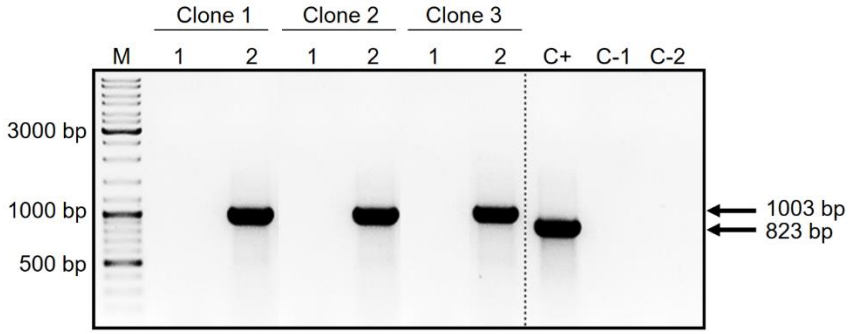

Figure 1. Agarose gel electrophoresis showing the PCR analysis to assess the segregation of *Synechocystis slr1074* mutant. Two primer pairs were used: one to check for the presence of the wild-type genomic region containing the *slr1074* gene (slr1074.5O + slr1074R2); and a second to check for the presence of the mutated genomic region containing the kanamycin-cassette (KmRRev + slr1074.3O). For full segregation of the *slr1074* mutant, no PCR product is expected to be amplified using the primers for the wild-type *slr1074* gene: Lanes 1; PCR product obtained using genomic DNA of the *slr1074* mutant and the primer pair KmRRev + slr1074.3O [expected product size – 1003 bp]: Lanes 2; C+, Positive control, using genomic DNA from *Synechocystis* sp. PCC 6803 wild-type and the primer pair slr1074.5O + slr1074R2 [expected product size – 823 bp]; C-1, Negative control for the primer pair for the *slr1074* gene; C-2, Negative control for the primer pair for the kanamycin-cassette; M, GeneRuler DNA Ladder Mix. The primers used to assess the segregation of this mutant are listed in Table S3.

The preliminary characterization (n=2) of the *slr1074* (*wzy*) mutant showed that the mutant grows similarly to the wild-type (Figure 2A), and does not exhibit any significant differences concerning the amounts of total carbohydrates, CPS or RPS produced compared to the wild-type (Figure 2B-D).

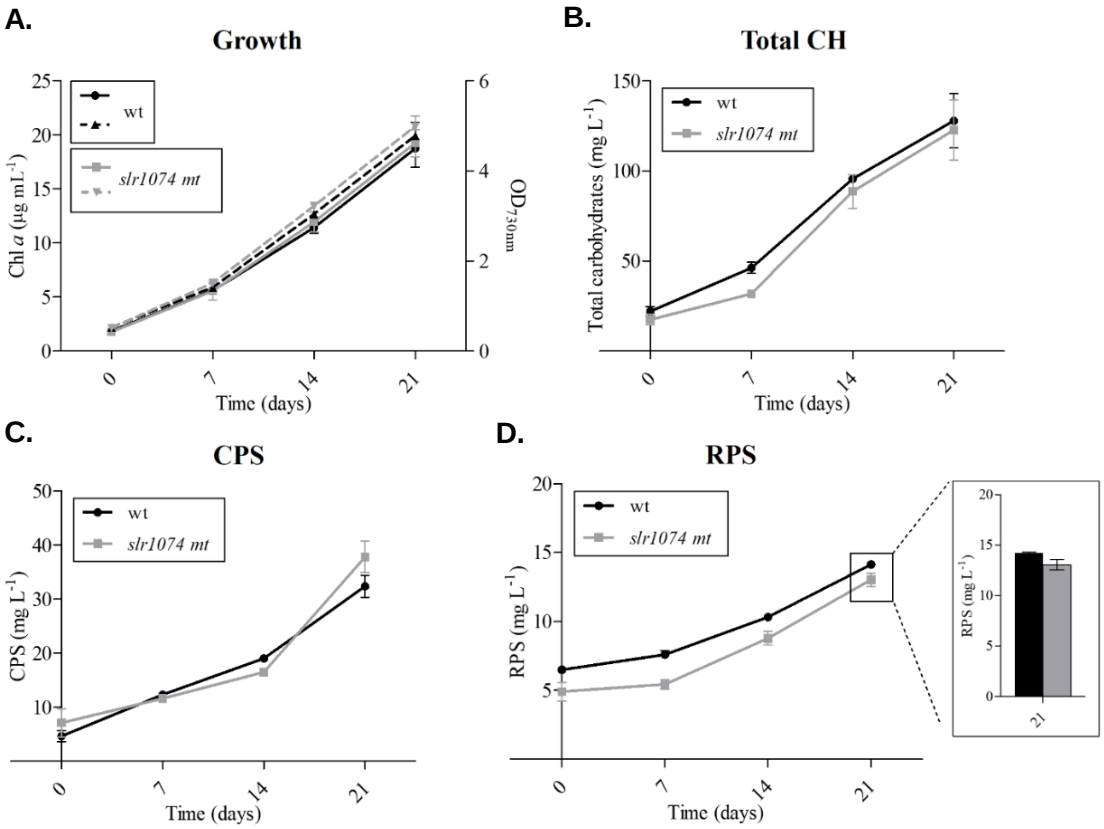

Figure 2. Growth curves and carbohydrate production by *Synechocystis* sp. PCC 6803 *slr1074* (*wzy*) mutant compared to the wild-type (wt). Growth was monitored by measuring the optical density at 730 nm (full lines) and chlorophyll *a* (Chl *a*) (dashed lines) (A). Total carbohydrates (B), capsular polysaccharides (CPS) (C), and released polysaccharides (RPS) (D) were measured by the phenol-sulphuric acid method (Dubois et al., 1951), and expressed as milligrams per liter of culture. Cells were grown in BG11 medium at 30°C under a 12 h light (50 µE m^{-2} s^{-1})/12 h dark regimen, with orbital shaking at 150 rpm.

The results obtained suggest that the absence of Slr1074, similarly to what was observed for the absence of Sll0737 (Pereira, Santos et al., 2019), does not impact EPS production, at least under the conditions tested, and that this gene is not essential for survival and growth. The Slr1074 protein might not be involved at all in EPS production or, alternatively, it could play a role in EPS production during the response to stress conditions. In 2002, Huang et al. reported a 3.7-fold up-regulation of the transcript levels of *slr1074* after exposure to high light (200 µE m^{-2} s^{-1}), suggesting that this condition triggers the expression of *slr1074* in *Synechocystis*. Exposure to high light could induce the production of EPS as a protective mechanism. However, the authors did not describe any data regarding the amount of EPS produced.

2. The *rfbC* (*slr0985*) mutant

Results previously obtained by Pereira, Santos et al. (2019) showed that the RPS produced by the Δ*wzb* (*slr0328*), Δ*wzc* (*sll0923*), Δ*wzb*:Δ*wzc* and wzc_{trunc} mutants, had a considerable increase in the percentage of rhamnose (Chapter II, Pereira et al., 2019). This led us to look into the rhamnose biosynthesis in *Synechocystis* (Figure 3). As stated previously, some of the genes encoding proteins involved in this pathway are located closely to other putative EPS-related genes, including *sll0923* (*wzc*), *slr0977* (*kpsM*) and *slr0982* (*kpsT*) that have already experimentally been shown to affect the amount of EPS produced and/or the composition of the polymers (Fisher et al., 2013; Jittawuttipoka et al., 2013; Pereira et al., 2019; Santos et al., 2021). The *slr0985* (*rfbC*) gene encodes an epimerase (Slr0985 – RfbC) that converts dTDP-4-oxo-6-deoxy-D-glucose into dTDP-4-dehydro-beta-L-rhamnose (Figure 3), and it was previously described as an inorganic carbon (C_i) responsive gene (Eisenhut et al., 2007).

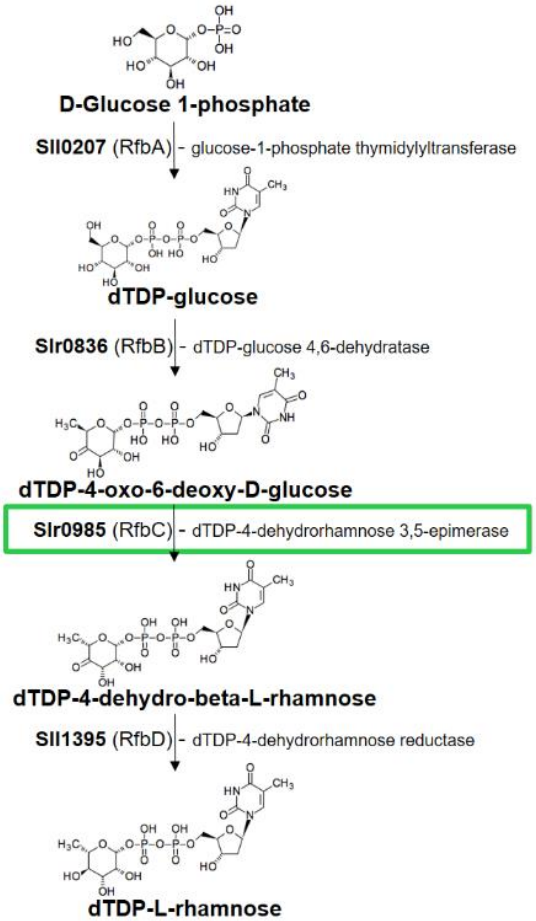

Figure 3. Pathway for rhamnose biosynthesis in *Synechocystis* sp. PCC 6803. The RfbC, dTDP-4-dehydrorhamnose 3,5-epimerase, is highlighted with a green box.

The *slr0985* (*rfbC*) knockout mutant was generated by double homologous recombination, partially replacing the gene with a kanamycin (Km) resistance cassette, as

previously described by Santos et al. (2021). The list of strains, plasmids and primers used for the generation/check segregation of the mutant are listed in Tables S1, S2 and S3, respectively. Full segregation of the mutant was confirmed by Southern Blot (Figure 4), and a preliminary quantification (n=2) of the total carbohydrates, CPS and RPS produced by the *rfbC* mutant, was performed.

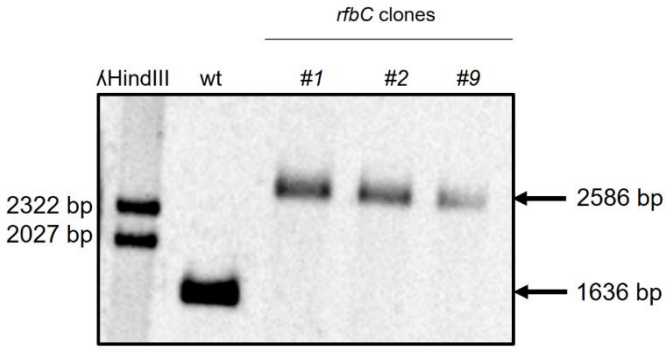

Figure 4. Southern blot analysis confirming the segregation of the *Synechocystis* sp. PCC 6803 *rfbC* mutant. The genomic DNA of the *Synechocystis* sp. PCC 6803 wild-type and *rfbC* mutant were digested with the endonuclease *DraI*. A dioxigenin labeled probe covering the 5' flanking region of *rfbC* was used. The primers used for the generation of this probe (333 bp) are listed in Table S3.The sizes of the DNA fragments hybridizing with the probe are indicated. wt – wild-type; # clone tested.

The *slr0985* (*rfbC*) mutant grows similarly to the wild-type (Figure 5A) and also produces a similar amount of total carbohydrates and CPS (Figure 5B and C). However, the amount of RPS was approximately 47% less than the wild-type (Figure 5D), suggesting that absence of Slr0985 (RfbC) impacts the amount of RPS secreted by *Synechocystis*.

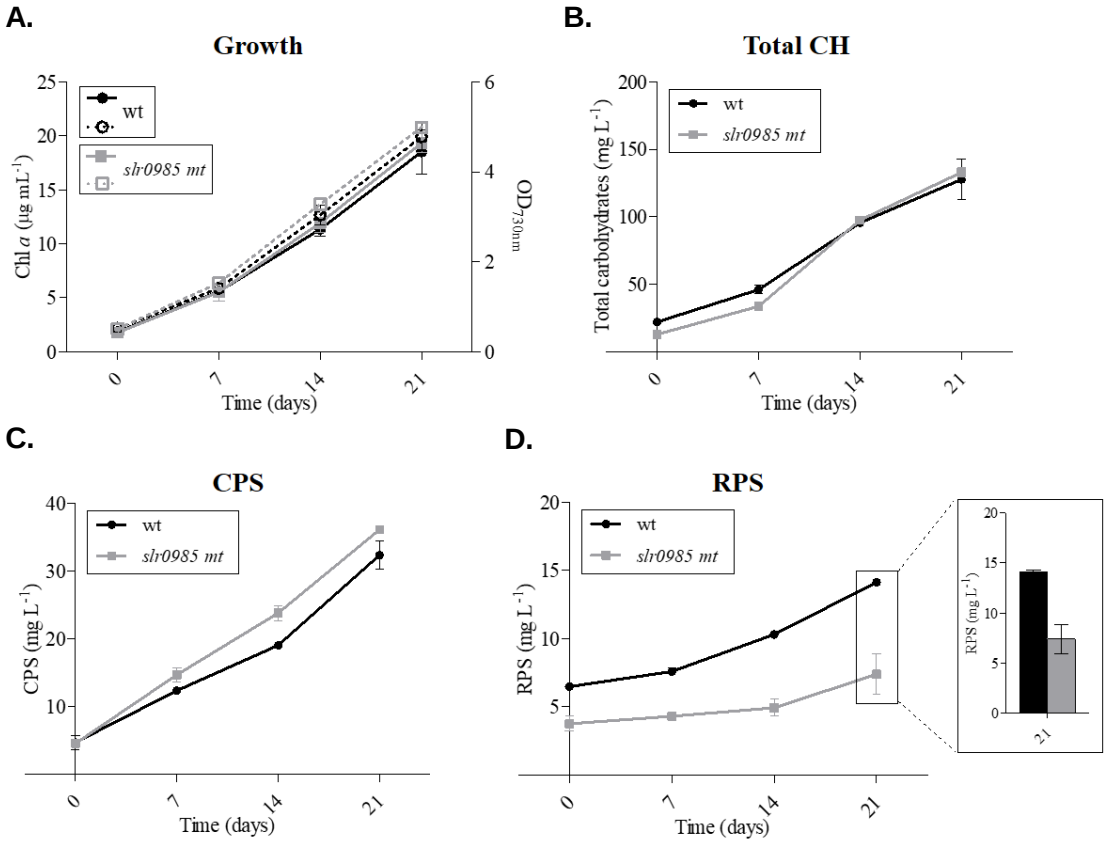

Figure 5. Growth curves and carbohydrate production by *Synechocystis* sp. PCC 6803 *slr0985* (*rfbC*) mutant compared to the wild-type (wt). Growth was monitored by measuring the optical density at 730 nm (full lines) and chlorophyll *a* (Chl *a*) (dashed lines) (A). Total carbohydrates (B), capsular polysaccharides (CPS) (C), and released polysaccharides (RPS) (D) were measured by the phenol-sulphuric acid method (Dubois et al., 1951), and expressed as milligrams per liter of culture. Cells were grown in BG11 medium at 30°C under a 12 h light (50 µE m^{-2} s^{-1})/12 h dark regimen, with orbital shaking at 150 rpm.

In addition, the proteomes and exoproteomes of the wild-type and *slr0985* (*rfbC*) mutant were analyzed, as previously described by Flores & Tamagnini, 2019 and Oliveira et al. (2016), respectively. For this purpose, the strains were cultivated in glass gas washing bottles with aeration, under a continuous light regime of 30-40 µE m^{-2} s^{-1}, at ~28°C (fast-growth conditions), until OD 1.5. No significant differences were observed regarding the intracellular proteome profiles (Figure 6A), however the mutant appears to secrete more proteins than the wild-type (data not shown). Moreover, the lipopolysaccharides (LPS) were also analyzed in the culture medium and outer membrane preparations of the wild-type and *rfbC* mutant, as previously described Oliveira et al. (2016) and Pereira, Santos, et al. (2019), respectively. Some differences were observed, namely the presence of less LPS in the concentrated medium of the *rfbC* mutant (Figure 6B), and differences on the O-antigen of the LPS from the outer membrane preparations, in the *rfbC* mutant compared to the wild-type (Figure 6C).

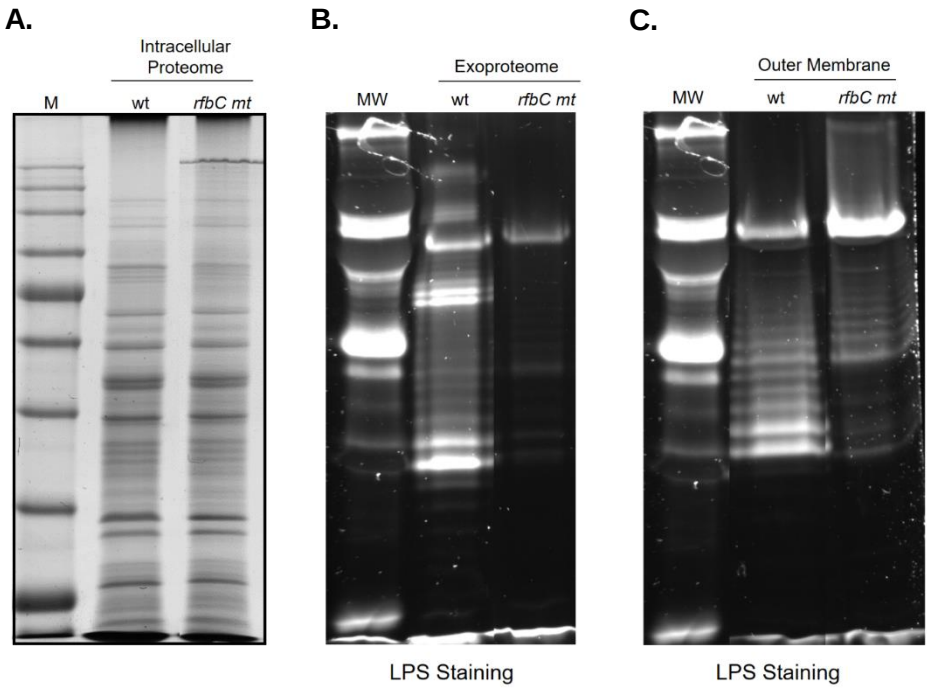

Figure 6. (A) Analysis of the intracellular proteomes of *Synechocystis* sp. PCC 6803 wild-type (wt) and *slr0985* (*rfbC*) mutant separated by electrophoresis on 12% SDS- polyacrylamide gels followed by staining with Roti-Blue. M, NZYColour protein marker II. Analysis of the lipopolysaccharides (LPS) in the culture medium (B) and outer membrane preparations (C) of *Synechocystis* sp. PCC 6803 wild-type (wt) and *rfbC* mutant (mt) strains by electrophoresis on 12% SDS- polyacrylamide gels followed by staining with Pro-Q Emerald 300 lipopolysaccharide. MW: CandyCane™ glycoprotein molecular weight standards.

After concentrating the extracellular medium of *Synechocystis* wild-type and the *slr0985* (*rfbC*) mutant, different color intensities were observed (Figure 7), suggesting a difference in the extracellular carotenoids content. Therefore, the pigment content in the extracellular medium of both cultures was analyzed. The absorption spectra showed the characteristic peaks of carotenoids for both strains although with a significantly higher amount for the wild-type (Figure 7).

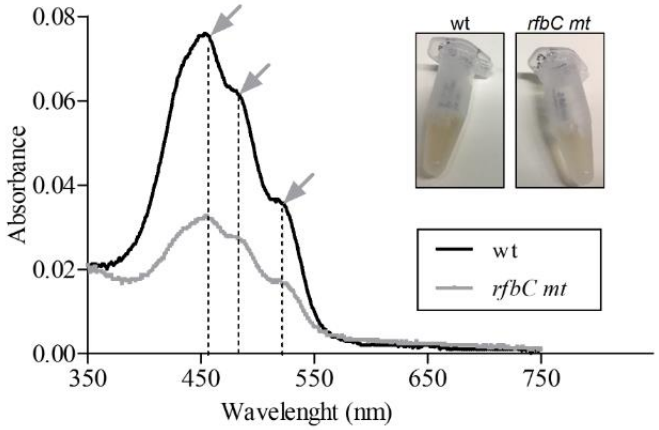

Figure 7. Absorption spectra of concentrated medium from *Synechocystis* sp. PCC 6803 wild-type (wt) and *rfbC* mutant cultures, with arrows indicating the characteristic carotenoid peaks at 460, 487, and 521 nm. The inset shows *Synechocystis* wt and *rfbC* mutant culture medium exhibiting different orange color intensities.

The results obtained suggest that the absence of Slr0985 strongly impacts RPS and the amounts of carotenoids in the medium. In addition, the monosaccharidic composition of the polymer produced by the *rfbC* mutant should be determined, since rhamnose represents approximately 6 to 14% (Flores et al., 2019; Panoff et al., 1988; Pereira, Santos et al. 2019) of the constitution of the polymer produced by *Synechocystis* wild-type.

References

Dubois, M., Gilles, K., Hamilton, J. K., Rebers, P. A., & Smith, F. (1951). A colorimetric method for the determination of sugars. *Nature*, *168*(4265), 167. https://doi.org/10.1038/168167a0

Eisenhut, M., von Wobeser, E. A., Jonas, L., Schubert, H., Ibelings, B. W., Bauwe, H., Matthijs, H. C. P., & Hagemann, M. (2007). Long-term response toward inorganic carbon limitation in wild type and glycolate turnover mutants of the cyanobacterium *Synechocystis* sp. strain PCC 6803. *Plant Physiology*, *144*(4), 1946–1959. https://doi.org/10.1104/pp.107.103341

Fisher, M. L., Allen, R., Luo, Y., & Curtiss, R. (2013). Export of extracellular polysaccharides modulates adherence of the cyanobacterium *Synechocystis*. *PLoS ONE*, *8*(9). https://doi.org/10.1371/journal.pone.0074514

Flores, C., Santos, M., Pereira, S. B., Mota, R., Rossi, F., De Philippis, R., Couto, N., Karunakaran, E., Wright, P. C., Oliveira, P., & Tamagnini, P. (2019). The alternative sigma factor SigF is a key player in the control of secretion mechanisms in *Synechocystis* sp. PCC 6803. *Environmental Microbiology*, *21*(1), 343–359. https://doi.org/https://doi.org/10.1111/1462-2920.14465

Flores, C., & Tamagnini, P. (2019). Looking outwards: Isolation of cyanobacterial released carbohydrate polymers and proteins. *Journal of Visualized Experiments : JoVE*, *147*. https://doi.org/10.3791/59590

Huang, L., McCluskey, M. P., Ni, H., & LaRossa, R. A. (2002). Global gene expression profiles of the cyanobacterium *Synechocystis* sp. strain PCC 6803 in response to irradiation with UV-B and white light. *Journal of Bacteriology*, *184*(24), 6845–6858. https://doi.org/10.1128/JB.184.24.6845-6858.2002

Jittawuttipoka, T., Planchon, M., Spalla, O., Benzerara, K., Guyot, F., Cassier-Chauvat, C., & Chauvat, F. (2013). Multidisciplinary evidences that *Synechocystis* PCC6803 exopolysaccharides operate in cell sedimentation and protection against salt and metal Stresses. *PLoS ONE*, *8*(2). https://doi.org/10.1371/journal.pone.0055564

Kopf, M., Klähn, S., Pade, N., Weingärtner, C., Hagemann, M., Voß, B., & Hess, W. R. (2014). Comparative genome analysis of the closely related *Synechocystis* strains PCC 6714 and PCC 6803. *DNA Research*, *21*(3), 255–266. https://doi.org/10.1093/dnares/dst055

Oliveira, P., Martins, N. M., Santos, M., Pinto, F., Büttel, Z., Couto, N. A. S., Wright, P. C., & Tamagnini, P. (2016). The versatile TolC-like Slr1270 in the cyanobacterium *Synechocystis* sp. PCC 6803. *Environmental Microbiology*, *18*(2), 486–502. https://doi.org/10.1111/1462-2920.13172

Panoff, J. M., Priem, B., Morvan, H., & Joset, F. (1988). Sulphated exopolysaccharides produced by two unicellular strains of cyanobacteria, *Synechocystis* PCC 6803 and 6714. *Archives of Microbiology*, *150*(6), 558–563. https://doi.org/10.1007/BF00408249

Pereira, S. B., Santos, M., Leite, J. P., Flores, C., Eisfeld, C., Büttel, Z., Mota, R., Rossi, F., De Philippis, R., Gales, L., Morais-Cabral, J. H., & Tamagnini, P. (2019). The role of the tyrosine kinase Wzc (Sll0923) and the phosphatase Wzb (Slr0328) in the production of extracellular polymeric substances (EPS) by *Synechocystis* PCC 6803. *MicrobiologyOpen*, *8*(6), e00753. https://doi.org/10.1002/mbo3.753

Santos, M., Pereira, S. B., Flores, C., Príncipe, C., Couto, N., Karunakaran, E., Cravo, S. M., Oliveira, P., & Tamagnini, P. (2021). Absence of KpsM (Slr0977) impairs the secretion of extracellular polymeric substances (EPS) and impacts carbon fluxes in

Synechocystis sp. PCC 6803. *mSphere*, *6*(1), 1–20. https://doi.org/10.1128/msphere.00003-21

Supplementary Material

Table S1. List of organisms/mutants used/generated.

Organisms		
Organism name/Genotype	**Description**	**Source**
Escherichia coli DH5α	Transformation/cloning strain	Invitrogen
Synechocystis sp. PCC 6803	Wild-type strain	Pasteur Culture Collection
slr1074 mutant	*Synechocystis* mutant with *slr1074* replaced by a Km resistance cassette.	This work
slr0985 mutant	*Synechocystis* mutant with *slr0985* replaced by a Km resistance cassette	This work

Table S2. List of plasmids used for the generation of the *slr1074* (*wzy*) and *slr0985* (*rfbC*) mutants.

Plasmids		
Plasmid	**Description**	**Source**
pGEM®-T easy	T/A cloning vector.	Promega
pGDslr1074.Km	pGDslr1074 with a Km resistance cassette inserted into the XmaI site.	This work
pGDslr0985.Km	pGDslr0985 with a Km resistance cassette inserted into the StuI site.	This work

Table S3. List of oligonucleotides used for the generation of the *slr1074* (*wzy*) and *slr0985* (*rfbC*) mutants, and to confirm mutant segregation.

Primers			
Mutant	**Name**	**Sequence (5'-3')**	**Reference**
***slr1074* (*wzy*) mutant**	slr1074.5O	CCGTTCTCTGTCCGTTACTTGGCTTTTCCT	This work
	slr1074.5I	GAATATAATCGTCGTGCCCGGGCATCCCAGCTTT GATTGACGGCATAATC	This work
	slr1074.3I	CAAAGCTGGGATGCCCGGGCACGACGATTATAT TCGAGAGCTATGCTGT	This work
	slr1074.3O	GGCATAAATACAAGCCTGGATTGCTTCG	This work
	slr1074R2	GCCTAATCACCGCCACTATGGT	This work
	KmRRev	GCATCGCCTTCTATCGCCTT	(Pereira et al. 2019)
***slr0985* (*rfbC*) mutant**	slr0985.5O	CGCCTGCGAAATCGTAGTAGCCAGTTATC	This work
	slr0985.5I	GATAATTCGGTAATTGAGGCCTATGGGCTGACG GATAACGGTTCTGAGT	This work
	slr0985.3I	TTATCCGTCAGCCCATAGGCCTCAATTACCGAAT TATCCCAGCGAGACC	This work
	slr0985.3O	GCTCATGGTAAACCGTATCAAATTGGGTC	This work
	slr0985_SB_Fwd	CCTGATGTTGTCCGCGCCCTA	This work
	slr0985_SB_Rev	CCAACTAGGACGATATCCCAGTA	This work

CHAPTER VI

Final Remarks and Future Perspectives

Final Remarks

Overall, this work contributes to provide a better and deeper understanding of some of the components involved in the production of extracellular polymeric substances (EPS), and of the importance of EPS as a carbon-sink in cyanobacteria. It also starts to address the genetic redundancy that is commonly pointed out as hindering the study of these mechanisms in cyanobacteria.

1. The tyrosine kinase Wzc (Sll0923) and the phosphatase Wzb (Slr0328) affect the amount and composition of EPS in *Synechocystis*

Using *Synechocystis* sp. PCC 6803 (hereafter *Synechocystis*) as a model organism, the role of Wzb (Slr0328) and Wzc (Sll0923) in the production EPS was addressed. Absence of Wzb resulted in 20% less RPS, while absence of Wzc affected both the amount of RPS and CPS, approximately 20% less of both (Pereira, Santos et al., 2019). Interestingly, a double mutant lacking both Wzb and Wzc did not show a cumulative phenotype, but exhibited a decrease in CPS and an increase in RPS, suggesting that in the absence of the two proteins, RPS production is likely to be diverted to an alternative route or, at least, employs different components to compensate for the absence of latter two. Altogether, these results support the involvement of different players, and raise the hypothesis of functional redundancy, either owing to the existence of multiple copies for some of the EPS-related genes/proteins and/or a crosstalk between the components of the different assembly and export pathways. Absence of Wzb and Wzc also affected the composition of the polymers produced by the mutant strains, resulting in a significant increase of the rhamnose content in the polymers produced by these mutants (Pereira, Santos et al., 2019). Wzb was shown to have the structure of LMW-PTP, though more closely related to the LMW-PTP of the unicellular eukaryote *Entamoeba histolytica* than of the LMW-PTPs of other bacteria. Wzc was described to possess ATPase and auto-kinase activities, and Wzb is able to interact *in vitro* with the C-terminal Y-rich tail of Wzc, suggesting that the phosphorylation state of Wzc is dependent on the activity of Wzb (Pereira, Santos et al., 2019). Overall, we clarified the roles of both proteins through biochemical and structural analysis, providing the first insights into the molecular mechanisms of EPS production in *Synechocystis,* highlighting, for the first time, tyrosine phosphorylation as a possible regulatory mechanism of EPS production in cyanobacteria.

2. Absence of KpsM (Slr0977) strongly impairs the secretion of EPS in *Synechocystis*

Since our previous results suggested that in the absence of two putative components from the Wzy-dependent pathway, Wzb and Wzc, RPS production was most likely diverted to a different route, we searched for a strong candidate outside this pathway that might be involved in EPS production. Thus, the *slr0977* gene, encoding a putative transport permease of the ABC transporter, was targeted taking into account previous works (Fisher et al., 2013; Flores, 2019; Kopf et al., 2014; Pereira et al., 2015). In agreement with the results obtained by Fisher et al. (2013), no significant growth differences were observed between the *kpsM* mutant and the wild-type, and the presence of a flocculent phenotype was also noticed, suggesting a light-sensitive clumping phenotype. In addition to the previously reported differences in the monosaccharidic composition of the EPS produced by the *kpsM* mutant generated by Fisher et al. (2013), our results show that absence of KpsM leads to a significant reduction of the amount of RPS (50%) and a less pronounced decrease of CPS (20%) (Santos et al., 2021). Overall, absence of KpsM significantly affects the amount of EPS in *Synechocystis*. Although there is a very evident decrease of the EPS content in the *kpsM* mutant, the total carbohydrate content remains similar between the mutant and the wild-type, suggesting a possible accumulation of carbon in the cells (Santos et al., 2021).

3. Absence of KpsM (Slr0977) impacts carbon fluxes, increasing the accumulation of PHB

As stated in Chapter III, our results showed that in the *kpsM* mutant, the decrease of EPS goes together with the intracellular accumulation of carbon in the form of the storage compound poly-hydroxybutyrate (PHB) (Santos et al., 2021). This is accompanied by extensive/broad alterations in the transcriptome and proteome of the *kpsM* mutant. Among these, are the upregulation of *sigE* and the lower abundance of the anti-sigma factor E enzyme, ChlH. SigE was previously described as a positive transcriptional regulator of sugar catabolic pathways in *Synechocystis* (Osanai et al., 2005, 2011, 2013; Tokumaru et al., 2018), with its activity being inhibited by ChlH (Osanai et al., 2009). The results of RNA sequencing and iTRAQ analyses also showed that players involved in sugar catabolic pathways, including glycolysis and the oxidative pentose phosphate pathway (OxPPP), are generally present in higher abundances in the mutant. Such as the upregulated phosphoglycerate mutase Pgm (Slr1945), operating at the beginning of lower glycolysis. Recently, this protein was proposed to play a key role in the regulation of cyanobacterial

carbon storage metabolism (Orthwein et al., 2021). It was suggested that the higher carbon flux through lower glycolysis results in higher pyruvate levels, thereby increasing the amount of PHB (Orthwein et al., 2021). It was previously suggested, that the total balance/distribution of the carbon flux could be the determinant factor when trying to improve the production of PHB (Lau et al., 2014). In accordance, Song et al. (2021) described that increasing the carbon flux from glucose to the precursor molecule acetyl-CoA, could lead to the production of value-added chemicals that require acetyl-CoA as a key precursor, such as PHB. A similar hypothesis was raised by Mittermair et al. (2021), which suggested that the availability of general energy supply should be further increased by the reduction of the EPS production, culminating in more precursors available to produce other metabolites, for e.g. PHB. Considering that plastics are now one of the most widely used materials worldwide, production of biobased and biodegradable bioplastics (with a lower environmental footprint), such as PHB, is currently environmentally and economically relevant (Price et al., 2020). Furthermore, PHB is the only poly-hydroxyalkanoate (PHA) produced photoautorophically, and a potential substitute for thermoplastic polymers, such as polypropylene, given its similar molecular structure (Koch & Forchhammer, 2021; Price et al., 2020).

Previous works reported that the amount of carbon flux directed towards PHB production is approximately 16% of the flux directed towards glycogen production (van der Woude et al., 2014). This is in agreement with our results, where the amount of PHB quantified corresponds to approximately 13% of the total amount of glycogen in the wild-type strain of *Synechocystis* (Chapter III, Santos et al., 2021). In Chapter III, we also show that the level of EPS produced by the *Synechocystis* wild-type strain (~6 µg μg^{-1} chlorophyll *a*) is approximately 6-fold higher than that of the most commonly abundant intracellular carbon storage compound, glycogen (~1 µg μg^{-1} chlorophyll *a*). This oftentimes-overlooked fact suggests that EPS can act as an incredibly effective carbon sink in cyanobacteria. Consequently, it stands to reason that re-directing the carbon flux from EPS production (through better understanding and controlling its biosynthetic pathways) should provide excess carbon towards production of other compounds, or vice versa. Thus, bearing in mind the significant reduction of the amount of EPS of the *kpsM* mutant, associated with its robust fitness, this genetic background can provide a starting point for the development of a solid platform/chassis for the production of carbon-based compounds or other compounds of interest.

4. Absence of KpsM (Slr0977) has a pleiotropic effect in *Synechocystis*

The absence of KpsM was also reported to increase the respiratory rate (O_2 consumption), to affect the amount of carotenoids present in the extracellular media, to alter protein secretion and pilin glycosylation (Santos et al., 2021). While the increase of the respiratory rate is significant in the *kpsM* mutant, the growth rate remains unchanged, suggesting that the differences observed do not affect growth under standard laboratory conditions and thus, that these physiological adjustments do not impact biomass formation. The smaller amount of carotenoids present in the extracellular medium of the *kpsM* mutant, together with the smaller amount of RPS, may contribute to the observed light-dependent clumping phenotype, since this mechanism provides self-shading for the cells, which may mitigate the absence of protection conferred by the carotenoids and EPS. While absence of KpsM clearly affects protein secretion, it is not simple to define why. It could be due to differences in the protein composition of the cytoplasmic membrane, as a strategy to compensate the decrease observed in the export of EPS, or, less likely, through a more direct role. Nevertheless, the differential PilA glycosylation profile may be closely related to the role of KpsM in polysaccharide transport, since previous works reported that mutants lacking proteins associated with the TolC-dependent secretion mechanisms also showed differential pilin glycosylation patterns (Gonçalves et al., 2018). Furthermore, in 2015, Khayatan et al. established a correlation between a type IV pilus-like nanomotor that drives motility and polysaccharide secretion in filamentous cyanobacteria. Although this correlation is not established for unicellular cyanobacteria, such as *Synechocystis*, it is possible that type IV pili may help to export the polysaccharide outside the cell (Mullineaux & Wilde, 2021).

5. Addressing the redundancy by using CRISPRi as a tool to repress multiple copies of EPS-related genes

Looking through and combining all the information on EPS biosynthesis and export collected from the literature and our previous work, it is reasonable to hypothesize that the cyanobacterial EPS biosynthetic pathways are more complex than the previously well-characterized bacterial ones. Up to now, the study of these pathways has been performed mainly through the generation and characterization of knockout mutants, by us and others. In cyanobacteria, due to its polyploid nature, this is a lengthy process. Therefore, the use of Clustered Regularly Interspaced Short Palindromic Repeats (CRISPR)-based technologies emerges as an alternative with a drastically shortened timescale for mutant segregation (Behler et al., 2018), which is particularly advantageous for work with

cyanobacteria. In addition, CRISPR interference (CRISPRi), enables targeted gene regulation as the dead Cas9/single-guide RNA (dCas9/sgRNA) complex blocks the RNA polymerase binding or the elongation, resulting in gene repression. Using CRISPRi has advantages over traditional gene knockouts namely, the possibility to study essential genes (that can not be knocked out), and the ability to be used in a multiplex format. Previous work by Yao et al. (2016) reported the repression of up to four genes, providing the proof-of-concept for the use of CRISPRi in multiplex in cyanobacteria. Thus, the use of this system to tackle the redundancy issue, which is frequently pointed out as hindering the study of the cyanobacterial EPS biosynthetic pathways, is particularly exciting. Keeping in mind the results obtained throughout Chapters II and III (Pereira et al., 2019; Santos et al., 2021), we opted to generate a mutant, using CRISPRi, where the 3 putative homologues of *kpsM* (*slr0977*, *slr2107*, *sll0574*) in *Synechocystis*, were targeted and successfully repressed (between ~60-80%) (Chapter IV). The repression levels obtained were within those previously reported for other targets in *Synechocystis* (Kirtania et al., 2019; Shabestary et al., 2018; Yao et al., 2016). The repression level of *slr0977* was the lowest among the three targeted genes, possibly because *slr0977* is part of an operon with a distant transcriptional start site (TSS). In this case, and as previously suggested by Yao et al. (2016), the use of more than one sgRNA targeting *slr0977* could increase the level of repression achieved. The 3-sgRNA *kpsM* mutant showed a similar phenotype, regarding the amount of carbohydrates produced, to the one obtained for the *slr0977* single mutant, generated by double homologous recombination (Chapter III, Santos et al., 2021). Through the comparison of the phenotype of the 3-sgRNA *kpsM* mutant to the individual phenotypes of the three conventional single knockout mutants (*slr0977*, *slr2107* and *sll0574*), we propose that Slr0977 is the key KpsM homologue involved in RPS export, at least under the conditions tested. In agreement, a comparative analysis of the transcriptomes of *Synechocystis* under ten different conditions, Kopf et al. (2014) reported that *slr0977* was the most expressed, while the transcript levels of *slr2107* increased under specific stress conditions (low temperature and nitrogen-depletion), and no data were reported for *sll0574* (consistent with the lower levels detected in our RT-qPCR experiment). In addition, previous RT-PCR results obtained by Pereira et al. (2019), also appear to suggest that *slr0977* is the most abundant of the three *kpsM* homologues in *Synechocystis*, strengthening our hypothesis. This study merely acts as a starting point for the use of CRISPRi as a tool to address the redundancy of EPS-related genes in cyanobacteria. The generation of other CRISPRi mutants, both targeting putative redundant components (for e.g. the 3 homologues of *kpsT* or the 5 homologues of *wzy*), but also targeting homologues that in other bacteria are associated with distinct pathways, are promising avenues to advance these studies. Moreover, in this work we used a constitutive CRISPRi system, in which both

the dCas9 and the sgRNAs were constitutively expressed, due to the high probability that the genes we were targeting were not essential and as such the mutants could survive even if the target gene was always repressed. In the future, the use of an inducible CRISPRi system could provide better control and allow a tighter regulation, and is envisioned as a valuable option.

Even though the application of CRISPRi in cyanobacteria is not yet widely used, it provided a novel approach to tackle the redundancy of EPS-related genes in cyanobacteria, thus enabling a faster screening of the different players, and allowing the now loose puzzle pieces to be put together to assist in the clarification of these molecular mechanisms/biosynthetic pathways.

6. Generation and characterization of other EPS-related mutants

Following the generation of a Δ*sll0737* (*wzy*) mutant that showed no phenotypic changes concerning the production of EPS (Pereira, Santos et al., 2019), we generated a *slr1074* (*wzy*) mutant. This gene encodes a putative polymerase, Wzy, associated to the Wzy-dependent pathway, however, one should keep in mind that there are 4 other homologues in the *Synechocystis* genome (*sll0737*, *slr0728*, *slr1515* and *sll5047*) (Pereira et al., 2015). As the Δ*sll0737* mutant (Pereira, Santos et al., 2019), the *slr1074* mutant does not show any significant differences regarding the amount of total carbohydrates, CPS or RPS produced compared to the wild-type, suggesting that both Sll0737 and Slr1074 are not involved in EPS production in *Synechocystis*, at least under the conditions tested. Overall, these results, taken together with our previous work (Chapters II, III and IV), seem to suggest a more prominent role for the components putatively associated with the ABC-transporter dependent pathway. Nevertheless, it does not exclude the involvement of other components from the EPS biosynthetic process, strengthening the hypothesis that the pathways of EPS biosynthesis in cyanobacteria deviate from the well-characterized bacterial ones.

The last steps of polymerization, assembly and export of EPS appear mostly conserved throughout bacteria, following one of three model mechanisms: the Wzy-, the ABC transporter- or the Synthase-dependent pathways. Thus, the work regarding the EPS biosynthetic pathways in cyanobacteria has mainly been focused on cyanobacterial homologues putatively involved in these last steps. However, as an initial approach to address EPS biosynthesis upstream of the assembly and export machinery, we generated a *slr0985* (*rfbC*) mutant. This gene encodes an epimerase, RfbC, involved in the rhamnose biosynthetic pathway in *Synechocystis*. Moreover, previous work showed that *Synechocystis*' mutants lacking the tyrosine kinase Sll0923 (Wzc) and/or the low molecular

weight tyrosine phosphatase Slr0328 (Wzb) produced EPS enriched in rhamnose (Chapter II, Pereira, Santos et al., 2019). Similar results were obtained for a mutant lacking Sll0982 (KpsT), the ATP-binding component of an EPS-related ABC-transporter (Fisher et al., 2013). The *rfbC* mutant produced approximately 47% less RPS, secreted more protein, showed some differences in terms of lipopolysaccharides (LPS), and had significantly less carotenoids in its concentrated medium compared to the wild-type (Chapter V, section 2), suggesting that absence of RfbC seems to have a broad effect in *Synechocystis*. In addition, the composition of the polymer produced by the *rfbC* mutant should be determined, since rhamnose is present in the polymer produced by the wild-type (Flores et al., 2019; Panoff et al., 1988; Pereira, Santos et al., 2019). Furthermore, the repercussions that a different composition will have in the bioactivity of the polymer should also be considered/evaluated. Especially since enrichment in rare sugars, such as rhamnose and fucose, can be advantageous to confer unique physical and bioactive properties to the polymers (Roca et al., 2015) and thus, their absence could strongly impact the bioactivity of the polymer.

7. Future Perspectives

Even though this work provided relevant information regarding the involvement of key proteins in the EPS biosynthesis, assembly and export pathways, and of the importance of EPS for cell homeostasis, and as a carbon-sink in cyanobacteria, several other questions were raised and other hypothesis/ideas were formulated/had during the course of this work, namely:

i) To overexpress *kpsM* (*slr0977*) with the aim of increasing the amount of RPS facilitating polymer isolation and its subsequent characterization and use;

ii) Using the *kpsM* (*slr0977*) mutant as a starting point to optimize a *Synechocystis* sp. PCC 6803 chassis for the production of poly-hydroxybutyrate (PHB), or other carbon-based compounds;

iii) To start piecing together the EPS biosynthetic pathways in *Synechocystis* sp. PCC 6803 by using KpsM (Slr0977) as bait and finding its interactors (protein-protein interaction [PPI]);

iv) Start addressing the hypothesis of crosstalk between components that are typically associated with distinct bacterial pathways (for e.g. Wzy- and ABC-transporter dependent pathways) by generating and characterizing multiple mutants (CRISPRi and/or traditional mutants);

v) Implement an hybrid system by using the traditional knockout mutants as genetic background, and use an inducible CRISPRi system to repress other components;

vi) Further characterize the *rfbC* (*slr0985*) mutant, and generate and characterize others, to continue to unveil the earlier steps of EPS biosynthesis, envisaging the polymer tailoring for specific applications.

References

Behler, J., Vijay, D., Hess, W. R., & Akhtar, M. K. (2018). CRISPR-Based technologies for metabolic engineering in cyanobacteria. *Trends in Biotechnology*, *36*(10), 996–1010. https://doi.org/10.1016/j.tibtech.2018.05.011

Fisher, M. L., Allen, R., Luo, Y., & Curtiss III, R. (2013). Export of extracellular polysaccharides modulates adherence of the cyanobacterium *Synechocystis*. *PLOS ONE*, *8*(9), e74514. https://doi.org/10.1371/journal.pone.0074514

Flores, C., Santos, M., Pereira, S. B., Mota, R., Rossi, F., De Philippis, R., Couto, N., Karunakaran, E., Wright, P. C., Oliveira, P., & Tamagnini, P. (2019). The alternative sigma factor SigF is a key player in the control of secretion mechanisms in *Synechocystis* sp. PCC 6803. *Environmental Microbiology*, *21*(1), 343–359. https://doi.org/10.1111/1462-2920.14465

Flores, C. (2019) Extracellular polymeric substances (EPS) from the cyanobacterium Synechocystis sp. PCC 6803: from genes to polymer application as antitumor agent (Doctoral thesis, University of Porto, Porto, Portugal). Retrieved from https://hdl.handle.net/10216/124611

Gonçalves, C. F., Pacheco, C. C., Tamagnini, P., & Oliveira, P. (2018). Identification of inner membrane translocase components of TolC-mediated secretion in the cyanobacterium *Synechocystis* sp. PCC 6803. *Environmental Microbiology*, *20*(7), 2354–2369. https://doi.org/10.1111/1462-2920.14095

Khayatan, B., Meeks, J. C., & Risser, D. D. (2015). Evidence that a modified type IV pilus-like system powers gliding motility and polysaccharide secretion in filamentous cyanobacteria. *Molecular Microbiology*, *98*(6), 1021–1036. https://doi.org/10.1111/mmi.13205

Kirtania, P., Hódi, B., Mallick, I., Vass, I. Z., Fehér, T., Vass, I., & Kós, P. B. (2019). A single plasmid based CRISPR interference in *Synechocystis* 6803 – a proof of concept. *PLoS ONE*, *14*(11): e0225375. https://doi.org/10.1371/journal.pone.0225375

Koch, M., & Forchhammer, K. (2021). Polyhydroxybutyrate : A Useful Product of Chlorotic Cyanobacteria. *Microbial Physiology*. https://doi.org/10.1159/000515617

Kopf, M., Stephan, K., Scholz, I., Matthiessen, J. K. F., Hess, W. R., & Voß, B. (2014). Comparative analysis of the primary transcriptome of *Synechocystis* sp. PCC 6803. *DNA Research*, *21*(5), 527–539. https://doi.org/10.1093/dnares/dsu018

Lau, N. S., Foong, C. P., Kurihara, Y., Sudesh, K., & Matsui, M. (2014). RNA-Seq analysis provides insights for understanding photoautotrophic polyhydroxyalkanoate production in recombinant *Synechocystis* sp. *PLoS ONE*, *9*(1), 1–11. https://doi.org/10.1371/journal.pone.0086368

Mittermair, S., Richter, J., Doppler, P., Trenzinger, K., Nicoletti, C., Forsich, C., Spadiut, O., Herwig, C., & Lackner, M. (2021). Impact of *exoD* gene knockout on the polyhydroxybutyrate overaccumulating mutant Mt_a24. *International Journal of Biobased Plastics*, *3*(1), 1–18. https://doi.org/10.1080/24759651.2020.1863020

Mullineaux, C. W., & Wilde, A. (2021). The social life of cyanobacteria. *eLife*, *10*, 3–5. https://doi.org/10.7554/elife.66538

Orthwein, T., Scholl, J., Spät, P., Lucius, S., Koch, M., Macek, B., Hagemann, M., & Forchhammer, K. (2021). The novel PII-interactor PirC identifies phosphoglycerate mutase as key control point of carbon storage metabolism in cyanobacteria. *Proceedings of the National Academy of Sciences*, *118*(6), e2019988118. https://doi.org/10.1073/pnas.2019988118

Osanai, T., Imashimizu, M., Seki, A., Sato, S., Tabata, S., Imamura, S., Asayama, M., Ikeuchi, M., & Tanaka, K. (2009). ChlH, the H subunit of the Mg-chelatase, is an anti-sigma factor for SigE in *Synechocystis* sp. PCC 6803. *Proceedings of the National Academy of Sciences of the United States of America*, *106*(16), 6860–6865. https://doi.org/10.1073/pnas.0810040106

Osanai, T., Kanesaki, Y., Nakano, T., Takahashi, H., Asayama, M., Shirai, M., Kanehisa, M., Suzuki, I., Murata, N., & Tanaka, K. (2005). Positive regulation of sugar catabolic pathways in the cyanobacterium *Synechocystis* sp. PCC 6803 by the group 2 σ factor SigE. *Journal of Biological Chemistry*, *280*(35), 30653–30659. https://doi.org/10.1074/jbc.M505043200

Osanai, T., Numata, K., Oikawa, A., Kuwahara, A., Iijima, H., Doi, Y., Tanaka, K., Saito, K., & Hirai, M. Y. (2013). Increased bioplastic production with an RNA polymerase sigma factor SigE during nitrogen starvation in *Synechocystis* sp. PCC 6803. *DNA Research*, *20*(6), 525–535. https://doi.org/10.1093/dnares/dst028

Osanai, T., Oikawa, A., Azuma, M., Tanaka, K., Saito, K., Hirai, M. Y., & Ikeuchi, M. (2011). Genetic engineering of group 2 sigma factor SigE widely activates expressions of sugar catabolic genes in *Synechocystis* species PCC 6803. *The Journal of Biological Chemistry*, *286*(35), 30962–30971. https://doi.org/10.1074/jbc.M111.231183

Panoff, J. M., Priem, B., Morvan, H., & Joset, F. (1988). Sulphated exopolysaccharides produced by two unicellular strains of cyanobacteria, *Synechocystis* PCC 6803 and 6714. *Archives of Microbiology*, *150*(6), 558–563. https://doi.org/10.1007/BF00408249

Pereira, S. B., Mota, R., Vieira, C. P., Vieira, J., & Tamagnini, P. (2015). Phylum-wide analysis of genes/proteins related to the last steps of assembly and export of extracellular polymeric substances (EPS) in cyanobacteria. *Scientific Reports*, *5*(July), 1–16. https://doi.org/10.1038/srep14835

Pereira, S. B., Santos, M., Leite, J. P., Flores, C., Eisfeld, C., Büttel, Z., Mota, R., Rossi, F., De Philippis, R., Gales, L., Morais-Cabral, J. H., & Tamagnini, P. (2019). The role of the tyrosine kinase Wzc (Sll0923) and the phosphatase Wzb (Slr0328) in the production of extracellular polymeric substances (EPS) by *Synechocystis* PCC 6803. *MicrobiologyOpen*, *8*(6), e00753. https://doi.org/https://doi.org/10.1002/mbo3.753

Price, S., Kuzhiumparambil, U., Pernice, M., & Ralph, P. J. (2020). Cyanobacterial polyhydroxybutyrate for sustainable bioplastic production: Critical review and perspectives. *Journal of Environmental Chemical Engineering*, *8*(4), 104007. https://doi.org/10.1016/j.jece.2020.104007

Roca, C., Alves, V. D., Freitas, F., & Reis, M. A. M. (2015). Exopolysaccharides enriched in rare sugars: Bacterial sources, production, and applications. *Frontiers in Microbiology*, *6*(APR), 1–7. https://doi.org/10.3389/fmicb.2015.00288

Santos, M., Pereira, S. B., Flores, C., Príncipe, C., Couto, N., Karunakaran, E., Cravo, S. M., Oliveira, P., & Tamagnini, P. (2021). Absence of KpsM (Slr0977) impairs the secretion of extracellular polymeric substances (EPS) and impacts carbon fluxes in

Synechocystis sp. PCC 6803. m*Sphere*, *6*(1), 1–20. https://doi.org/10.1128/msphere.00003-21

Shabestary, K., Anfelt, J., Ljungqvist, E., Jahn, M., Yao, L., & Hudson, E. P. (2018). Targeted repression of essential genes to arrest growth and increase carbon partitioning and biofuel titers in cyanobacteria. *ACS Synthetic Biology*, *7*(7), 1669–1675. https://doi.org/10.1021/acssynbio.8b00056

Song, X., Diao, J., Yao, J., Cui, J., Sun, T., Chen, L., & Zhang, W. (2021). Engineering a central carbon metabolism pathway to increase the intracellular acetyl-CoA pool in *Synechocystis* sp. PCC 6803 grown under photomixotrophic conditions. *ACS Synthetic Biology*, *10*(4), 836–846. https://doi.org/10.1021/acssynbio.0c00629

Tokumaru, Y., Uebayashi, K., Toyoshima, M., Osanai, T., Matsuda, F., & Shimizu, H. (2018). Comparative targeted proteomics of the central metabolism and photosystems in SigE mutant strains of *Synechocystis* sp. PCC 6803. *Molecules*, *23*(5). https://doi.org/10.3390/molecules23051051

van der Woude, A. D., Angermayr, S. A., Puthan Veetil, V., Osnato, A., & Hellingwerf, K. J. (2014). Carbon sink removal: Increased photosynthetic production of lactic acid by *Synechocystis* sp. PCC6803 in a glycogen storage mutant. *Journal of Biotechnology*, *184*, 100–102. https://doi.org/10.1016/j.jbiotec.2014.04.029

Yao, L., Cengic, I., Anfelt, J., & Hudson, E. P. (2016). Multiple gene repression in cyanobacteria using CRISPRi. *ACS synthetic biology, 5*(3), 207–212. https://doi.org/10.1021/acssynbio.5b00264